FLASH FLOODS AND THEIR EFFECTS ON THE DEVELOPMENT IN EL-QAÁ PLAIN AREA IN SOUTH SINAI, EGYPT, A STUDY IN APPLIED GEOMORPHOLOGY USING GIS AND REMOTE SENSING

Dissertation

Zur Erlangung des Grades

"Doktor der Naturwissenschaften"

im Promotionsfach Geographie

am Fachbereich Chemie, Pharmazie, Geowissenschaften

der Johannes Gutenberg- Universität Mainz

Vorgelegt von

YOUSSEF SHAWKY YOUSSEF SHERIEF

Geboren in Sharqia, Ägypten

Mainz, 2008

Tag der mündlichen Prüfung: 20/10/2008

Erklärung:

Ich versichere hiermit, die vorliegende Arbeit selbständig und unterVerwendung der angegebenen Quellen und Hilfsmittel verfaßt zu haben.

Assertion:

All views and results presented in this thesis are those of the author unless stated otherwise

Dedication

TO MY HOMELAND: EGYPT
TO MY WIFE AND CHILDREN
TO MY BIG FAMILY
AS A CONFESSION OF KINDNESS

TO ALL PEOPLE WHO HAD DAMAGE FROM FLOODS
WITH MY BEST WISHES AND BETTER FUTURE

Zusammenfassung

Die Trockengebiete der Erde sind in viel stärkerem Maße von extremen Naturereignissen betroffen als die humiden Klimaregionen. Obwohl Ägypten ganz überwiegend im ariden Klimabereich liegt, wird es im Norden häufig von stärkeren Winterregen betroffen, die insbesondere auf der Halbinsel Sinai Wadifluten hervorrufen können. Solche Fluten sind gekennzeichnet durch hohe Geschwindigkeit bei kurzer Dauer und einen hohen Maximalabfluss. Durch Wadifluten werden meist auch große Sedimentmengen transportiert, wodurch Felder und Siedlungen beschädigt oder gar zerstört werden, ja es kann sogar zu Todesopfern unter der ansässigen Bevölkerung kommen. Der lokale Charakter seltener Starkregen, der bei den Menschen der Wüste bekannt ist, macht eine wirksame Vorhersage fast unmöglich. Obwohl eine Fülle an Messdaten aus dem Gelände vorliegt, werden die Möglichkeiten, ein Frühwarnsystem für Wadifluten einzurichten, eher zurückhaltend beurteilt. Die meist nur kurzzeitige Abflussspitze als ein Charakteristikum von Wadifluten bedeutet eine zusätzliche Unsicherheit der Schadensabschätzung in einem Vorwarnsystem.

Die vorliegende Dissertation ist nach der Einführung in 5 Kapitel gegliedert. Im ersten Kapitel wird die physisch-geographische Ausstattung des Untersuchungsraumes beschrieben. Dabei geht es vor allem um die Gesteine und ihre Lagerung, einschließlich der Darstellung des Kluftnetzes, und die Lockersedimente. Im speziellen Fall wurden die sandigen Sedimente des kleinen Wadi Moreikh genau untersucht, um die Ablagerungsprozesse und die paläoklimatischen Bedingungen zu erforschen. Das Alter der Sedimente wurde mit Hilfe mehrerer OSL-Datierungen ermittelt. In Kapitel 1 wird außerdem das heutige Klima, gegliedert nach Temperatur und Feuchtegang, Windverhältnisse und Verdunstung beschrieben. Weiterhin geht es um die Darstellung von Wüstenböden und der in geringem Maße vorhandenen Vegetation, deren Dichte über Satellitenbildauswertung ermittelt wurde.

In Kapitel 2 wird eine morphometrische Analyse der Einzugsgebiete der großen Wadis im Untersuchungsgebiet vorgenommen. Sie ist in drei Teile gegliedert: Der erste Teil enthält die morphometrische Analyse der Wadinetze, die aus zwei Hauptquellen, topographischen Karten und DEMs übernommen wurden. Wadi- bzw. Gewässernetze werden als wichtige Einflussfaktoren von Wadifluten angesehen. Eine Reihe statistischer Größen, wie etwa Gewässerordnung, Bifurkationsgrad, Gewässerlänge, Gewässerdichte und Gewässergeometrie werden im Einzelnen untersucht. Im zweiten Teil dieses Kapitels wird die morphometrische Analyse der Einzugsgebiete, beruhend auf Relief, Ausdehnung und Grundrissform vorgestellt.

Der dritte Teil enthält die morphometrische Analyse der Schwemmfächer, aus der sich die El-Qaá -Ebene zusammensetzt.

Kapitel 3 enthält die Darstellung des Oberflächenabflusses bei Starkregen sowie der Versickerungsverluste. In erster Linie geht es um die detaillierte Beschreibung der Genese und der Intensität von Regenfällen. Sie sind neben den Substratbedingungen die Hauptursache für Wadiabfluss. Alle wichtigen Parameter werden untersucht, wie etwa Niederschlagstyp, -verteilung, -intensität, -dauer, und -häufigkeit sowie die enge Beziehung zwischen Niederschlag und Abflussgeschehen. Im zweiten Teil dieses Kapitels werden Abschätzungen zu den Wasserverlusten durch Verdunstung und Infiltration vorgenommen, da sie einen unmittelbaren Einfluss auf die Abflusshöhe haben. Im dritten Teil des Kapitels werden alle abflusserzeugenden Faktoren zusammenfassend erläutert.

Kapitel 4 enthält grundlegende Aussagen zur Abschätzung von Flutereignissen; dies ist wichtig, um eine Karte der von Fluten evtl. betroffenen Gebiete zu erstellen. Das Kapitel besteht aus vier Teilen. Im ersten Teil geht es um die Abflussschätzung, die hierfür verwendeten unterschiedlichen Methoden und deren Variablen, wie etwa Abflussbeginn, Hauptabfluss, Abflussmenge sowie um eine Häufigkeitsanalyse von Wadifluten. Im zweiten Teil wird eine Untersuchung extremer Abflussereignisse vorgestellt. Der dritte Teil enthält die Karte der von Wadifluten betroffenen Bereiche, gegliedert nach Wadieinzugsgebieten und nach Fluthöhe. Hierfür wurde ein DEM benutzt, um die Abflussbahnen genau zu erfassen, vor allem aber um die Hauptabflussrinnen festzulegen, die erfahrungsgemäß bei Fluten am gefährlichsten sind. Als Synthese wird im vierten Teil die Risikokarte des gesamten Untersuchungsgebietes präsentiert, die von großer Bedeutung für die Planung in der Region sein dürfte.

Im fünften und letzten Kapitel werden Ausführungen zur möglichen Dämpfung von starken Abflussereignissen gemacht. Es besteht aus drei Teilen. Im ersten Teil geht es um eine Methode, die geeignet erscheint, Wadifluten voherzusagen. Im zweiten Teil geht es um die Diskussion der Vor- und Nachteile von Methoden, die helfen könnten, die Auswirkung von Flutereignissen abzumildern. Hier sind im Wesentlichen technische Eingriffe gemeint. Zum Schluss werden im dritten Teil die Entwicklungsperspektiven für das Untersuchungsgebiet, die El-Qaá -Ebene aufgezeigt, die in der ägyptischen Landesplanung einen hohen Stellenwert besitzen.

Summary

The arid regions are dominated to a much larger degree than humid regions by major catastrophic events. Although most of Egypt lies within the great hot desert belt; it experiences especially in the north some torrential rainfall, which causes flash floods all over Sinai Peninsula. Flash floods in hot deserts are characterized by high velocity and low duration with a sharp discharge peak. Large sediment loads may be carried by floods threatening fields and settlements in the wadis and even people who are living there.

The extreme spottiness of rare heavy rainfall, well known to desert people everywhere, precludes any efficient forecasting. Thus, although the limitation of data still reflects pre-satellite methods, chances of developing a warning system for floods in the desert seem remote. The relatively short flood-to-peak interval, a characteristic of desert floods, presents an additional impediment to the efficient use of warning systems.

The present thesis contains introduction and five chapters, ***chapter one*** points out the physical settings of the study area. There are the geological settings such as outcrop lithology of the study area and the deposits. The alluvial deposits of Wadi Moreikh had been analyzed using OSL dating to know deposits and palaeoclimatic conditions. The chapter points out as well the stratigraphy and the structure geology containing main faults and folds. In addition, it manifests the pesent climate conditions such as temperature, humidity, wind and evaporation. Besides, it presents type of soils and natural vegetation cover of the study area using unsupervised classification for ETM+ images.

Chapter two points out the morphometric analysis of the main basins and their drainage network in the study area. It is divided into three parts: The first part manifests the morphometric analysis of the drainage networks which had been extracted from two main sources, topographic maps and DEM images. Basins and drainage networks are considered as major influencing factors on the flash floods; Most of elements were studied which affect the network such as stream order, bifurcation ratio, stream lengths, stream frequency, drainage density, and drainage patterns. The second part of this chapter shows the morphometric analysis of basins such as area, dimensions, shape and

surface. Whereas, the third part points the morphometric analysis of alluvial fans which form most of El-Qaá plain.

Chapter three manifests the surface runoff through rainfall and losses analysis. The main subject in this chapter is rainfall which has been studied in detail; it is the main reason for runoff. Therefore, all rainfall characteristics are regarded here such as rainfall types, distribution, rainfall intensity, duration, frequency, and the relationship between rainfall and runoff. While the second part of this chapter concerns with water losses estimation by evaporation and infiltration which are together the main losses with direct effect on the high of runoff. Finally, chapter three points out the factors influencing desert runoff and runoff generation mechanism.

Chapter four is concerned with assessment of flood hazard, it is important to estimate runoff and tocreate a map of affected areas. Therefore, the chapter consists of four main parts; first part manifests the runoff estimation, the different methods to estimate runoff and its variables such as runoff coefficient lag time, time of concentration, runoff volume, and frequency analysis of flash flood. While the second part points out the extreme event analysis. The third part shows the map of affected areas for every basin and the flash floods degrees. In this point, it has been depending on the DEM to extract the drainage networks and to determine the main streams which are normally more dangerous than others. Finally, part four presets the risk zone map of total study area which is of high inerest for planning activities.

Chapter five as the last chapter concerns with flash flood Hazard mitigation. It consists of three main parts. First flood prediction and the method which can be used to predict and forecast the flood. The second part aims to determine the best methods which can be helpful to mitigate flood hazard in the arid zone and especially the study area. Whereas, the third part points out the development perspective for the study area indicating the suitable places in El-Qaá plain for using in economic activities.

Table of content

List of Tables

List of figures

List of photos

Introduction

1. Location of the study area

El-Qaà plain area is located on the eastern coast of the Gulf of Suez between 27° 43́ 44″ to 28° 54́ 55″ N and 33° 11́ 50″ to 34° 15́ 24″ E within the southwest Sinai rift zone Fig. (1). The study area is an elongate northwest-trending zone running for approximately 150 km and 20-30 km wide parallel to the Gulf of Suez.

It is bounded in the east by Wadi Aat El-Sharqy, Wadi Kid, Wadi Dahab and Wadi Wateer, in the west by the Gulf of Suez, in the north by Wadi Sedry, and by the Red see in the south. It covers an approximate surface of 6070 km^2, which is estimated 10 % of the Sinai Peninsula, with a maximum length of 150 km approximately and a maximum width of 20 km.

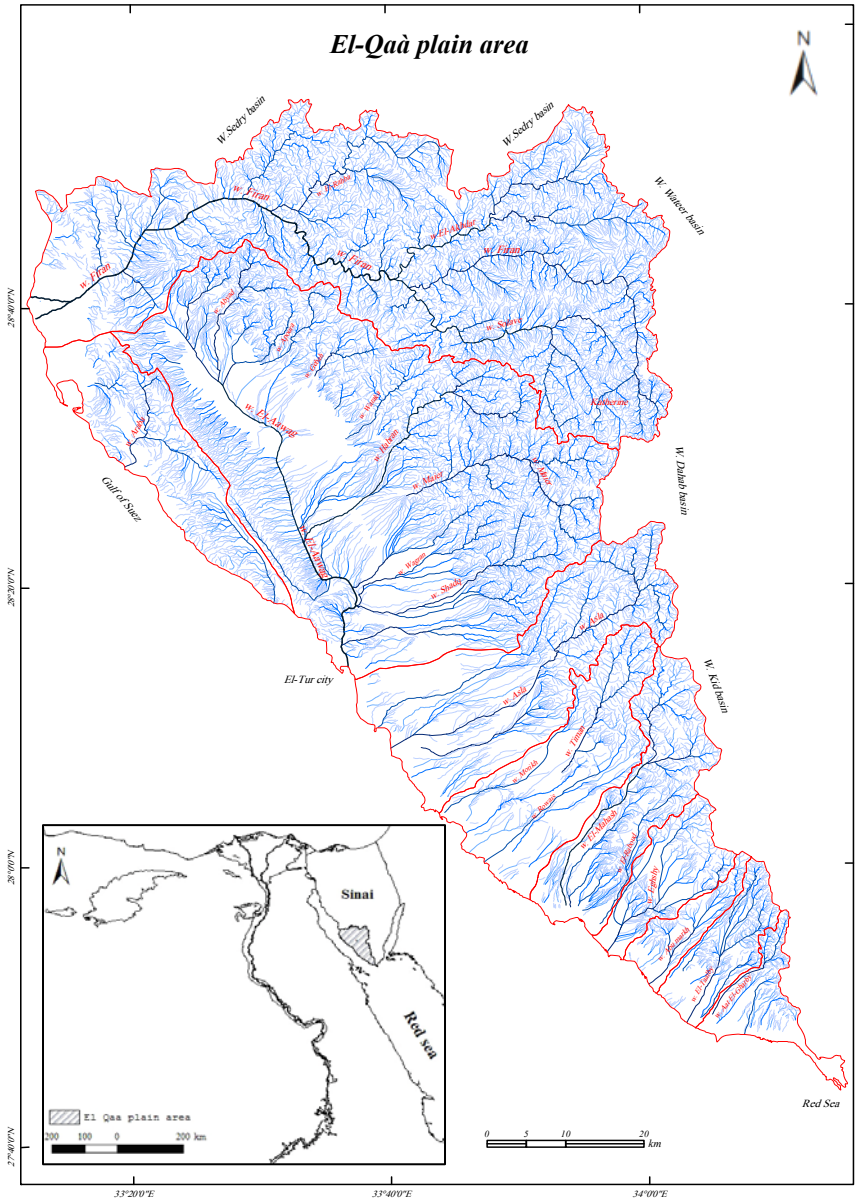

Fig (1) Location of El-Qaà plain area

El-Qaà plain is covered by quaternary alluvial fans from several wadis and bounded by both Pre-Cambrian granites and old Carboniferous clastics. Upper Tertiary deposits (marine Miocene sediments and most probably, non-marine Pliocene sediments) are forming El-Qaà plain below the surface (ABDALLAH AND ABU KHADRA, 1976). I will focus this point with details in the next chapter.

The surface of the plain is slightly dipping towards southwest; the average slope degree is estimated at 2°. The plain is subjected to floods from several wadi basins, i.e from north to south Wadi Firan, Wadi El-Aawag, Wadi Habran, Wadi Meiar, Wadi Asla, Wadi Timan, Wadi Eghshy, Wadi El-Taalby, Wadi Amlaq, and Wadi Aat El-Gharby Fig (1). They are all active during rainy periods (HAMAD, 1980).

2. Problem definition

The arid regions are dominated to a much larger degree by major catastrophic events (Baker 1977). Such events are rare, they tend to be scattered also in space, and their scientific documentation is mostly inadequate. Although most of Egypt lies within the great hot desert belt; it experiences some torrential rainfall, which causes flash floods all over Sinai Peninsula. Flash floods in hot deserts are characterized by high velocity and low duration with a sharp discharge peak (ASHOUR, M, 2002). Large sediment loads may be carried by floods threatening settlements in the wadis and people who are living there.

The extreme spottiness of rare heavy rainfall, well known to desert people everywhere, precludes any efficient forecasting. Thus, although the limitation of data still reflects pre-satellite methods, chances of developing a warning system for floods in the desert seem remote. The relatively short flood-to-peak interval, a characteristic of desert floods, presents an additional impediment to the efficient use of warning systems. Nearly all catastrophic desert floods have a flood-to-peak interval of less than one hour, and often the flood comes as a wall of water.

A big problem inherent in the opening up of the deserts to modern development is one of perception. Urban planners and highway engineers become insensitive to the potential even though infrequent dangers of dry wadi beds and closed basins, which must carry and store excess surface water. The alluvial fans of El-Qaà plain area bording the mountains are of main interest in this respect.

On the one hand, they strongly attract human occupancies because they represent preferred sites in terms of local topography, accessibility and, mainly, water supply. On the other hand, the alluvial fan is located at the outlet of a mountain watershed into a lower foreland such as a rift valley or a major valley, threatening Bedouin villages especially in Wadi Firan.

Because settlements and other structures in deserts are also widely scattered, a spatial combination of the area affected by a violent desert flood with an area of settlement is relatively rare. However, such events seem to be more frequent during recent years than in past decades. One reason for this is undoubtedly the great expansion of economic activity, mainly various forms of mining. There are today more objects to be affected in the desert, because they are more widely distributed and, furthermore, they are served by a much more widespread and organized network of roads (SHECK, A.1979)

In south Sinai, wadis are developed as a deeply incised valley network in the mountain area, and as an alluvial fan network in the foreland plain. Due to human activities and the extension of human settlements, the impacts of flash floods have become much more serious, causing loss of human life, loss of livestock, damage of infrastructure, and socioeconomic problems. Generally, in Sinai study area runoff calculation is very difficult because of a lack of direct runoff data. Therefore, the problem is remaining unsolved until long-term runoff data will be available (JICA AND WRRI, 1999), but it may be helpful to use other methods to estimate runoff in the study area such as morphometric analyses and climatic data evaluation.

These methods are fit for wadis that have been formed within basement or metamorphic rocks. Several wadis in southern Sinai are famous for their activity during flood such as Wadi Wateer, Wadi Dahab and Wadi Kid in the eastern part of Southern Sinai and Wadi Firan, Wadi Sedry, Wadi Gharandal and Wadi Meiar in the western part of southern Sinai.

The study area is considered representing a promising and strategic target for urban and agricultural expansions, but usually it is attacked by natural hazards, especially flash floods although rainfall is scarce in Sinai Peninsula; it is well known for its flash floods with high velocity. Each runoff causes more damages of bedouin villages, the infrastructure in urban centers such as electric poles, water and oil pipes, bridges and roads photos (1, 2 and 3).

Photo (1) the highway and bridge in Wadi Wateer were destroyed by a flash flood

Photo (2) the flash flood attacked the road and eroded it vertically of about 100 cm

Photo (3) the highway Suez- Sharm El-Sheikh was destroyed by a flash flood of Wadi El-Aawag

History of strong flash floods in Sinai during the period extending from 1975 - 2004

Date of runoff	***Location***	***Human and Natural Damage***	***remarks***
20-25/2/1975	***Wadi El-Arish***	*Flash floods caused damages along the Wadi El-Arish in the north of Sinai.The water submerged the coastal area and extended to about 200 km till central Sinai and formed a deep lake with length of 8 km and width of 3 km. the results were as follows: 17 persons died and 105 inhabitants became homeless because about 200 homes were destroyed*	*- The restricted flash flood to Wadi El-Arish.* *- The location of lake is not determined and the probable location of it may be El-Halal strait.*
18/10/1987	***Wadi Wateer***	*Destroy and damage of Nuweiba and Ras El-Naqab road as well as destroying parts of coastal road between Nuweiba and Taba especially these parts which cross the mouths of wadis. This flash flood led to the injury of 27 persons with snake poison.*	*The flooding took away the cars in the roads and buried some of them with every thing inside, i.e. people and their belongings.*
6/1/1988	***Wadi Sudr***	*The flood in a wadi close to Ras Sudr caused the death of 5 passengers inside a car.*	*The flood happened 60 km far from Sudr town.*
13/10/1991	***Wadi Firan***	*The main road following Wadi Firan and some houses in El-Tarfa village had been partly destroyed.*	*The flash flood originated in Saint. Catherine area.*
20-22/3/1991	***Wadi El-Aawag***	*The big flash flood in Wadi El-Aawag destroyed some houses in El-Wadi village and some animals died.*	*The flood developed in Wadi Meiar and Wadi El-Mahash.*
25-27/10/2004	***Wadi Wateer***	*The runoff in Wadi Wateer destroyed the highway to Nuweiba to 40% photo (2).*	*The flood developed in the whole basin resulted in a big runoff.*

- Source: some reports about flash floods in Sinai, meteorological authority magazine, and newspaper archive.

Wadi Firan is one of the most active wadis of Sinai; former floods have destroyed long parts of the road and damaged houses in two Oasis areas (Firan and El-Tarfa). But the outlet of Wadi Firan –El Tur is in contrast, not dangerous. The surface flows from El-Qaà plain are carryng a lot of sediments sometimes daming the highway. The point where the Wadi El-Aawag crosses the highway near El Tur is a risky zone due to the absence of any sutibale structure to mitigate the flow path photo (3).

3. Objectives

The main objective of this work is flood hazard assessment in El-Qaà pain area considering the study area is one of the main development areas in Egypt and southern Sinai. Because of the development in this area several times has been attacked by flash floods which caused severe economic and social damages. It will be focused on the recognition of different indicators and factors which play an important role to estimate and mitigate the runoff in the study area such as geological setting, climate conditions, basins and network morphometric analysis, slopes, and hydrological setting using remote sensing and geographical information systems. It can be determining the objective in the following points:

1- The work aims to focus on geological and climate setting which are considered as the main influence factors on the flash flood assessment.

2- Morphometric analysis of the main basins and networks of the study area whereas the basins parameters, area, shape, and slope have a direct effect on runoff.

3- Calculation rainfall amounts in all basins in the study area, and losses through evaporation and infiltration to estimate runoff.

4- Determination of the areas which are threatened by flash floods, to give an understanding of the causal factors.

5- Definition of extreme event analysis of flash floods to make a risk zone map of the study area

6- Determination of development perspectives for the study area.

7- This work aims to find an answer for some questions such as:

- What are the best methods to estimate runoff in arid regions?
- What are and where are the affected areas by flash floods?
- What the best methods of GIS and remote sensing techniques to study flash floods?
- What are the best methods to mitigate flash floods in arid regions, such as the study area?

4. Field work

Geomorhological field work in the study area of southern Sinai is considered an essential element, although the study area is nearly covered by topographic and geologic maps with different scales, satellite images, and DEM map, There were organized two field trips between 23.3 to 1.4.2005, and from 26.2 to 1.3.2007. The field work was very necessary to carry out the following investigations:

1. During both trips were measured several transverse sections along some potentially flash flood active channels such as Wadi Firan and El-Aawag especially at narrow trunks. In additional some cross sections for the main wadi channel were taken.

2. During the second field trip, we tried to make hydrological sections in some wadi channels such as Wadi Meiar and Wadi Moreikh to determine the depth of groundwater and estimate the amount using new equipment from Regensburg University managed by Prof. J, VÖLKEL, and Dr. M, LEOPOLD (photo 4).

3. Determination of erosion and damage results from flash flooding in the study area especially on roads, culverts, and the site of Wadi floor.

4. Taking about 26 samples from delta sediments in El-Qaà plain for physical analysis, and 7 samples for OSL dating.

5. Determination of suitable tools to avoid or mitigate flash flood hazards and definition of the safe and protected areas for development.

6. Determination of the location of urban and touristic sites in El-Qaá plain area which were selected and built up without threatening of flash flooding hazard.

Photo (4) *hydrological cross section for the main channel of Wadi Meiar*

5. Available Data

5.1. Geologic maps

- The geological map of Egypt scale 1:100000 is the first source for outcrop lithology in the study area. It had been produced by Remote Sensing Authority in 2002.
- The second source of geological data are three sheets of geological maps of Sinai scale 1:250000 which have produced by Egyptian General Survey Authority in 1994. They have more details about lithology and structure of the study area
- Several previous studies and reports about lithology, structure and stratigraphy of the southern Sinai.

5.2. Topographical maps

Several sheets of topographic maps scale 1:100000 and 1:50000 are available. They have been used by the following steps:

- The first step was scanning all sheets and rectifying the projection as UTM using ERDAS imagine program.
- The sheets have been collected to make a mosaic map for the total area.
- The third step was digitizing all topographic features such as contour lines, elevations, urban areas, roads, and wadi networks which required about eight months.
- The last step was the classification of drainage network orders, road orders and urban areas as individual layers

5.3. Satellite images

Satellite images are considered one of the main sources of geological, topographic, and geomorphic data. There were several images used in the present study which can be classified as followings:

- TM images (Thematic Mapper) which were produced in years 1976 and 84 (three bands), 87 and 96 (seven bands) giving details until 28m lengths.
- ETM+ images (Enhanced Thematic Mapper plus) were produced in 2001 (9 bands); every pixel represents about 30m lengths.

- Spot images produced in 2001 (3 bands) which give details smaller than 20m, and some images of a band of panchromatic spot which give details to give details smaller than 10m lengths.

- SRTM images (Shuttle Radar Topography Mission) are produced in 2003 and give details until 90m lengths; these images were used to make DEM, contour and relief map, in addition, they can be used to extract drainage networks.

- ASTRA images (Advanced Spaceborne Thermal Emission and Reflection Radiometer) produced by NASA in 2005 giving details until 15 m lengths; they were used to make also DEM with more details than SRTM.

- Quick Bird images (2.5m) of Google earth which were used to show the effect of flash floods in the study area.

- METEOSAT images were used to see the evolution of rain storms by sequential images. they show the rain storm movement every half hour during the flash flood in Southern Sinai at 17.11.1996.

5.4. Climatic and hydrologic data

There are 6 meteorological stations in and around the study area. Their climatic data recorded until 2004 were used. During the record periods, there is a lack at the time of wars which has been explained in chapter three. The climatic data are considered the main data to study rainfall and runoff estimation in the study area depending on the maximum rainfall in one day.

Additionally, there are used reports about flash floods in Sinai, documented by climatological and hydrological studies.

6. The main tools

6.1. Laboratory analysis

- The laboratory analysis of 26 samples was carried out after field work to determine the grain size of samples (physical analysis), and to determine the salt ratios of the samples (chemical analysis). OSL dating was made in a laboratory in Denmark for 7 samples of Wadi Moreikh to determine sedimentation an palaeoclimatic conditions.

- The second laboratory activties of the present study was scanning, digitizing, and stereoscopy of some air photos of the study area. In addition, new available programs and techniques were used.

6.2. Programs used

Several programs were used to analyze the data of the study area. These programs are related to GIS, remote sensing, statistical analysis, and painting programs. I have developed myself some GIS and remote sensing programs because I have bee fittd by some courses in GIS labor of Mainz University. I used the programs classified as followings:

6.2.1. GIS and remote sensing programs, there are several programs had been used with adding some modifications and skills to favour layout they are ARC view (3.2- 3.3), ARC GIS (9- 9.1- 9.2), ERDAS IMAGINE (8.7- 9- 9.1), ENVI 4.3, LANDSERVE 2.2, and AUTO CAD 14.

6.2.2. Statistical and paint programs such as SPSS (13-15), Excel 2003, paint shop, Photo shop, and Surfer 8, whereas, the full text of the thesis is typed using Microsoft office (2003- 2007).

7. Structure of thesis

The present thesis contains introduction and five chapters as followings:

Chapter one points out the physical settings of the study area. It shows the geological settings such as outcrop lithology and deposits. In addition, it manifests the climate conditions such as temperature, humidity, wind, and evaporation. Besides, it describes the soils and natural vegetation.

Chapter two points out the morphometric analysis of the main basins and their drainage network in the study area. It was divided into main three main parts; the first part manifests the morphometric analysis of the drainage networks which had been extracted from two main sources, topographic maps and DEM images. The second part of this chapter shows the morphometric analysis of basins such as area, dimensions, shape, and surface. Whereas, the third part points out the morphometric analysis of alluvial fans which form main part of El-Qaá plain.

Chapter three manifests the surface runoff through rainfall and losses analysis. The main part in this chapter is deicated to rainfall which was studied in detail; it is considered

as the main reason of runoff. While the second part of this chapter concernes with water losses estimation such as evaporation and infiltration which have direct influence on the runoff. Finally, chapter three points out all factors influencing desert runoff and runoff generation mechanism.

Chapter four concernes with assessment of flood hazard, it is important to estimate runoff and to determine affected areas. Therefore, the chapter consists of four main parts; the first part manifests the runoff estimation, the different methods to estimate runoff and its variables such as runoff coefficient lag time, time of concentration, runoff volume, and frequency analysis of flash flood. While the second part points out the extreme event analysis. The third part shows the map of affected areas for every basin and the flash flood degrees. Finally, part four points out the risk zone map of total study area.

Chapter five as the last chapter concernes with flash flood hazard mitigation, it consists of three main parts. First part is flood prediction and the method which can be used to predict and forecast the flood. The second part aims to determine the best methods which can be helpful to mitigate flood hazard in the arid zone and in the study area, whereas, the third part points out the development perspective for the study area.

Chapter one: Physical sittings

1.1. Geological setting

El-Qaà plain area is considered as one of the complex areas in geological settings, located at the old Archean Triangle which is composed by igneous, metamorphic and sedimentary rocks. The igneous and volcanic rocks cover nearly 2629.21 km² at about 43.3 % of the study area, where the metamorphic rocks cover about 179.41 km², which is nearly 3% of total area and the sedimentary rocks expand on the surface for 791.49 km² at about 12.9%. But recent deposits cover 2468.49 km² nearly at 40.8%; they are distributed on deltas and alluvial fans, terraces, Wadis deposits and sabkhas.

The study area has been included in some studies by previous work. Precambrian was presented by BARRON, (1907), SAID, and SHUKRI, (1955). , EL-SHAZLY and ABDEL-HADY, (1974), and STERN and MATON, (1987). They described in detail these geological formations and their distribution in the study area. Whereas the early descriptive work concerning the stratigraphy and sedimentology of Gulf of Suez region was done by HUME et al. (1921), MOON and SADEK (1921), and SAID (1962, 1992). Authors gave details about geology of Gulf of Suez and Sinai region.

Additional structure studies were presented by ROBSON (1971), MOUSTAFA, (1976), GARFUNKEL and BARTOV (1977), PATTON (1982), MOSTAFA, A., R., (1992) and JACKSON et al. (2006). They investigated main structure features such as faults and folds in the area of study. Only few studies focused the stratigraphy and sedimentology of the study area e.g. GARFUNKEL and BARTOV (1977), ISSAWI et al. (1988), NOWEIR and EL-SHISHTAWY (1996). The deposits studies were presented by Rögner et al (2002) had made dating for lacustrine deposits in Wadi Firan channel, and Grunert, J., Völkel, Leopold and Sherief, Y. (2008) had also made OSL dating for alluvial deposits of Wadi Moreikh.

The geological settings can be subdivided into thee distinctive units:

1.1.1. Outcrop lithology.

1.1.2. The structure.

1.1.3. The stratigraphy.

1.1.1. Outcrop lithology of El-Qaà plain area consist of four main kinds of rocks and deposits, igneous and volcanic rocks, metamorphic rocks, sedimentary rocks and old, recent and sabkha deposits.

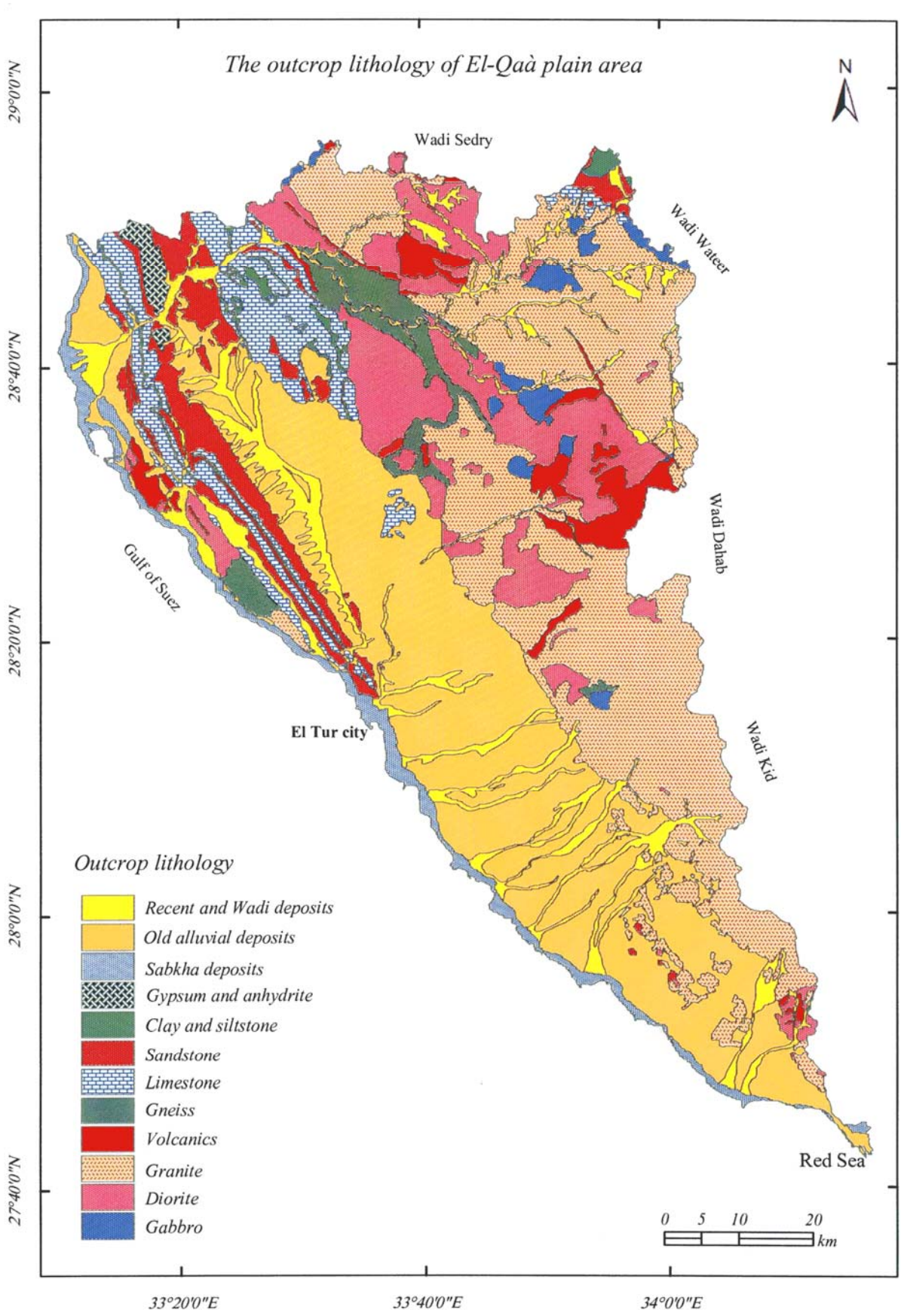

Fig (1-1) ***the outcrop lithology of El-Qaà plain area,*** *the source: Geological map of Sinai, A.R.E., (sheet No. 1) scale 1: 250 000, 1994, Geological map of Egypt –digital- scale 1: 250 000, 2003, modified by the researcher.*

1.1.1.1. The igneous rocks

This kind of rocks is distributed in the southern and eastern part of the study area, covered 2629.21 km² for about 43.3% of total area. It can be divided into:

1.1.1.1.1. Diorite rocks, Diorites usually occur as small isolated masses of different composition that crop out sporadically over the study area (EL-MASRY et al. 1992). These rocks consist of coarse to medium – grained quartz diorite and hornblende – biotite granodiorite, partly schlieric, foliated and commonly xenolithic (GEOLOGICAL SURVEY OF EGYPT, 1994). It covers nearly 691.22 km² at about 11.4% distributed in Serbal and Moeen mountains and in the east of El-Aàwag and Wadi Habran basins, (Photo 1-1) and (Fig. 1-1).

Photo (1-1) diorite rocks in Wadi Habran basin

1.1.1.1.2. Granite rocks, these are comprising from coarse to medium-grained alkaline granite ± riebekite and monzogranite locally megacrystic and foliated, covered of about 1626.52 km² nearly 26.8% of the study area. The distribution and areal extent of granite rocks in the study area is shown in (Fig. 1-1). They are distributed in southern and eastern of El- Qaa plain area in Wadi El-Aat El gahrby basin, Wadi Egshy basin, Wadi El-Tàalby basin (photo 1-2), Wadi Maier basin and Wadi Firan basin.

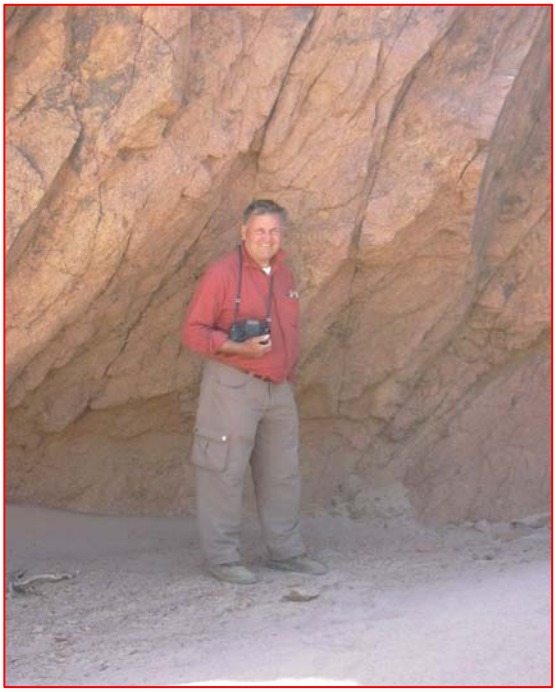

Photo (1-2) Granite rocks in Wadi El-Táalby

1.1.1.1.3. Metagabbro rocks, which contain coarse to medium grained metgabbro, variably deformed, locally banded, hornblende and olivinebearing, covered about 88.86 km² for about 1.5% of total area and distributed in Wadi El-Achdar basin, Wadi Solav basin and Wadi Shadq basin (Fig. 1-1).

1.1.1.1.4. Volcanic rocks, these rocks cover about 221.61 km² for about 3.6% of total area, allocated in St. Catherine area in Wadi Firan basin, Qabeliat Mountain, El-Banat Mountain and Wadi Emlaha basin (Fig. 1-1). These rocks contain a metamorphosed pyroclastic volcaniclastic group: tuffs, agglomerate, tuffaceous laminates, turbidites, conglomerates, but also and greywacke. The other group is formed by metamorphosed acid volcanics: rhyolite, dacite and quartz porphyry (GEOLOGICAL SURVEY OF EGYPT, 1994).

1.1.1.2. Metamorphic rocks

the metamorphic rocks in the plain area consist of Firan Sulaf Gneiss rocks, coarse to medium – grained banded hornblende – biotite gneiss, porphyroblastic and mylonitic in part, with interbanded migmatite amphibolite and metabasite dykes (photo 1-3). These rocks cover about 179.41 km² for about 3% and are surrounding the middle part of Wadi Firan (Fig. 1-1).

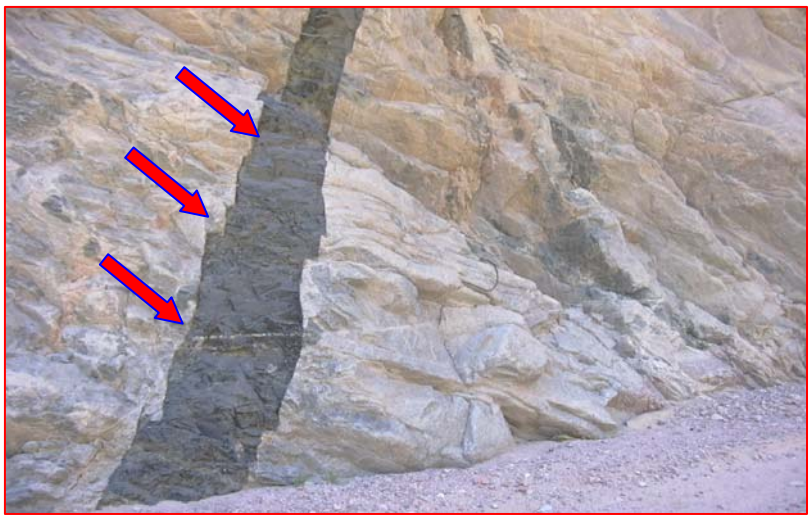

Photo (1-3) dyke from gneiss rocks in the north side of Wadi Mair

1.1.1.3. Sedimentary rocks

The most prominent sedimentary rocks in the study area comprise limestone, sandstone, siltstone and gypsum.

1.1.1.3.1. Limestone consists of Wata formation, Sudr formation, Thebes's formation, Darat formation and Samalot formation. Limestone in the study area is usually thinly layered (0.5 – 2.0 m thick) and in some places contains fragments of fossils including gastropods, echinoderms and foraminifers; these were probably deposited in a low energy environment with normal marine salinities (NOWEIR and EL-SHISHTAWY, 1996). The distribution and area of extend of the limestone in the study area is shown in (Fig. 1-1) in Qabaliat Mountain in the middle part of Wadi Firan basin in Abu Turayfiyah Mountain.

1.1.1.3.2. Sandstone the main component of this kind of rocks is Araba formation which consists of the Nubian sandstone. This is considered to be one of the largest sandstone bodies on earth, rocks of which consist mainly of varicolored sandstones of white, yellow, red, brown and gray colors. The Nubian sandstone attains a vertical thickness of about 120 m in the study area. Recently, some geologists divided the Nubian section into the Araba, the Naqus and the Malha formations (e.g. ISSAWI and JUX, 1982). It covers nearly 286.34 km² for about 4.3% and is exposed on the surface in the study area in Wadi Firan basin, Qabaliat Mountain and the lower part of Wadi Abu Khshaib basin and Wadi Um Markha basin (Fig. 1-1).

1.1.1.3.3. Siltstone (Matulla formation) is composed mainly of brown to reddish siltstone, shale, sandy shale, sandstone and less abundantly limestone and dolomite. This suite of rocks was deposited during a time of fluctuating sea-level on a low energy shelf environment (NOWEIR and EL-SHISHTAWY, 1996). These rocks cover approximately 63.81 km² for about 1% of the total area and appear on the surface in Qabaliat Mountain and the lower part of Wadi Firan basin (Fig. 1-1).

1.1.1.3.4. Gypsum and anhydrite rocks in the study area are named the Sudr formation which consists of mainly gypsum, anhydrite with interbeds of marl, and of white chalk a bout 40 m thick, chalky porcelanite and calcareous and siliceous shale. The base of the unit is easily recognized in the field by the presence of the white chalk, but the chalky porcelanite is white to light brown and hard. These lithologies were deposited in deep, marine water environments. Microfossils are sometimes recognized in these lithologies and from the calcareous and siliceous shales (Noweir and El-Shishtawy, 1996). These rocks cover nearly 37.55 km² of about 0.6% from the study area and are located in north and south of the main stream of Wadi Firan (Fig. 1-1).

1.1.1.4. Alluvial deposits

Alluvial deposits are widely distributed and represent, therefore, an important outcrop lithology in the study area, extending nearly 2389.45 km^2 that is 39.59 % of the study area. Due to important of the alluvial deposits which build up El-Qaá plain, they should be studied in details such as distribution, mechanical and chemical analysis and OSL dating. It is necessary to know the deposition conditions and the paleoclimate evoluation study area ranging between arid and semiarid conditions.

1.1.1.4.1. Distribution of deposits

1.1.1.4.1.1. Old alluvial deposits are considered to be one of the largest deposits in south Sinai, extending in nearly 1850.09 km² for about 30.6% of the study area. They are composed by several old alluvial fans of Wadi Habran, Wadi Maier, Wadi El-Mahash, Wadi Asla, (photo1-4) and other wadis fans covering most of El-Qaá plain (Fig 1-1).

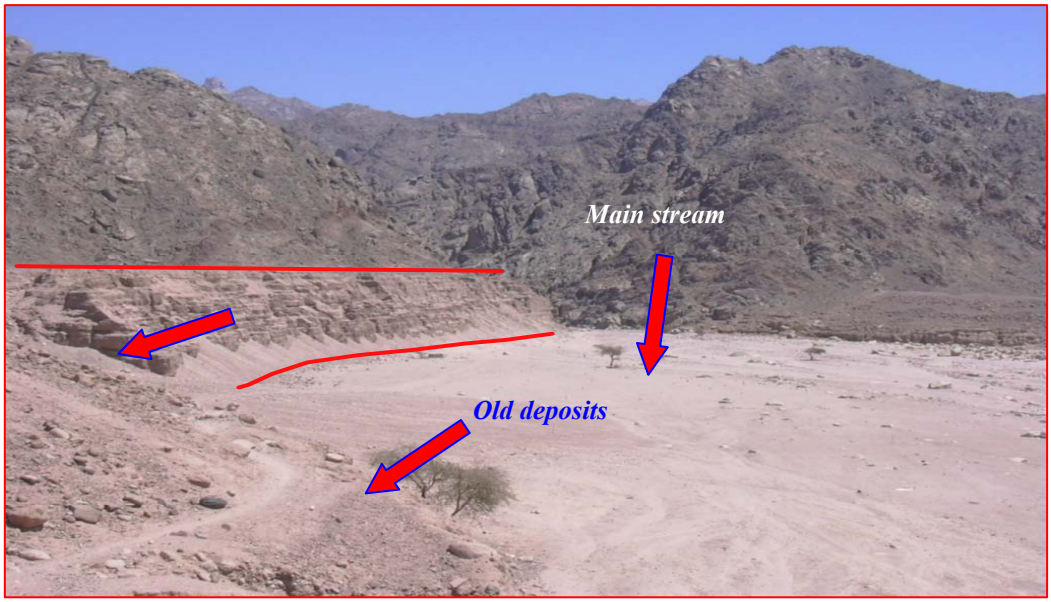

Photo (1-4) the old alluvial fan of Wadi Asla- southern Sinai

The field observations reveal that the alluvial fans sediments are mostly composed of coarse material such as boulders and gravels which become significantly smaller in size as we move away from the fan axis. Big boulders are observed along the fans of the relatively large Wadis which drain solid crystalline basement rocks such as Wadi Maier and Wadi Shadq; in addition boulders are of lower size extend along the fans situated in the eastern side of Qabaliat Mountain. They may be related to the watershed areas in sedimentary rocks.

1.1.1.4.1.2. Wadi deposits are distributed in Wadi floors such as Wadi Firan, Wadi El-Aàwag and other Wadis (Fig. 1-1). These deposits are covering about 543.36 km² of nearly 8.9% of the total area. Most of these deposits consist of gravels and soft material; however, they differ from one Wadi to another depending of the source of these deposits, the slope angle, and the extent of basin and wideness of Wadis. Wadi Maier for example drains from basement area and its average of wideness is 50 m. Here, most of deposits are boulders and gravel (photo 1-5). On the other hand most of the deposits in Wadi El-Aàwag which has a typical wide floor and slow slope. Draining mostly from sedimentary area consist of soft material, few gravel and small boulders (photo 1-6).

Photo (1-5) the deposits in Wadi Maier floor

Photo (1-6) the deposits in Wadi El-Aàwag floor

1.1.1.4.2. Grain size and chemical analysis

The present study gives a view about the grain size distribution in the study area and traces the depositional conditions. Spot samples were taken from several locations in El-Qaá plain. Tab (1-1) shows about 26 samples taken for mechanical and chemical analysis. 7 samples were taken for OSL dating.

Tab. (1-1)*: distribution number of deposit samples and type of analysis in basin areas.*

Basin	No.	Type of analysis
Aat El-Gharby	2	Grain size and chemical analysis
Amlaha	1	Grain size and chemical analysis
Amlaq	1	Grain size and chemical analysis
Asla	11	Grain size and chemical analysis
El-Aawag	6	Grain size and chemical analysis
El-Taalby	2	Grain size and chemical analysis
Meiar	3	Grain size and chemical analysis
Moreikh	7	OSL dating

The samples were taken during two periods of field work; 9 samples for grain size analysis were taken during the first field trip in November 2004, 17 samples were taken during the second field trip between Feb. 26th and March 2nd 2007. All samples were analyzed in the Geolabor of the Geographical Institute of Mainz University, whereas 7 samples for OSL dating taken during the second field trip and were dated in a special laboraroy of Aarhus University, Denmark.

Tab. (1-2) grain size and chemical analysis of 26 deposit samples of El-Qaá plain area

S	area	T	fU	mU	gU	ffS	fS	mS	gS	pH	$CaCO_3$	EC
		%	%	%	%	%	%	%	%	$CaCl_2$	%	MS
1	**El-Taalby**	1.48	0.07	0.39	1.48	1.90	2.02	21.62	71.04	7.22	2.75	164.1
2	**El-Taalby**	2.35	0.78	1.49	5.71	7.35	4.81	26.77	50.3	7.78	3.76	107.2
3	**Aat El-Gh1**	2.56	0.48	0.33	4.09	13.03	14.89	31.10	33.53	7.75	12.71	400
4	**Aat El-Gh2**	2.60	0.40	0.15	1.35	11.96	26.7	45.35	11.82	7.82	23.45	21
5	**Amlaha**	1.74	0.34	1.00	2.52	4.42	5.47	35.75	48.76	7.86	3.11	129
6	**Amlaq**	1.27	0.17	0.26	1.07	4.38	14.36	50.62	27.87	7.80	6.10	165.5
7	**Asla 1**	1.12	0.22	0.34	1.33	2.29	3.86	44.46	46.39	7.80	1.23	85
8	**Asla 2 del.**	6.55	1.38	1.11	2.45	20.10	21.01	26.90	20.50	8.08	15.50	216
9	**Asla 3 dune**	7.40	2.15	3.94	4.12	4.87	6.54	27.74	43.24	7.44	0.00	2032
10	**Asla 4**	3.24	0.87	0.87	1.54	4.20	7.05	33.86	48.35	7.64	0.00	797.0
11	**Asla 5**	2.05	0.75	0.88	0.00	2.12	4.15	27.85	62.20	7.57	0.00	86.0
12	**Asla 6**	3.45	0.91	0.81	3.66	5.35	7.53	37.20	41.09	7.67	0.00	162.3
13	**Asla 7**	2.32	0.88	0.70	3.85	6.14	5.32	28.68	52.13	7.81	2.21	145.2
14	**Asla 8**	2.26	0.48	0.26	1.26	10.94	27.37	42.49	14.94	7.85	6.35	118.9
15	**Asla 9 bed**	1.96	0.59	0.51	2.27	4.09	6.17	38.46	45.96	7.89	2.12	83.8
16	**Asla 10 bed**	2.67	0.29	0.29	1.91	4.61	5.85	46.07	38.31	7.94	2.24	85.0
17	**Asla11dune**	1.98	0.24	0.10	1.55	1.74	3.04	58.60	32.75	7.91	1.12	98.0
18	**El-Aawag1**	5.68	1.38	5.61	36.34	23.38	15.83	9.67	2.10	8.13	19.48	3587
19	**El-Aawag2**	43.02	17.43	14.71	15.07	7.52	0.87	0.85	0.53	7.85	29.52	4503
20	**El-Aawag3**	3.40	0.75	0.43	1.07	2.61	5.38	57.93	28.43	7.93	9.77	1062
21	**El-Aawag4**	56.23	26.86	13.56	1.81	1.18	0.15	0.17	0.03	7.65	40.87	1628
22	**El-Aawag5**	3.55	1.27	0.63	0.80	4.39	11.19	51.03	27.15	7.89	11.41	1365
23	**El-Aawag6**	5.87	1.56	1.06	1.47	4.92	5.17	55.69	24.26	8.19	5.84	3403
24	**Meiar 1**	1.36	0.23	0.17	1.30	4.43	6.46	31.51	54.54	7.79	1.92	135.3
25	**Meiar2 rez.**	2.63	0.12	1.17	0.88	2.42	2.95	30.45	59.40	7.55	1.53	83.0
26	**Meiar 3 ter.**	17.69	4.83	8.46	43.23	15.32	3.45	4.34	2.67	7.36	0.00	705.0

- Source: the samples were analyzed in the Geolabor of the Geographical Institute of Mainz University.

Each sediment sample shows a range of sizes. This variant must be characterized statistically so that samples may be compared and interpreted. To achieve that goal, the data obtained from grain-size analysis are represented graphically by histograms (Fig 1-2) which show the variation among samples owing to the source of deposits and the flash flood activities in different basins.

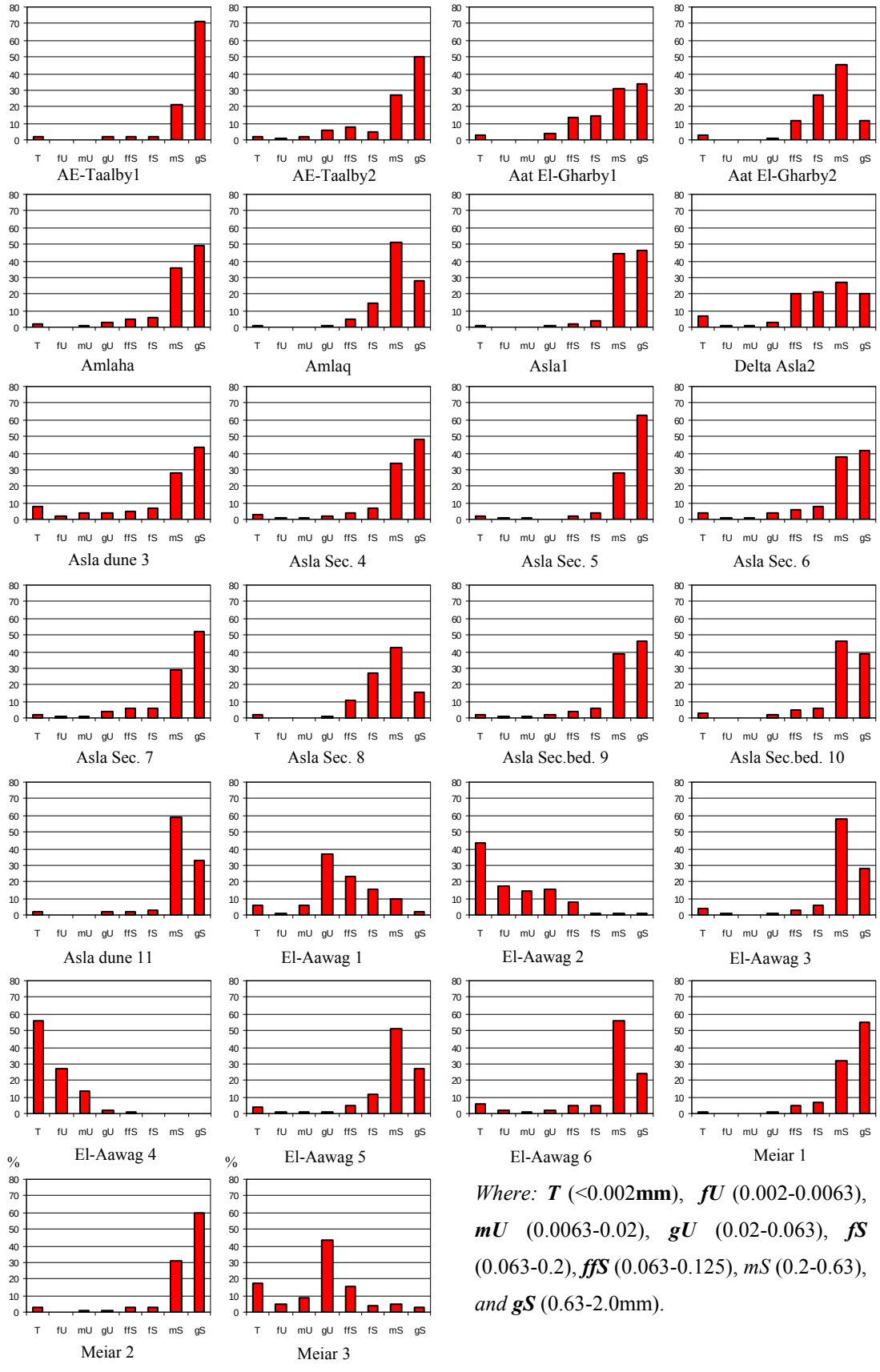

Fig (1-2) *grain size analysis of 26 deposits samples of El-Qaá plain area*

It can be said that the texture of deposits in the study area is coarse in most of the basins, but Wadi El-Aawag has different types of texture which relate to the position of sample such as coarse texture in El-Aawag terraces, medium texture in El-Aawag delta, and fine texture in wadi bottom. The constructed histograms (Fig 1-2) are unimodal having single maximum, and show that:

1- *Clay deposits* (< 0.002mm) ratios have more variations between the main basins of the study area, the clay ratio was found very low in the basins which drain from igneous and metamorphic rocks. The ratio of clay represent 1.12 % of total sample 1 of Wadi Asla, 1.27% in Wadi Amlaq, 1.48% in sample 1 of Wadi El-Taalby 1, and 1.36 in sample1 of Wadi Meiar. The clay ratios also vary between different samples in the same basin related to the local position of the samples. In Wadi Asla, the clay ratio range among 1.12% of total samples in Wadi bottom, 6.55% among the samples of terraces, and 7.40% of dune sand. In Wadi El-Aawag the clay ratio has a big variation which ranges between 3.40% to 56.23% of total sample while the clay ratio of Wadi Meiar ranges only between 1.36% to 17.69% of total sample.

2- *Silt deposits* (FU, mU, and gU 0.002- 0.063mm) in the study area have a low ratio. The total ratios of these categories have been recorded as low ratios in basins such as Wadi El-Taalby 4.9%, Wadi Aat El-Gharby 3.4%, and Wadi Asla 3.54%, whereas the average of silt ratios of all samples in Wadi Meiar, and Wadi El-Aawag have represented about 20.1%, and 23.6% respectively.

3-*Sand deposits* (ffS, fS and gS 0.063- 2.0mm) represent the predominate ratios of weight samples in the study area. Sand deposits form about 93% of Wadi El-Taalby samples, 94% of Wadi Amlaq samples, 92% of Wadi Asla samples, 56.7% of Wadi El-Aawag samples, and 72.6% of Wadi Meiar samples. Consequently, it can be concluded that the deposits of the study area consist of mostly coarse deposits which may have been keeped a big amount of paleoflood water resulting in big ground water storage.

4- Tab (1-2) shows also that the samples have about equal ratios of pH ranging between 7.22% in Wadi El-Taalby to 8.13% in Wadi El-Aawag; the ratios of Calcium Carbonate $CaCO_3$ vary among 0.0% of some samples in Wadi Asla and Wadi Meiar to 23.45 % in the samples2 of Wadi Aat El-Gharby, and reach to 40.87% in the samples 4 of Wadi El-Aawag.

1.1.1.4.3. Deposits dating

Several geosientists have studied the thick fossile deposits in Wadi Firan. The sedimentological, geochemical and geomorphological results are published in: (RÖGNER and SMYKATZ-KLOSS 1991a, b, 1993, 1998; EL SHERBINI 1993; SMYKATZ-KLOSS et al. 1997, 1998, 1999/2000, 2000; RÖGNER et al. 1999, KNABE 2000; NAGUIB 2000, and RÖGNER et al 2004). Two different methods of dating were applied: Thermoluminescence (TL) by RÖGNER et al 2004 and OSL by GRUNERT, VÖLKEL, LEOPOLD, and SHERIEF 2007. The results are as following:

1.1.1.4.3.1. Thermo-luminescence (TL) dates

RÖGNER, et al 2004 had used the Quaternary TL Surveys in Bonn University which was set up in 1993 as an independent commercial laboratory providing thermoluminescence (TL) date measurement services to archaeologists and geologists. The well- bedded silts of Wadi Firan (photo 1-7) and its tributaries (central Sinai, Egypt) are up to 50m heigh. Despite they have been the subject of several geoscientific studies their formation and origin is still under discussion (i.e. lacustrine? fluvial? fluvial- aeolian? true loess? river terraces?).

RÖGNER, ET AL 2004 concluded that the layered silts of Wadi Firan and moreover, the wadis of the central Sinai are alluvial loesses. They contain Miocene foraminifera, which originate from the center of the Ataqua anticline in the Gulf of Suez, where loose Miocene globigerina marls formed outcrops at the surface 20-27 ka ago. From there, aeolian processes transported the loess eastwards during the global ice-periods and the consequent sea-level decrease until the loess was sedimented on the slopes of the wadis (Firan, El-Sheikh, and Solav).

Photo (1-7) *the alluvial loess deposition in the main channel of Wadi Firan.*

After the l.g.m. - period, especially at the beginning of Holocene, when the climate changed to more humidity, rain washed out the fine-grained aeolian material and transported it towards the main stream of the wadi where it was deposited in ponds, oxbow-lakes and swamps aside the river. During river floods the suspended fine-grained, silty material passed over the banks of the meandering river ("overbank-fines") and sedimented on the flat areas behind the levees. Ten TL data range between 27 and 11 ka, thus indicating that the alluvial loess deposition of central Sinai took place during the Late Glacial (RÖGNER, ET AL 2004).

1.1.1.4.3.2. OSL dates

OSL is a trapped charge dating method based on the time-dependent accumulation of electrons and holes in the crystal lattice of certain common silicate minerals. When a mineral is formed, all its electrons are in a ground state. Naturally occurring radioactive minerals emit rays which ionize atoms, causing negatively charged electrons to be transferred from the atoms in a valence band to a conduction band. After a short time most electrons recombine with the positively charged holes which remain near the valence band. However, all natural minerals contain defect sites such as lattice defects, at which electrons and holes can be trapped. Some of the traps are light sensitive. In OSL dating, trapped electrons are activated by light exposure, which causes most of them to recombine with the holes (KOUKI, P., 2006 after GRÜN, 2001).

In practize sampling is complicated. Try to avoid sediments that show any post-depositional disturbances such as root penetration, krotovinia (bioturbation), carbonates, ground-water leaching, certain soil formations or large stones that may hamper sampling. If the only exposure that is available is one in which cracks, roots or krotovina may be encountered at depth, or the sediment is so hard that it will be difficult to remove a tube driven in at depth, and then take a cube block sample at the site. Mark the sample as to the side exposed to the surface. Wrap it in aluminum foil, a black bag (several layers if being shipped) and tape tightly to prevent disintegration *http://crustal.usgs.gov/laboratories/luminescence_dating/section4.html.*

7 Samples for OSL analysis were taken by J. VÖLKE and M. LEOPOLD during the second field trip in February 2007. Six of them were taken from one place which is pointed in fig (1-3) and one sample (7) was taken from other place beside the previous position. All samples were analyzed by Andrew Murray in Nordic Laboratory for Luminescence Dating, Department of Earth Sciences, University of Aarhus, Roskilde Denmark.

Fig (1-3) *position of OSL dating (A and B) and vertical section for the three main units of OSL samples*

GRUNERT, VÖLKEL, LEOPOLD, and SHERIEF interpreted the OSL dates in fig (1-3) and concluded as follows:

On top of Unit 3 a desert pavement isremarkably well developed. As the rock fragments of the pavement are partly big (> 30 cm) the surface must have existed some time affected by flashfloods or even debris flows. This gives a first morphological indication on the age of the section which can't be young.

Unit 3 consists of layers which frequently change between coarser and finer material. The sediments are less $CaCO_3$ cemented compared to those of unit 1 and 2. The coarse sediments, which can be as thick as 30 cm, consist of angular and partly rounded fragments up to a maximum of 5 cm in length and are mixed with sands. The fine sediment bands, which have a thickness up to 10 cm, consist of sand and silt. The clasts are horizontally orientated and give, therefore, indication of constant fluvial activity during sedimentation.

Unit 2 consists of rather fine, mainly silty to sandy sediments. No fragments larger than 2 mm were found. Silty layers up to 30 cm thick are divided by sandy layers up to 10 cm in thickness. The sediments are party cemented and they remind of aeolian sediments which, in a second phase, have been transported by fluvial processes. Such sediments have been described by Rögner et al. (2004) in the Wadi Firan 100 km north of wadi Moreikh. The sediments of unit 2 differ drastically from those of unit 1a and 1b. As both types of sediments can be found in the alluvial fan at the wadi outlet, we interpret the differences in the sediment types primarily as changes in the processes of sediment production and not necessarily in a change of water availability.

Unit 1b consists like 1a of angular clasts but of minor size which are partly orientated. The amount of sand and silt increases more and more towards the top of Unit 1b and the sediments are $CaCO_3$ cemented. The layering is horizontal to sub-horizontal. Frequently, layers of pure sand and silt over- or underlay the typical coarser deposits. The direction of the layering is along the valley which partly can be followed over hundreds of meters. Again the transportation distance of these sediments must have been short due to the angular shape of the rocks. Compared to unit 1a the size and number of the clasts as well as the increase of finer material indicate either a change in the amount of water or a change in the geomorphologic process which provided the sediments.

Unit 1a consists of angular not well orientated clasts up to 20 cm in diameter and sands. Silt and clay are a minority group. The cemented sediments are well layered. The

layers are 5 to 25 cm thick and get partly replaced by pure coarse sand bands. The oblique layers have different angles and directions.

We interpret unit 1a as sediment which has been transported only a short distance. The sediments of unit 1a are similar to debris flow sediments but they are clearly orientated along the gorge and show no genetic connection to the valley sides.

During the accumulation phase of unit 1a either the production of sediments (angular clasts) was very high and/or the amount of water in the wadi system during the several flood events was rather low. Based on the observation of grain size, round boulders degree and dating analysis of deposits in Wadi Firan and Wadi Moreikh, it can be conclouded that the study area was influenced during the Pleistocene by aemiarid periods.

1.1.1.5. Sabkha deposits

Sabkha is an Arabic word for salt pan which has become entangled with playa. Sabkhat is the correct plural, despite the prevalent use of sabkhas (NEAL, 1975). Originally the term was applied to both coastal and inland saline depressions in North Africa and the Middle East, such as the salt – encrusted, supratidal flats of Abu Dhabi, along the Persian Gulf (CHRISTIAN et al. 1957; SHEARMAN, 1966), but NEAL (1975) describes a sabkha as a geomorphic surface the level of which is dictated by the water table (PETER, 2000). Sabkha sediments are dominated usually by carbonates, evaporates, fluviatile, aeolian and marine debris and are sometimes cemented with carbonate or gypsum (COOKE et. al 1993).

Alluvial deposits

The distribution and areal extent of the sabkhas in El-Qaá plain area is shown in (Fig. 1-1). They cover nearly 75.04 km² for about 1.3% of the study area along the Gulf of Suez (photo 1-8).

Photo (1-8) Sabkha deposits in El-Qaá plain along the Gulf of Suez

1. 1.2. Structure of the study area

The structure geology of the area under study is dominated by high- angle normal faults (Fig. 1-4). Most faults are curved in plain (sinuous) or have zigzag shape delimiting many blocks which are usually tilted (Fig. 1-6). Folds are of minor importance in deforming the area except for the regional Hadahid monocline, described by MOUSTAFA (1992), which occupies the western side of the area (Fig. 1-6). This monoclinal fold was first described by Patton (1982).

1.1.2.1. Faults

Faulting is more predominant than folding in El-Qaá plain area. Faults in the eastern part of El-Qaá plain have a predominant NNE-SSW orientation whereas those in El-Qaá plain and the western part of it have a predominant NW-SE orientation (Fig. 1-5). El-Qaá plain area has been affected in a complicated way by different type of faults, mainly normal, although some have subordinate oblique-slip components and few are strike-slipped. The faults the faults of the area belong to tow main sets which are oriented NW (N35˚W), and NNE.

Tow major oblique-slip normally are bounding the area:

First, the Precambrian-phanerozoic fault which exists on the eastern most side of the mapped area (Fig. 1-6). This fault was called the "G. El-Tur Fault" by MOUSTAFA (1992). It is the longest fault in the area and extends for more than 30 km.

The fault has a zigzag shape with two NS oriented segments connected by a tow of NW-NNW oriented fault segments. It is a high-angel oblique-slip normal fault with a dip up to 75˚ and horizontal slip component. Its dip slip component has throw ranges from 400-500m (NOWEIR and EL-SHISHTAWY, 1996).

The second major normal fault exists on the western side of the area and extends for 20 km, but in some places is hidden beneath the alluvium deposits of El-Qaá plain. This fault includes two main segments. The longest one has a NW orientation, whereas a short one has a NS orientation (Fig. 1-6). This fault is called herein "Hadahid Fault". In addition to the two major faults, a number of main faults are recognized and mapped in the area. These faults have different trends; they include: NW, NNW, NE, NNE, EW and NS directions. The EW set characterizes generally the strike slip faults (Fig. 1-5).

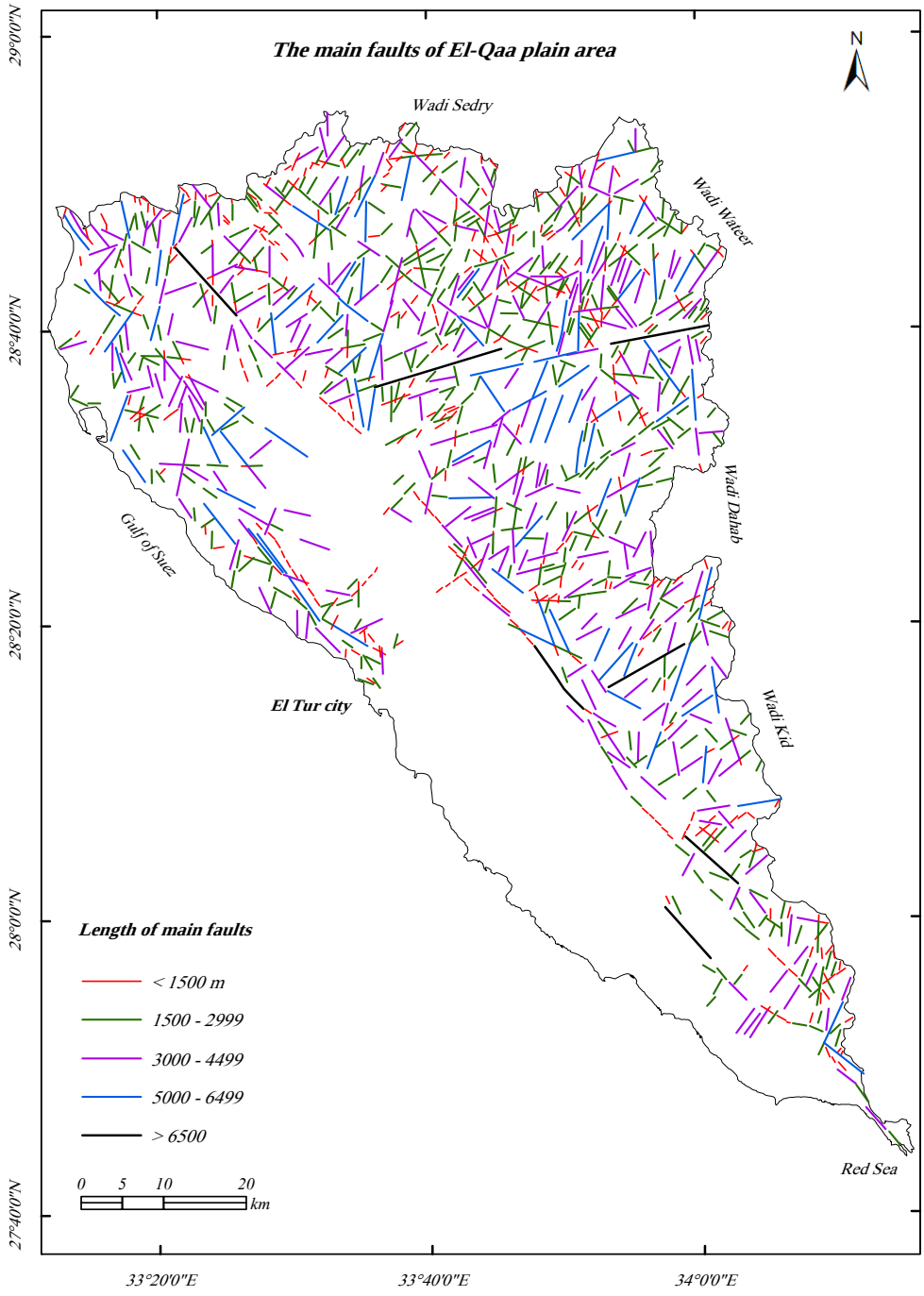

Fig (1-4) ***the main faults in El-Qaá plain area***, *data source: Conoco coral, geological map of Egypt scale 1:500 000, 1987, sheet Quseir and south Sinai, modified by the researcher from ETM Satellite images 2001.*

The structure study over a distance of about 30 Km in the eastern part of the NW-trending zone, east of El-Qaá plain, indicates that the main structural features affecting the area are faulting and tilted blocks. The dominant trend of the faults is NW-SE, which corresponds with the average regional trend of the structures throughout the region. These faults slice the rocks into a series of tilted blocks. The blocks dip westward, towards the Suez rift, and are generally bounded by synthetic normal faults.

Therefore, the NW strike-slip faults are considered being the main faults in the eastern area of El-Qaá plain, which trend in NNE between 10˚ and 40˚ (Fig. 1-4 and 1-5), but the NE strike-slip faults are the main faults in El-Qaá plain respectively.

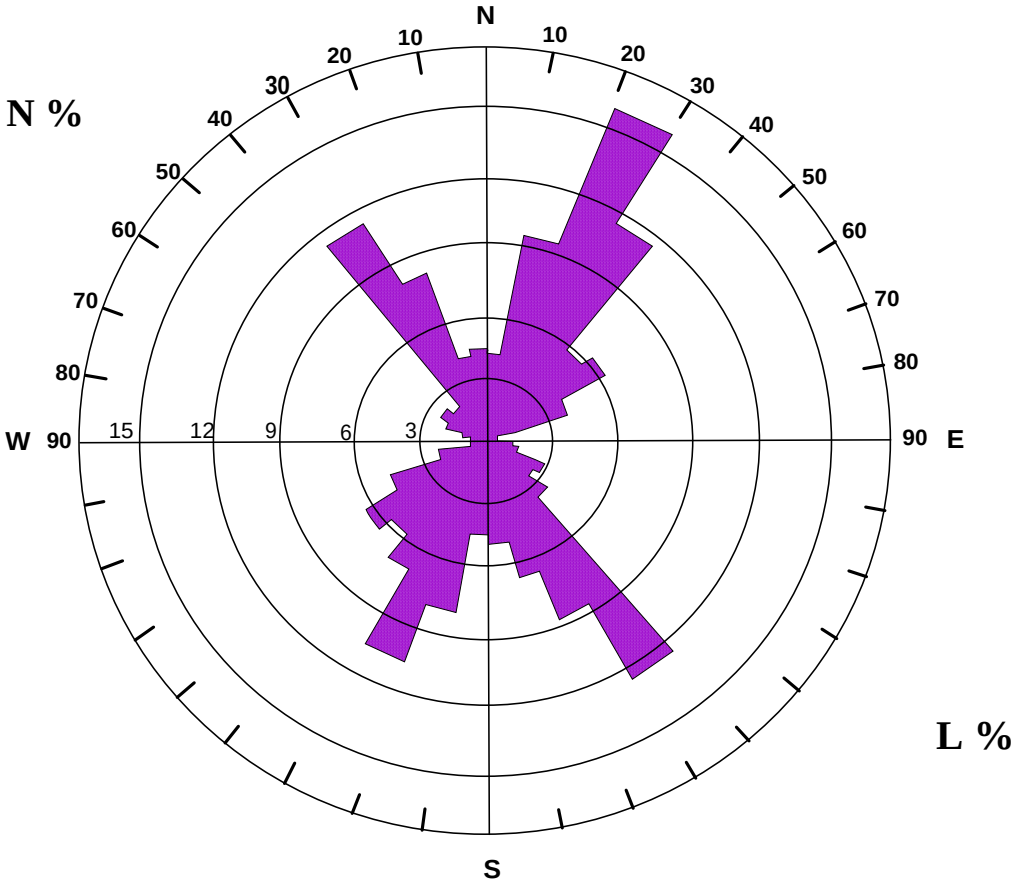

Fig (1-5) ***Rose diagram of the main faults detected in El-Qaá plain area***, *the upper half shows the number of faults in percent while the lower half shows their equivalent length in percent*

1.1.2.2. Folds

Folding is of secondary importance than faulting and plays a minor role in the structural setting of the area. Folds are represented by the southwest facing Hadahid monocline which occupies the western part and extends parallel to the western boundary of the study area. The monocline has a gentle to steep dip towards the W and SW ranging from 10-15˚ up to 75-80˚ in some places (photo 1-9).

PATTON (1982) modeled the deformation that led to the development of Hadahid Monocline. He indicated that the steep flank of this monocline was formed by draping (STREAMS, 1971) of the ductile Upper Cretaceous and the competent Eocene rocks over a fault cutting the underlying brittle Precambrian basement and pre-Cenomanian sandstones (MOUSTAFA and EL-RAEY, 1993).

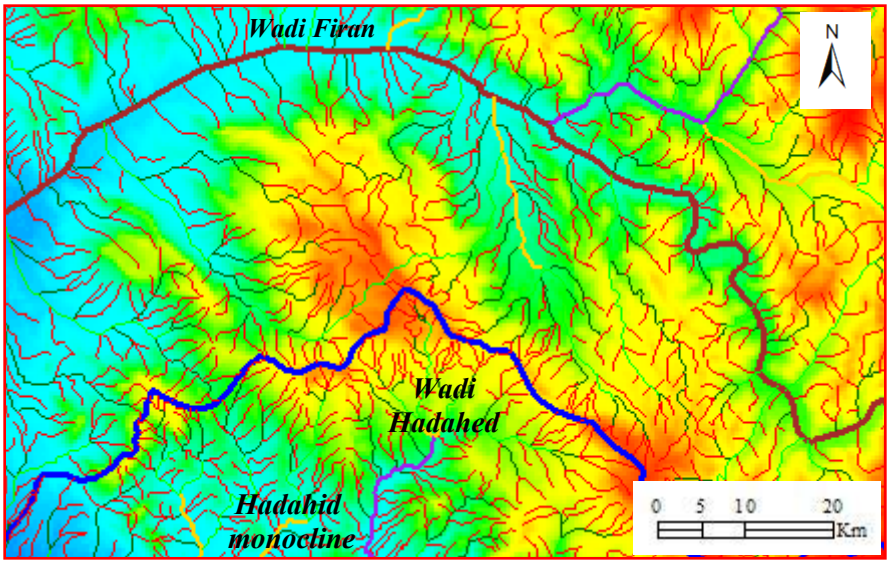

Photo (1-9) Hadahid monocline south of the main stream of Wadi Firan

There are many synclines which are mapped in the area under (Fig. 1-6); the longest one exists in the southeastern part of the area. This fold is divided into two synclines. They are called "Gebaah Syncline" and "Tar Syncline" with syncline axis parallel to the NS segment of the Precambrian fault. Another plunging syncline, located around Wadi Araba, is called "Araba syncline" by GARFUNKEL and BARTOV (1977).

The core is covered by Miocene rocks forming a north-plunging syncline. The syncline axis is roughly parallel to the main strike of the major Precambrian-Phanerozoic fault. The fold axes are trending NW, NNW and NS. The difference in trend of the three fold axes could be due to different stresses at different times.

1.1.2.2.1. Structural setting

The regional structure of the area is represented by one major tilted block bounded by two major faults. This block is called the "Firan block". It is located between the topographically low land of El-Qaá plain to the west and the structurally high mountains in basement rocks of the Sinai massif to the east (NOWEIR and EL-SHISHTAWY, 1996). Based on this regional structure setup, -NW-SE elongated blocks can be recognized in the area (Fig. 1-6). They are:

1- El-Qaá block, which occupies the western part of the area. It is covered by Quaternary deposits that form together with the underlying Oligocene-Miocene rocks the Hadahid monocline.

2- The Firan block. This major tilted block is arbitrarily divided into three smaller sub-blocks which dominate the area. These are the western, central and eastern sub-blocks.

3- The rift which is occupied by the Precambrian rocks of Sinai massif and occurs in easternmost side of the mapped area (Fig. 1-6).

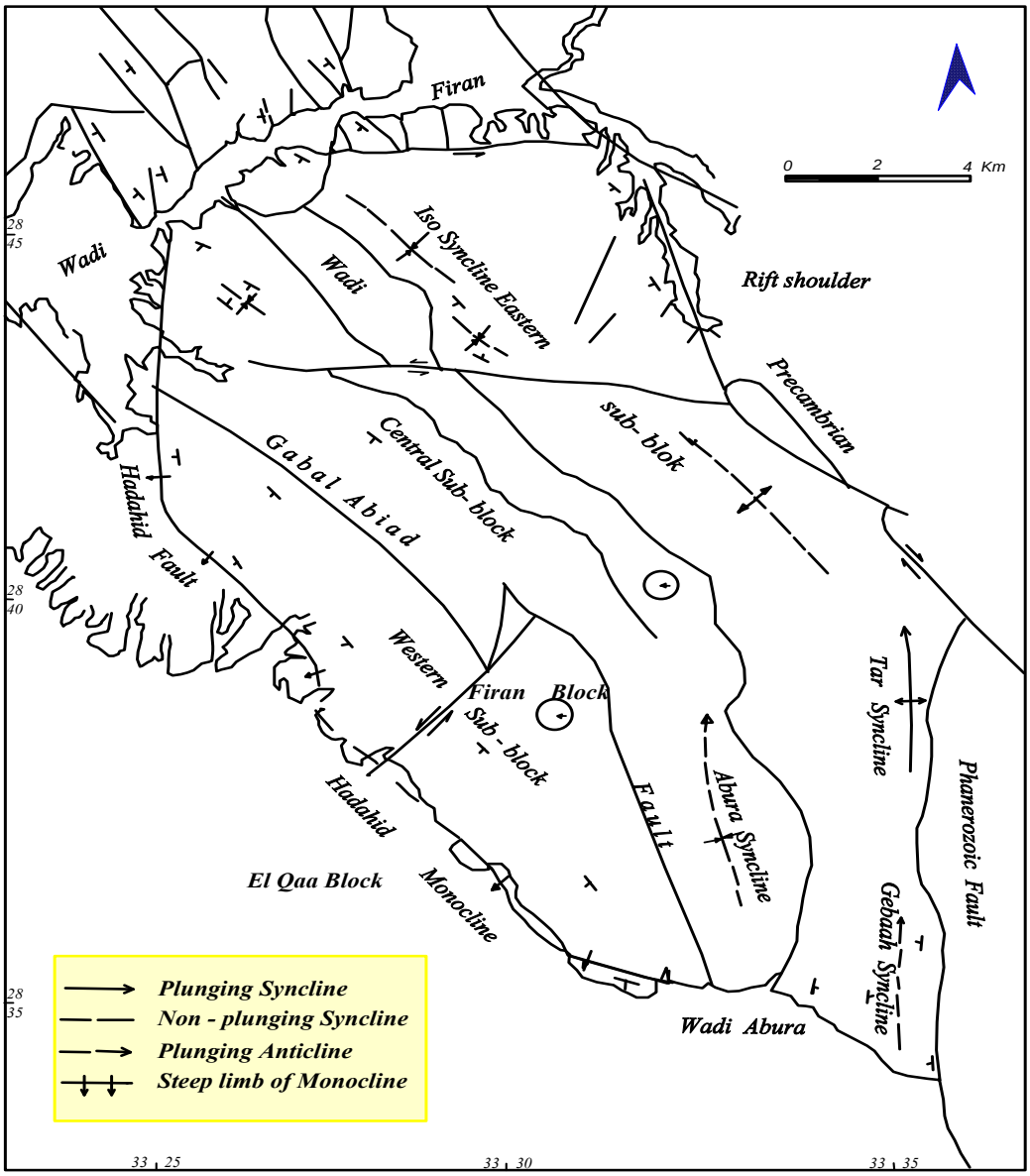

Fig (1-6) ***the different blocks and sub-blocks and the structural features in the study area,*** *after Noweir and El-Shishtawy, 1996*

1.1.3. Stratigraphy of El-Qaá plain

El-Qaá plain is covered by a Cambrian- to Miocene- age sedimentary sequence (Fig. 1-1). Precambrian basement rocks surround the area from the east and northeast. A composite stratigraphic succession of the area is shown in (Fig. 1-7).

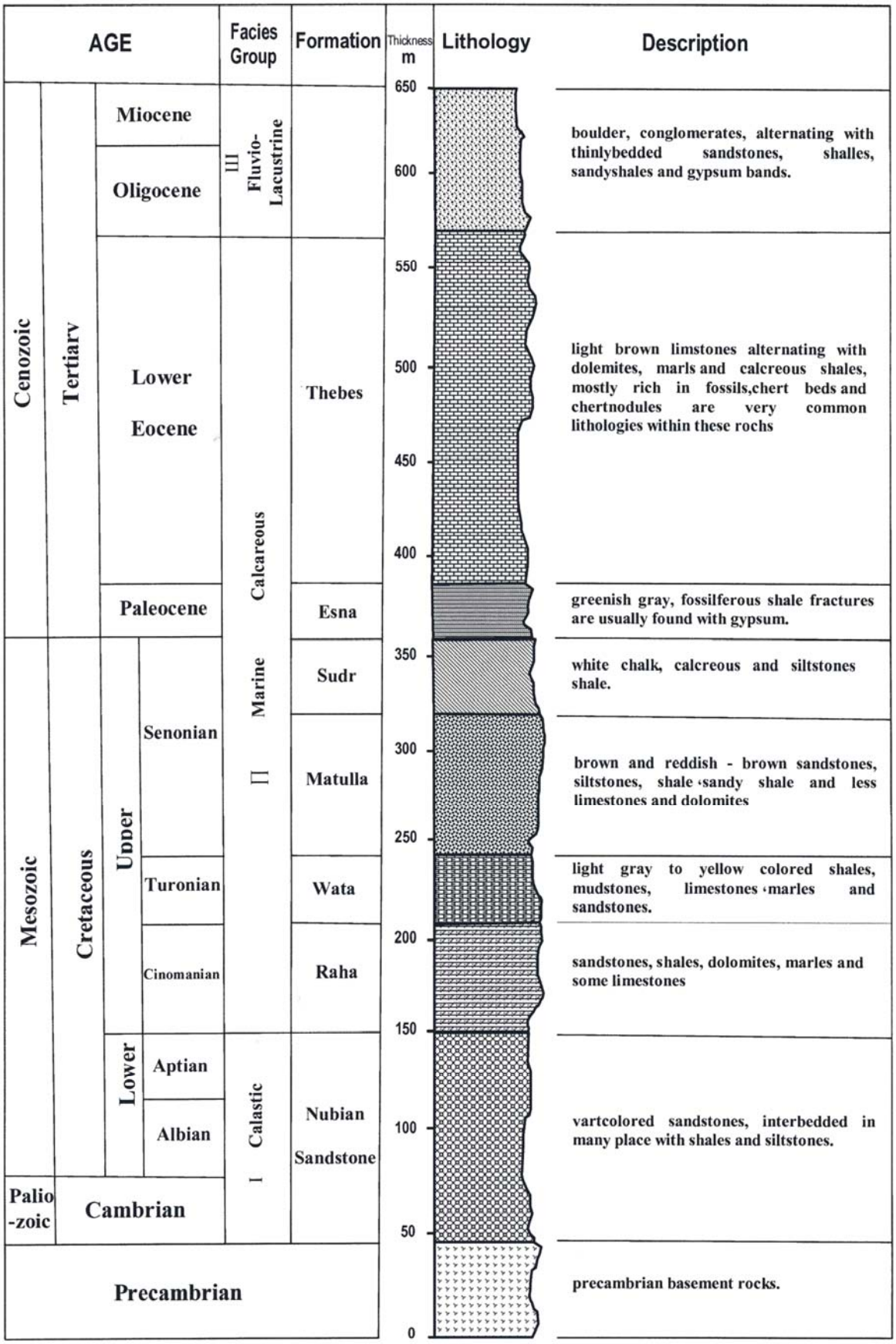

Fig (1-7) ***Stratigraphy and facies characteristics of El-Qaá plain*** *modified after NOWEIR and EL-SHISHTAWY 1996.*

Three characteristic facies groups can be recognized in this area:

A lower group of clastic sedimentary rocks of Cambrian to Early Cretaceous age; a middle group o marine, predominantly calcareous facies of Cenomanian to Middle Eocene age and an upper fluvio-lacustrine clastic facies of Oligocene to Miocene age (NOWEIR and EL-SHISHTAWY, 1996).

1.1.3.1. The lower clastic group

The main component of this group is the Nubian Sanstone formation which is considered to be one of the largest sandstone bodies on the earth, in regard to both time and space. The rocks of this formation rest unconformably on Precambrian basement rocks. These rocks are well-stratified in some places and characterized by the presence of cross-bedding structures. The sandstones are in many places interbedded with shales and siltstones. Nubian Sandstone sequences of Early Cambrian to Early Cretaceous age are locally present in this area. The Nubian Sandstone Formation attains a vertical thickness of about 120 m in the study area (Fig. 1-7). Recently, some studies divided the Nubia section into the Araba, the Naqus and the Malha Formation (ISSAWI and JUX, 1982).

1.1.3.2. The middle marine, calcareous facies

The main components of this group comprise Cenomanian to L. Eocene age rocks of the Raha, Wata, Matulla, Sudr, Esna and Thebes Formations. The U. Cretaceous rocks (Raha, Wata, Matulla, and Sudr formations) have a total thickness of about 220m in the study area (Fig. 1-7).

1.1.3.2.1. The Raha formation consists mainly of sandstones, shales, dolomites, marls and some limestone intercalcations (KASSAB and OBAIDALLA, 2001). The rocks of this group are easily distinguished from the underlying Nubia sandstone formation by the distinct changes in lithology. The sandstone of Raha formation is fine-to medium-grained and is usually cemented by calcite and/or dolomite cement. The thickness of the Raha Formation is about 60m in the study area.

1.1.3.2.2. The Wata Formation (Turonian age) consists of light gray to yellow colored shales, mudstones, limestones, marls and sandstones. The formation overlies the shales and limestones of the Raha Formation and its base is recognized by the appearance of oyster shales and muddy- limestone with oyster banks. The Wata formation attains a thickness of about 40m in the study area (Fig. 1-7).

1.1.3.2.3. The Matulla Formation (GHORAB 1961), type section of Wadi Matulla (west-central Sinai) is composed mainly of brown to reddish- brown sandstones, siltstones, shales, sandy shales and less abundantly limestones and dolomites. This suite of rocks was deposited during a time of fluctuating sea-level on a low energy shelf environment (BAUR, et. al 2001). The dolomites are dark grey and characterize the base of unit. The formation attains a thickness of about 80m (Fig. 1-7).

1.1.3.2.4. The Sudr Formation (Campanian- Maastrichtian) consists of 40m thick sequence of white chalk (Fig. 1-7), chalky porcelanite and calcareous and siliceous shale. The overlying formation is the brown to dark gray shale of Esna Formation. The chalk of the Sudr Formation is white in color and moderately hard. The chalky porcelanite is white to light brown and hard. These lithologies were deposited in deep, marine- water environments (NOWEIR and EL-SHISHTAWY, 1996).

1.1.3.2.5. The Esna Formation (Paleocene age) consists mainly of shale which is moderately fissile and fractured. This formation overlies the Sudr Formation and is characterized by its greenish grey color and the presence of gypsum bands. The overlying formation (Thebes Formation) is recognized by the change in lithology to the limestones with nodular and bedded cherts of light brown color. The Esna Formation has a thickness of about 30m in the study area (Fig. 1-7).

1.1.3.2.6. The Thebes Formation (L. Eocene age) is light brown in color and consists of alternating beds of limestones, dolomites, marls and calcareous shales. The Eocene rocks in this area are overlying grey shale with thin limestone and chalk interbeds of the Esna Formation and underlying limestone, shale, marl, gypsum, chalk and conglomerate of Oligocene- Miocene age (NOWEIR and EL-SHISHTAWY, 1996). The thickness of the Thebes Formation ranges from 150-200m in the study area (Fig. 1-7).

1.1.3.3. The upper fluvio - lacustrine clastic facies

The upper fluvio- lacustrine clastic facies comprises rocks of Oligocene- Miocene age. The thickness of the sequence is highly variable and ranges from 20-80m (Fig. 1-7). The base of the sequence is marked by the presence of a boulder conglomerate ranging in size from 2-50cm. The boulders are mostly found in a matrix of silt to coarse-grained sand. Thinly- bedded sandstones and limstones are in some cases present intercalated with the conglomerates (NOWEIR and EL-SHISHTAWY, 1996).

1.2. Climatic conditions

The climatic conditions of the Sinai Peninsula are similar to those, which characterize desert areas in other parts of the world. They include extreme aridity, long hot and rainless summer months and a mild winter. During the winter months some areas of Sinai experience brief but intensity of rainfall that makes Wadi beds overflow and sometimes cause severe flash floods which damage the roadways and, sometimes, human lives (JICA, 1999).

The climate of any particular place is influenced by several interacting factors. These include latitude, elevation, nearby water, topography, vegetation, and prevailing winds. In the present study, the climatic conditions of El-Qaá plain area are discussed in the light of available records. There are six meteorological stations in Southern Sinai including Sharm El-Sheikh, El- Tor, Abou Rudeis, Ras Sudr, St. Catherine and Nekhel. No regular records are available from the majority of these stations. They were stopped after the 1967 war and renewed after 1982 (Tab. 1-3).

Tab (1-3) *lat, long, elevation and record period of meteorological stations in the study area*

Station	*Latitude N.*	*Longitude E.*	*Elevation(m)*	*Record period*
Ras Sudr	29˚ 46	32˚ 42	15.67	1976 -2005
Abu Rudeis	28˚ 33	33˚ 12	6.27	1961 - 67, 1976 - 2005
Nekhel	29˚ 55	33˚ 44	460	1963 - 67, 1980 - 2005
St. Catherine	28˚ 21	34˚ 04	1350	1934 - 37, 1979 - 2005
El- Tur	28˚ 14	33˚ 37	2.7	1961 -67, 1984 -2005
Sharm El-Sheikh	27˚ 58	34˚ 33	36.5	1982 - 2005

The climate settings are known in El-Qaá plain area from studying the following climate elements:

1.2.1. Temperature

It is recognized that the monthly mean and annually temperature don't directly influence geomorphological processes, because the effect of temperature with regard variability between maximum and minimum values which are important to know. It may play a main role in isolation weathering which involves the idea that rocks and minerals are ruptured as the result of large diurnal and/or seasonal temperature changes, and steep temperature gradients from the surface into the rock. Such changes are said to cause tensions, expansion and contraction of rocks and minerals, depending on coefficients of thermal expansion and other properties of the affected material that can lead to fracture (GOUDIE, 1993).

Tab (1-4) *monthly means values of daily maximum and minimum temperature at meteorological stations (˚C)*

Station		Jan.	Feb.	Mar.	Apr.	Mai.	Jun.	Jul.	Aug.	Sep.	Oct.	Nov.	Dec.	Aver.
Ras Sudr	*Max.*	19.3	20.3	22.9	27.1	31.2	34.2	35.5	34.5	32.3	29	21.3	20.6	**27.4**
	Min.	8.4	9.4	10.7	14.2	17.4	20.3	22.0	22.5	19.8	17.5	13.4	9.6	**15.4**
Abu rudeis	*Max.*	19.5	21.0	23.4	27.9	30.8	32.5	32.9	32.3	31.3	28.7	24.6	21.2	**27.2**
	Min.	9.8	9.1	12.9	16.9	20.3	21.1	24.7	25.3	24.0	20.2	15.1	11.1	**17.5**
Nekhel	*Max.*	17.7	19.2	22.4	27.4	30.6	34.4	35.4	35.3	31.8	29.2	23.6	19.5	**27.2**
	Min.	0.7	1.8	4.6	8.1	11.1	13.5	15.1	16.0	14.6	12.2	5.5	9.0	**8.7**
ST. Catherine	*Max.*	14.4	15.1	18.7	23.8	27.9	31.0	32.1	33.1	33.6	25.8	19.3	16.8	**24.3**
	Min.	0.5	0.9	5.0	8.4	12.1	14.7	16.0	16.1	14.7	10.7	5.8	1.8	**8.9**
EL-Tur	*Max.*	21.2	21.7	24.2	27.1	30.7	33.5	34.6	34.8	32.6	29.6	26.6	22.5	**28.3**
	Min.	9.9	10.9	13.6	16.8	19.6	22.8	23.2	24.3	23.1	19.0	14.7	11.5	**17.5**
Sh. El-Sheikh	*Max.*	22.0	23.3	25.3	29.2	33.5	36.8	37.2	35.2	31.1	27.8	27.8	22.8	**30.1**
	Min.	13.3	14.0	16.2	19.7	23.8	26.2	27.3	27.8	26.4	22.9	18.2	14.7	**20.9**

- *Source: the Egyptian meteorological authority from 1934 to 2002*

A study of the temperature data reveals the following general characteristics:

1- The change from the Mediterranean depressions of the winter to the Khamasin[1] depressions of spring causes a rather sudden rise in temperature.

2- The great change from the summertime regime to the winter regime, often occurring in late October, induces a very drastic alteration in monthly mean temperature, maxima, minima, and means (SOLIMAN, 1972).

The spatial change of minimum and maximum temperature in El-Qaá plain area depends on the latitude and altitude. The study area has a long summer, from April to October; and a short winter from January to March, separated by a transitional period (November-December).

It can be observed from monthly mean values of daily maximum and minimum temperature at study stations in (Tab.1-4) and (Fig 1-8) that:

- July is considered having the highest temperature during the year, while the daily mean temperature has recorded for about 37.2˚C at Sharm El-Sheikh, 35.5˚C at Ras Sudr, 35.4˚C at Nekhel and 32.9˚C in Abu Rudeis. August has the highest temperature during the year at El-Tur with average 34.8˚C, and September has the highest temperature at St. Catherine whereas the temperature reaches 33.6˚C.

[1] *The winds which originated in the Libyan-Egyptian desert in North Africa are a seasonal pattern known as al-Khamasin. The Egyptian capital, Cairo and other parts of the country have been wrapped in the yellowish haze of dust since Sunday http://www.arabicnews.com/ansub/Daily/Day/980317/1998031712.html.*

- January has the lowest temperature at St. Catherine with mean value 0.5˚C, 0.7˚C at Nekhel, 8.4˚C at Ras Sudr and 9.9˚C at El-Tur, while the lowest mean of temperature in December is recorded at Nekhel with 0.9˚C and 1.8˚C at St. Catherine.

The range between maximum and minimum temperature at Nekhel and St. Catherine stations is the largest, and computed for about 18.5˚C and 16.4˚C respectively. This average affects during long time on geomorphological processes this favorers Insolation weathering and frost weathering in January and has therefore, a remarquable effect on geomorphological processes.

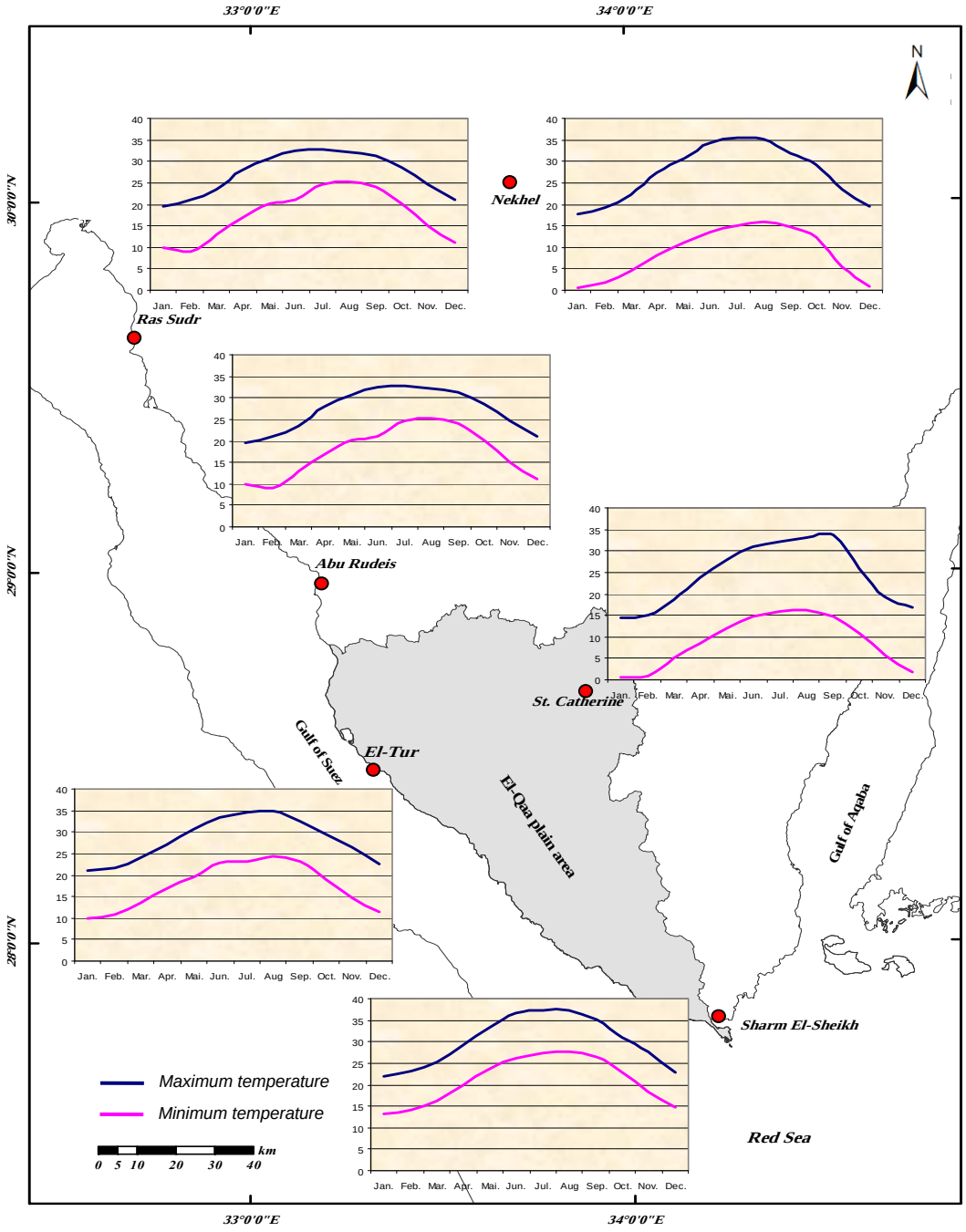

Fig (1-7) ***Monthly mean values of daily maximum and minimum temperature in the study area***

- it shows that the daily mean of maximum temperature increases in the inland areas toward the east because it is less affected by Suez Gulf, while the mean of maximum temperature at Nekhel reaches to 27.2˚C with differential range from 1˚C to 3˚C, while the mean of daily minimum temperature has decreased toward the east resulting of the affect of the Gulf of Suez (SALEM, 1993).

1.2.2. Evaporation

The Evaporation is considered being one of the most important elements of climate, which is focused from many sciences such as Hydrology, Botany, Geology, and Geomorphology especially in the arid zones.

Tab (1-5) Mean daily amount of evaporation of study stations (mm).

Station	Jan.	Feb.	Mar.	Apr.	Mai.	Jun.	Jul.	Aug.	Sep.	Oct.	Nov.	Dec.	Aver.
RasSudr	7.4	8.8	9.7	11.9	14.8	16.2	16	15.5	13.2	10.5	8	6.9	**11.6**
Abu Rudeis.	8	9	10.3	11.7	13.2	14.3	13.4	13	12	9.8	5.5	8.4	**11**
Nekhel	5.6	7.1	10.4	13.1	15.5	17.5	16.7	14.7	12.2	10.6	7.2	5.9	**11.4**
St. Catherine	5.7	6.9	9.1	13.4	15.6	18.2	16.6	15.9	13.4	10.7	6.9	6.2	**11.6**
El-Tur	7.2	8	9.5	11.1	12	12.5	12	11.9	11	8.2	7.5	7.3	**9.9**
Sh. El-Sheikh	11.1	13.2	14.7	17.6	21	26.8	25	22.6	21.1	16.4	13	11.7	**17.9**

- *Source: the Egyptian meteorological authority from 1934 to 2002*

To study evaporation in these areas is very important because it is mostly higher than precipitation; the values of evaporation depend on some factors such as temperature, relative humidity, wind speed, the cover of plant and solar radiation. So, the amount of evaporation is dependent upon the individual location.

Due to the values of mean daily evaporation (Tab.1-5) and (Fig 1-8) it can be concluded, that:

- The values of evaporation increase toward south Sinai Peninsula with regard to the continental effect, whereas the annually range of evaporation is measured at Ras Sudr for about 11.6 mm/day, 11 mm/day at Abu Rudeis, 9.9 mm/day at El-Tur and 17.9 mm/day at Sharm El-Sheikh. It is the result of the Gulf of Suez and wind speed in the study area (SALEM, 1993).

- The mean of evaporation in the high altitude area of St. Catherine area (2000-2650m) increase, whereas the annual range is recorded about 11.6 mm/day. The July is considered being the month with highest evaporation and lowest relative humidity, with regard to wind speed, especially of Al-khamasin wind (SOLIMAN, 1978).

- The lowest evaporation is recorded during the cool months with calm winds while it reaches less than 1 mm at 27-1-1987 (SALEM, 1993).

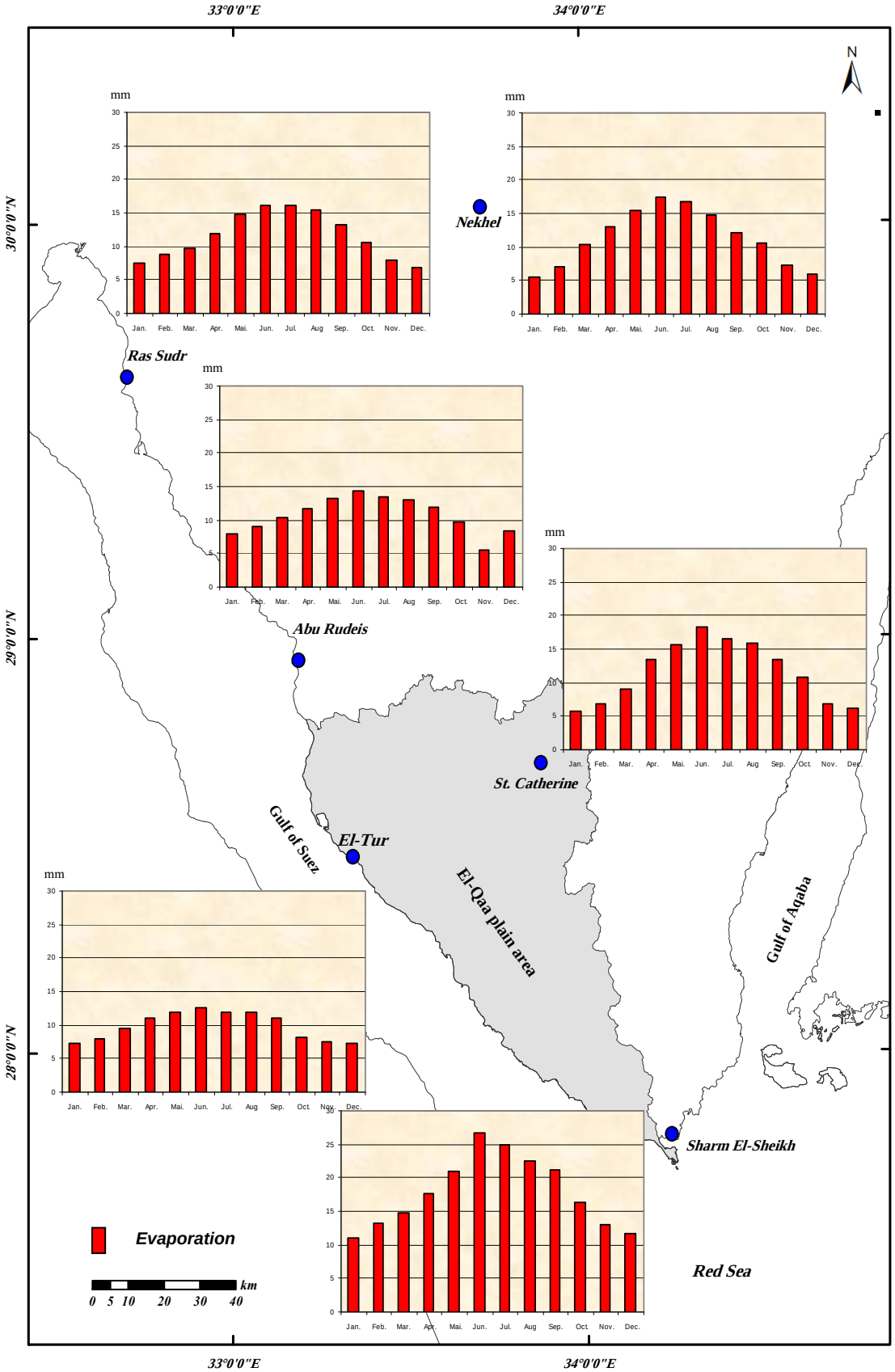

Fig (1-8) ***Monthly mean of daily evaporation in the study area (****mm/day****)***

1.2.3. Relative humidity

Relative humidity is the ratio of the real amount of water vapor in air to the maximum amount of water vapor that could be in the air if the vapor were at its saturation conditions. Often the concept of air holding water vapor is used in the description of relative humidity. Relative humidity is wholly understood in terms of the physical properties of water alone and therefore is unrelated to this concept.

$$RH = \frac{P\,(H_2O)}{P^*(H_2O)} \times 100\%$$

Where:

RH is the relative humidity of the gas mixture being considered.

P (H_2O) is the partial pressure of water vapor in the gas mixture.

P *(H_2O) is the saturated vapor pressure of water at the temperature of the gas mixture.

The relative humidity of a system is dependent not only on the temperature but also on the absolute pressure of the system of interest. Therefore, a change in relative humidity can be explained by a change in system temperature, a change in the absolute pressure of the system, or a change in both of these system properties (*http://en.wikipedia.org/wiki/Relative* humidity)

Anywhere, the air in the study area is considered arid when the relative humidity is less than 50%, semi arid when it ranges from 60% to 70% and humid when relative humidity rises up to 70%.

Tab (1-6) monthly means values of daily relative humidity of study stations.

Station	Jan.	Feb.	Mar.	Apr.	Mai.	Jun.	Jul.	Aug.	Sep.	Oct.	Nov.	Dec.	Aver.
Ras Sudr	59	56	59	54	52	53	55	57	61	63	61	60	58
Abu Rudeis.	55	52	51	49	50	55	58	60	62	62	58	58	56
Nekhel	62	56	51	44	44	41	46	50	59	61	61	59	53
St. Catherine	43	30	32	23	20	25	24	27	27	31	33	40	29
El-Tur	57	54	53	58	58	60	60	62	64	62	58	56	59
Sh. El-Sheikh	43	40	43	39	34	32	34	37	42	46	45	46	40

- Source: the Egyptian meteorological authority from 1934 to 2002

From the (Tab.1-6) and (Fig.1-9) we can see that:

- Relative humidity has increased at the coastal stations more than the inland stations such as Ras Sudr station 58%, Abu Rudeis 56% and El-Tur 59% especially in summer season due to the evaporation increasing. By contrast at inland stations it has decreased at Nekhel 53% and at St. Catherine 29% with regard to low temperature, high topographic position and stations far from the sea breeze.

- January is considered being the most humid month at inland station resulting by the effect of the cool and humid air which attends the Mediterranean depressions, but October is the most humid month at coastal stations such as Ras Sudr 63% and Abu Rudeis 62%. September has reached at El-Tur to 64%. These characters depend on; a high temperature which has affect directly the evaporation raise, sea breeze effect during this period and the role of temperature inversions which influence the evaporation in lower stratosphere (SALEM, 1993).

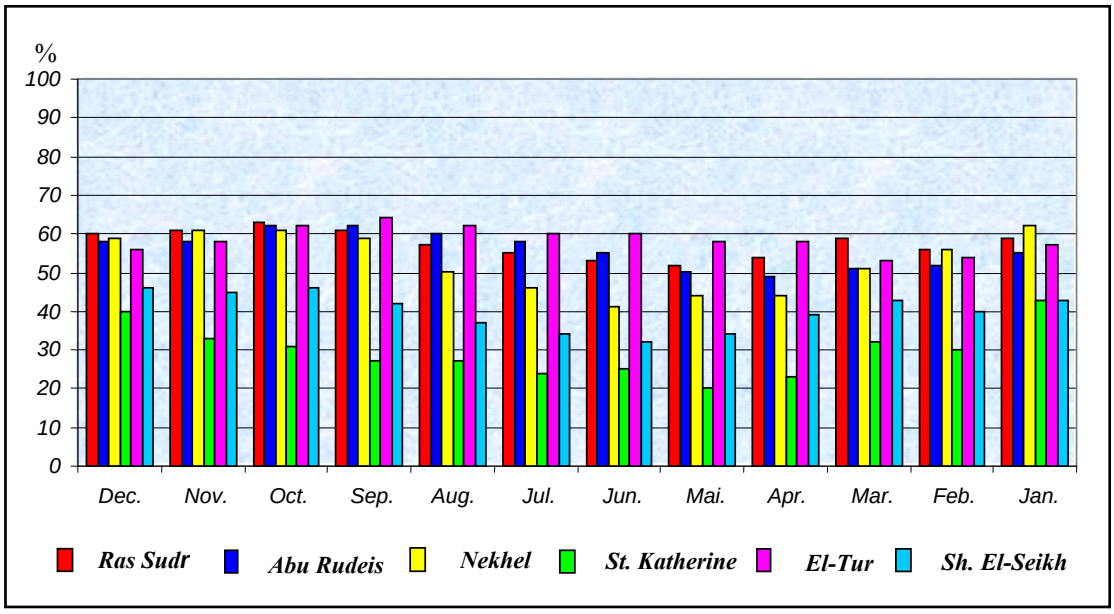

Fig (1-9) ***Monthly mean values of daily relative humidity of stations in the study area***

- Due to the very high rate of evaporation from the warm water of the Gulf of Suez and Red Sea, the area has the ability to be hot and moist. Along the coast, humidity is usually rather low than over the sea and generally increases from north to south. The Meteorological Reports reveals that in winter the humidity vibrates around 44%. The monthly mean values of humidity are around 50 % throughout the year for morning observations and some 5-10% higher in the afternoons.

1.2.4. Surface wind

Surface wind plays an important role for horizontal and vertical thermal exchange and dominates the most of climate elements such as evaporation, humidity and precipitation. On the other hand, wind speed is different from one area to another and from season to season depending on pressure distributions, topographic and local relief (SALEM, 1993).

In spite of the Mediterranean depressions which affect in winter Northern Egypt directly, causing variable surface winds, both in speed and direction, the study area is practically unaffected by these depressions and remains for most of the time, under the eastern flank of the sub-tropical high pressure gradient. Orographic effects in the southern Sinai may transform these winds into strong ones.

It has been noticed that the frequency of strong and gale winds decreases considerably in southern Sinai. Northeasterly winds become more frequent in the spring and autumn months along the Mediterranean coast line. This fact reveals that the eastern Mediterranean is becoming an area of relatively high pressure. In southern Sinai northerly winds prevail during this period; they are interrupted only temporarily by the passage of depressions. Autumn, especially October, is the time of lowest wind speed (SOLIMAN, 1972).

Tab (1-7) the percent of wind directions and calm periods in the study area

Station	N	NE	E	SE	S	SW	W	NW	Calm
Abu Rudeis	12.9	5	4.1	4.5	2.5	1.8	15.2	50.9	**3.1**
St. Catherine	2.6	6	3.2	9.1	12.2	32	20.6	8.3	**6.1**
El-Tur	12.3	11.4	2.6	2.9	2.8	3.6	27.2	37.1	**.1**
Sh. El-Sheikh	4.2	6.2	5.6	6.3	5	5.4	19.6	42.2	**5.5**

- Source: the Egyptian meteorological authority from 1934 to 1994 and http://www.windfinder.com from 4-2002 to 10-2006.

It can be shown from (Tab.1-7) and (Fig.1-10) that:

- Wind direction is predominantly from NW at Abu rudeis 50.9%, Sh. El-Sheikh 42.2% and El-Tur 37.1%, whereas the predominant direction at St. Catherine is SW with percent 32%, with regard to relief and topographic factors of this area; especially in winter December is considered being the month of highest wind activity 41% at St. Catherine area.

- The lowest percent of wind direction has been computed to 2.6% E, at El-Tur, to 2.6% N at St. Catherine, to 5% NE at Abu Rudeis and to 5% S at Sh. El-sheikh.

- The calm periods decrease in the area along Gulf of Suez reaching to 0.1% at El-Tur, 3.1 at Abu rudeis. The calm period is typical for December, while it is measured at Sharm El-Sheikh to 5.5%, and at St. Catherine to 6.1% due local relief and altitude which is over 2600m asl.

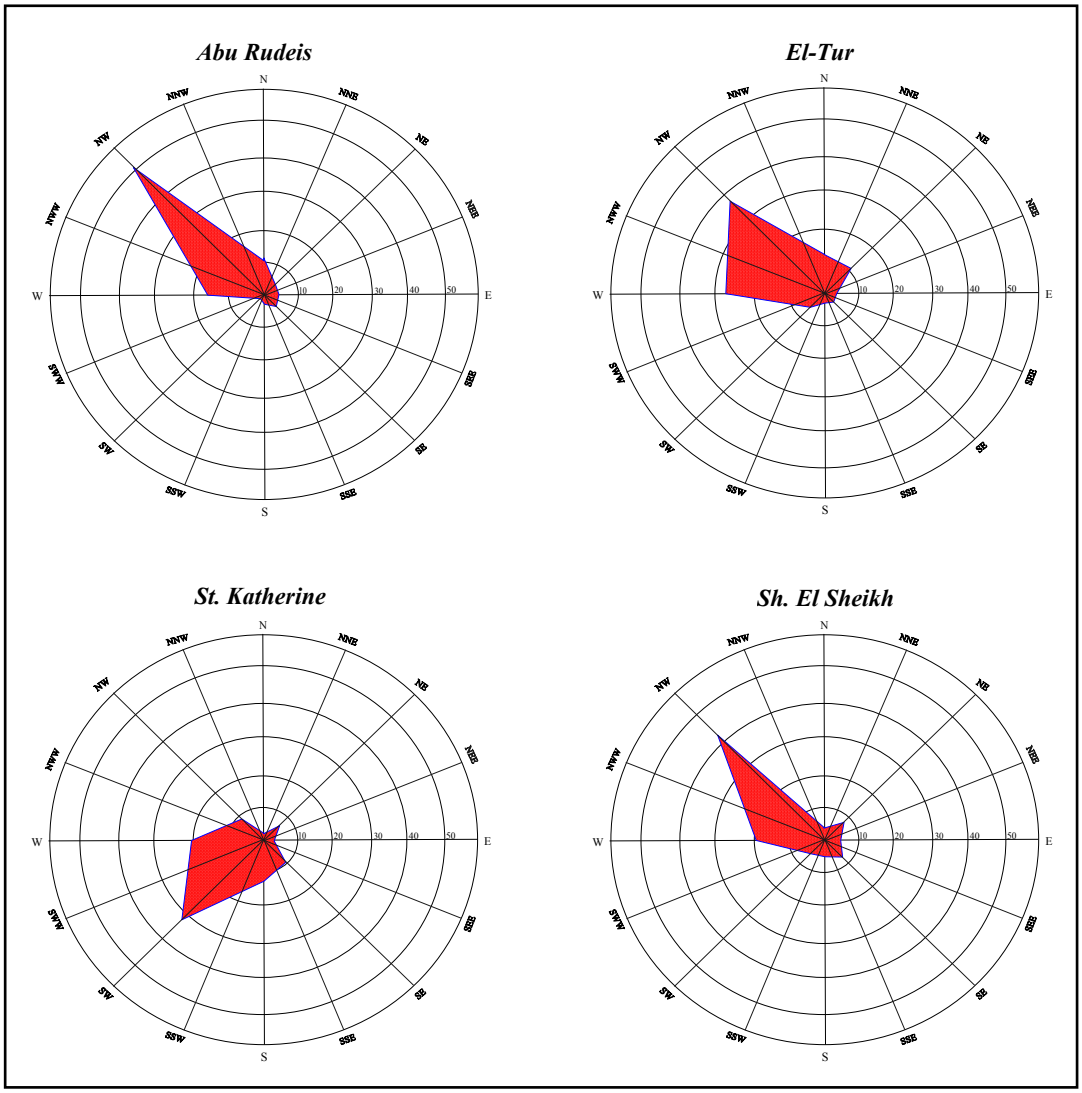

Fig (1-10) ***The percent of wind directions in the study area***

It is observed from (Tab.1-8) that the average wind speed is about 5-20 knot/h. Maximum speed has been recorded at El-Tor to 20 knot/h in June, 19 knot/h in August and September, but, at St. Catherine maximum speed has recorded in October and November to 18 knot/h. Relative high speed is reported in summer during June and July along Gulf of Suez at El-Tur and Abu Rudeis stations, while the minima speed has measured to 4 knot/h in February at Ras Sudr and St. Catherine stations.

Tab (1-8) monthly mean of wind speed in the study area (knot/h).

Station	Jan.	Feb.	Mar.	Apr.	Mai.	Jun.	Jul.	Aug.	Sep.	Oct.	Nov.	Dec.	Aver.
RasSudr	5	4	7	6	7	7	6	8	7	5	5	4	5
Abu Rudeis.	6	5	8	7	9	11	9	11	11	9	6	5	8
St. Catherine	7	4	6	9	9	11	11	11	7	18	18	12	10
El-Tur	13	14	17	16	18	20	18	19	19	16	14	13	16
Sh. El-Sheikh	9	10	13	12	13	14	12	14	15	11	11	9	11

- Source: the Egyptian meteorological authority from 1934 to 1994 and http://www.windfinder.com from 4.2002 to 10.2006.

1.2.5. Precipitation (Introduction)

Deserts occur mainly in areas associated with presence of high-pressure cells, where air is subsiding, the atmosphere remains relatively stable, and divergent air flows are predominant. This is typical for low altitudes such as El-Qaá plain area. Precipitations in these areas are also commonly associated with small, convective cells that can produce intense, short- duration storms. Thus, for example, winter rainfall in Sinai tends to be associated with convective cells formed in conditions of atmospheric instability at the front of a belt of low-pressure (YAIR and LAVEE 1985).

Usually the rain in deserts, as elsewhere, is variable in frequency, intensity, duration and spottiness, so that generalizations are difficult. Nevertheless, certain features of desert precipitation are important in the context of fluvial processes.

The spatial and temporal variability is not unique to deserts, but it is exceptionally important because it means that commonly only parts of drainage systems are affected by rainfall and activated by runoff at any time. Equally important, the location of runoff often varies from event to event. It can be noticed that the location of precipitation and runoff may be predictable where the cause is fixed: for example the escarpment at Taif (Saudi Arabia) provides a firm local topographic control of rain fall (GOUDIE, et al. 1993).

The study area is characterized by an arid (< 100 mm / year) to extremely arid climate with Mediterranean influences, and often receives less than 50 mm annually. The southern Sinai massif is receiving more an average of 65-100 mm but the precipitation comes almost exclusively in winter and may sometimes occur as snow on the high peaks. Flooding, resulting from convective rains has been observed during all seasons (DAMN, 1983). According to SALEM (1993) the mean annual rainfall ranges between 10.4 mm / year at El-Tur. 15.4 mm / year at Ras Sudr, 21.5 mm / year at Abu Rudeis, and 63 mm / year at St. Catherine, and these amounts indicate that the rain increases toward the east of the study area (St. Catherine).

The hydrographical basins of the study area have high surface water potentialities. This is due to the fact that the eastern branches of their steep sloping channels drain the highlands of south and central Sinai where high rates of rainfall prevail (SAAD et. al., 1980). However, chances for infiltration are limited due to the steep rocky slopes of their Wadis. The precipitations of the study area will be discussed later in more details (see chapter 3).

1.3. Soils and natural vegetation

1.3.1. Soils

El-Qaá plain constitutes of several geomorphologic units each of which is characterized by a particular assemblage of landforms and soils. This study area is a part of the Gulf of Suez rift zone covered with Quaternary alluvial Wadi deposits and underlain by Pliocene rocks called El-Qaá formation. It is composed primarily of alternating beds of sandstones with gypseous interbeds, (HAMMAD, et al, 1998).

Due to the stratigraphy (see above) the geologic section at the base of El-Qaá formation consists of the Miocene Qabilyat formation composed essentially of a fossiliferous limestone, and the Eocene rocks below are composed essentially of limestone. ABDULLAH and ABU KHADRA (1976), stated that El-Qaá plain is covered by Quaternary deposits and bounded by upper Tertiary deposits, (marine Miocene and most probably non-marine Pliocene sediments), which share in the surface geology of El-Qaá plain area.

The soils of the study area can be classified by using remote sensing techniques; unsupervised classifications of ETM image for El-Qaá plain area depend on *ISODATA*. It is iterative in the manner that it repeatedly performs an entire classification (outputting a thematic raster layer) and recalculates statistics. "Self-Organizing" refers to the way in which it locates the clusters that are inherent in the data. The *ISODATA* clustering method uses the minimum spectral distance formula to form clusters. It begins with either arbitrary cluster means or means of an existing signature set, and each time the clustering repeats, the means of these clusters are shifted. The new cluster means are used for the next iteration. Then this classification was represented on a computer assisted map.

The visual analysis of the contrast map and colored composite image allows noting the main geomorphologic units. Also, it provides some indications related to the spectral behaviors of different surface. This analysis determines the location of six kinds of soils (Fig 1-11):

***1.3.1.1. Rocky surface*s** are restricted mainly to mountainous south-east Egypt. They are found in combination with calcisols and gypsisols in the most mountainous parts of the Eastern Desert and Red Sea Mountains, in a belt extending from the Sudanese border north to about 29^{o} N, and on the southern tip of the Sinai Peninsula.

Soils of this unit are classified as *Lithic leptosols*. They are distributed mostly in the east and north east of the study area and the Qabilyat mountain area in the north west of El-Qaá plain area (*http://www.fao.org/ag/agl/swlwpnr/reports/y_nf/egypt/e_soils.htm*).

1.3.1.2. Crusty and gravelly surface can be recognized by gypsum and /or carbonates crust covering more than 60% of the area (ABD EL-HADY et. al, 1991). It is distributed mostly in the north east of the study area (Qabilyat mountain area), in the north west of El-Qaá plain and the lower part of Wadi Firan basin.

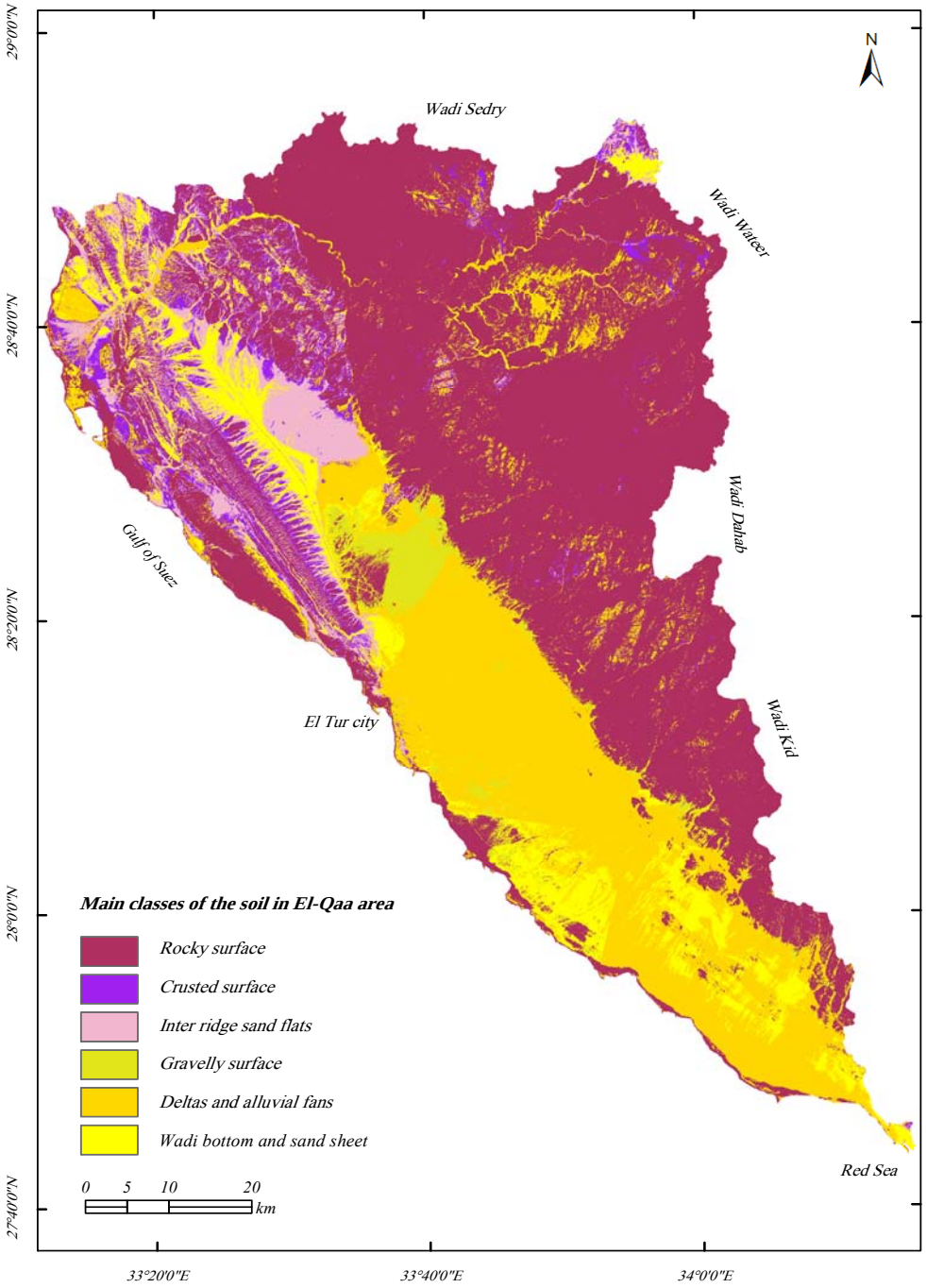

Fig (1-11) *Soil classification in El-Qaà plain area using unsupervised classification of ETM image* **(**remote sensing techniques**).**

1.3.1.3. Inter ridge sand flats, inclined surfaces representing the foot of the southern triangular mountains. Depth of soils is ≤ 50 cm, soil texture class is coarse sand; saturation percentage of these soils ranges between 21 – 22,pH values tend to be slightly alkaline (PH values are 8.0 – 8.4), EC values range between 2.5 to 5.0 dS/m and $CaCO_3$ content ranges between 7.7 – 8.7 %. Lithic contact at 50 cm defines the depth of this soil profile (EL NARY and SALEH, 2003). Soils of this unit are classified as *Lithic Torripsamments*. They are typic for miscellaneous geomorphologic units, marine spitsinclined limestones, ridges, rocky hills and cuestas. A type of sedimentary rock containing a large quantity of weathered quartz grains is restricted between elongated ridges. These deposits were found in the northern part of El-Qaá plain and Qabilyat area.

1.3.1.4. Gravelly surface, these deposits were found at the Wadi mouth, mostly coarser than the other deposits that built up fans. Wadi outlet occurs after heavy rains in the uplands. They produce floods bringing down coarse textured sediments. Soils of this unit are classified as *Typic Torripsamments*.

1.3.1.5. Deltas and alluvial fans, large deposits of alluvial sediments become located at the mouth of channels where stream velocity reduces quickly. Soils of this unit are classified as *Typic Torripsamment,* on the other hand Bajadas and alluvial fans. Consecutive series of alluvial fans are forming a foot plain along the edge of a linear mountain range. This landform normally occurs in arid climates. Soils of this unit are classified as *Typic Torripsamments* and were found at several places of El-Qaá plain such as the fans of Wadi Maier, Wadi Eghshy and the delta of Wadi Firan (Fig.1-12).

1.3.1.6. Wadi bottom and sand sheet, the Wadi bottom is covered mostly by sandy and silty sediments. Soils of this unit are classified as *Typic Haplocalcids*. They were found mostly at the bottoms of Wadi Firan and Wadi El-Aawag (Fig.1-12). Stratified and sorted poor sand deposits at the surface are supposed being formed when windblown materials were transported among patchy rocks. Such sand sheets could be categorized to high, moderately high, moderately, moderately low and low velocity. Soils of this unit are classified as *Typic Torripasmments* (EL NARY and SALEH, 2003).

It has been noticed from ETM image analysis and field work that these soils especially in northern parts of El-Qaá plain are derived from several common rocks of different igneous, metamorphic and sedimentary origins, whereas in northern extremities of the plain in the area of country hills, Wadis are cutting through the three types of major common rocks (HAMMAD et al. 1998).

1.3.2. Nature vegetation

El-Qaà plain area is characterized by young tertiary and quaternary alluvial sediments, sandstone, gypsum and limestone. Much of the alluvial sediments originate from the hills to the east. Alluvial fans derived from magmatic and metamorphic parent rocks are common in the southern part of Sinai Massif. Limestone derived from local weathering and transported by wind, mixes with the alluvium or forms individual dunes (DANIN, 1983). The plain is divided into six geomorphologic units: terraces, active alluvial plains, Wadi channels, alluvial fans, playas and coastal shore.

The analysis of the relationships between variations in vegetation composition and those in environmental factors indicates that the distribution of vegetation in the study area is mainly controlled by elevation, percentage of surface sediments of different size classes, soil moisture, organic matter, salinity and pH. Elevation is obviously of major importance in controlling the amounts of water received or lost by runoff, and in controlling the temperature in a site. The percentage of surface sediments of different size classes determines the spatial distribution of soil moisture (EL-GAREEB, R. and SHABANA, M. 1990). Studies carried out in a Negev desert watershed at Sade Boqer by YAIR *et al.* (1980) have demonstrated that surface properties of rocks and soils are the main factors controlling the spatial distribution of soil moisture at various scales.

In the same desert, WHITTAKER *et al.* (1983) pointed out that the distribution of soil moisture in a rocky desert (with patches of rock alternating with patches of soil) depends on the distribution and ratio of rock surface to soil volume. High soil moisture can be predicted where the rock: soil ratio by volume is high. Future studies on the structure of vegetation in Sinai Wadis should take into account the effects of micro-scale variations in the patterns of soil surface properties. The role of organic matter in soils as a key element in fertility is well known. It is largely related to the human and animal remains, and is also influenced by the litter supply from the vegetation. Soil pH is relatively low (7.1) in a few stands of the present study, which may be attributed to the effect of air-dried storage of the soil samples.

El-Qaà plain can be divided into three ecological districts, which contain some environmental conditions as background material for the study of species diversity using multi spectral classification of ETM image (Fig.1-12):

District 1 *(coastal plain of the Gulf of Suez),* young sediments of tertiary and Quaternary, mainly alluvium, sandstone, sands, gypsum and limestone characterize this district. Vegetation of this part is restricted to Wadis.

District 2 *(Lower Sinai Massif),* this district contains much granite, other magmatic and metamorphic rocks and wide valley floors filled with arkose and alluvium; small and large outcrops of smooth-faced rocks also occur. Lower altitudes of this district support vegetation only in Wadis while that of upper altitude forms a diffuse pattern (DANIN, A. 1978).

District 3 *(Upper Sinai Massif),* the rock sequence is similar to that of district 2, but with large outcrops of smooth-faced rocks building up several mountain peaks. Springs and wells supply water for intensive agriculture in the valleys (HADIDI et al. 1970). Due to the higher amounts of available water, as a result of altitude, much more habitats are occupied by plants. Large outcrops of smooth-faced granite characterize several mountains of this district. Most of the area supports diffuse vegetation (photo 1-10).

Photo (1-10) Acacia (mimosa) trees at Wadi Maier bottom, and Phoenix (dactylifera) at Wadi Firan

Plants in the study area are restricted to microenvironments (as in Wadis, channels and depressions) where runoff water collects and provides sufficient moisture for plant growth. This is described by MONOD (1954) as contracted vegetation, runoff desert (ZOHARY, 1962), and restricted desert (WALTER, 1963).

The vegetation is characterized by sparseness of plant cover (does not exceed 5% on the average; KASSAS, 1966), a limited number of plant species (16 on the average in each site), and poverty of trees (5% of the recorded species).

Nevertheless, a flora of total 480 species is recorded in south Sinai, 389 species of these belonging to rare species, which have a limited distribution. Out of these, rare species are of 31 endemic, 23 endangered 16 vulnerable, and three (3) extinct species.

Gebel Catherine, Wadi El Arnaeen, Gebel Musa, the surrounding of the famous monstary and the Wadi El Deir are extraordinarily rich in species with a considerable amount of endemic. There are also several endangered and vulnerable species. About 36.1% of the endemic species are recorded from gebel Catherine and the Wadi El Deir. Moreover 54.5% of the endangered and vulnerable species are found in Gebel Catherine, Gebel Musa and the Wadi El Deir (JICA, 1999).

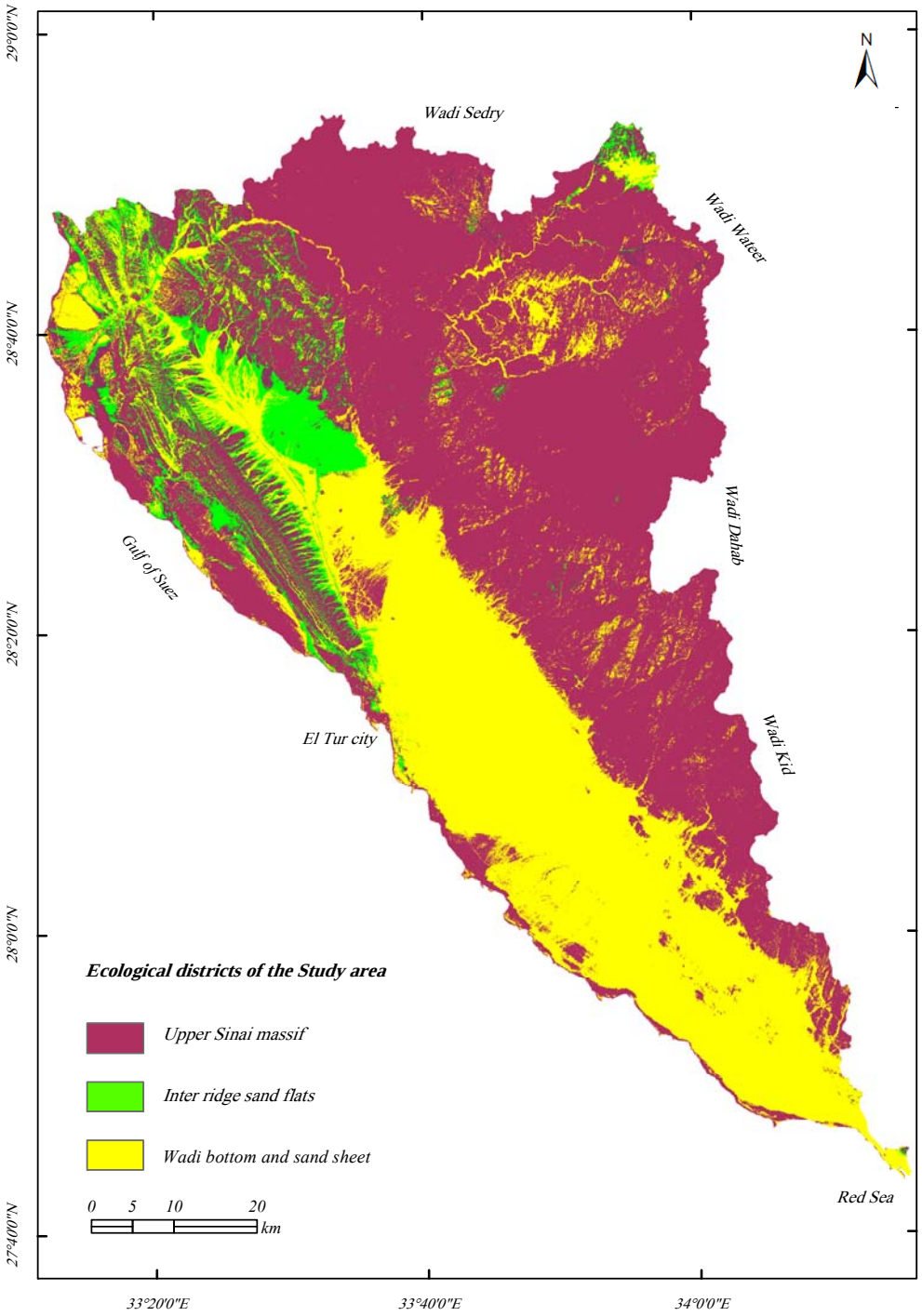

Fig (1-12) *Ecological districts in El-Qaà plain area using unsupervised classification of ETM image* (remote sensing techniques).

Chapter 2
Morphometric analysis

Landforms are the result of geologic and geomorphologic processes that occur on the earth's surface. The term landforms as used by geoscientific modelers denote a portion of the earth that unites the qualities of homogeneous and continuous relief due to the action of common geological and geomorphological processes. This concept of landforms is essentially an idealized one; it follows that the closer the studied landform conforms to its definition, the greater the accuracy of the obtained model. Geomorphometry, a subdiscipline of geomorphology, means the quantitative and qualitative description and measurement of landforms (PIKE AND DIKAU, 1995; DEHN ET AL., 2001; PIKE, 2002) and is based principally on the analysis of variations in elevation as a function of distance. A basic principal underlying geomorphometrics is that there exists a relationship between relief form and the numerical parameters used to describe it, as well as to the processes related to its genesis and evolution.

Derivation of landform units can be carried out using various approaches, including classification of morphometric parameters, filter techniques, cluster analysis, and multivariate statistics (DIKAU ET AL., 1995; DIKAU, 1989; SULEBAK ET AL., 1997; AND ADEDIRAN ET AL., 2004). A common focus of the study of landforms is to consider them as formed by small and simple elements topologically and structurally related. Morphometric studies usually begin with the extraction of basic components of relief, such as elevation, slope, and aspect; a more complete description of the landform may be achieved by using spatial derivatives of these initial descriptors, as well as useful indicators, e.g., the topographic wetness index (MOORE AND NIEBER, 1989), stream power index (MOORE ET AL., 1993A), and aggradations and degradation index (MOORE ET AL., 1993B).

Therefore, morphometric analysis of landforms is considered being one of the important fundamentals in geomorphological studies, it was presented by Horton (1945); Smith, (1950, 58); Strahler (1952, 54, 64,); Scheidegger (1965); Morisawa (1962); Sherve (1966); Chorley (1957); Carlston (1963); Leopold and Miller (1956); Melton (1958), and Schumm (1954, 56, 1973).

Systematic description of geometry of a drainage basin and its network-channel system requires measurements of two main elements:

2.1. Morphometric analysis of drainage network.

2.2. Morphometric analysis of basins

2.3. Morphometric analysis of Alluvial fans

2.1. Morphometric analysis of drainage network

The drainage network constitutes the basic system for studies in climatic geomorphology. It is a basic system in which inputs of energy, both potential and kinetic, carry out work and its variable components control the structure of the drainage system (IGNACIO & LUIS A, 1982).

2.1.1. Stream orders

The first step in drainage-basin analysis is the designation of stream orders, following a system introduced by Horton (1945) and slightly modified by Strahler (1952); Melton (1958b) has explained the mathematical concept involved. Assuming the availability of a channel-network map including all intermittent and permanent flow lines located in clearly defined valleys, the smallest fingertip tributaries are designated order 1 (Fig. 2-1). Where two first-order valleys join, a channel segment of order 2 is formed; where two of orders 2 join a channel of order 3 is formed; and so on. The trunk stream by which all discharge of water and sediment passes is therefore the stream segment of highest order.

Beneficial of the stream-order system depends on the premise that, on the average, if a sufficiently large sample is treated, order number is directly proportional to size of contributing watershed, to channel dimensions, and to stream discharge at the place in the system. Because order number is dimensionless, two drainage networks differing greatly in linear scale can be compared with respect to corresponding points in their geometry by use of order number (STRAHLER, 1964).

According to Strahler's classification and to the drainage network map of El-Qaà plain basins (Fig. 2-1) one can say that there are two streams carrying the seventh order (Tab. 2-1). These are Wadi Firan and Wadi El-Aawag. In addition, there are six streams of sixth order: two of Wadi Firan, two of Wadi El-Aawag, one of Wadi Esla, and one of Wadi El-Mahash.

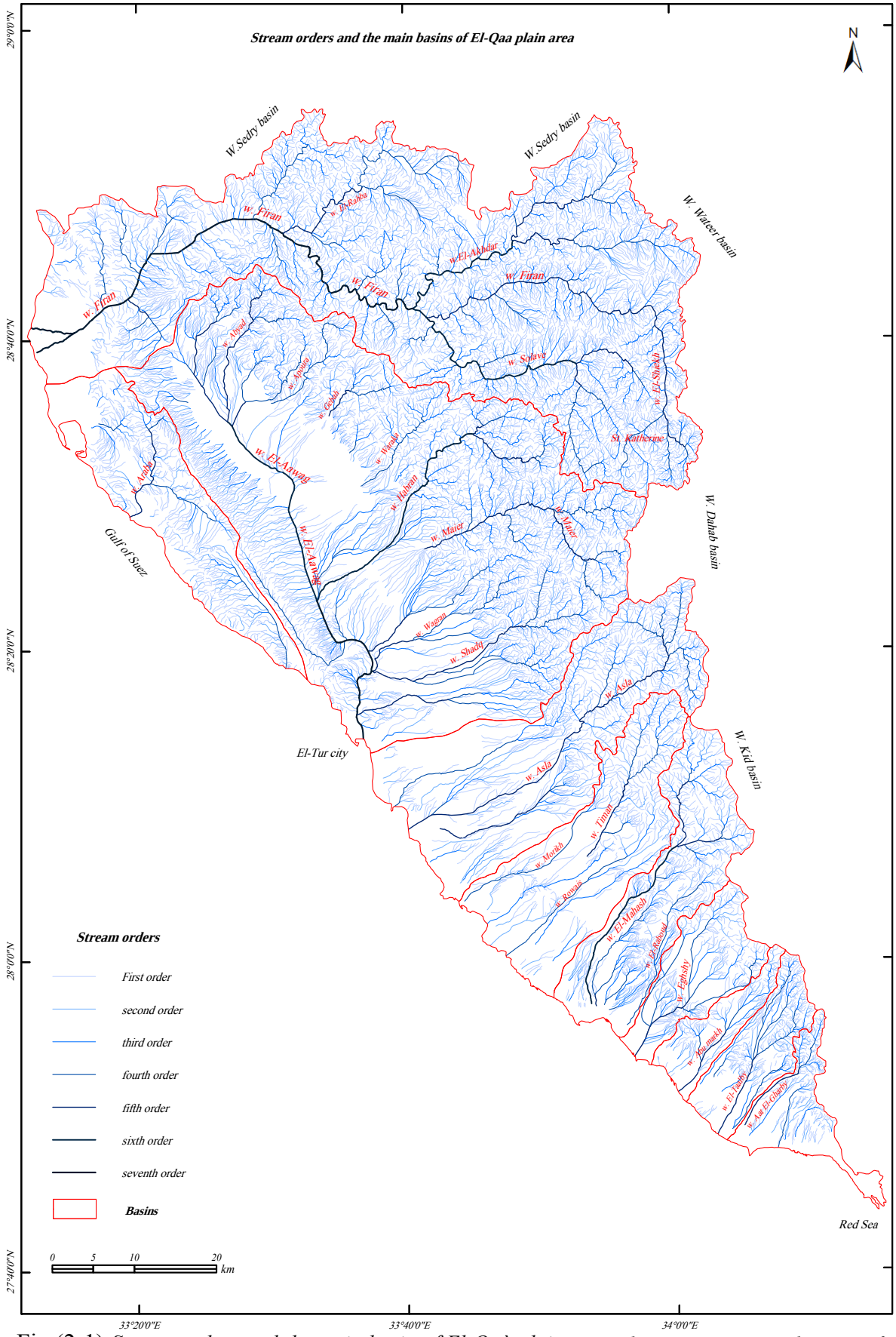

Fig (2-1) *Stream orders and the main basin of El-Qaà plain area, the source: topographic map of Egypt scale 1: 50 000, aerial photograph scale 1: 40 000, and ETM Image 2003, using Arc GIS and Erdas imagine programs.*

Tab. (2-1) Stream orders and bifurcation ratio of the main wadis in El-Qaà plain area

Orders / Wadis		first	second	third	fourth	fifth	sixth	seventh
w. Firan	***SN***	4800	879	242	42	7	2	1
	Rb	**5.5**	**3.6**	**5.8**	**6**	**3.5**	**2**	-
w. El-Aawag	***SN***	4334	835	203	40	11	2	1
	Rb	**5.2**	**4.1**	**5.1**	**3.6**	**5.5**	**2**	-
w. Araba	***SN***	438	102	26	5	1	-	-
	Rb	**4.3**	**3.9**	**5.2**	**5**	-	-	-
w. Asla	***SN***	859	154	34	9	2	1	-
	Rb	**5.6**	**4.5**	**3.8**	**4.5**	**2**	-	-
w. Timan	***SN***	813	162	17	5	1	-	-
	Rb	**5**	**9.5**	**3.4**	**5**	-	-	-
w. El-Mahash	***SN***	733	144	34	11	2	1	-
	Rb	**5.1**	**4.2**	**3.1**	**5.5**	**2**	-	-
w. Eghshy	***SN***	286	58	15	5	1	-	-
	Rb	**4.9**	**3.9**	**3**	**5**	-	-	-
w. Abu Markh	***SN***	148	40	9	3	1	-	-
	Rb	**3.7**	**4.4**	**3**	**3**	-	-	-
w. El-Taalby	***SN***	349	89	24	5	1	-	-
	Rb	**3.9**	**3.7**	**4.8**	**5**	-	-	-
w. Aat El-gharby	***SN***	244	65	13	3	1	-	-
	Rb	**3.8**	**5**	**4.3**	**3**	-	-	-
study area	***SN***	13004	2548	617	128	26	6	2
	Rb	**5.1**	**4.1**	**4.8**	**4.9**	**4.3**	**3**	-

- Source: topographic map scale 1: 50 000 (digital), aerial photograph scale 1: 40 000, and ETM Image 2003, using Arc GIS and Erdas imagine programs.

The Wadis above represent the five big basins in the study area. As for the fifth order, it has 28 streams; the fourth order has 128 streams; the third order has 617 streams; the second order has 2548 streams; and the first order has 13004 streams. The numbers of streams of the first order represent a ratio of 79.6%, the second order sreams represent a ratio of 15.6% of total streams, and the third orders streams represent about 3.8%.If the streams of the second and third order were added to the first, the ratio will be 99% of the total stream numbers.

This high number almost coincides with many studies applied on dry valleys in different Egyptian territories, for example: the ratio of the the first order, second order and third order of Wadi Baba basin (southern Sinai) reached to 95.6% of total stream numbers (SHERIEF, Y. 1999), and reached to 97.8% in Wadi Tayyibah basin in the west central of Sinai (AKL, 1994).

This means that the channels of dry areas are distinguished by their increased numbers streams of the first, second, and third orders, a fact which could be related to the hyper arid climate which causes the rarity or the nonexistence of the plant cover.

Therefore, floods may have been eroded many streams due to sheet flows being the dominant fluvial process. It can be concluded that the geological and climatic conditions and the slops degree have been played the main role to increase the numbers of streams. The greatest number of streams of all basins in El-Qaà plain area (6025 streams) in Wadi Firan, and Wadi El-Aawag basin (5435 streams) is covering mostly sediment rocks, whereas, Abu Markh basin which receives the least number of streams (201 streams) is covering mostly igneous rocks.

According to King and Al-Saleh (1991) there is an actual correlation between stream orders and alluvium thickness. The coefficient of determination of Wadi alluvium thickness on stream orders is about 0.77 in Wadi Al-Khanagah basin, central Saudi Arabia. Thus about 77% of the variability in the observed values of alluvium thickness is explained by stream orders. It has drawn the attention to the importance of establishing the relationships between landforms and rapid applied hydrogeomorphological studies in areas lacking systematic data base.

2.1.2. Bifurcation ratios (Rb), the basin and sub-basins stream length ratios have been calculated by applying the following formula:

$$Rb = \frac{Nu}{Nu + 1}$$

Where **Rb** is the bifurcation ratio, **Nu** is the number of stream order and **Nu + 1** is the number of streams in the next higher order.

Strahler (1964) declared that the bifurcation characteristically range between 3.0 and 5.0 for watersheds in which the geologic structures do not distort the drainage pattern. The theoretically possible minimum value of 2.0 is rarely approached under natural conditions. Because the bifurcation ratio is a dimensionless property, and drainage systems in homogeneous materials tend to display geometrical similarity, it is not surprising that the ratio shows only a small variation from in different regions.

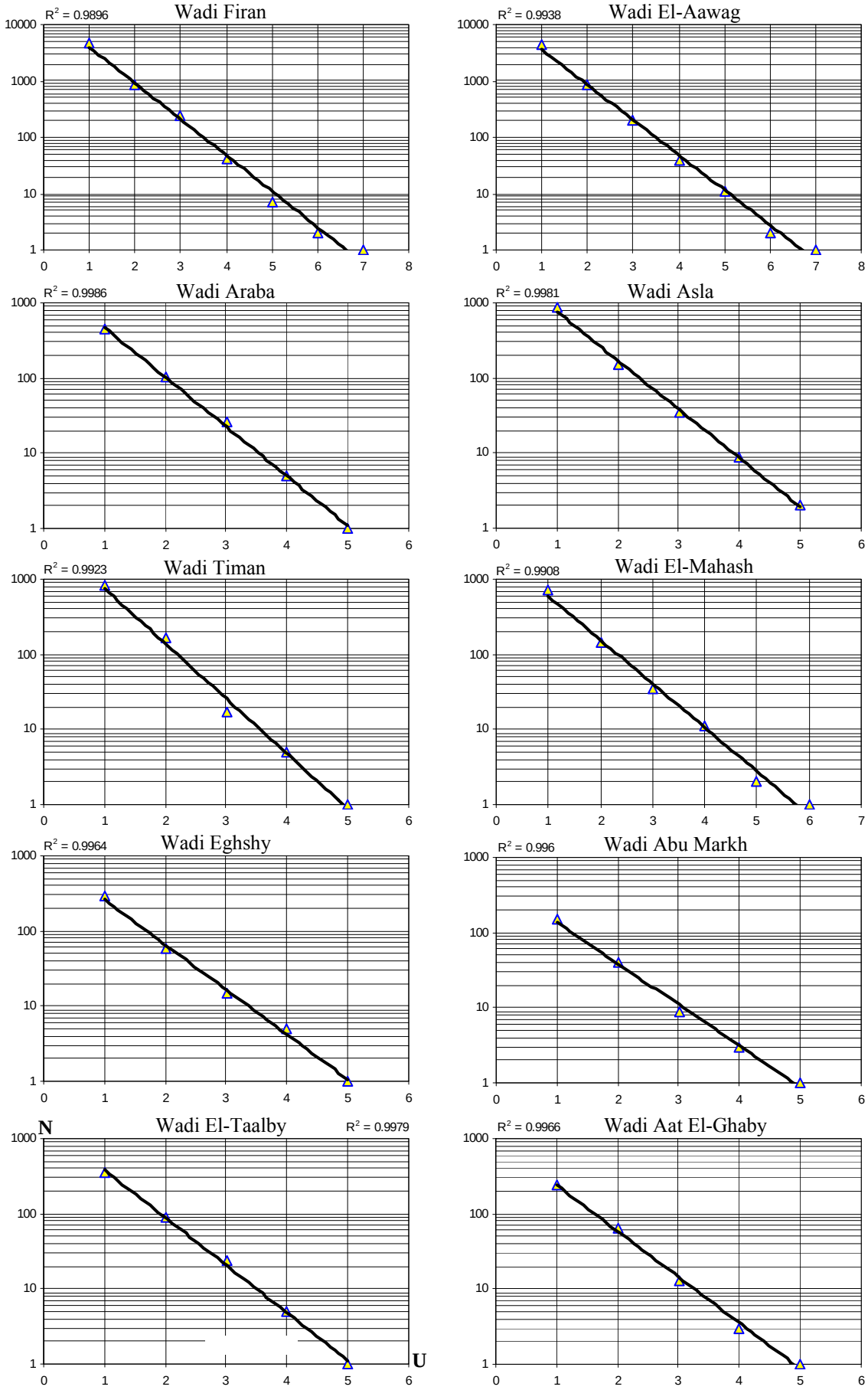

Fig (2-2) *The relationship between stream* ***numbers*** *(**N**) and stream* ***orders*** *(**U**) in the* study area

(Tab. 2-1) shows that the bifurcation ratio of all streams confirms Strahler's law with the exception between the second and fifth orders of the majority of Wadis in the study area; while the maximum ratio reaches 5.8 and 6 in the third and fourth order of Wadi Firan consecutively, and reaches in Wadi El-Aawag 5.5, 5.1, and 5.5 in the first, third, and fifth orders consecutively. This is related to the steams of these orders in Wadi Firan and Wadi El-Aawag basins originating from a high mountain area (2300-2600m). Abnormally, high bifurcation ratio might be expected in regions of steeply dipping rock strata where narrow valleys are confined between hogback ridges such as the upper parts of Wadi Firan basin and tributaries of Wadi El-Aawag basin.

According, Horton's Law (1945) which is known as (the Law of Stream Numbers), saying "the Numbers of stream segments of successively lower order in a given basin tend to form a geometric series, beginning with a single segment of the highest order and increasing according to a constant bifurcation ratio."

The relationship between stream orders and stream numbers is shown in (Fig. 2-2), which shows that the relationship between two elements is a strongly inversely proportion; i.e. with the increase of stream orders, the number of drainage streams decreases. In addition, most of the points are mostly located on the same straight line, whereas, the point that deflects from this line belongs to the order before the last. This shows that the number of mountain tributaries, those of lower order, that enrich the principal drainage, resemble a high number; besides, the drainage of middle sectors of basins are of less numbers. This might be related to the little step with the eminence of limestones that form most parts of Wadi El-Aawag basin and the lower part of Wadi firan bain.

2.1.3. Stream lengths means length **L** of stream-channel segment of order **U** is a dimensional property revealing the characteristic size of components a drainage network and its contributing basin surface (STRAHLER, 1964). The first order stream channel with its contributing first-order drainage-basin surface area should be regarded as the unit cell, or building block, of any watershed. Because first-order drainage basins tend to be geometrically similar over a wide range of sizes, it is not important which length property is chosen to provide the characteristic measurement of size by which systems are being compared from region to region?

The total stream lengths of the basins in the study area reach 15621.6 km. The streams of the first order occupy 63.4%, of the second order 19.6%, of the third order 8.6%, and the seventh order 0.6% (Tab. 2-2). On the other hand, there is an obvious increment in the total length of high tributary streams (1st, 2nd and 3rd 81.6%) and an obvious decrease in the total of the streams of higher order. The reason is related to the increment in the number of the first, second and third order streams. In addition, the average length of the streams of the first order is 0.76km, the second order 1.2km, third order 2.2km, and the seventh order 46.2km.

Actually, the streams of the first order resemble the mountainous surface which is characterized by a steep slope. These streams are short, obstructive, fast flowing and combine soon with each other to form the streams of the second order, whereas the streams of the higher order always record a higher average length. They have reach in the seventh order Wadi Firan 70.1km and in Wadi El-Aawag 22.2.

Tab. (2-2) *Stream lengths of the main wadis in El-Oaà plain area*

Orders / Wadis	first	second	third	fourth	fifth	sixth	seventh
w. Firan	3613.3	1072	461.4	188.8	109.5	48.4	70.1
w. El-Aawag	3424.2	1069.1	463.8	240.7	131.6	57.8	22.2
w. Araba	476.3	154.1	36.5	30	13.6	-	-
w. Asla	781.1	241.7	99.7	53.1	61	-	-
w. Timan	410	102.9	75.2	63	11.3	-	-
w. El-Mahash	541.6	165.4	84.7	55.1	17	23.5	-
w. Eghshy	206.6	77.3	36.5	43.1	10	-	-
w. Abu Markh	196.4	76.6	45	42.4	10.7	-	-
w. El-Taalby	109.4	47.6	20.6	8.2	9.4	-	-
w. Aat El-gharby	132.9	56.4	23.8	13.3	10	-	-
study area	**9891.8**	**3063.1**	**1347.2**	**737.7**	**359.8**	**129.7**	**92.3**
%	**63.4**	**19.6**	**8.6**	**4.7**	**2.3**	**0.8**	**0.6**

- Source: topographic map scale 1: 50 000(digital), aerial photograph scale 1: 40 000, and ETM Image 2003, using Arc GIS and Erdas imagine programs.

The relationship between the total stream lengths and the stream orders is an inversely proportion, this means the higher order of stream, and the less total length of the streams (Fig. 2-3), but the relationship between the average length of stream and the basin order is a strong positive proportion.

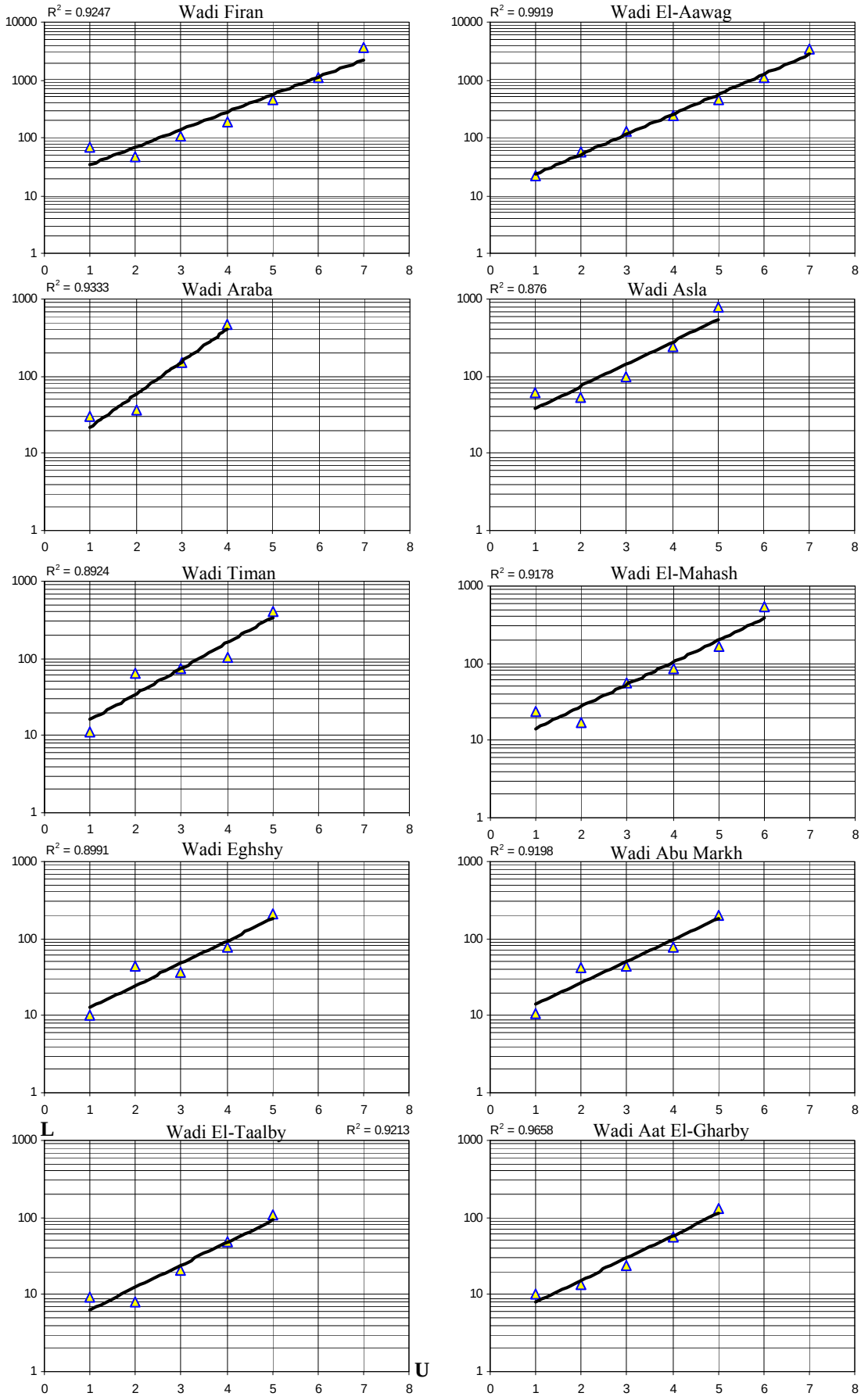

Fig (2-3) *The relationship between the total stream* ***length*** *(**L**) and stream* ***orders*** *(**U**) in the* study area

2.1.4. Texture ratio is considered being an important element to study the discharge networks and the extent of the surface cutting of basins within this watershed, regarding as that the surface of basin has been affected by another factor such as: geological formations, wild, nature plants, and the stage of the cycle of erosion the basin has reached.

The texture ratio can be computed by:

$$Tr = \frac{Ns}{Lp}$$

Where ***Tr*** is the Texture ratio, ***Ns*** is the Number of streams, and ***Lp*** is the length of perimeter of the basin.

Morisawa (1958) had composed a classification for texture rate which consists of:

- *Less than 8 streams / km (coarse texture).*
- *From 8 to 20 streams / km (medium texture).*
- *From 20 to 200 streams / km (soft texture).*
- *More than 200 streams / km (very soft texture).*

(Fig. 2-4) and (Tab. 2-3) show that 5 basins lie in category one (*coarse texture*) and 4 basins in category two (*medium texture*) to range between 8.4 streams/km in Wadi El-Mahash basin, 8.58.5 streams/km in Wadi Timan basin and 17.7 streams /km in Wadi Firan basin, whereas texture ratio in Wadi El-Aawag basin reaches to 23.7 streams/km (*soft texture*). The structural factor has a main effect in the texture ratio especially in Wadi El-Aawag basin and Wadi Firan, but, types of geological formations and slopes have had a big influence to increase the texture ratio in Wadi El-Aawag basin which lies mostly in a sedimentary rocks region.

Strahler, (1954) studied the relationship between the texture ratio and drainage density in some Wadis in USA and had found it being a direct proportion. the concluded that the basins which have less than 5 streams/ km are covered by carbonic and sandstone rocks and have coarse texture, from 5 to 10 streams/ km consist mostly of metamorphic and igneous rocks, and have a middle texture , from 10 to 100 streams/ km they have a soft texture and are covered by Pleistocene sedimentary rocks. The very soft texture ratio has been classified in the badlands.

So, it can be concluded that the basins which are similar in geological, structural, hydrological conditions the sources of the Wadis networks have nearly the same category of texture ratio.

Tab. (2-3) *Texture ratio of the major basins of study area*

Basins	w. Firan	w. El-Aawag	w. Araba	w. Asla	w. Timan	w. El-Mahash	w. Eghshi	w. Abu Markh	w. El-Taalby	w. Aat El-Gharby
Texture ratio	17.7	23.7	4.7	7	8.5	8.4	5.3	3.5	7.4	3.8

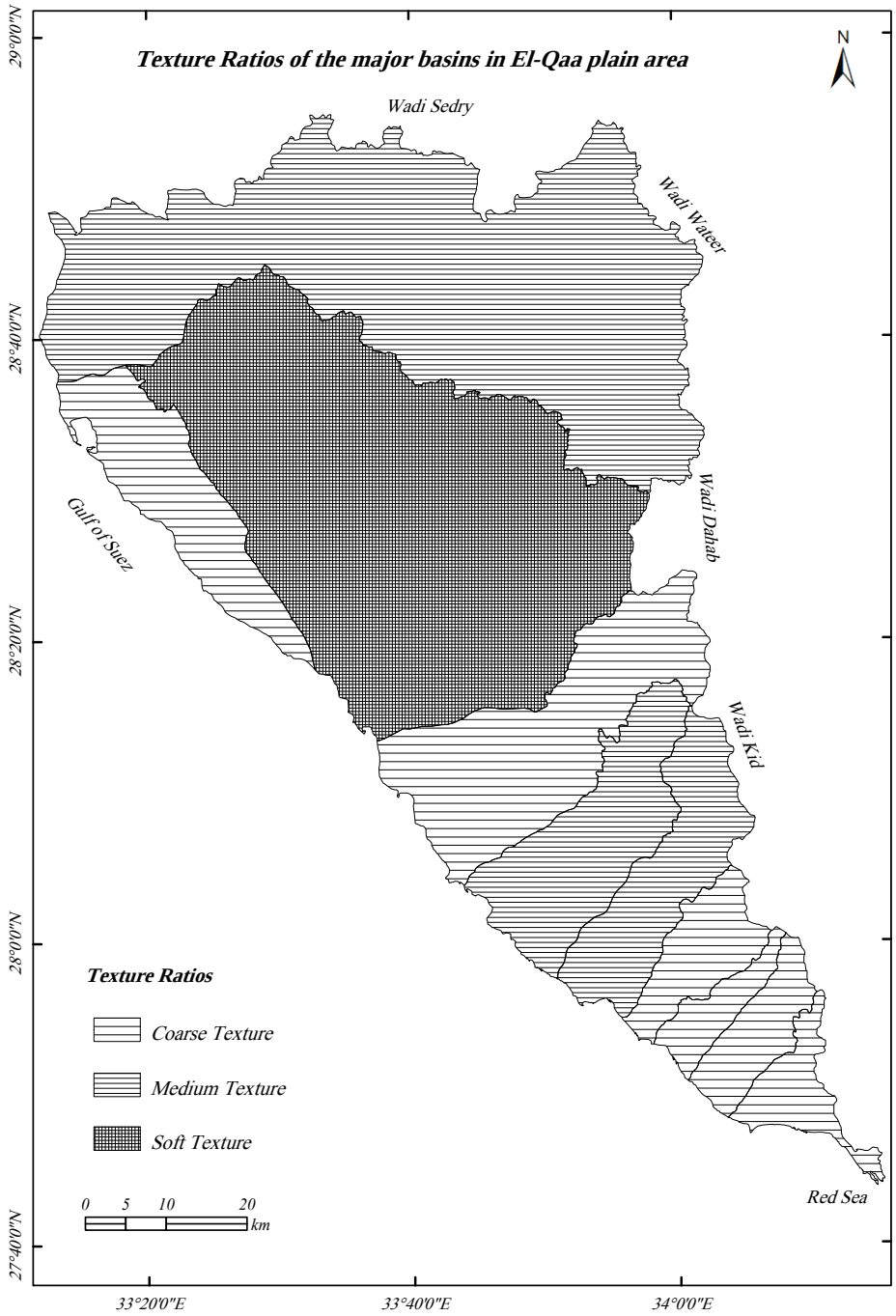

Fig (2-4) *The texture ratios of the major basins in the study area*

2.1.5. Stream frequency (Fs), is one of rates which discusses the forms of drainage networks; the level of surface basins erosion in addition gives an impression about the drainage density. Stream frequency has been calculated by applying the following formula:

$$Fs = \frac{\sum Nu}{A}$$

Where Fs is stream frequency, $\sum Nu$ is total number of stream segments of all orders, and A is Basin area.

Tab. (2-4) *Stream frequency in the major basins of study area*

Basins	w. Firan	w. El-Aawag	w. Araba	w. Asla	w. Timan	w. El-Mahash	w. Eghshi	w. Abu Markh	w. El-Taalby	w. Aat El-Gharby
Stream frequency	3.1	2.7	1.7	1.8	2.5	2.8	2.2	2.3	3.5	2.9

According to, Horton, (1945) the stream frequency for small and large drainage basins is not directly comparable because it usually varies with the size of the drainage area. A large basin may contain as many small or fingertip tributaries per unit of area as a small drainage basin, and in addition it usually contains a larger stream or streams. This effect may be masked by the increase of drainage density and stream frequency on the steeper slope generally according with smaller drainage basin.

From studying the values of the stream frequency of the study area (Tab. 2-3), it has been noticed that sub-basins of vast basins contain a number of streams related with their areas. If stream consists of more than one stream, it means that the ratio of stream frequency between small basins and huge basins is equal, while the escarpments perform an important role to vary streams frequency ratio, i.e. the upper parts of Wadi Firan basin, Wadi Maeir basin and Wadi El-Taalby basin.

In addition, the values of stream frequency ranged between 1.7/km in Wadi Araba basin, 1.8 in Wadi Asla basin, and the maximum value reached 3.5/km in Wadi El-Taalby basin. The values of stream frequency are different from one area to another depending on the source of watershed, the kind of geological formations, orders of streams, and the slope, while the stage cycle has a small effect on the values of stream frequency.

2.1.6. Drainage density, (Dd) is probably the parameter which most globally represents the interaction between climate and geomorphology in the development of the drainage network (IGNACIO & LUIS A, 1982). *It* is a measure for the degree of fluvial dissection and is influenced by numerous factors, among which resistance to erosion of rocks, infiltration capacity of the land and climatic conditions rank high (VERSTAPPEN, 1983).

According to Horton (1945), the drainage density (Dd) is defined as the total length of streams per unit area divided the area of drainage basin. It is expressed as:

$$D\,d \;=\; \frac{\sum L\,t}{A}$$

Where $\sum Lt$ *is the total length of all the ordered streams, and* ***A*** *is the area of the basin.*

Drainage density, which has been defined as total stream length per unit area of a river basin (HORTON, 1932, 1945), has often been used to express the degree of fluvial dissection. Numerous researchers have measured values of Dd from topographic maps or other sources and have analyzed variables controlling Dd. The results indicate that Dd is related to climate (CHORLEY, 1957; CHORLEY and MORGAN, 1962; GREGORY and GARDINER, 1975), vegetation (MELTON, 1958), bedrock geology (SMITH, 1958; Wilson, 1971), time (RUHE, 1952), and the hypsometric integral (STRAHLER, 1952). Some researchers (e.g. SCHUMM, 1956) have also found that Dd is strongly influenced by relative relief (R), which means the maximum height dispersion of a terrain normalized by its length or area.

The climatic and geologic controls of Dd are widely recognized and well understood: Dd tends to be large in arid regions of sparse vegetation (El-Qaà plain area), in temperate to tropical regions subjected to frequent heavy rains, and in areas underlain by rocks with low infiltration capacity or transmissibility (CARLSTON, 1963; COTTON, 1964; MADDUMA BANDARA, 1974; GREGORY AND GARDINER, 1975). By contrast, the general relation between rainfall and drainage density remains uncertain. In humid badlands, SCHUMM (1956) found a positive correlation between Dd and the relief ratio, basin height divided by basin length. According to GARDINER et al. (1977), such a correlation is plausible from the widely observed inverse correlation between both drainage density and relief (R) and basin area. An experimental analysis of rill erosion performed by MOSLEY (1972) also revealed that drainage density (Dd) was positively correlated with ground slope.

Tab. (2-5) *Drainage density in the major basins of study area*

Basins	w. Firan	w. El-Aawag	w. Araba	w. Asla	w. Timan	w. El-Mahash	w. Eghshi	w. Abu Markh	w. El-Taalby	w. Aat El-Gharb
Drainage density	3.1	2.7	2.1	2.1	1.7	2.7	2.3	2.2	2.7	2.1

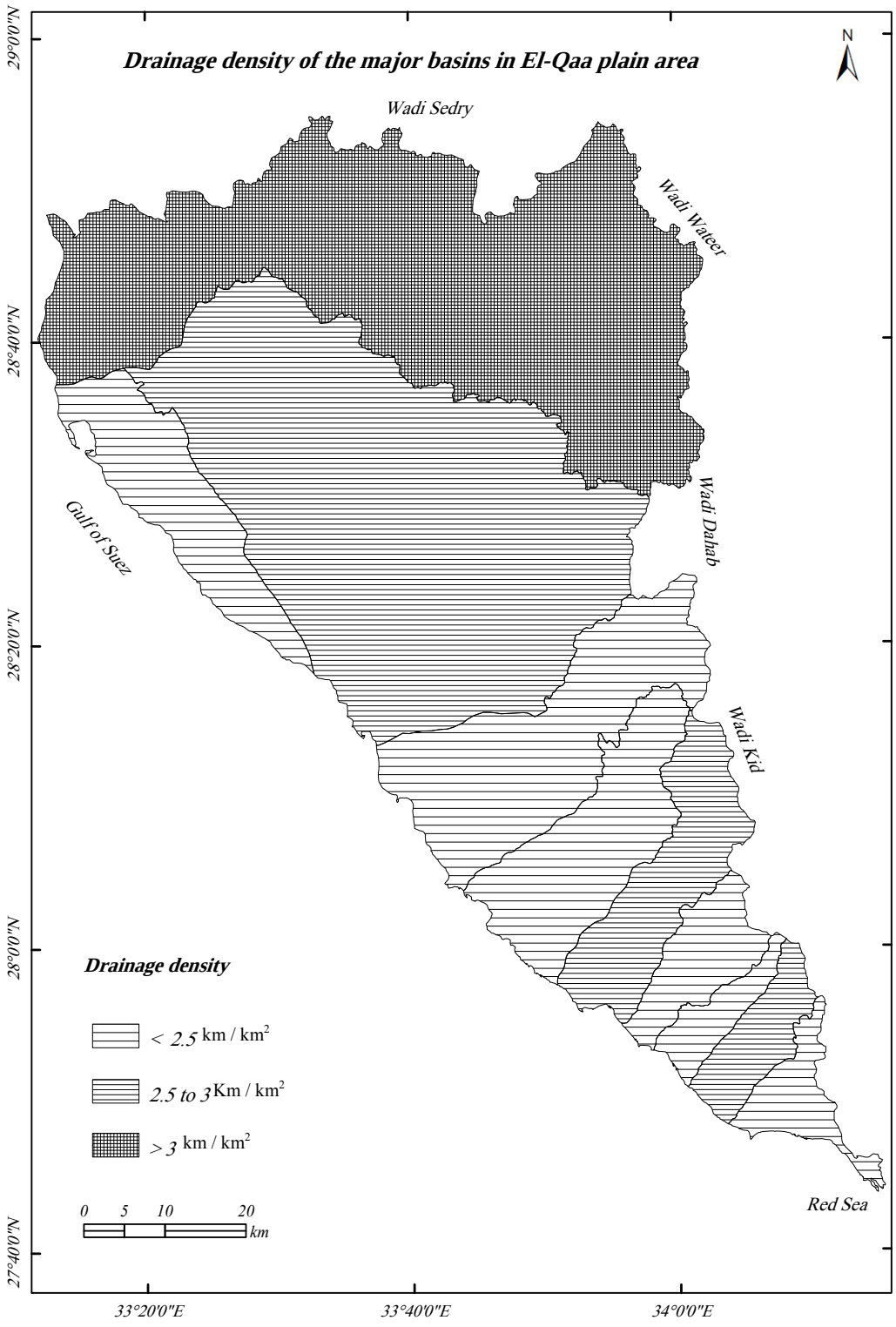

Fig (2-5) *Drainage density of the main basins in the study area*

(Tab. 2-5) and (Fig. 2-5) show the drainage density in the main basins of study area, the values range between 1.7km/km^2 for Wadi Timan basin and 2.9km/km^2 in Wadi Firan basin with average 2.4km/km^2 of total study area. The relative increase of drainage density in Wadi Firan basin is related to the morphology of basin surface which is characterized by rugged relief and steep slopes especially in the upper part of the basin.

Moreover, it has been noticed that the higher values of drainage density have been registered in the huge basins of Wadi Firan basin, and Wadi El-Aawag. These values indicate that the basins with a big area, steep slopes and a cover of sedimentary rocks, have a high value of drainage density. But the steep slope plays an essential role increasing the drainage density in the basins which have medium areas in the study area i.e. Wadi El-Mahash basin and Wadi El-taalby basin.

2.1.6.1. Drainage density and relief

Notably, although the theory predicts a positive correlation between *Drainage density* and *Basin relief* for Hortonian, creep-dominated landscapes, it also predicts a strong inverse correlation for landslide. Most studies show a positive correlation between *Dd* and *R. SCHUMM* (1956) found a positive correlation between *Dd* and the relief ratio in a humid badland area. MONTGOMERY AND DIETRICH (1989, 1994a) reported a positive correlation between drainage density and valley gradient in stream-head hollows in the western United States. A positive correlation between drainage density and slope has also been observed in experimental work (*SCHUMM ET AL.*, 1987). In El-Qaà plain area, there is a positive correlation between *Dd* and R (*A*), and negative correlation between *Dd* and Rr (*B*), but the low values are due to other factors which have a direct effect such as lithology, slopes and climate.

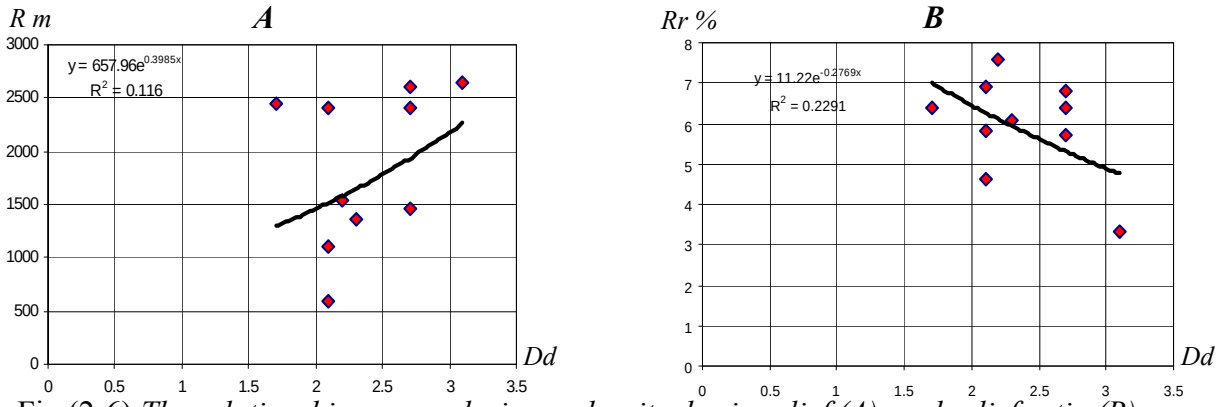

Fig (2-6) *The relationship among drainage density, basin relief (A), and relief ratio (B)*

In contrast to the data from these mostly (though not exclusively) low- to moderate-relief cases, OGUCHI (1997) found an inverse relationship between relief and the density of deep valleys in mountainous terrain in Japan. Also the analysis of different methods for measuring *Dd* showed that the results depend on the criteria used. If only well-defined valley forms are identified as drainages, there is a clear inverse *Dd-R* relationship, whereas if all contour inflections are considered, the relationship disappears. (GREGOR, TUCKER and RAFAEL, 1998) suggested that the varying behavior of *Dd* with respect to *R* may reflect differences in process dominance on hillslopes. Given that landsliding is active in the basins studied by OGUCHI (1997) and colleagues, they suggested that their findings reflect an increasing areal proportion of planar, landslide dominated hillslopes in steeper terrain.

2.1.6.2. Drainage density and climate

Most studies of the relationship between climate and *Dd* show either an inverse relation (MELTON, 1958) or a humped curve in which *Dd* increases with mean annual precipitation under semiarid to arid climates, and decreases under more humid climates (GREGORY AND GARDINER, 1975; MOGLEN ET AL., 1998). MOGLEN et al. (1998) emphasize the importance of vegetation as a limiting factor on *Dd*.

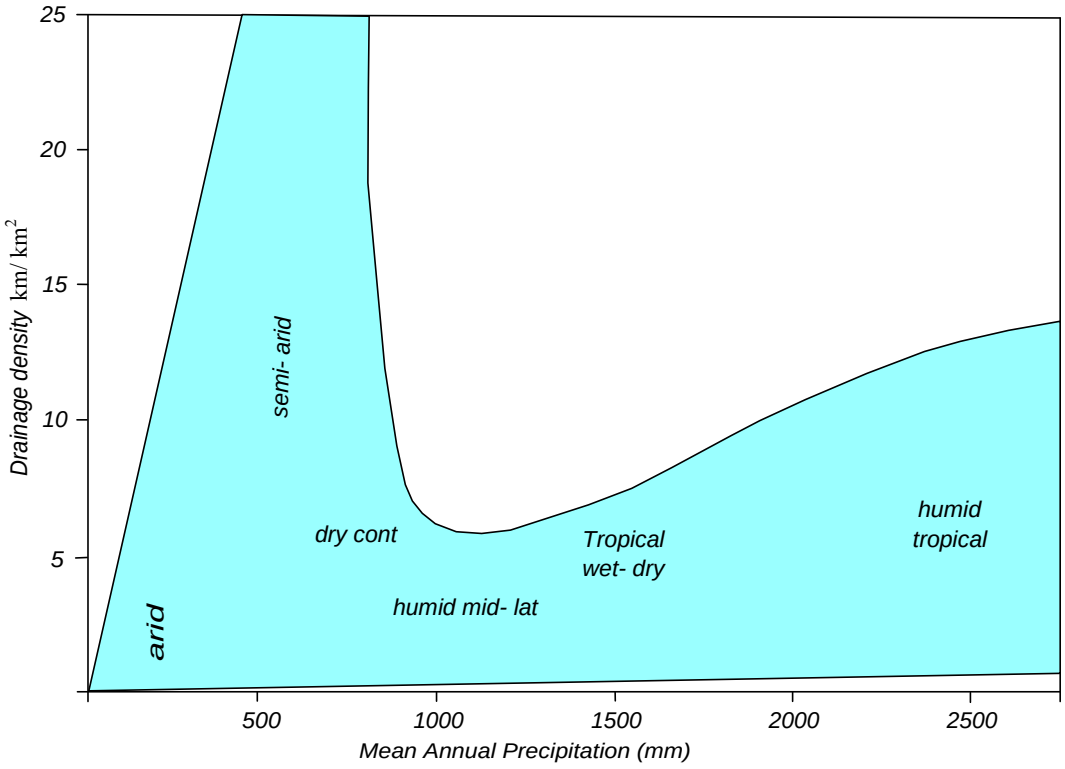

Fig (2-7) *Relation between drainage density and mean annual precipitation (modified after Gregory, 1976)*

Higher diffusivity under a humid climate would tend to decrease *Dd*, and conversely for an arid climate. Increased weathering rates under a humid climate would also tend to increase regolith thickness, thereby increasing transmissivity and decreasing drainage density. All of these factors may contribute to counterbalancing the positive effects of increased rainfall on *Dd*. In addition, changes in precipitation variability would likely influence drainage density (TUCKER AND SLINGERLAND, 1997).

World pattern of drainage density conforms broadly to morphoclimatic zones and reflects the combined effect of climate and vegetation on network development (Fig. 2-7). In the United States, drainage density progressively increases from areas of sparse precipitations in arid regions to a maximum in semiarid environments. From its peak, drainage density successively decreases and reaches a minimum in temperate regions. Finally, in more humid areas, drainage density maintains a relatively steady value (SANDRA, L.1984).

2.1.7. ***Correlation relationships among the main elements of network in the study area***

(Tab. 2-6) shows the correlation relationships (matrix) among seventh elements of morphometric analysis for the network in El-Qaà plain area, whereas ***U*** is orders, ***Nu*** is number of streams, ***A*** is area of orders. ***L*** is length of streams, ***Dd*** is drainage density, ***Tr*** is texture ratio, and ***S*** is slopes of streams in the study area.

Tab. (2-6) *Correlation matrix between morphometric characteristics of drainage network in study area*

Element	U	Nu	A	L	Dd	Tr	S
U	1.00	-0.92	0.90	0.75	-0.88	0.92	-0.92
NU		1.00	0.99	0.80	0.74	0.94	0.98
A			1.00	0.77	-0.61	0.95	-0.73
L				1.00	0.66	0.68	0.95
Dd					1.00	0.64	0.97
Tr						1.00	0.82
S							1.00

- The relation is negative and strong between the stream orders (**u**) and each of stream numbers, length, drainage density, and slope while it is positive between the orders and stream length (0.75), and the area of these orders (0.90). This means that, the more the number of streams, the more the area of basins and their lengths and widths.

- The correlation relation is positive and strong between the stream numbers (**Nu**) and each of slopes of streams (0.98), stream length (0.80), area of orders (0.99), drainage density, and texture ratios.
- The relationship is negative between the area (**A**) and each of drainage density (-0.61), and slopes (-.73). This is because basins of a large area, especially, like Wadi El-Aawag basin and Wadi Firan Basin, might include large areas of interfluves with no drainage lines where the area is of great account. But it is positive between the area and length of stream (0.77), and strongly positive between area and texture ratios (0.95)
- The relation is positive between length of stream (**L**) and each of drainage density (0.66), the texture ratios (0.68), and strongly positive between **(L**) and slope (0.95).
- There is a strong positive relationship between drainage density (**Dd**) and each of slopes of streams (0.97), and texture ratios (0.64). Finally, the relation is positive and strong between texture radios and slops (0.82).

2.1.8. Drainage patterns

The patterns which are formed by streams form are determined by inequalities of surface slope and inequalities of rock resistance. This being true, it is evident that drainage patterns may reflect original slope and original structure or the successive episodes by which the surface has been modified, including uplift, depression, tilting, warping, folding, faulting, and jointing, as well as depositions by the sea, glaciers, volcanoes, winds, and rivers. A single drainage pattern may be the result of one or of several of these factors. Moreover, as streams are long lived, comprising a lot of physiographic features "some of the oldest survivors or surviving remnants and also some of the youngest developments in response to earth movements," they may embody a long record of the geologic history of a region (ZERNITZ, 1932).

Drainage patterns or nets are classified on the basis of their form and texture. Their shape or pattern develops in response to the local topography and subsurface geology. Drainage channels develop where surface runoff is enhanced and earth materials provide the least resistance to erosion. The texture is governed by soil infiltration, and the volume of water available in a given period of time to enter the surface (*http://www.uwsp.edu/geo/faculty/ ritter/geog101/textbook/fluvial_systems/drainage_patterns.html*).

If the soil have only a moderate infiltration capacity, and a small amount of precipitation strikes the surface over a given period of time, the water will likely soak in rather than evaporate away. If a large amount of water strikes the surface more water will evaporate, soak into the surface, or stay on leveled ground. On sloping surfaces this excess water will runoff. Fewer drainage channels will develop where the surface is flat and the soil infiltration is high because the water will soak into the surface.

2.1.8.1. Dendritic drainage

A dendritic drainage pattern is the most common form and looks like the branching pattern of tree roots. It develops in regions underlain by homogeneous material. In this case the subsurface geology has a similar resistance to weathering so there is no apparent control over the direction the tributaries take. Tributaries are joining larger streams at acute angle (less than 90 degrees). Rocks differing in composition but of equal resistance may occur in regions which have suffered intense metamorphism. Original differences in rock hardness tend to be obliterated by metamorphic action, and on such rocks there may develop a pattern essentially dendritic.

In the study area, the dentritic drainage pattern has been found in all basins which have similar lithological conditions especially in the upper parts of basins. (Fig. 2-8-A) shows the dentritic pattern in Wadi Abyad which has a fifth order, and is one of the tributaries in Wadi El-Aawag basin.

2.1.8.2. Trellis drainage

The essential characteristic of trellis drainage pattern in Catherine area (Wadi Firan) (Fig. 2-8-B) is the presence of secondary tributaries parallel to the master-stream or other stream into which the primary tributaries enter, these secondary tributaries are usually conspicuously elongated and approximately at right angles to the streams into which they flow.

The term (trellis) should not be applied where only one set of tributaries joins a master-stream at right angles; one may represent the beginning of dendritic or rectangular drainage. By contrast the trellis pattern implies a lattice effect which is furnished by the elongated parallel secondary tributaries (ZERNITZ, 1932).

Trellis drainage patterns look similar to their namesake, the common garden trellis. Trellis drainage develops in folded topography like that in the Qabaliat and Hadahid Mountains in the study area whereas short tributary streams enter the main channel at sharp angles as they run down besides of parallel ridges called anticlines.

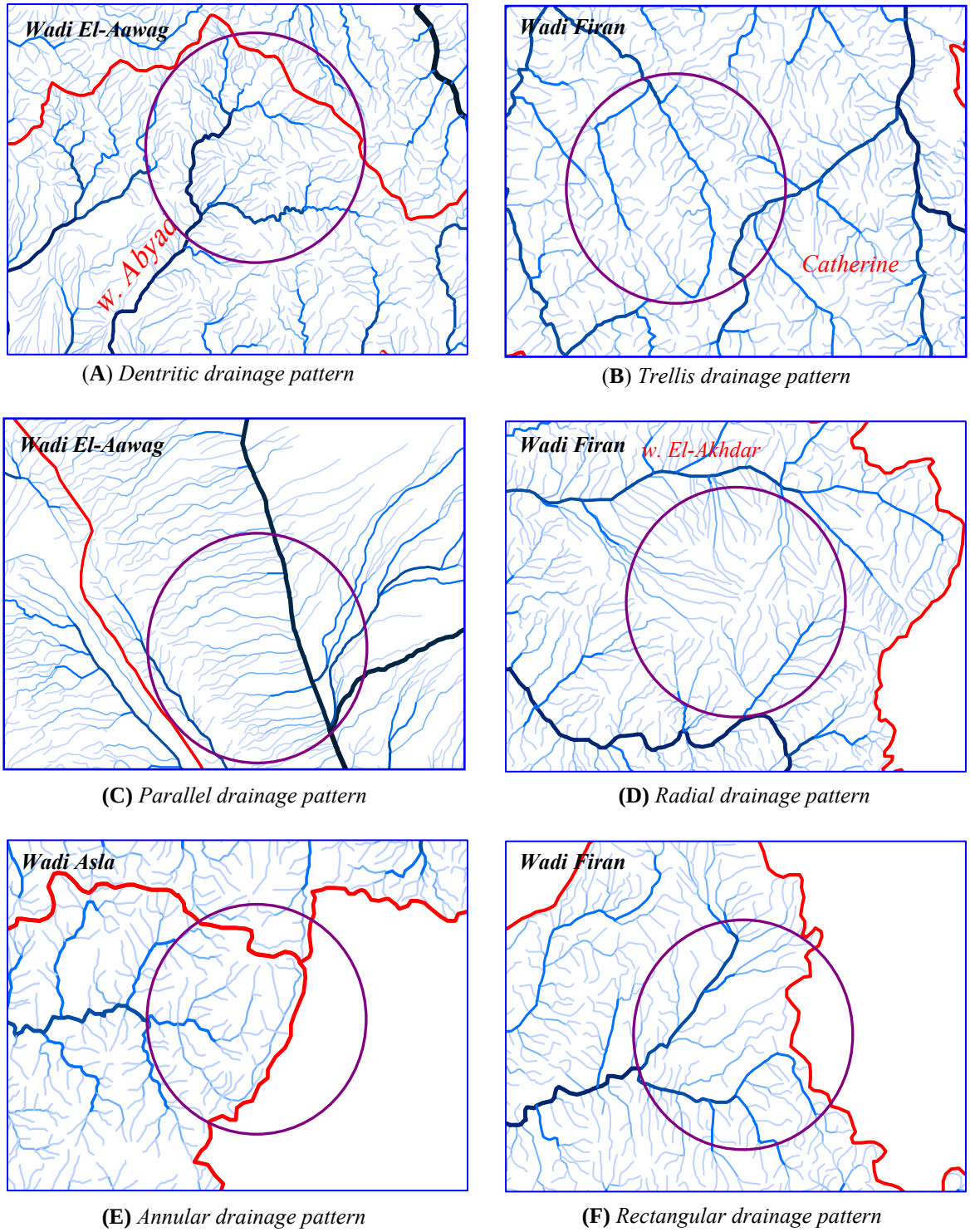

(**A**) *Dentritic drainage pattern*

(**B**) *Trellis drainage pattern*

(C) *Parallel drainage pattern*

(D) *Radial drainage pattern*

(E) *Annular drainage pattern*

(F) *Rectangular drainage pattern*

Fig (2-8) *The drainage patterns in main wadis networks of El-Qaà plain area*

2.1.8.3. Parallel drainage

Parallel drainage patterns form where there is a pronounced slope of the surface. A parallel pattern also develops in regions of parallel, elongate landforms like outcropping resistant rock bands. Tributary streams tend to stretch out in a parallel-like fashion following the slope of the surface. A parallel pattern sometimes indicates the presence of a major fault that cuts across an area of steeply folded bedrock. All forms of transitions can occur between parallel, dendritic, and trellis patterns.

The drainage pattern is called parallel (Fig. 2-8-C) when the streams over a considerable area or in a number of successive cases flow nearly parallel to one another. Parallel drainage implies either a pronounced regional slope or a slope control by parallel topographic features such as some tributaries of Wadi El-Aawag basin in Qabaliat Mountain area. Parallel streams may develop along parallel faults (in Wadi Firan); the streams etching out subsequent valleys along fault zones; or faulting may cause parallel "rift valleys" in which the consequent streams would be parallel.

2.1.8.4. Radial drainage

The radial drainage pattern develops around a central elevated point. This pattern is common to such conically shaped features as volcanoes. The tributary streams extend the headward reaches upslope toward the top of the volcano. All the streams do not necessarily flow away from each other in normal radial pattern. Individual streams may, owing to irregularities in the initial slope of dome or volcano, or to other causes, flow for parts of their courses obliquely toward each other.

A new lava flow may spread across several valleys and cause those parts of the drainage to unite. As erosion advances some of the streams may become tributaries of their more aggressive neighbors through capture. Gullies may develop on certain valley walls, then grow head-ward up the slope, and therefore nearly parallel to the main stream. These are all parts of the normal radial pattern (ZERNITZ, 1932). Numerous examples of radial drainage on un-breached domes and Mountains are given in the upper parts of the main basins i.e. Wadi Firan in El-Banat Mountain, and Akhsima Mountain (Fig. 2-8-D), Wadi El-Aawag in Madsus and El-Leada Mountains, Wadi Asala in Ramhan Mountain, and several other Wadis.

2.1.8.5. Annular drainage

Annular drainage pattern (Fig. 2-8-E), as the name implies, is ringlike in pattern. It is subsequent in origin and associated with maturely dissected dome or basin structures. The annular drainage pattern, like the trellis pattern, is an excellent illustration of the increasing influence of structure over slope as drainage approaches to maturity. Slope alone controls the initial courses of streams; structure and slope, the adjusted courses of maturity. The annular valleys carved out by subsequent streams on domes and basins will be separated from one another by rimming hogbacks, the outcrops of resistant strata (ZERNITZ, 1932).

The annular pattern develops most perfectly where erosion of the dome exposes rimming sedimentary strata of greatly varying degrees of hardness. The more fortunate subsequent streams will, furthermore, increase their length at the expense of less fortunate subsequents by extending their valleys headward in the soft rock which encircles the dome. Holding their own, in this struggle for survival, will be a few consequent master streams that have dug channels deeper than those of the piratical subsequents. Thus there results a series of subsequent streams which tend to assume a circular or annular pattern and a few trunk streams which are consequent in origin and radial in pattern.

2.1.8.6. Rectangular drainage

The rectangular pattern is characterized by right-angled bends in both the main stream and its tributaries. It differs from the trellis pattern by its greater irregularity, there is not such perfect parallelism of side streams. The latter ones are not necessarily as conspicuously elongated; and secondary tributaries need not being present. Structural control is prominent, as the pattern is directly conditioned by the right-angled jointing or faulting of rocks.

In addition, the rectangular patterns have a more ordered appearance than dendritic stream patterns. They typically develop in areas where streams flow along zones of weakened rocks adjacent to intersecting faults. Because of fault control, streams generally meet at right angles and have similarly shaped bends (SHERIEF, Y. 1999). Examples for this are the upper parts of Wadi Firan, Wadi El-Aawag, and Wadi Asla basins which are characterized by a lot of faults and joints, especially in the areas which are covered with Igneous rocks (Fig. 2-8-F).

It can be concluded from a previous discussion that:

- There are many drainage patterns in the study area because of variation of geological formations, which consist of sedimentary rocks in the northwestern El-Qaà plain area, and metamorphic, igneous rocks in the eastern part of the study area (Fig. 1-2).
- The structure geology has been played an important role to form the surface of the study area, i.e., faults and joints which were detected as rectangular positions to contribute a parallel drainage.
- The geomorphological stage has played a significant role to the occurrence of some consequent drainage patterns such as dendritic parallel pattern, whereas, the dendritic (first) drainage pattern is considered a preamble to form the parallel drainage pattern (second) with prescription. This means that the stage has played a main role to change types of drainage patterns.
- Finally, the drainage patterns are different from one place to another in the study area depending on variation of the slope, due to the fact that some particular drainage patterns have been jointed with a steep slope (parallel pattern); other patterns are correlated with soft slopes (radial pattern) http://museum.gov.ns.ca/mnh/nature/nhns/t3/t3-2

2.2. Morphometric analysis of basins

A drainage basin is an area where water from rain or snow melt drains downhill into a body of water, such as a valley, river, lake, dam, estuary, wetland, sea or ocean. The drainage basin includes both the streams that convey the water as well as the land surfaces from which water drains into those channels. The drainage basin acts like a funnel - collecting all the water within the basin area and channeling it into a waterway. Each drainage basin is separated topographically from adjacent basins by a ridge, hill or mountain, which is known as a water divide.

The morphometric analysis of the main basins in the study area depends mostly on measurements of these basins from topographic maps (large scale), areal photographs, photo maps, satellite images (TM, ETM, SPOT and SRTM), and field work measurements to make a data base which can be analyzed mathematically, geometrically, and statistically by means of different equations using remote sensing and geographical information systems.

Drainage basin is a system which is morphologically governed and geometrically characterized by some functional relationships. These relationships are determined by measuring the different elements which describe the basin as following:

2.2.1. Basins area

*2.2.2. Basins dimensions (*Length, width, and perimeters*)*

2.2.3. Basins shape

2.2.4. Basins surface

2.2.5. Correlation relationship between the elements of basins and networks

2.2.1. Basins area

Area characteristics are considered as one of the most important elements in the morphometric analysis of the stream systems. Strahler (1958) says that basins which have similar characteristics in area and form are also similar in their geomorphological characteristics. Shape and area are deeply related to the geomorphological processes and the geological characteristics of the studied area, in addition to the initial surface of the earth. It is of no doubt that these elements have a great influence on the drainage network and the topographic characteristics of the basin (AKL, 1994).

Tab. (2-7) *the average of orders area in the main basin and the correlation between them*

Orders / Wadis	first	second	third	fourth	fifth	sixth	seventh	Total area	R
w. Firan	0.31	1.6	3.2	25.6	136.2	320.4	998.5	**1918.5**	**0.794**
w. El-Aawag	0.34	1.7	4.5	28.4	168.8	368.4	870.3	**1982**	**0.817**
w. Araba	0.46	2.1	5.3	28.4	152.6	-	-	**338.2**	**0.801**
w. Asla	0.42	2.4	4.8	28.8	185	-	-	**601.1**	**0.786**
w. Timan	0.38	2.2	6.3	31.2	175	-	-	**399**	**0.799**
w. El-Mahash	0.36	2.1	4.4	27.4	150.5	227	-	**329.7**	**0.886**
w. Eghshy	0.31	2.1	4.1	24.6	163	-	-	**163.7**	**0.785**
w. Abu Markh	0.39	1.9	4.3	26	71	-	-	**88**	**0.872**
w. El-Taalby	0.24	1.8	4.5	22.4	103	-	-	**139.8**	**0.817**
w. Aat El-gharby	0.24	1.5	3.7	32.3	57	-	-	**117.8**	**0.910**

(Tab. 2-7) shows the total area of the main basins in the study area which were separated to ten main basins regarding every basin is as a geomophological unit. Wadi El-Aawag basin is considered the biggest basin 1982km^2, and Wadi Firan basin 1918.5km^2, but the smallest basin is Wadi Abu Markh basin 88km^2.

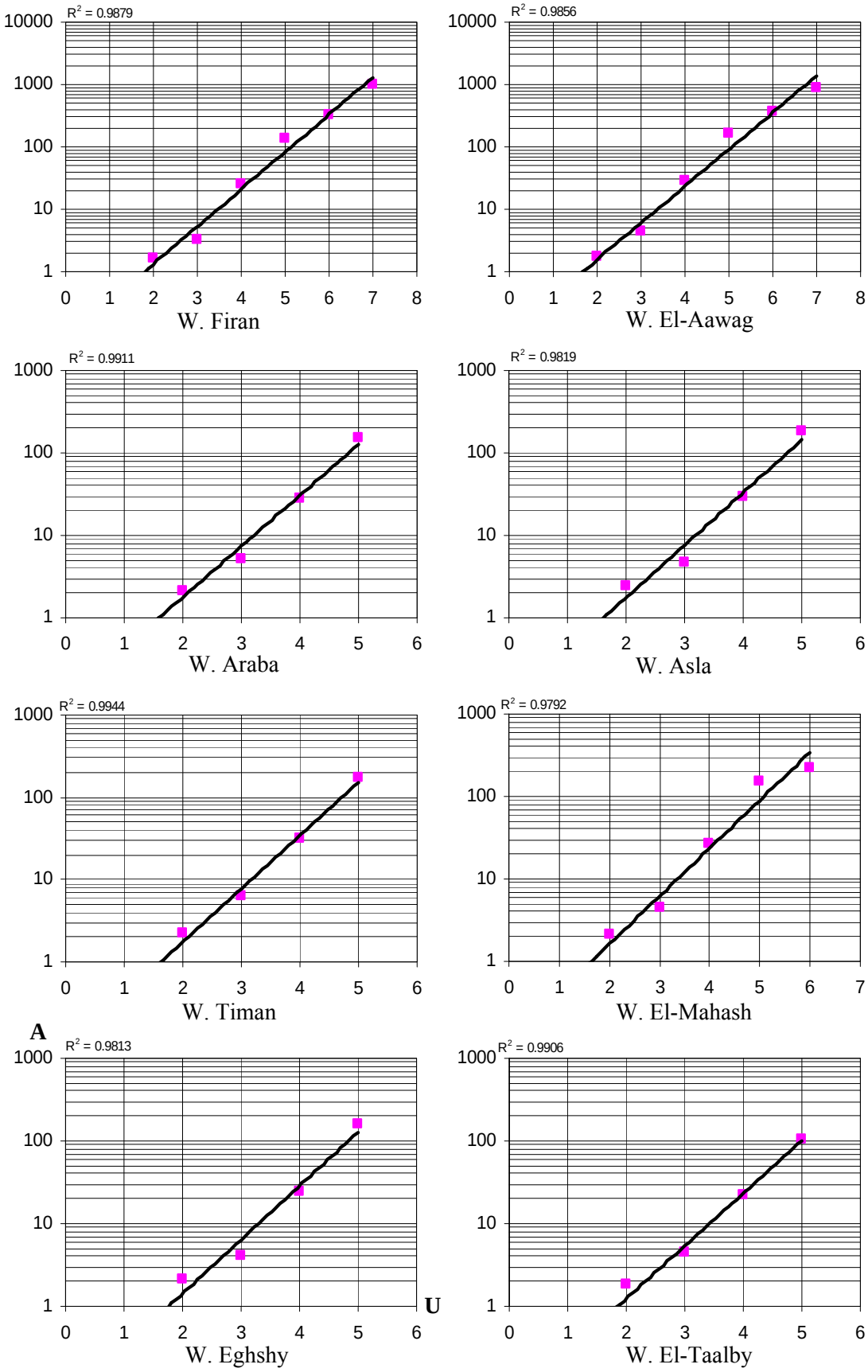

Fig (2-9) *The relationship between orders and the average area of orders in the main basins*

The averages of order areas are different from one basin to another in El-Qaà plain area ranging in the first order between 0.24 km in Wadi El-Taalby basin, and 0.46km^2 in Wadi Araba, whereas, in the second order, the average of area ranges from 1.5 km^2 in Wadi Aat El-gharby to 2.4 km^2 in Wadi Asla, while in the fifth order the area alternated between 57km^2 in Wadi Aat El-gharby, and 168.8km^2 in Wadi El-Aawag. Generally, the average basin area increases with the increase of the stream orders. It is quite logical because the geomorphological processes of the first order streams are focused on the vertical erosion saving the lateral erosion. In addition, the small areas indicate that the processes erosional by water are inactive in the area.

The relationship between the area and orders is a strong direct proportion which range between 0.910 in Wadi Aat El-gharby basin and 0.786 in Wadi asla basin. This means that whenever the order was increasing the average area of stream order increased directly.

2.2.2. Basins dimensions (Length, width, and perimeters***)***

2.2.2.1. Basin length, there are many ways to measure the basin length. The first is length in a straight line from the mouth of a stream to the highest point on the drainage divide of its basin (SCHUMM, 1936). The researcher followed Gardiner's method that depends on measuring the direct distance between the pouring point and the farthest point on the basin perimeter, avoiding having any portion of the line outside the basin limits (GARDINER, 1975).

Tab. (2-8) *the dimensions of the major basins in El-Qaà plain area*

element / Wadis	Length km (L)	Width km (W)	Permiter km (P)	L / W
w. Firan	79.1	27.4	337.9	2.9
w. El-Aawag	45.4	31.3	228.6	1.5
w. Araba	12.7	12.4	123.9	1
w. Asla	41.8	12.2	152.3	3.4
w. Timan	37.8	8.4	118.4	4.5
w. El-Mahash	37.7	8.2	110.9	4.6
w. Eghshy	22.1	6.4	69.4	3.5
w. Abu Markh	19.9	4.2	57.3	4.7
w. El-Taalby	21.4	6.4	63.1	3.3
w. Aat El-gharby	15.9	4.2	86.9	3.7

- *Source: Topographic map scale 1: 50 000 (digital), aerial photograph scale 1: 40 000, and ETM Image 2003, using Arc GIS and Erdas imagine programs.*

(Tab. 2-8) clarifies the length of the major basins in the study area, which is different from one basin to another due to differences of the area: slopes, lithology and structure. Wadi Firan basin is the longest basin 79.1km, whereas the shortest basin is Wadi Araba basin 12.7km.

2.2.2.2. Basin width, The main limitation of the width of a basin is the surface slope. If this is steep, the basin should be narrow; otherwise too much sediment movement will be needed to obtain level basins. Basin width is an important element to study the shape of basins and the ratio of L/W to determine the final shape of these basins (MULLER, 1974). At least, there are three possibilities to measure the width of a basin; the first is the average of some measurements of basin width, the second is the result of division of the basin area with the basin length, whereas the third way is to compare the maximum width of the basin with the maximum length in the basin.

(Tab. 2-8) shows that Wadi El-Aawag basin is the widest basin in the study area 31.3km, Wadi Firan 27.4 km. this average of width is relatively high because of the nature of rocks, i.e. limestones that were easily eroded. Therefore, the basins are formed as a result of vertical and lateral erosion. Especially process of lateral erosion increases in the Wadi El-Aawag basin and the lower part of Wadi Firan basin. But Wadi Abu Markh basin is considerd the narrowest basin in the study area whereas the width reaches only 4.2km.

2.2.2.3. Basin perimeter is considered as the main element of basin dimensions because it is used to compute a lot of elements in morphometric analysis i.e. basin shape, circulation ratio, compactness coefficient, and relief ratio. In addition, the basin perimeter is the total length of the drainage basin boundary which reflects the geomorphological stage of basins. It can be measured by following the dividing line between the basin and the other neighboring basins. Wadi Firan basin comes in the top of basin where its length reaches to 337.9km, followed by Wadi El-Aawag basin 228.6km. Wadi Abu Markh basin has the lowest length of perimeter 57.3 km (Tab. 2-8).

Generally, it is obvious that the perimeters of the main basin in the study area have a lot of zigzags related to the effect of structure especially, so in the basins which are covered by soft rocks (sedimentary rocks): Wadi El-Aawag basin and Wadi Araba basin.

2.2.3. Basins shape

The shape, or outline form of a drainage basin, as it is projected upon the horizontal plane of a map is another factor affecting the stream discharging characteristics. As explained above, long narrow basins with high bifurcation ratios would be expected to have attenuated flood- discharge periods, whereas rotund basins of low bifurcation ratio would be expected to have sharply peaked flood discharge (STRAHLER, 1964). Circular basins produce larger floods than longitudinal watersheds if they are of similar sizes. This is obvious because a shorter time of accumulation of the flood is expected. Generally, the shape of basins is related with amount of discharge, velocity, Peak of runoff and log time (SALEM, A. 1989).

The shape of basin is described by some elements such as:

2.2.3.1. Elongation ratio

2.2.3.2. Circularity ratio

2.2.3.3. Form coefficient

2.2.3.1. Elongation ratio (***Re***), was defined for Schumm (1956) as the ratio between the diameter of circle with the same area basin (D) and the basin length (L). This ratio runs between 0.6 and 1.0 over a wide variety of climatic and geologic types. Values near to 1.0 are typical of regions of very low relief, whereas values in the range 0.6 to 0.8 are generally associated with strong relief and steep slopes (STRAHLER, 1964).

The elongation ratio is calculated by using the following formula:

$$\mathrm{Re} = \frac{D}{L} = 1.128\,\frac{\sqrt{A}}{L}$$

Where ***A*** is area of basins, ***L*** is basin length, and ***1.128*** is a constant (MESA, L. 2006).

Tab. (2-9) *Elongation ratio of the main basins in El-Qaà plain area*

Basins	w. Firan	w. El-Aawag	w. Araba	w. Asla	w. Timan	w. El-Mahash	w. Eghshi	w. Abu Mark	w. El-Taalby	w. Aat El-Gharb
Elongation Ratio	0.31	0.55	0.81	0.33	0.30	0.27	0.33	0.27	0.31	0.38

- *Source: Digital maps and ETM, Spot Images*

(Fig. 2-10) and (Tab. 2-9) clarify the elongation ratios of the major basins in the study area which run between 0.27 and 0.81. These values can be divided into three categories as:

- The first category less than 0.30, which contains Wadi El-Mahash basin and Wadi Abu-Markh basin 0.27. This means that these basins are near from elongation and far from circulation.

- The second category ranges between 0.30 and 0.60; it contains most basins in the study area (Fig. 2-9), whereas Wadi El-Aawag basin is relatively far from elongation, but the other basins are near from elongation such as Wadi Firan basin 0.31 and Wadi Timan basin 0.30.

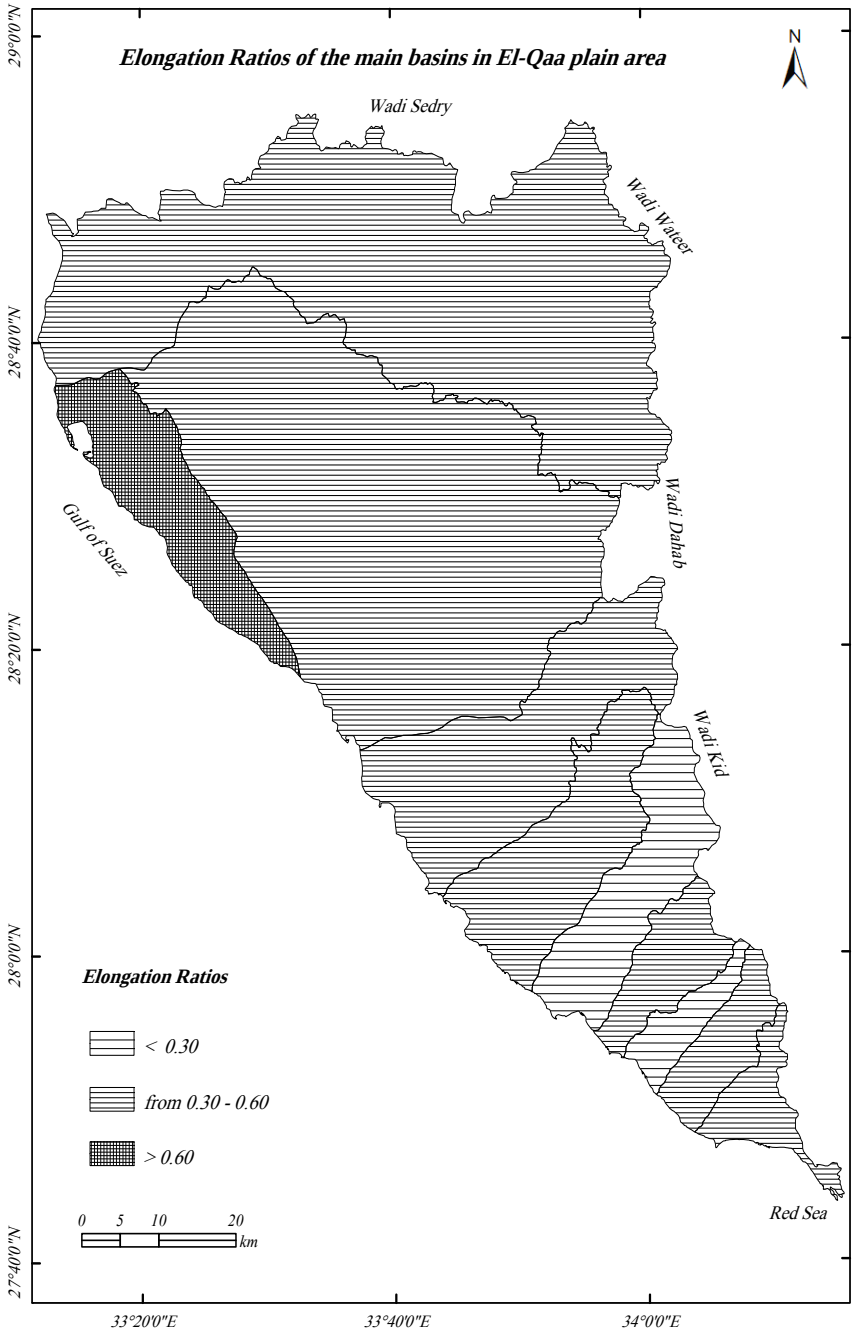

- The last category more than contains only one basin (Wadi Araba basin) 0.81, this value mostly associated with strong relief, the type of geological formations and steep ground slopes.

Fig (2-10) *Elongation ratios of the major basins in the study area*

2.2.3.2. Circularity ratio (***Rc***), the circularity ratio (MILLER 1953; STRAHLER 1964)is expressed as the ratio of the basin area (A) and the area of a circle with the same perimeter as that of the basin (P) :

$$\mathrm{R}\,c = \frac{4\pi A}{P^2}$$

Where ***Rc*** is basin circularity, ***P*** is basin perimeter, ***A*** is area of the basin and ***4*** is a constant.

Tab. (2-10) *Circularity ratios of the major basins in El-Qaà plain area*

Basins	w. Firan	w. El-Aawag	w. Araba	w. Asla	w. Timan	w. El-Mahash	w. Eghshi	w. Abu Markh	w. El-Taalby	w. Aat El-Gharby
Circularity Ratios	0.21	0.48	0.28	0.33	0.36	0.34	0.43	0.34	0.44	0.20

- Source: Digital maps and ETM, Spot Images

(Tab. 2-10) and (Fig. 2-11) show that the circularity ratios in the study area vary from one basin to another rangeding from 0.20 in Wadi Aat El-Gharby basin and 0.21 in Wadi Firan basin, whereas the more values of circularity decrease the more a basin is far from regular shape the more circularity values increase the more a basin is near of the regular shape. In the study area, Wadi El-Aawag basin is the nearest basin to regular shape while its values are considered the biggest values reaching to 0.48.

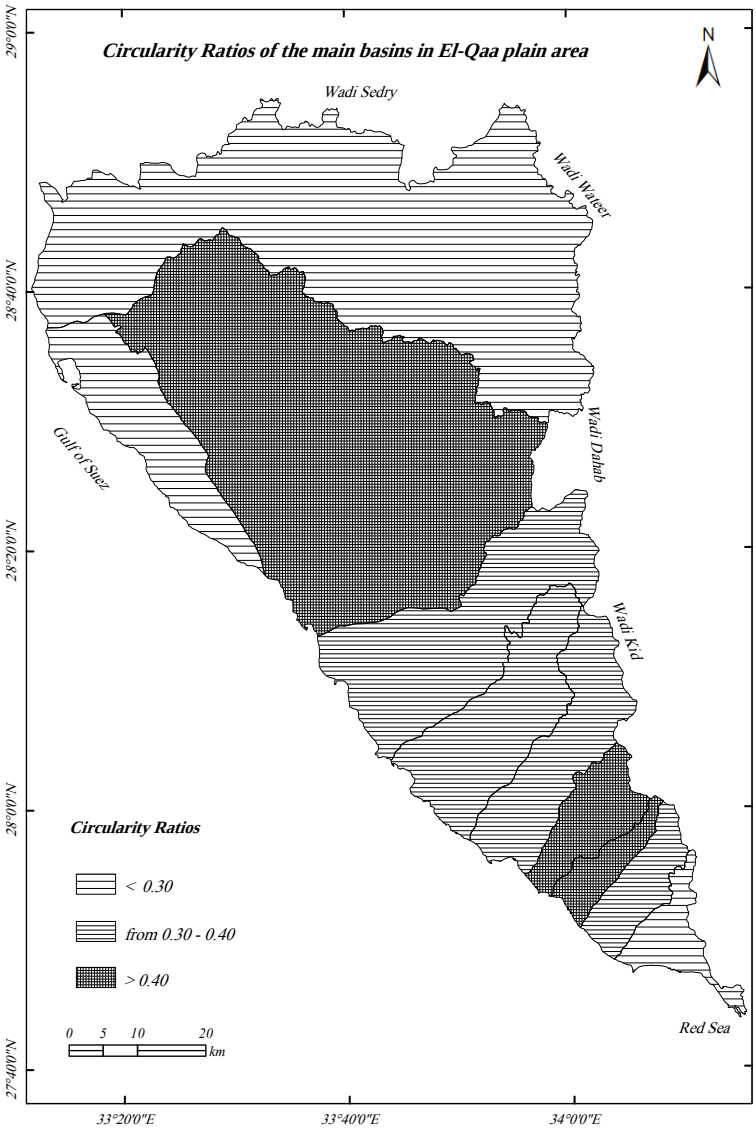

Fig (2-11) *Circularity ratios of the major basins in the study area*

2.2.3.3. Form coefficient shows the relationship between the length and the width of basin and is computed with Horton's formula (1932):

$$Cf = \frac{A}{L^2}$$

Where ***Cf*** is form coefficient, ***A*** is the area of basin, and L^2 is the square of length of basin. The low values make evident that the area of basin is small, and the shape is near to the triangular or longitudinal shape; the high values show that the basin is near to square or circular shape.

Tab. (2-11) *Form coefficient of the major basins in El-Qaà plain area*

Basins	w. Firan	w. El-Aawag	w. Araba	w. Asla	w. Timan	w. El-Mahash	w. Eghshi	w. Abu Markh	w. El-Taalby	w. Aat El-Gharb
Coefficient Shape	0.30	0.96	1.2	0.34	0.27	0.23	0.33	0.22	0.30	0.46

- Source: Digital maps and ETM, spot images

From Tab. 2-11 it seems that the values of coefficient shape range from 1.2 in Wadi Araba basin, 0.96 in Wadi El-Aawag basin and 0.22 in Wadi Abu Markh basin. These values reveal that both Wadi El-Aawag basin and Wadi Araba basin are the nearest basins to regular shape because of the type of geological formations. By contrast, Wadi Abu Markh basin and Wadi Timan basin are near to the longitudinal shape.

Schumm, (1956) noticed that the relationships between basin shape and drainage density are less clear, but after early variations in which the basin is close to circular shape the influence of increased relief is obvious and the elongation ratio decreases to a constant of about 0.5 representing 40 percent mass removal and indicating that the basin maximum length is twice the diameter of a circle of the same area.

Generally, structure conditions have played the main role by changing the shape of basins, especially in the southern basins of the study area which is mostly covered by metamorphic and igneous rocks, whereas the hydrologic and climatic conditions in this area are strongly limited. But north basins (Araba, El-Aawag) have been affected by hydrologic and climatic conditions compared with structure condition (faults, joints and folds) and geomorphological stage.

2.2.4. Basins surface

It includes the study of the following elements:

2.2.4.1. Relief ratio

2.2.4.2. Relative relief

2.2.4.3. Ruggedness value

2.2.4.4. Slope

2.2.4.5. Hypsometric curve

2.2.4.1. Relief ratio (Rr), is defined as the ratio between total basin relief, the maximum elevation difference within the catchments, and basin length, measured as the longest dimension of the drainage basin (SCHUMM, 1956). It can be computed by using Schumm's equation (1963):

$$\mathrm{R}\,r = \frac{R}{L}$$

Tab. (2-12) *Relief ratio, relative relief and ruggedness value of the major basins in El-Qaà plain area*

element / Wadis	Relief ratio	Relative relief	Ruggedness value
w. Firan	33.3	7.8	1.4
w. El-Aawag	57.4	11.4	1.3
w. Araba	46.5	4.8	0.24
w. Asla	57.7	15.8	0.96
w. Timan	64.5	20.6	0.78
w. El-Mahash	63.7	21.6	1.2
w. Eghshy	61.4	19.5	0.59
w. Abu Markh	77.8	27	0.65
w. El-Taalby	67.9	23.	0.74
w. Aat El-gharby	69.1	12.6	0.44

- Source: Digital maps and SRTM image

Tab (2-12) and Fig. (2-12) show that Wadi Firan basin registers the lowest relief ratio among all other basins (33.3m/km), followed by Wadi Araba basin (46.5m/km), then Wadi El-Aawag basin (57.4m/km), whereas Wadi Abu Markh basin register the highest ratio in relief (77.8m/km). This means that basins of bigger area and of more length are getting more effective erosion processes than basins of lesser area and of lesser length. This shows furthermore that with the development of the erosional cycle, the surface of the valley is subjected to degradation in ratio with an increase in length towards the high springs.

As a result, the values of relief ratio decrease. As for the relief ratio in Wadi Abu Markh basin has been registered 77.8m/km which is related to the fact that the erosion factor has not been strong enough to lower down the basin surface.

Besides, the headward erosion actions have not been active. Consequently, the length of the basin has been little which is reflected on the relief ratio.

According to HADELLY AND SCHUMM, 1961 there is a direct relation between relief ratio and accumulated sediments in small basins in Arizona. They found other factors included in this relation like the power of runoff and the amount of sediments. But MORISAWA (1962) had found an inverse relation between the hydrology of basin and stream gradient, circularity, and relief ratio.

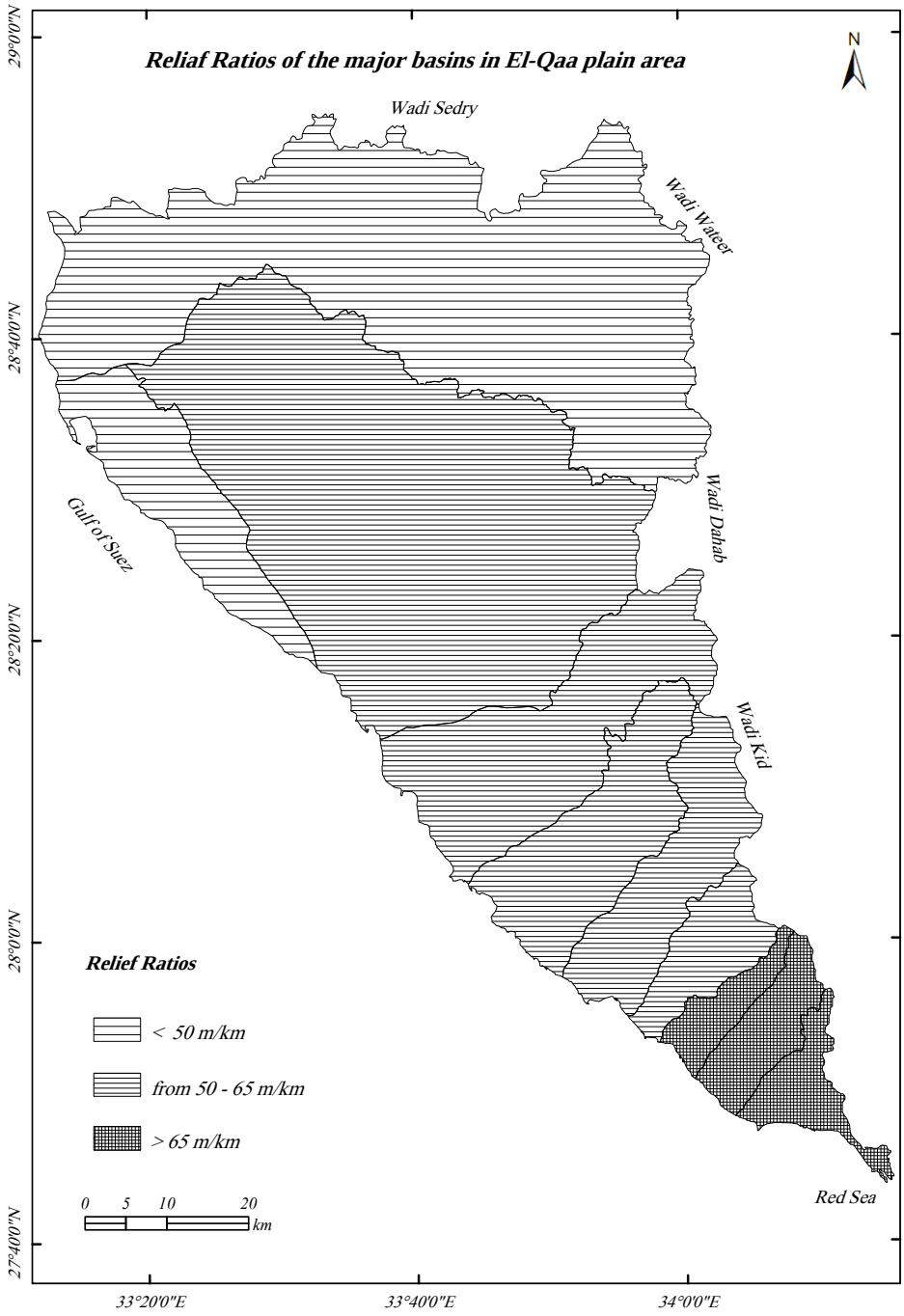

Fig (2-12) *Relief ratios of the major basins in the study area*

2.2.4.2. Relative Relief (Ri is defined as the ratio between total basin relief, the maximum elevation difference within the catchments, and basin perimeter. Relative relief is the difference between summit level, the highest altitude for a given area, and base level, lowest altitude for a given area. Relative relief can be used as an index of the relative velocity of vertical tectonic movements *http://iflorinsky.narod .ru/rr.htm*. It can be computed by Melton's formula (1957):

$$\mathrm{R}\ i = \frac{R}{P}$$

Where as **Ri** is the relative relief, ***R*** is the maximum elevation, and ***P*** is perimeter of basin.

The values of relative relief are different from one basin to another in the study area, whereas it ranges from 4.8m/km in Wadi Araba basin, and 27 m/km in Wadi Abu Markh basin (Tab. 2-12), these values can be distributed into three categories:

- The first category (less than 10m/km) contains Wadi Firan basin and Wadi Araba basin (Fig. 2-13).
- The second category (from 10-20m/km) consists of four basins like Wadi ElAawag basin and Wadi Eghshy basin
- The last category (more than 20m/km) includes also four basins such as Wadi Timan basin and Wadi El-Taalby basin (Fig. 2-13).

The previous values of relative relief show that if the value increases gradually every time the area decreases until it reaches 27m/km in Wadi Abu Markh. This means that basins with large areas underwent a faster progress in erosion actions than the basins with small areas. This relation is mostly perfect between relief ratio and relative relief (0.95) because they both confirm the fact that with the progress of the erosional cycle their values decrease (AKL, 1994)

Due to the fact that basins of large areas possess a bigger number of tributaries (Wadi Firan- Wadi El-Aawag) they help to create a drainage network which accelerates the development of these basins compared with that of smaller basins. There is a converse relation between relative relief and rock resistance against erosional forces in fixed climatic conditions, where the values of relative relief decrease according to the increase of rock resistance. But this is not the only powerful factor, because the degree of slope of the original surface, where streams flow in its valleys has a clear influence on the increase of the erosion power and hence on the degradation of the surface (SCHUMM, 1954).

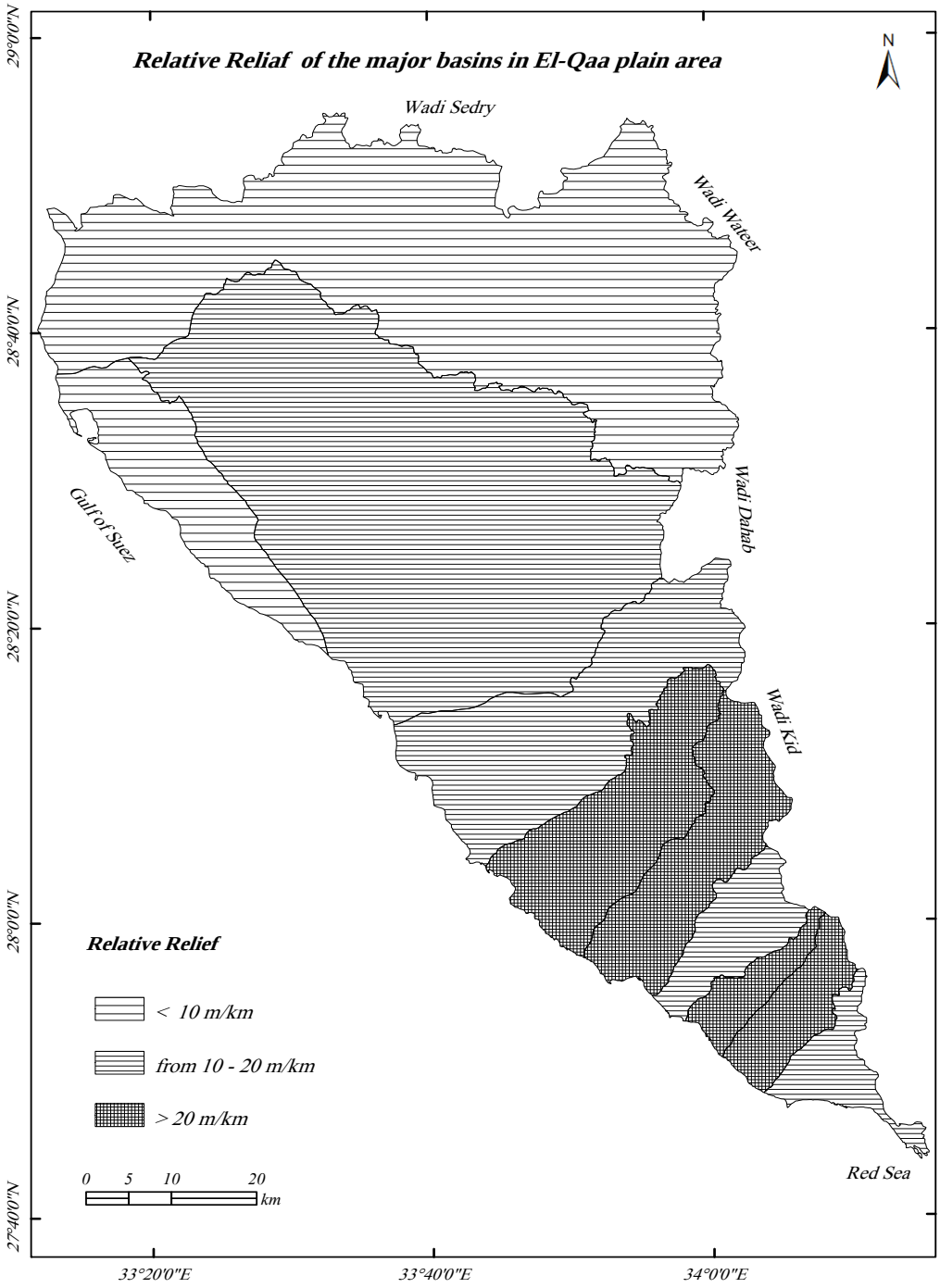

Fig (2-13) *Relative relief of the major basins in the study area*

2.2.4.3. Ruggedness Value is estimated by multiplying the basin relief by the drainage density and therefore this is a dimensionless number. As its name suggests, ruggedness indicates the extent to which the topography of a landscape is dissected, and it represents the outcome between erosional and depositional processes. Furthermore, rugged landscapes tend to have a high degree of connectivity between hillslopes and channels, suggesting a high potential for sediment delivery.

This factor shows the relation between the basin relief and both length of its drainage network and the area of basins; it can be computed by the low of DOORNKAMP and KING 1971:

$$\mathrm{R}v = \frac{Ri \times Dd}{5280(\text{constant})}$$

Where **Rv** is ruggedness value, ***Ri*** is relative relief, ***Dd*** is drainage density, and 5280 is a constant

Applying this factor on the basins of the study area, it has been shown that all their values range between 0.24 in Wadi Araba basin and 1.4 in Wadi Firan basin (Tab. 2-12), due to the area and length of basin. These factors play the main role to increase or decrease the values, but it has been noticed that the basin with has the smallest area (Wadi Abu Markh basin) has a relatively big value of ruggedness 0.65.

The heightening of ruggedness value in the area means that the area has made good progression in the erosional cycle by the way that the Young stage has came to an end reaching the mature stage. This stage is characterized by the increase of the value of ruggedness because the stream will be in dissension between vertical and lateral erosion all the way on its basin length. Lands then will be divided among low areas covered by the stream and high areas that are not influenced by erosional forces (AKL, 1994). This is contrary to both, the young stage and the old stage. The basin lands have been high in the first stage and low and flat in the second because of the processes of deposition.

2.2.4.4. Surface Slope

The slope is the rate of rise or fall against horizontal distance. It may be expressed as a ratio, decimal, fraction, percentage, or the tangent of the angle of inclination. The concept of measuring slopes from a topographic map is a familiar one for most professionals in the landscape planning/surveying professions. Slope is a measurement giving the steepness ground surface. Slope is measured by calculating the tangent of the surface. The tangent is calculated by dividing the vertical change in elevation by the horizontal distance.

Slope gradient is a key factor influencing the relative stability of a slope. It determines the degree to which gravity acts upon a soil mass. Slopes are often irregular and complex, with gradients varying greatly throughout a given profile. Each slope profile section should be treated as a separate management and restoration site unit.

The gradient of slopes is calculated from a 3 x 3 cell window as shown below. The window below represents the eight neighboring elevations (Z) surrounding the cell at column i row j. (Fig. 2-14) shows the window (kernel) used for computing derivatives of elevation matrices. This 3x3 window is successively moved over the map to give the derivatives of slope and aspect. In addition, maximum slope is calculated from the maximum gradient of 8 neighbors. NB. Arc View calculates by slope this way with the result given in degrees. Maximum downhill slope is calculated from the maximum gradient of the cell or cells which are less or equal in elevation to the central cell. If there is no downhill neighbor the cell is assigned a value of -1.

Zi-1, j+1	***Zi, j+1***	***Zi+1, j+1***
Zi-1, j	***Zi, j***	***Zi+1, j***
Zi-1, j-1	***Zi, j-1***	***Zi+1, j-1***

Fig (2-14) *The window used for computing derivatives of elevation matrices, after* (http://www.sli.unimelb.edu.au/gisweb/DEMModule/DEM_T_Sl. Htm).

If average slope is requested, east-west gradients are calculated as follows

$$dEW = [(Zi+1,j+1 + 2Zi+1,j + Zi+1,j-1) - (Zi-1,j+1 + 2Zi-1,j + Zi-1,j-1)]/8dX$$

The north-south gradient is calculated by

$$dNS = [(Zi+1,j+1 + 2Zi,j+1 + Zi-1,j+1) - (Zi+1,j-1 + 2Zi,j-1 + Zi-1,j-1)]/8dy$$

Where dx = the east-west distance across the cell (cell width) and dy = the north-south distance across the cell (cell height)

The previous system is considered being one of the best techniques to compute the slope surface and degree (DEM Module) from satellite images, especially SRTM image (The Shuttle Radar Topography Mission). This method was followed in El-Qaà plain area using ARC-GIS program, a special module for analyzing slope degrees. These range between 0º and 85º (Fig. 2-15), whereas the low values (0º-20º) are found in Wadi bottoms, alluvial fans, and the lower parts of pediment areas. The middle values (20º-45º) expand in the upper parts of pediments, Qabalialt Mountain and the north eastern part of Wadi Firan. The high values (more than 45º) are found in the belt of igneous and metamorphic rocks which have many escarpments. Examples are the upper parts of basins such as of Wadi Asla, Meiar, El-Taalby, El-Mahash, and Abu Markh (Fig. 2-15).

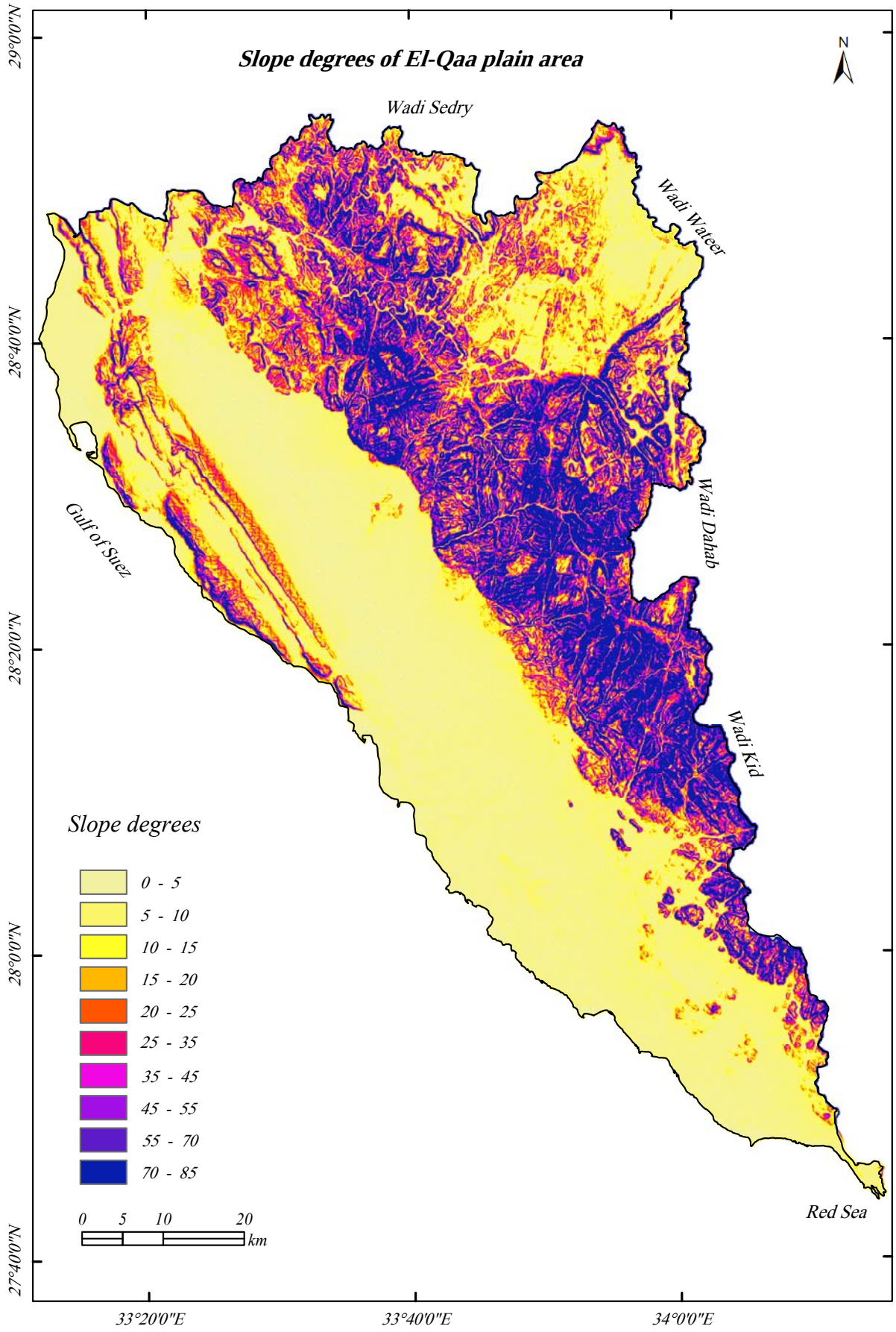

Fig (2-15) *Slope degrees for the surface of El-Qaà plain area, using SRTM (90m) image*

2.2.4.5. Hypsometric Curve

A hypsometric curve is a simple graph showing the proportion of land area that exists at various elevations by plotting relative area against relative height. It was first used in fluvial geomorphology when LANGBEIN et al. (1947) employed hypsometric (area-altitude) analysis to express the overall slope of selected drainage basins. The hypsometric curve had often been used throughout the 1950's (STRAHLER, 1952; MILLER, 1953; SCHUMM, 1956). Then, the curve and its integral were incorporated into research dealing with erosional topography.

Differences in hypsometric curves between various landscapes arise because the geomorphic processes that shape the landscape may be different. The hypsometric curve may also be shown as a continuous function and graphically displayed as an x-y plot with elevation on the vertical or ordinate axis and an area above the corresponding elevation on the horizontal or abscissa. The curve can also be shown in non-dimensional or standardized form by scaling elevation and area by the maximum values. The non-dimensional hypsometric curve alloowes hydrologists and geomorphologists to assess the similarity of watersheds, but it is only one of several characteristics.

Stages of youth, maturity, and old age in regions of homogeneous rocks give a distinctive series of hypsometric forms, but, mature and old stages give identical curves unless monadnock masses are present. In general, drainage basin height, slope steepness, stream channel gradient, and drainage density show a good negative correlation with mean integrals. Lithologic and structural differences between areas or recent minor uplifts may explain certain curve differences.

Fig. 2-16 shows that the all basins in the study area are within the mature stage according to Strahler's classification (1952), whereas all values are less than 40%. Wadi Aat El-Gharby basin has the lowest value of stable mass (14%) and 86% of basin surface are eroded, followed by El-taalby basin (16%), while the stable mass of Wadi Firan basin reaches to 37%. It is noticed also that more than 65% of basin areas lie at elevations lower than 500m a.s.l., for El-Aawag basin these are 66.3%, 62.9 % for Firan basin, and 63.3% for El-Mahash basin. Asmaller percentage of basin areas (nearly 35%) lies between 500m and 2500m a.s.l. giving evidences for the mature stage of the study area.

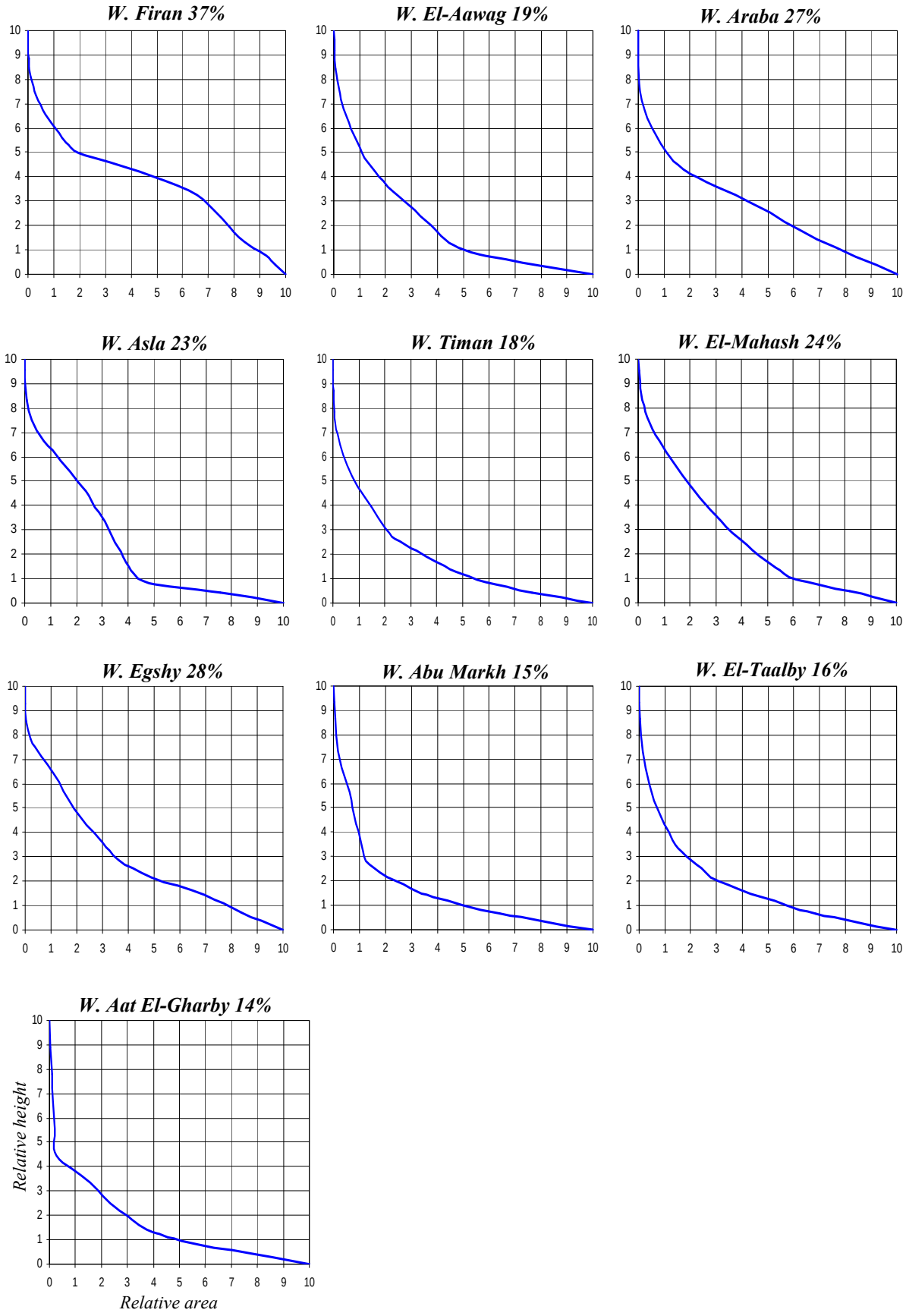

Fig (2-16) *Hypsometric curves for the major basins in El-Qaà plain area*

2.2.5. Correlation relationship between the elements of basins and networks

From morphometric analysis of the drainage networks with all their different elements like area, shape, and basin surface, we can make a correlation matrix between the elements of the network and the basin characteristics (Tab. 2-13). In this matrix, depending on the strong relation whether positive or negative, the weak relations between these elements were skipped.

Tab. (2-13) *Correlation matrix between morphometric characteristics of drainage basins and their network*

	A	***L***	***W***	***P***	***Rv***	***U***	***Nu***	***Dd***	***Tr***
Area (**A)**	1	0.77	0.98	0.91	0.73	0.90	0.99	-0.69	0.95
basin length (**L)**		1	0.66	0.86	0.86	0.75	0.80	0.66	0.68
Basin width (**W**)			1	0.88	0.62	0.87	0.96	0.66	0.66
Basin perimeter (**P**)				1	0.69	0.82	0.93	0.70	0.70
Ruggedness value (**Rv**)					1	0.83	0.74	0.72	0.76
Orders (**U**)						1	-0.92	-0.88	0.92
Stream numbers (**Nu**)							1	0.74	0.94
Drainage density (**Dd**)								1	0.64
Texture ratio (**Tr**)									1

It could be noticed from this matrix that:

- The area has a strong positive relation with each stream number (0.99), basin width (0.98), texture ratio (095), basin perimeter, and basin length, but this relation is negative between the area and drainage density (-0.69). Whereas, the more the basin area the more basin dimensions and decrease of the drainage density.
- The relation is positive between basin dimensions (length, width, and perimeter) and such of area, stream numbers and length, and ruggedness value. The increase in the basin dimensions has been early followed by an increase in the area as a direct result of the increase in stream number and their length (Tab. 2-13).
- the combination between basin dimensions is of a negative correlation in spite of their frequency, drainage density, elements of the basin shape (elongation and circulation) and the surface factors (relief ratio and relative relief), where the increase in basin dimensions lead to a decrease in the basin surfaces and thus to a decrease in values of relief ratio.
- The stream orders have a strong negative correlation with stream numbers (-0.92), drainage density (-0.88), and texture ratio (-0.92).

2.3. Morphometric analysis of alluvial fans

Alluvial fans are depositional landforms which occur where confined streams emerge from mountain catchments into zones of reduced stream power. An abrupt reduction in stream location (BULL, 1979), and here fans may be built up progressive deposition, especially of the course fraction of stream's sediment load. The gross topography of mountain fronts may be tectonically or erosionally controlled. At faulted mountain fronts, alluvial fans sediments may from part of thick sequence of sedimentary basin-fill deposits, but at erotsionally controlled mountain fronts the fan deposits may be thinner, burying former erosional pediment surface. In both situations the alluvial fans form a transitional environment between mountains and plain photo (2- 1)

Alluvial fans generally have a conical surface form with slopes radiating away from an apex at the point where the stream issues fro the mountain catchment. some fans, especially along active faults, may have asingel stream source at the apex; others, especiallz where pedimentation has occurred prior to burial bz the fan deposits, or where the fan sediments have backfilled into the mountain cachment maz have more complex multiple sources. The relationships between the stream channels and fan surface reflect the erosional/ depositional behavior of system as a whole. Withen the mountain source area the stream network has a conventional tributary pattern of channels which issue as one channel onto the fan suface (HARVY, M. 1997).

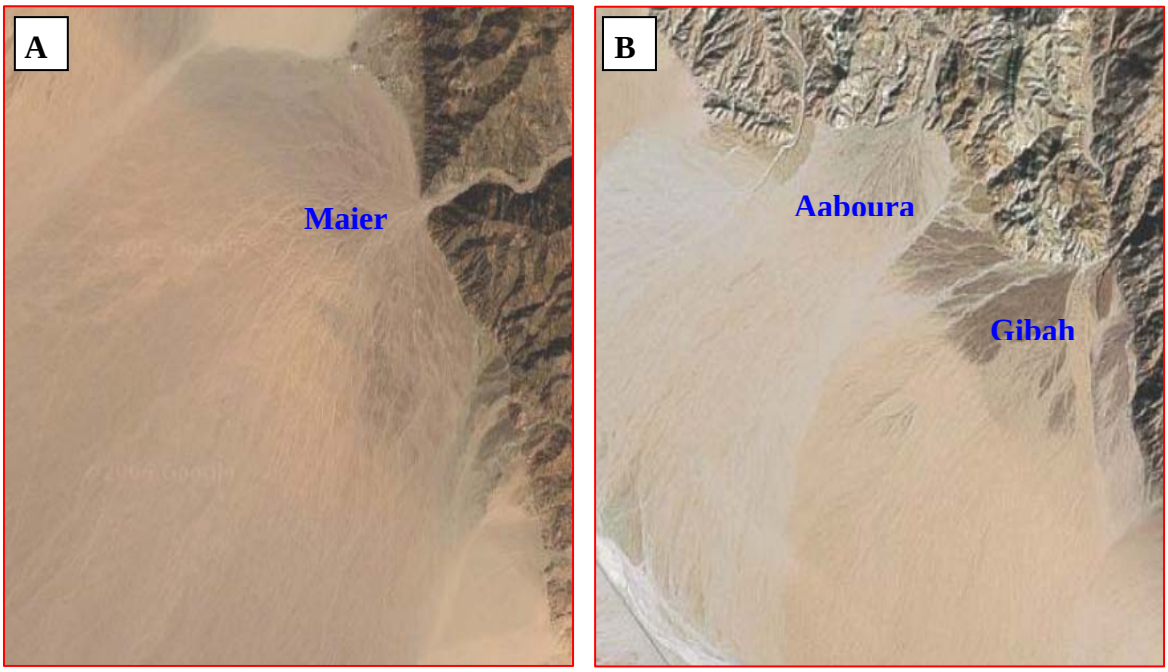

Photo (2- 1) *shows topographic relationship with alluvial fan forms (a) Meiar alluvial fan, (B) switching and successive fan surface age of two alluvial fans (Wadi Gibah and Wadi Aaboura).*

Alluvial fans in a various physiographic environments are particularly abundant in structurally disturbed regions. According to the main depositional process (HARVEY, 1984) they can be classified as debris-flow or fluvial dominated fans (KOSTASCHUK et al., 1986). Fans of intermediate depositional type are also common (Harvey, 1990). Based on the position with respect to the source area, fans can be described as valley side or mountain front fans (HARVEY, 1988). The latter are very well developed in places, where the mountain front correlates with a tectonically active mountain chain. Alluvial fans can be single (BULL, 1977) or coalesce into a continuous depositional belt, i.e., like El-Qaà plain, which has developed at the foot of the high front of south Sinai Mountains.

The availability of altitude data in digital format and the possibility of constructing digital elevation models (DEMs) that faithfully represent the landscape at a given scale, provide us new tools for quantitative analyzing topography (PIKE, 1993). A review of the literature has shown that no attempt has been made in using DEMs to characterize alluvial fans. We describe the methodology to prepare a detailed DEM for a large part of the Southern Sinai, as well as the construction of digital morphometric maps which have been used to identify and to map in total 22 alluvial fans

Boundaries of alluvial fans, shown by subtle changes in terrain gradient and aspect, were recognized and mapped using a set of digital derivatives of altitude and shaded-relief. Fan boundaries were drawn interactively on the shaded relief image displayed on the computer screen, and successively adjusted locally to match the spatial distribution of slopes (Fig. 2-17), local relief and curvature (both plan and profile), and the location of braided and meandering channels.

Fan boundaries were distinct in the upper part, where slopes are steeper (0.5° to 2.1°), but much more difficult to map in the lower part, where the transition of distal-fan to external-plain is defined by very subtle changes in slope (0.5° to 1.5°). In this area the definition of boundaries was subjective. For each of the 22 fans we computed a set of geometrical (i.e., length, perimeter, area,) and morphometrical (i.e., descriptive statistics of altitude, relief and slope) criteria (Tab. 2-14). Fan area and perimeter were automatically computed in vector format. Fan length was measured interactively from digital maps. Altitude, relief and terrain gradient statistics were computed from the altitude matrix.

Both the geometric and morphometric analyses were carried out individually for all fans as well as for their source areas.

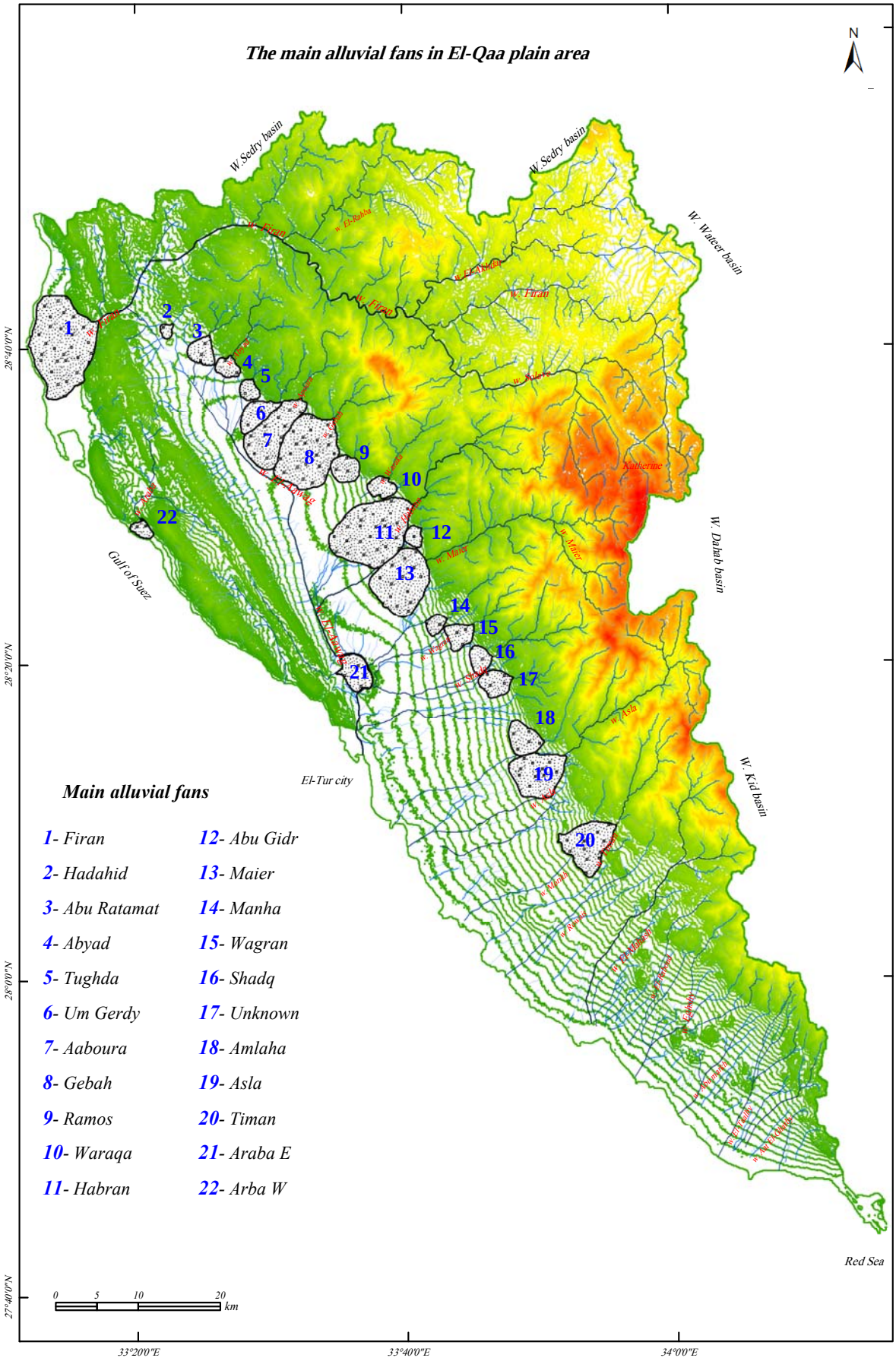

Fig (2-17) *The main alluvial fans in El-Qaà plain area.*

2. 3.1. Alluvial fan area and slopes

Fans area ranges from a few 2.1 to 69.3 of square kilometres with an average value exceeding 18.5 km^2. The largest mapped fans are Firan (69.3 km^2) and Habran (58.5 km^2). Fan length, measured along the steepest gradient (i.e., at right angle to contour lines), from the apex to the distal boundary contacting the external plain, varies from Hadahid with 1.8 km to Habran with 11.4 km. Within the mapped features, altitude ranges from sea level at Araba W fan to 520 m at Timan fan.

Tab. (2-14) *Geometrical and morphological parameters for the main alluvial fans in the study area*

Fan Name	Fan area (Km^2)	Perimeter (km)	Length (km)L	Elevation range (m)H	Slope (°)	H / L	Basin area *(Km^2)*
Firan	69.3	3.9	9.2	98	0.6	0.012	1908
Hadahid	2.1	5.7	1.8	35	1.1	0.019	12
Abu Ratamat	8.1	11.1	3.4	72	1.2	0.021	37
Abyad	5.4	9.2	2.5	75	1.7	0.03	53
Tughda	4.6	8.1	2.5	47	1.1	0.019	25
Um Gerdy	11	14.4	5.9	86	0.8	0.015	28
Appoura	30.6	24.8	9.6	220	1.3	0.023	37
Gebah	49.4	27.4	9.2	255	1.6	0.028	55
Ramos	8.8	10.9	3.4	75	1.3	0.022	23
Waraqa	6.5	10.3	2.5	65	1.5	0.026	53
Habran	58.5	29.7	11.4	280	1.4	0.025	152
Abu Gidr	4.1	7.8	2,4	80	1.9	0.033	15
Maier	39.5	23.6	7.3	165	1.3	0.023	231
Manha	3.4	8.1	2.8	92	1.8	0.033	27
Wagran	8	11.5	3.6	115	1.8	0.032	31
Shadq	6.4	9.6	2.7	90	1.9	0.033	77
Unknown	9.5	11.9	3.9	130	1.9	0.033	37
Amlaha	12	13.3	4.1	85	1.2	0.021	47
Asla	27.5	20.4	6.9	195	1.6	0.028	601
Timan	26.5	22	6.5	235	2.1	0.036	399
Araba E	12	14.3	4.3	35	0.5	0.008	338
Arba W	3.9	8.1	2.1	43	1.2	0.020	702
average	**18.6**	**14.4**	**5**	**117**	**1.4**	**0.023**	**222.18**

- Sourse: The values were measured from ASTER image (15m), SRTM image (90m) and digital topographic maps scale 1:50 000, and computed from the altitude matrix

Total relief within the fans ranges from 35m for the Hadahid fan, to more than 280m for the Habran fan. According to GUZZETTI, ET AL (1997) low values of total relief are mostly associated with the smallest fans (Hadahid, Araba west, and Taghda). The spatial distribution of relative relief and slopes of the alluvial fans in the study area ranges between 0.5° in Araba east fan and 2.1° in Timan fan respectively and reaches to 0.6° in Firan fan (Fig 2-18).

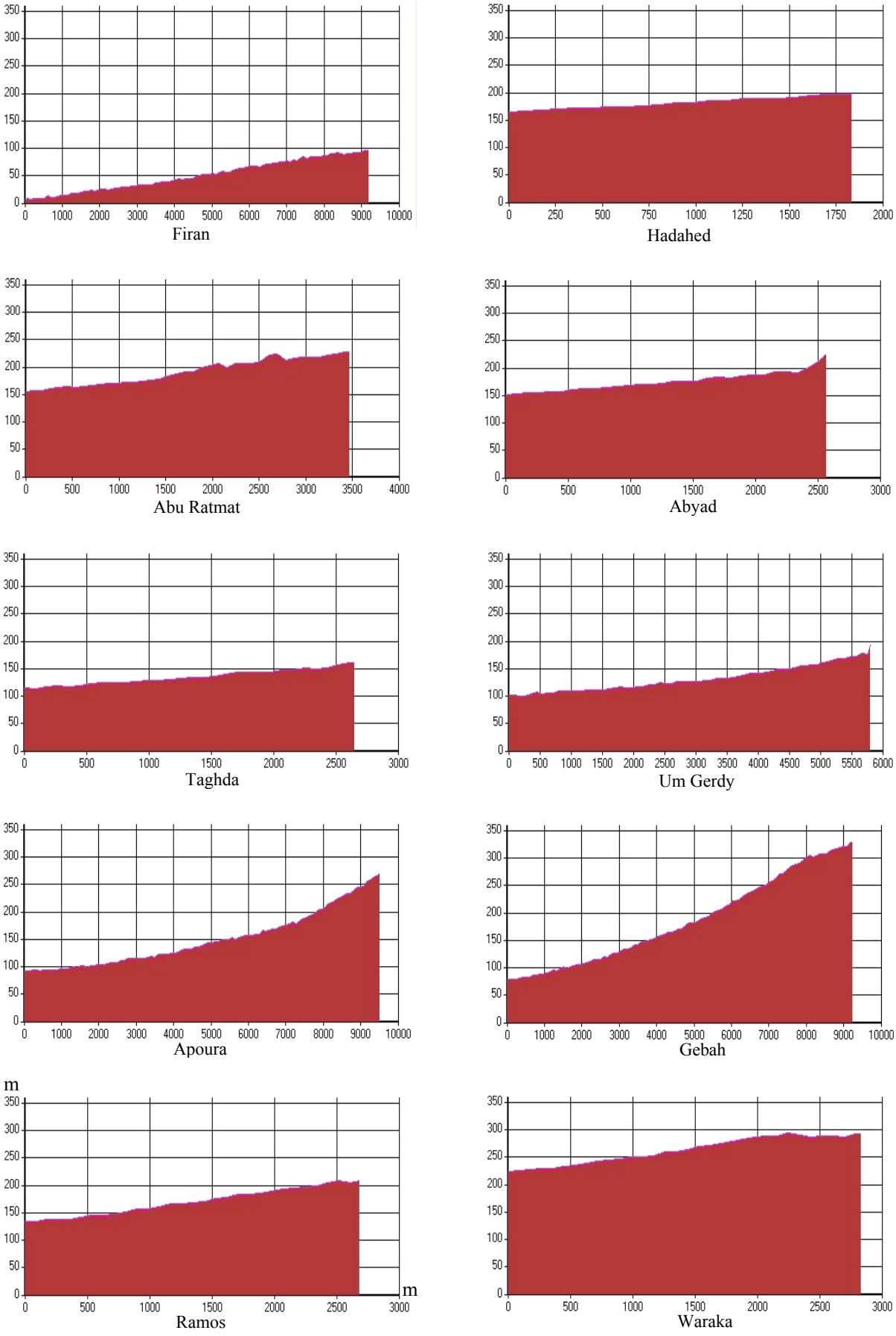

Fig (2-18-a) *The average slopes of the main alluvial fans in El-Qaà plain area.*

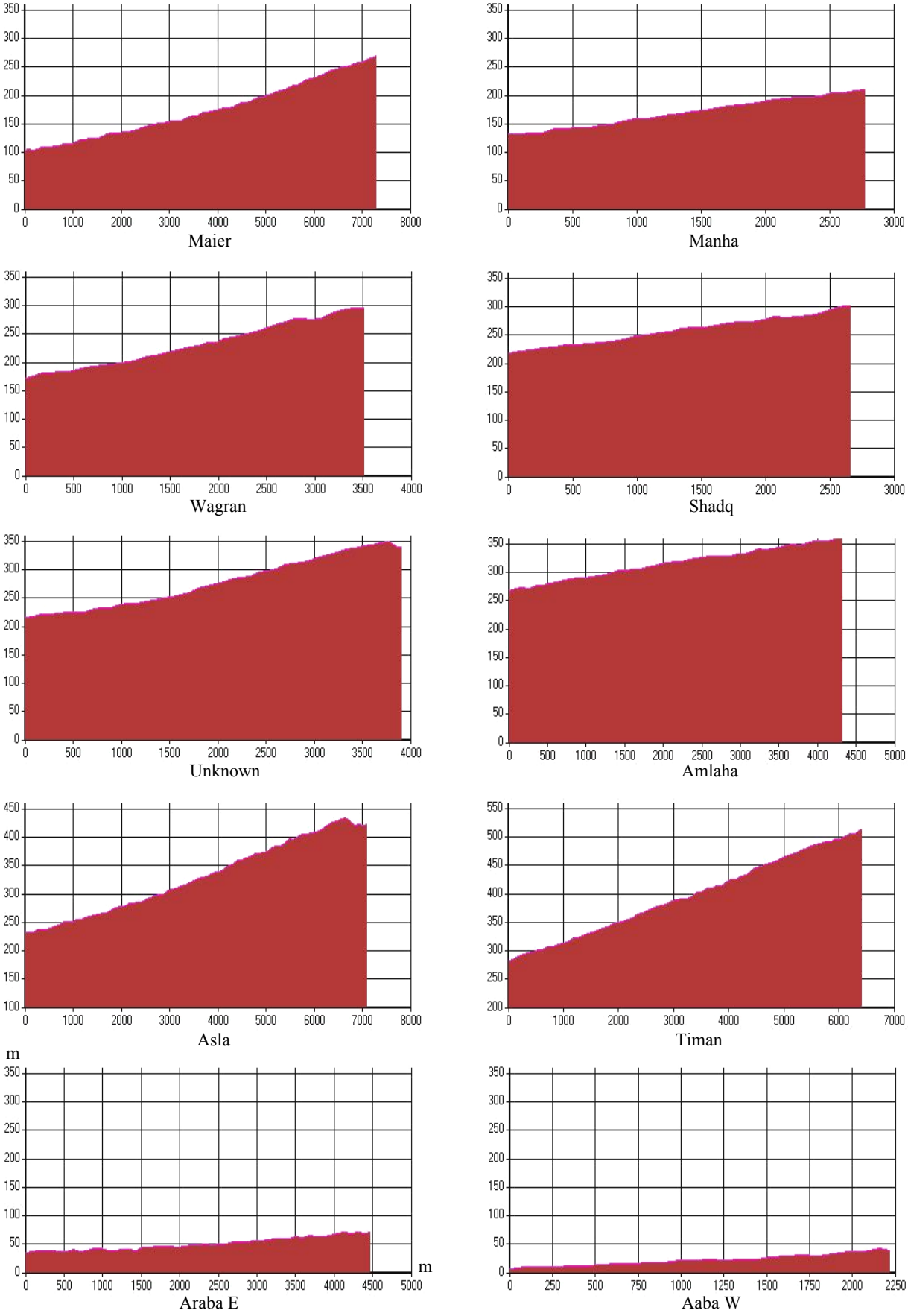

Fig (2-18-b) *The average slopes of the main alluvial fans in El-Qaà plain area*.

(Tab. 2-7) shows that the ratio of fan relief to fan length (H/L) is another element to measure mean slope. For most of the fans the ratio coincides more or less with the mean terrain gradient computed from the DEM. The relationship between mean slopes and total relief shows that fans with high average topographic gradients exhibit small total relief but high values of relative relief. These fans are small (i.e. Hadahid). On the contrary, alluvial fans with high values of total relief (with the exception of Firan) show low values of topographic gradient and a large areal extent (i.e. Habran).

2.3.2. Fan-catchments relationships

Fan size, shape, location and dominant morphological processes are controlled by drainage-basin characteristics such as size, slope, erodibility of the exposed rocks, rainfall and flood combined with sediment yield. Geomorphologists have attempted to establish relationships between geomorphological characteristics of alluvial fans and their drainage basins (BULL, 1964, 1977; LECCE, 1990, 1991; HARVEY, 1990). These empirical expressions take the forms of power functions, suggesting a degree of self-similarity or of scale invariance (SCHROEDER, 1991).

Fan size increases with drainage size giving an isometric i.e. positive relationship (CHURCH and MARK, 1980), or, fan area increases less than drainage basin area (BULL, 1964, OGUCHI and OHMORI, 1994). Fan slope shows a negative relationship to fan area and drainage basin area (HOOKE, 1968); catchments ruggedness exhibits a positive correlation to fan slope (KOSTASCHUK et al., 1986; CHURCH AND MARK, 1980); and fan area is positively correlated to the dispersion of altitude within the basin (OHMORI, 1978).

In the study area the relationship between fan area and drainage basin area is positive. Inspection of Fig 2-19 reveals that the scatter in the data is large and the regression line is quite poorly fitted. Uncertainty in the definition of the extent of alluvial fans and of drainage basins may only partially account for this large scatter. A positive relationship between fan area and drainage basin area was established. Increasing the catchment area the fan area increases at a reduced rate. In the study area this is obvious because of the presence of very large basins.

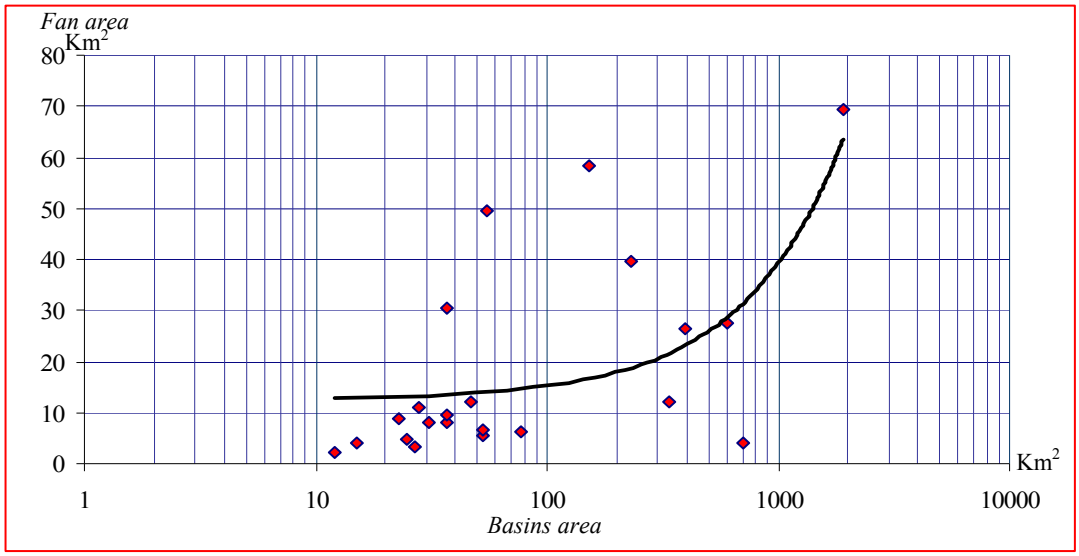

Fig (2-19) *The relationship between fan area and drainage basin area*

The quantitative analysis of altitude data and its derivatives was less efficient in outlining the differences amongst the fans. Average values of altitude and its derivatives were quite similar for all fans and showed high standard deviations. Similarity between fans was higher than their internal homogeneity. The slope of the regression line is lower than that commonly proposed for arid and humid regions. Discrepancies may be due to the large size of the fans and the catchments, as well as to the complex, and to a large extent unknown, geomorphological history of the fans (GUZZETTI, ET AL 1997).

Fan morphometric criteria in the study area are related to the present drainage basin characteristics which have a direct influence on the fan area and slope such as:

1 - Lithologic variations have a strong influence on fan area and slopes. BULL (1962) demonstrated the effect of drainage basin lithologies on the area and slopes and concluded that drainage basins consisting of erodible lithologies, such as mudstone and shale, produce fans that are steeper than, and almost twice as large, as those produced by basins underlined by more resistant sandstone.

2 – Tectonic activity has also an affect on the relationship between the area of an alluvial and its drainage basin area. VISERAS et al. (2003) determined that the stratigraphic stacking patterns of alluvial deposits reflect geographic differences in eustacy and tectonics. Fans along tectonically active mountain fronts tend to be smaller and steeper due to the vertical aggradation of alluvial deposits. Fans at moderately active mountain fronts tend to be elongated and large in relation to their drainage basin. This is the case with all fans in El-Qaà plain area.

Chapter 3

Surface runoff

During the last few decades, flash floods have developed as one of the most dangerous natural disasters, which may occur almost everywhere in the world. In recent times, great attention was given to flash floods due to several catastrophic events in different countries. Flash floods are one of the most impressive hazardous manifestations of the environment, which directly affect human activities and security. Their origin and development are not yet well enough understood. There are many ways to prevent flash floods, but no matter how well anyone method works its effect is always limited (LIN, 1999).

Surface runoff can be considered as one of the major problems in the desert, especially, in Arabic deserts. Actually, Arabic countries have created many development projects, such as reclamation, agriculture, industry, tourism, settlements and others. Runoff, especially flash flood is a real danger for the development in these areas, and is considered being the main reason to loose big quantities of fresh water besides the destruction of life stocks and infrastructure in the desert.

Climatic and hydrologic conditions are considered to be the important factors which have a direct influence on rivers and valley basins to form their surface i.e. on the evolution of fluvial landforms. The effectiveness of the hydrological factor related to many elements such as kind of rocks, structure, basins characteristics and their runoff networks as well as the hydrologic conditions has a direct influence on the present processes in the study area and the human activities (SALEM, A. 1985).

Runoff measured in the study area requires sufficient data about climate conditions such as rainfall, evaporation, infiltration and transpiration. In addition geomorphological and geological setting is needed as well as data with regard to flash flood, i.e gauge height, if available, water quantity, velocity and the time which is running until reaching the estuary coast by flash flood.

The climatological and hydrological data of El-Qaà plain area have been collected from a lot of sources such as meteorological stations of the period between 1934 and 2005 (Tab.1-1), from reports about flash floods in Sinai, several projects, references and own field work. They have been computed with some meteorological programs such as "met 1" and "cropwat 4.3" to calculate evaporation and evapotranspiration in the study area.

It is noticed in these data that there are some discontinuities in time, especially the warfare times but it can be compensated from the other reports.

The surface runoff will be discussed in this chapter concerning two main elements:

3.1. Factors influencing desert flood

3.2. *Runoff generation mechanisms*

1. ***Factors influencing desert flood***

Runoff in the desert is considered as a result of many factors and variations which affect each other by different degrees. These factors are the follows:

3.1.1. Rainfall

3.1.2. Water losses

3.1.3. Basins and channel network

3.1.4. Climate and vegetation

They determine the runoff which is resultant between rainfall, water losses, and water infiltration.

3.1.1. Rainfall

The desert is characterized by rare rainfall which normally don't increase 25.4mm annually. Rainfall in arid and semi-arid zones results largely from convective cloud mechanisms producing storms typically of short duration, relatively high intensity and limited areal extent (COOKE AND WARRAN. 1973). However, low intensity frontal-type rains are also experienced, usually in the winter season. In Sinai and in Jordan, relatively low-intensity rainfall may represent the greater part of annual rainfall during this period.

Flash floods are often the result of convectional storms or of high-intensity rain cells associated with frontal storms (WILLIAM, I. 1988). These storms produce large amounts of rain within a brief period, often measured in minutes rather than hours. Furthermore, a storm which affects a steep, bare, impermeable surface such as a narrow mountain valley like Wadi Maier in the study area or a densely built-up urban area (El-Tur city), is resulting in high flood peaks passing too rapidly for giving adequate flood warnings (SMITH AND WARD, 1998).

3.1.1.1. Rainfall types

There are three distinct, main types of rainfall in the study area:

3.1.1.1.1. Convectional rainfall

3.1.1.1.2. Frontal or cyclonic rainfall

3.1.1.1.3. Orographic or relief- induced rainfall

3.1.1.1.1. Convectional rainfall usually occurs in places with warmer or tropical climates, i.e. in countries close to the equator. In the Middle East and Sinai, this type of rainfall mostly occurs during the autumn and spring months. Convection is the mechanism where currents of warm or heated air are rising separated by larger areas of gradually dropping air. This is commonly the cause of particularly powerful thunderstorms that occur during hot seasons, i.e. in summer. Convectional rain is caused by a hot soil surface so that the atmosphere becomes heated and hotter than normal, which in turn causes the damp pressure of the air to rise. During the following cooling process clouds can be formed.

They are mostly of the cumulonimbus type, eventually developing to large thunder clouds which may release their great amount of water in a massive downpour photo (3-1). This type of rain is not related at a steady place or time and moreover, the rain varies from year to year in the same place (NAGIB, M., 1970). It is known from St. Catherine mountainous area in the north east of El-Qaà plain.

Photo (3-1) *large cumulonimbus cloud with rainfall (convectional rainfall)*

3.1.1.1.2. Frontal rainfall, this rain type is caused mainly by the occurrence of low pressure areas, and happens when warm and often tropical air meets cooler air masses. During this process the warm air becomes lifted by the colder air, resulting in condensation and rainfall.

Fronts can be either cold fronts or warm fronts. Warm fronts occur in the situation presented above, when warm and cold air are meeting, and the warm air 'overrides' the cooler air and moves upward. Warm fronts are usually followed by several days of intense rainfall due to the endurance conversation of the period. Cold fronts occur when a mass of cooler air moves towards warm air (Photo 3-2). This however, causes a similar effect to a warm front, but the ensuing rain duration is shorter and often more intense than that of a warm front. This type of rain is typical for the coastal area from El-Tur city towards Sharm El-Sheikh.

3.1.1.1.3. Orographic rainfall, this type of rainfall is caused when masses of air pushed by wind encounter sizeable objects or land formations they cannot pass, such as high mountains (hence its name of orographic rainfall). This pushes the air across the object/land form in question, and, if the air is pushed high enough, it becomes condensed and transforms into a cloud, which may cause rainfall. This type of rainfall is also known as relief rainfall. One of the rainiest places in Egypt, South Sinai Mountains, is an example for orographic rainfall.

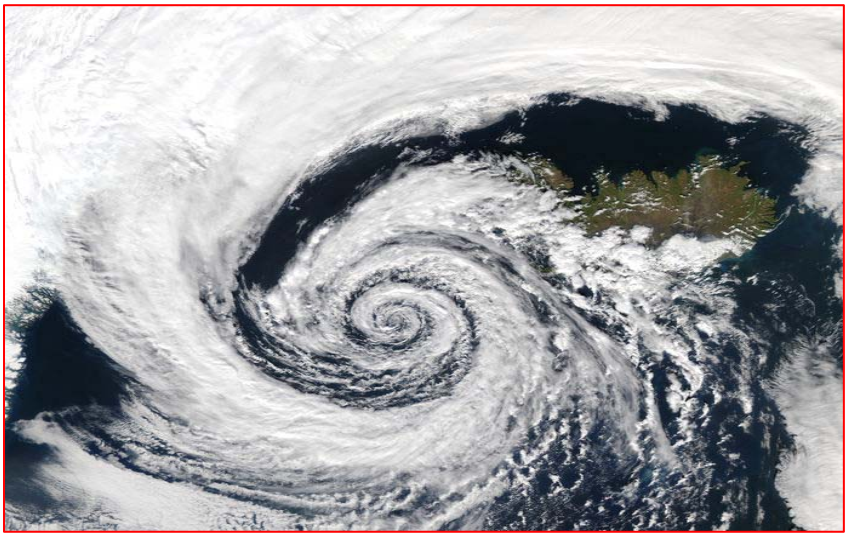

Photo (3-2) *An example from meteorological satellite (showing a depression)*

These previous types of rain develop mostly to thunder storm in the study area, especially in the mountainous area east of El-Qaà plain.

3.1.1.2. Synoptic weather patterns

(NAGIB, M., (1970), ZAKARIA, T., (1993), DAYAN, U., and MORIN, E (2006) concluded that the synoptic weather patterns leading to heavy rainfall are related with three effectual factors as the followings:

3.1.1.2.1. Mediterranean Mid-latitude Cyclones

The most active cold fronts from the Mediterranean, which are accompanied by high amounts of rain, are associated with mid-latitude, extra-tropical cold depressions developing over the eastern Mediterranean e.g., the Cyprus depressions; (Fig 3-1 A) (GOLDREICH, 2003). They are activated leeside of the Turkish Mountains preferably over the Aegean Sea, where the air-sea contrast is maximized (SHAY-EL AND ALPERT, 1991). The very humid winds associated with these depressions may lead to heavy rainfall over the Dead Sea region as a result of forced convection while crossing the western and eastern ridges at both sides of the basin.

Intensive rainfall in the southernmost parts of the drainage basin i.e. Sinai Peninsula, is generated mainly by the Syrian branch of the Cyprus depression (Fig 3-1B). This means Mediterranean mid-latitude cyclone that deepens while approaching Syria. It differs substantially from normal conditions which are: Mediterranean cyclones tend to decay before reaching Syria. Under such conditions, the escarpments along the Dead Sea rift and the Sinai Mountains are less effective in blocking moisture transport across them.

The Syrian depressions are the second frequent, synoptic-scale cyclone type, producing major floods over the northern part of the study area (KAHANA ET AL., 2002, 2004). A comparison of all eastern Mediterranean cyclones for four consecutive winters (1982–1986) undertaken by ALBERT AND NEEMAN (1992) revealed that such Syrian cold cyclones are in general slightly more baroclinic than average latent heat fluxes, indicating the importance of local convection.

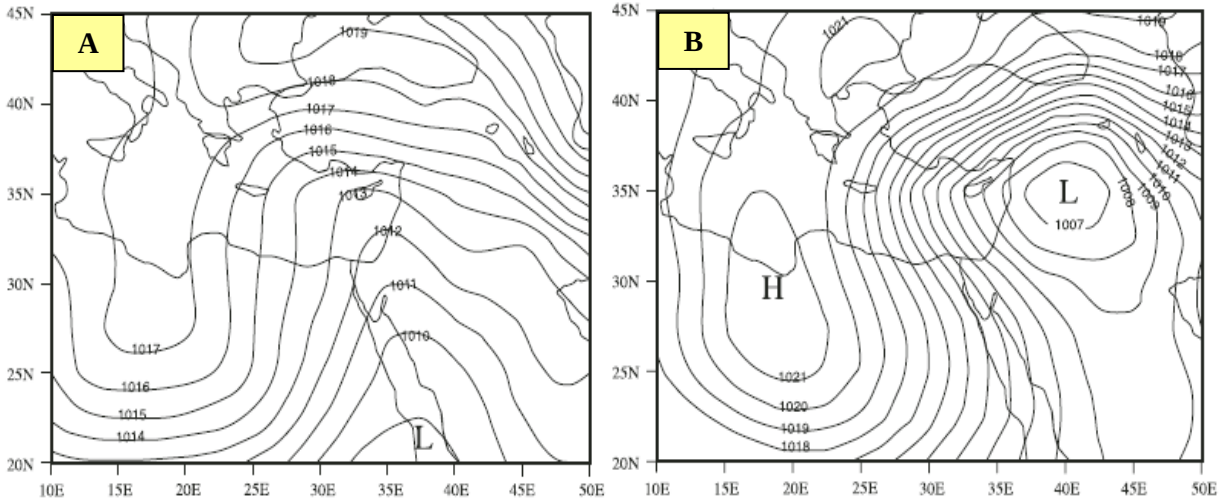

Fig (3-1): (A) *Composite sea level pressure with 1* hPa *interval, for all flash floods in Sinai (provided by the National Oceanic & Atmospheric Administration–Cooperative Institute for Research in Environmental Sciences Climate Diagnostic Center,(B) Composite sea-level pressure, with 1* hPa *interval, for all flash flood cases resulting from the Syrian cold cyclones modified after* DYAN *et al (2006)*

3.1.1.2.2. The Active Red Sea Trough

The Red Sea Trough is one of the most frequent atmospheric circulation patterns over the southeastern Mediterranean. In contrast to the Mediterranean mid-latitude cyclones, a tropical synoptic-scale system named "Active Red Sea Trough" (KAHANA et al., 2002), accounting for most of the major floods over the southern Dead Sea watershed, occurs mainly during fall and penetrates from the south (DAYAN et al., 2001). This barometric trough extends from equatorial eastern Africa towards Sinai, northwards along the Red Sea, and is accompanied by widespread rainfall. All these cases are characterized by southerly winds over Sinai at the 500 hPa level. This parameter is the most powerful predictor for major floods and crucial for activation of the frequent Red Sea Trough at the surface. This is transporting moisture of tropical origin to Sinai (KAHANA et al., 2004).

The knowledge gained from detailed synoptic-scale analysis of several rainstorms associated with an active Red Sea Trough impacting southern Israel and eastern Sinai (ZIV et al., 2004) provides a basis for the generalization of the main characteristics of this synoptic system. In all cases, the storm was initiated while hot and dry air blew from the east at lower levels, resulting in a buildup of conditional instability throughout the troposphere in their initial stage. These storms were characterized by a mesoscale convective system (MCS) with an intensive warm core moving from Sinai northward over the Negev desert and the Dead Sea basin (photo 3-3).

They are organized in multiple cells and exhibit moist convective Zones, which sustain thunderstorms (HIRSHBOECK, 1999). Their physical characteristics were defined on the basis of enhanced infrared satellite imagery developed by MADDOX (1980) and appear as a large circular region composed of high clouds that gradually become colder at their surface and higher toward the center of the system (photo 3-3). Such cloud clusters crossing the Negev Desert and the Dead Sea basin can produce intense rainfall, inducing floods due to their large aerial extent and long duration.

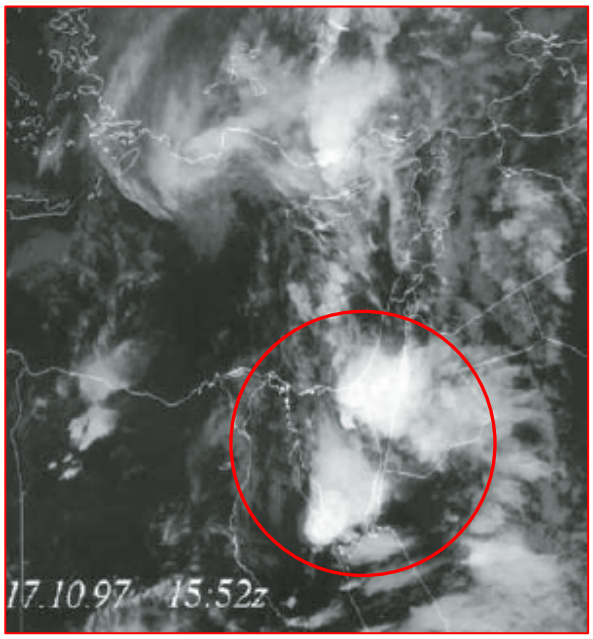

Photo (3-3) *U.S. National Oceanic & Atmospheric Administration satellite IR image (NOAA) for a developing Mesoscale Convective System over Sinai and the Negev at 15:52 UTC 17 Oct 1997.*

3.1.1.2.3. Jet Stream Disturbances

Upper troposphere jet streams play a role in the development of rainstorms and extreme floods over southern Sinai. The subtropical jet (SJT) stream serves as a conveyor belt of moisture in mid- and upper tropospheric layers, often originating from tropical Africa. In addition to this important role, the synergetic interaction of these jets with the mid-tropospheric diabatic processes produces intensified cyclogenesis of other synoptic scale patterns and contributes significantly to deep synoptic scale ascent over the region (ZIV et al., 2004). KRICHAK et al. (1997a) suggests that the Active Red Sea Trough developes as a result of a lee-type cyclogenesis in association with the position of the jet over the area, i.e. the northern part of the Red Sea. In addition to the conditional instability established by the preexistence of the Red Sea barometric trough, the upper-level divergence induced by both polar jet (PJ) and SJT streams over the region supported the formation and intensification of this storm (Fig 3-2).

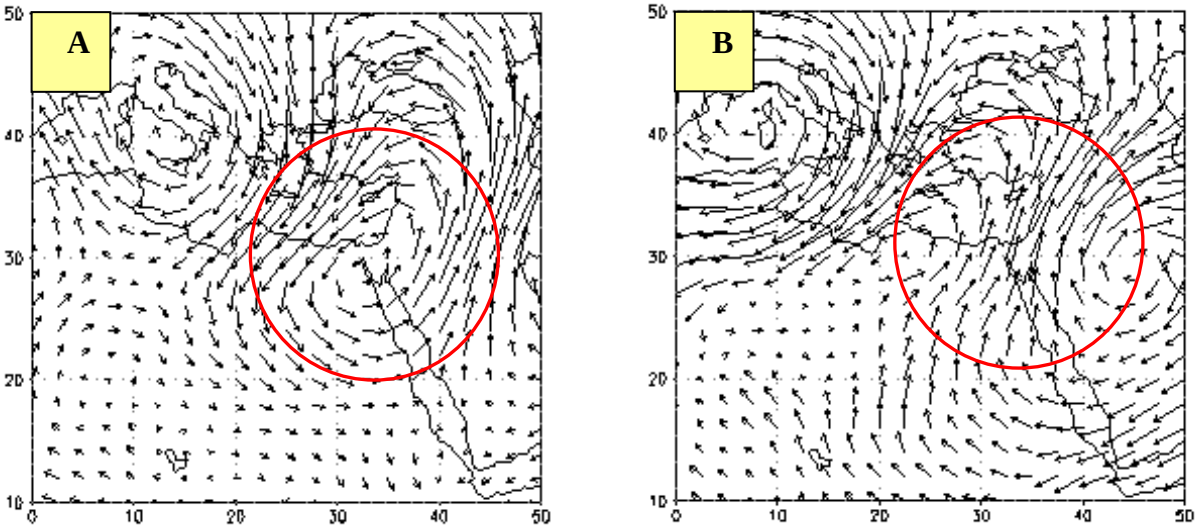

Fig (3-2) Composed charts of 200 hPa wind vector deviation from the (1985-1995) - monthly mean, in March: (A) non RST rain; (B) RST rain, after (TSVIELI, Y., and YANGVIL, A., 2007).

In the Fig 3-2, a mid-latitude upper trough approaches the region accompanied by intensification of the SJT over northern Africa and formation of a PJ over Turkey. The eastern Mediterranean is then situated simultaneously to the left of the SJT exit and to the right of the PJ entrance, implying divergence near the tropopause. The SJT structure can play an important role in inducing torrential rain and floods over the entire eastern Mediterranean and Sinai. DAYAN and ABRAMSKI (1983) found, for instance, an abnormal feature in the SJT's structure in which, contrary to the usual conditions, the jet stream had an anticyclonic curvature and moved northward with increasing altitude.

The previous analysis of the rainfall producing factors shows that the rainfall in the northern Sinai is more affected by these factors, but the southern Sinai is more affected by khamasin depressions and thunder storms (ZAKARIA, T., 1993).

Tab. (3-1) The annual and monthly mean of thunder storm days in the study area.

Station	**Jan.**	**Feb.**	**Mar.**	**Apr.**	**Mai.**	**Jun.**	**Jul.**	**Aug.**	**Sep.**	**Oct.**	**Nov.**	**Dec.**	**Sum**
Ras Sudr	0.0	0.0	0.0	0.0	0.0	0.0	0.0	0.0	0.0	0.0	0.0	0.0	***0.0***
Abu Rudeis	0.0	0.0	0.0	0.0	**0.1**	0.0	0.0	0.0	0.0	0.0	**0.1**	**0.1**	***0.3***
Nekhel	**0.4**	**0.2**	0.0	**0.2**	**0.2**	0.0	0.0	0.0	0.0	0.0	**0.4**	0.0	***1.4***
St. Catherine	**0.1**	0.0	**0.3**	**0.1**	0.	0.0	0.0	**0.2**	**0.2**	**0.4**	**0.3**	0.0	***1.8***
El-Tur	0.0	0.0	0.0	**0.2**	**0.3**	0.0	0.0	**0.1**	0.0	**0.1**	**0.1**	**0.2**	***1.0***
Sh. El-Sheikh	0.0	0.0	0.0	0.0	00	0.0	0.0	0.0	0.0	0.0	**0.1**	0.0	***0.1***

- Source: The archive of Meteorological authority, reports none published.

It can be noticed from (Tab. 3-1) that:

1- The relief plays an important role to increase the number of thunder storm days in the study area which ranges between 1.8 days in St. Catherine station (1350m), 1.4 days in Nekhel (460m), and one day in El-Tur station.

2- There are no thunder storm days in summer months in the study area, due to stable anticyclonic weather conditions.

3- The thunder storm days in St. Catherine and El-Tur stations increase significantly in autumn and spring months. It is, therefore possible to forecast flash flood events in El-Qaà plain area during these periods.

3.1.1.3. Rainfall distribution

Factors controlling the distribution of rainfall over the earth's surface are the belts of converging-ascending air flow, air temperature, moisture-bearing winds, ocean currents, inland distance from the coast, and mountain ranges. Ascending air is cooled by expansion, which results in the formation of clouds and eventually, the production of rain. Conversely, in the broad belts of descending air masses the great desert regions of the earth are found. Descending air becomes warmer by compression and consequently it absorbs moisture instead of releasing it. Furthermore, if the temperature is low, the air has a small moisture capacity resulting in small amounts of rainfall.

The topography plays a considerable role in increasing rainfall in some areas, such as St. Catherine area where deeply incised valleys funnel moisture transporting clouds. The highest peaks of the northeast ranges up to (2614m) and their western slopes dipping down to El-Qaà plain area, experience the highest mean annual rainfall (Fig 3-3, 3-4).

This general influence of topography on rainfall formation and its areal distribution has been focused by many investigations during the last several decades. In most cases the influence of mountains or ridges on horizontal scales of 10s to 100s of kilometres has been treated. Obviously, the focus has mostly been laid on the so-called orographic effect, i.e., the increase in rainfall caused by topography inducing cloud formation processes. Both dynamic/numerical and statistical models have been quite widely dealt within the literature, more recently by ALPERT and SHAFIR (1989), HAIDEN et al. (1992), STEIN and ALPERT (1993), BARROW and LETTENMEIER (1994), WESTON AND ROY (1994), BASIST et al. (1994), KUHN and YAIR (2004), and KATRA, I. et al. (2007). In general, more rainfall occurs on windward slopes, especially on their upper parts, than on the leeside in the 'rain shadow' (Fig 3-4).

Tab. (3-2) The annual and monthly mean of rainfall quantity in the study area (mm).

Station	**Jan.**	**Feb.**	**Mar.**	**Apr.**	**Mai.**	**Jun.**	**Jul.**	**Aug.**	**Sep.**	**Oct.**	**Nov.**	**Dec.**	**Sum**
Ras Sudr	2.5	2.4	3.6	1.0	0.2	0.1	0.0	0.0	0.0	0.4	1.3	2.9	***14.4***
Abu Rudeis	3.0	2.3	1.3	0.5	0.1	0.0	0.0	0.0	0.0	0.2	2.3	6.7	***16.4***
Nekhel	10.2	6.5	3.3	1.4	0.0	0.0	0.0	0.0	0.0	3.7	7.6	5.2	***37.9***
St. Catherine	1.7	1.4	13.5	8.9	6.4	0.0	0.0	0.0	0.1	3.4	21.7	7.2	***64.3***
El-Tur	0.6	1.2	0.7	0.6	0.3	0.0	0.0	0.0	0.0	0.6	1.1	2.7	***7.8***
Sh. El-Sheikh	0.2	0.0	0.0	0.2	0.0	0.0	0.0	0.0	0.0	0.0	0.0	23.4	***23.8***

- *Source: The archive of Meteorological authority, reports none published.*

3.1.1.3.1. Annually and monthly distribution

It can be noticed from (tab. 3-2) and (fig 3-3) that:

1- The amount of rainfall decreases from west toward east, while, the annually average of rainfall during observation years in Ras Sudr station has reached 14.4mm, Abu-rudeis staion 16.4mm, El-Tur Station 7.8mm, and Sharm El-Sheikh station 23.8mm, but the amount of rainfall in Nekhel and St. Catherine stations have reached 37.9mm and 64.3mm consecutively (Fig3-4), because of the much higher location of these stations.

2- December is considered having the highest rainfall in most stations of south Sinai during the year, where the monthly rainfall has recorded for about 6.7mm in Abu Rudeis, 2.7mm in El-Tur, and 23.4mm In Sharm El-Sheikh (Fig 3-3).

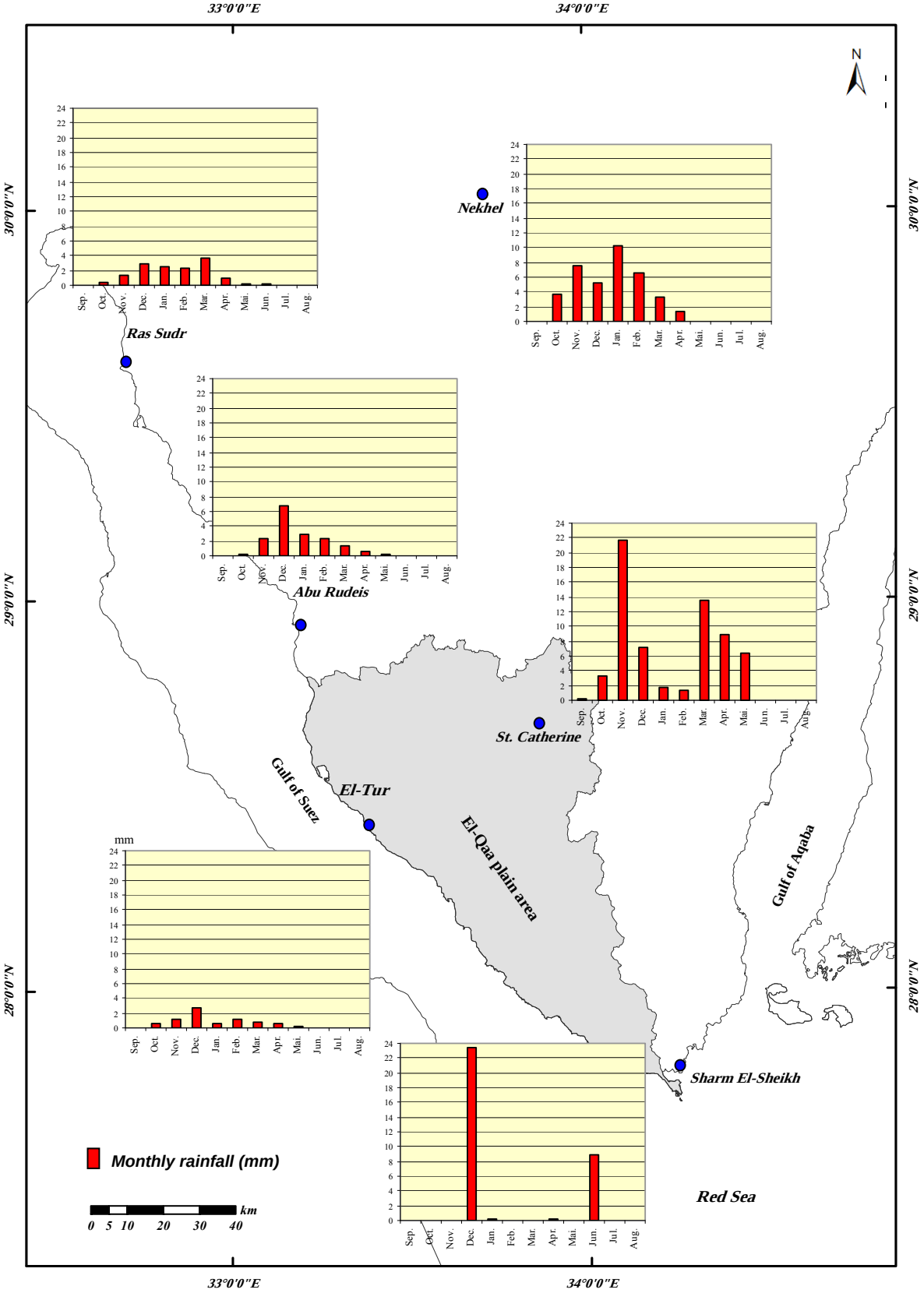

Fig (3-3) *Monthly mean of rainfall in the study area (mm)*

3- The summer months in the study area have no rainfall, whereas in the autumn and spring month's representative by May and September sometimes few rains occur, due to the active pressure depressions in this period of year, especially in St. Catherine area which has 8.9mm in April, 6.4mm in Mai, and 21.7mm in November (Fig, 3-3).

3.1.1.3.2. Seasonal rainfall distribution

The rainfall season starts in September and enduring to Mai, while June, July, and August are rainless. The summer season is characterized by stable high air pressure.

Tab. (3-3) The season's rainfall amount and their ratio from annual average

Station	**Annually Rain**	**Spring Rain**	**%**	**Summer Rain**	**%**	**Autumn Rain**	**%**	**Winter Rain**	**%**
Ras Sudr	**14.4**	4.8	**33.3**	0.1	0.7	1.7	11.8	7.8	**54.2**
Abu Rudeis	**16.4**	1.9	11.6	0.0	0.0	2.5	15.2	12.0	**73.2**
Nekhel	**37.9**	4.7	12.4	0.0	0.0	11.3	**29.8**	21.9	**57.8**
St. Catherine	**64.3**	28.8	**44.8**	0.0	0.0	25.2	**39.2**	10.3	16.0
El-Tur	**7.8**	1.6	20.5	0.0	0.0	1.7	21.8	4.5	**57.7**
Sh. El-Sheikh	**23.8**	0.2	0.8	0.0	0.0	0.0	0.0	23.6	**99.2**

- Source: The archive of Meteorological authority, reports none published.

From (Tab.3-3) and (Fig 3-4) can be concluded that:

1- Winter season has the highest values of rain in the study area bating Saint Catherine station. The highest values are recorded to 23.6mm and 12.0mm which represent 99%, 73.2% of total rain consequently in Sharm EL-Sheikh and Abu Rudeis stations. In winter season, the pressure depressions animate and cause the troposphere to be unstable inducing sometimes heavy rainfall in the coastal area.

2- Rainfall increases in autumn and spring seasons, especially in the mountainous area (Catherine Mountain). Every year during the same period, this area is subjected to thunder storms due to the movements of Sudan depressions from south to north. Subsequently, this depressions cause the troposphere to be unstable leading to heavy rain and flash flood in the mountainous.

3- The highest rainfall in autumn season is recorded to 25.2mm and 11.3 mm which represent 39.2 %, 29.8% of total rainfall respectively in St. Catherine and Nekhel stations, but low rainfall values in this period is recorded in the coastal stations, 0.0mm, 1.7mm respectively in Sharm El-Sheikh and El-Tur stations. Whereas, the highest rainfall in spring season is recorded to 28.8mm, and 4.8mm respectively, this represents 44.8%, and 33.3% of total rainfall in St. Catherine and Nekhel stations.

4- The lack of effective depressions in summer explains that the climate in the study area remains i.e. stable arid.

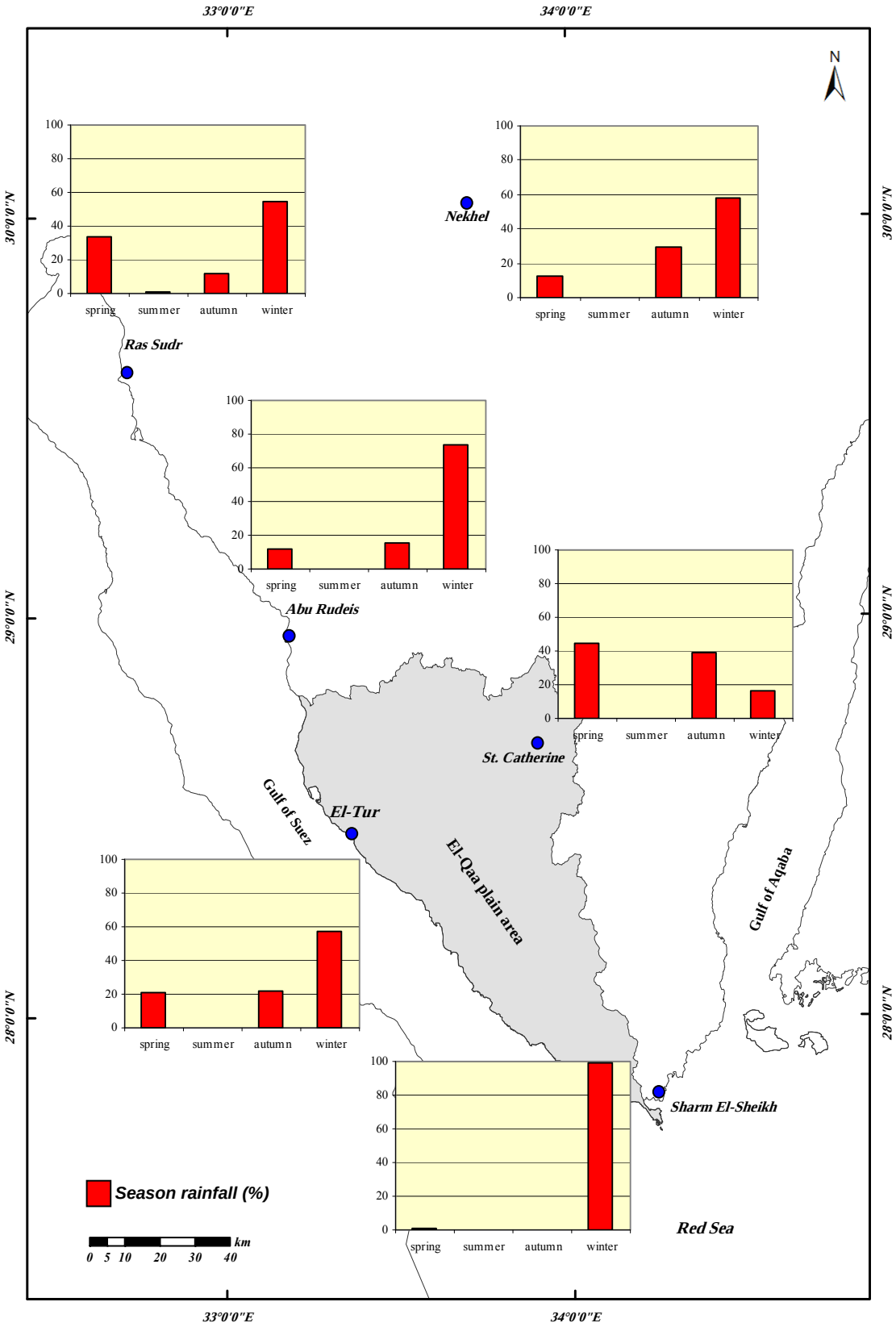

Fig (3-4) *Seasonal rainfall distribution in the study area (%)*

3.1.1.3.3. Seasonal rainfall concentration is considered a good indicator to discuss seasonal rainfall in any region. MARKHAM, C., (1970) has developed a method to compute the seasonal rainfall concentration. The assumption can be made that mean monthly rainfall values are vector quantities with both magnitude and direction, whereas magnitude being the month of the year expressed in units of arc.

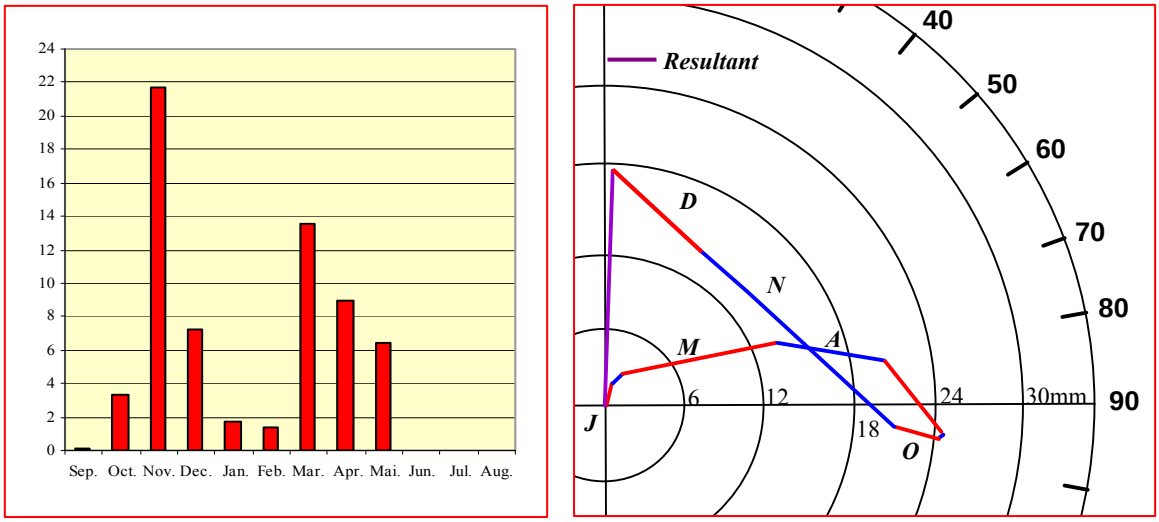

Fig (3-5) *Example of seasonal rainfall concentration of Saint Catherine station, modified after* MARKHAM, C., (1970)

Vector direction for mean monthly rainfall is thus 015° for January, 044° for February, 074° for March, etc.

The next step is to add the twelve monthly vectors (fig 3-5). The vector resultant is a measure of the seasonality of rainfall, its magnitude is representing the degree of seasonality, and its direction is representing the period of seasonal concentration. The ratio between the magnitude of the resultant and the total mean annual rainfall, expressed as a percentage, is here called the Seasonality Index. Large values show high, small values low seasonality. The maximum possible value for the Seasonality Index is 100 percent, and would occur when all the rainfall occured in a single month. The minimum value is zero percent, occurring if rainfall is evenly distributed throughout the year.

The resultant vector for St. Catherine rainfall has a direction of 09° (Fig3-5) and a magnitude of 17.4 mm. Converted to time; the direction is January 10, or simply January, since the resultant should not be ascribed of greater accuracy than its components. St. Catherine mean annual rainfall for the period is 64.3mm. Its Seasonality Index is thus 17.4/64.4, or 27.1 percent.

Tab. (3-4) The time and ratio of rainfall concentration in the study area

Station	**Rainfall concentration %**	**Time of concentration**
Ras Sudr	**62.5**	*From 10 to 30 January*
Abu Rudeis	**60.5**	*From 18 December to 3 January*
Nekhel	**69.7**	*From 26 December to 10 January*
St. Catherine	**27.1**	*From 25 December to 9 January*
El-Tur	**71.5**	*From 24 December to 7 January*
Sh. El-Sheikh	**98.4**	*From 9 to 23 December*

- Source: The archive of Meteorological authority, reports none published, (computed by researcher).

(Tab. 3-4) shows that:

1- The highest percent of rainfall concentration has been computed in Sharm El-Sheikh station to 98.4% which concentrates in the period from 9 to 23 December.

2- The lowest percent of rainfall concentration has been recorded in St. Catherine station to 27.1% and concentrates during the period from 25 December to 9 January.

3- Rainfall predominantly occurs in winter season (December and January), because of the depression activity in this time of year.

3.1.1.3.4. Rainy day number

This is considered being an indicator to determine the days and months which have heavy rainfall and a strong effect on the rural development in the study area. The decrease of rainy days is related with the summation of annual rainfall, especially in the area which is characterized by a sub-tropical desert climate (ZAKARIA, T., 1993).

Tab. (3-5) Rainy days and their percentage of total rainfall summation

Station	**Rainy days (day)**	**0.1 to 1.0 mm (%)**	**1 to 10 mm (%)**	**> 10 mm (%)**
Ras Sudr	**6.2**	65.4	32.4	2.2
Abu Rudeis	**9.6**	64.6	32.3	3.1
Nekhel	**20.8**	50.0	45.2	4.8
St. Catherine	**33.4**	60.2	32.3	7.5
El-Tur	**5.0**	58.0	34.0	8
Sh. El-Sheikh	**7.2**	70.4	27.2	2.4

- Source: The archive of Meteorological Authority, reports none published, (computed by researcher).

It can be noticed from (tab.3-5) that:

1- The rainy days number in the upland stations is higher than those of coastal stations. Nekhel and St. Catherine as upland stations reach 20.8 days, and 33.4 days respectively, whereas the coastal stations El-Tur and Abu Rudeis only reach 5 and 9.6 days consecutively.

2- The first category of rainy days ranges from 0.1 to 1.0 mm, which represents in Sharm El-Sheikh station 70.4% of rainy days, and 50.0 % in Nekhel station.

3- The second category ranges between 1.0 to 10.0 mm, which represents in Nekhel Station 45.2% of rainy days, and in El-Tur station 34.0%.

4- the last category of rainy days gives more than 10mm. St. Catherine and El-Tur stations have the highest percentage of such rainy days (7.5%, 2.4 days, and 8.0%, 0.4 days) respectively. This amount of rainfall has normally a direct effect in the study area producing quick runoff.

3.1.1.3.5. The highest amounts of rainfall and their dates

The highest amount of rainfall that is recorded in one day is considered being one of the important variables to study distribution of rainfall and runoff especially in arid and semi arid zones. The values that record > 10mm of rainfall in one day lead often to runoff and flashflood, thus, it could be based on these values in the study area to estimate the capability of runoff events.

Tab. (3-6) The highest amount of rainfall which had been recorded in one day

Station		Jan.	Feb.	Mar.	Apr.	Mai.	Jun.	Jul.	Aug.	Sep.	Oct.	Nov.	Dec.	St.Dev
Ras Sudr	*mm*	***13.7***	5.3	***21.2***	***10.3***	2.1	0.0	0.0	0.0	0.0	2.5	9.8	9.7	***6.7***
	Day	***4/88***	7/97	***11/94***	***1/86***	18/76	0.0	0.0	0.0	0.0	19/77	23/84	17/85	-
Abu rudeis	*mm*	**11.2**	5.6	4.0	2.4	1.8	0.0	0.0	0.0	0.0	2.2	***19.7***	***23.9***	***8.4***
	Day	9/79	7/82	13/76	1/86	13/76	0.0	0.0	0.0	0.0	24/76	***8/82***	***12/64***	-
Nekhel	*mm*	***14.4***	***16.0***	5.4	3.0	1.9	0.0	0.0	0.0	0.0	9.7	***22.7***	***10.1***	***7.6***
	Day	***18/65***	***10/63***	25/67	20/64	23/97	0.0	0.0	0.0	0.0	31/3	***11/66***	***9/2000***	-
ST. Catherine	*mm*	9.6	7.6	***18.2***	***12.9***	***37.1***	0.0	3.4	***14.5***	0.8	***20.2***	***11.6***	***15.8***	***10.5***
	Day	1/94	7/99	***20/80***	***8.82***	***27/97***	0.0	30/96	***27/99***	5/92	***17/97***	***9/82***	***26/80***	-
EL-Tur	*mm*	3.4	6.0	8.2	0.2	0.0	0.0	0.0	0.0	0.7	4.0	***18.6***	***11.6***	***6.2***
	Day	26/91	3/93	22/91	21/93	0.0	0.0	0.0	0.0	24/94	16/86	***2/94***	***17/85***	-
Sh. El-Sheikh	*mm*	6.0	3.8	***10.3***	0.3	4.2	0.0	0.0	0.0	0.8	7.1	***48.3***	3.0	***14.1***
	Day	10/92	21/89	***9/89***	23/92	10/98	0.0	0.0	0.0	25/94	16/87	***17/96***	17/85	-

- Source: The archive of Meteorological Authority, reports none published.

(Tab. 3-6), (Fig 3-6) and (Fig 3-7) expressed the highest amount of rainfall which had been recorded in one day and their dates; it can be noticed from that:

1- Sharm El-Sheikh station had recorded the highest amount of rainfall in one day to 48.3mm at 17.11.1996 that is, compared with others stations, very high (Fig 3-6). This amount of rainfall leaded to a big flash flood in one of the best tourist areas in Egypt.

2- St. Catherine station has had the secondary high amount of rainfall in one day that reached 37.1mm at 27.5.1997 (spring season). This station had 6 runoff events during the recording period (25 years), whereas, rainfall was more than 10.0mm /day and this range of rainfall is sufficient to produce runoff. The autumn months have the highest probability of rainfall in this station (Fig 3-6).

3- Nekhel Station has also had some high amounts of rainfall in one day (>10.0mm/day)represented by 22.7mm at 11.11.1966, and 16.0mm at 10.2.1963, but the effectiveness of these amounts of rainfall is less than those in Catherine area, because of sedimentary rocks and deposits with high infiltration rates. The summit area of Sinai around Catherine consists of primary rocks.

4- The relief plays an important role or increasing the amount of rainfall in the study area represented in the two upland stations St. Catherine and Nekhel.

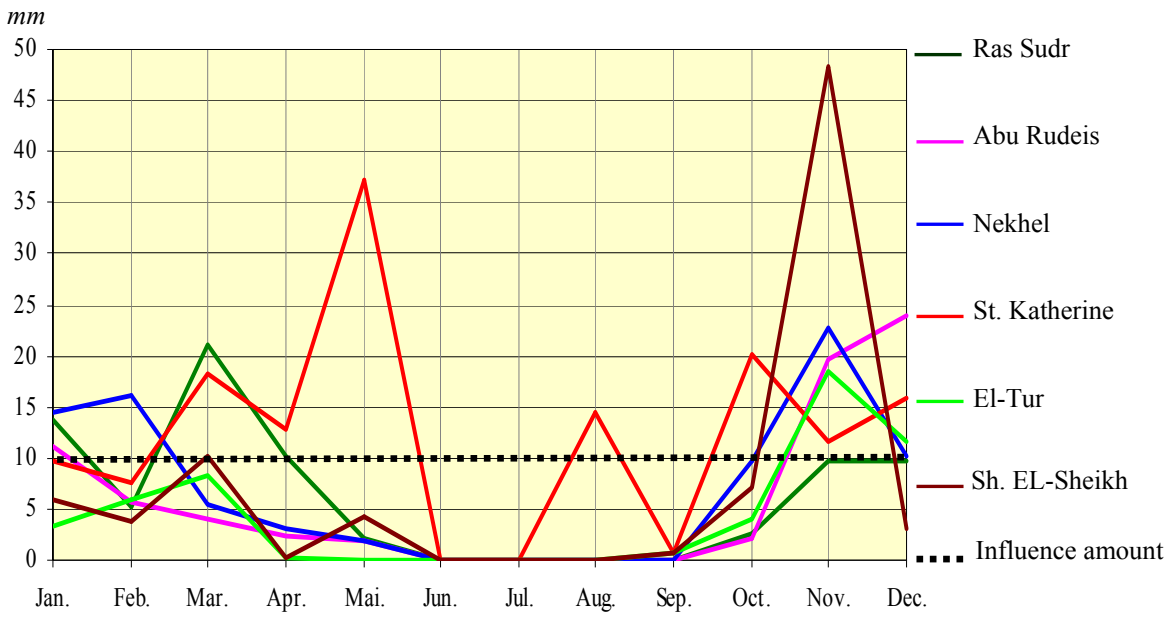

Fig (3-6) *The highest amount of rainfall in the study area that recorded in one day*

5- The values of standard deviation indicate the big variation between the amounts of rainfall in the stations of the study area and moreover present the variations of the amounts of rainfall in the same station among the months. The values ranges between 6.2 in El-Tur station, and 14.1 in Sharm El-Sheikh station which has a big variation of the amount of rainfall between all months (Fig 3-6). The more values of standard deviation increase the more variations of the amounts of rainfall increase between months in the same station.

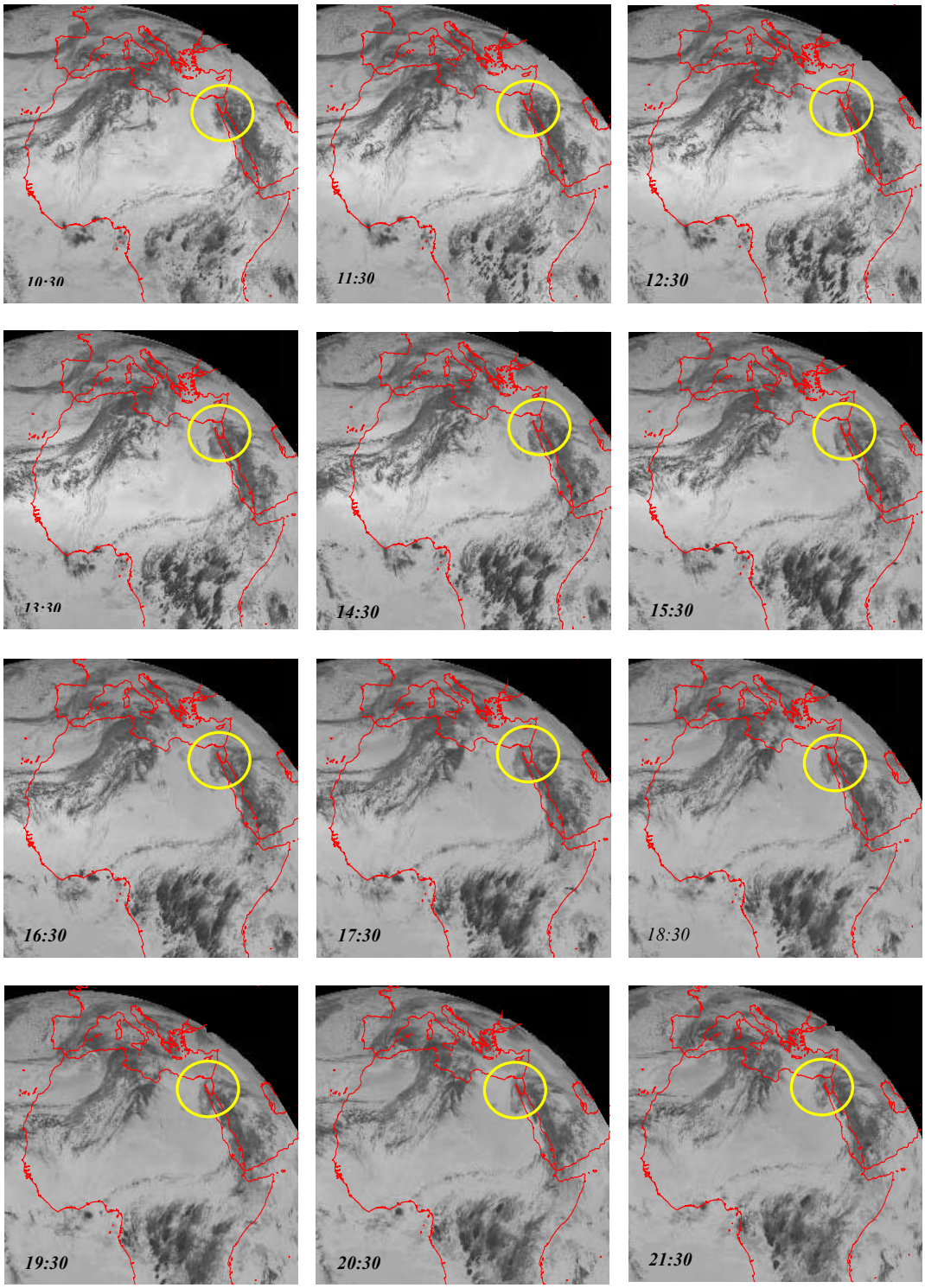

Fig (3-7) *Sequencial Meteosat images showing the rainy storm movements every half hour during the flash flood in the Southern Sinai at* ***17.11.1996.***

It can be noticed from Fig 3-7 that the rainy storms can be following to forecasting the flash flood from Satellite images to avoid the flood hazards; it can be used to calibrate rainfall estimates from other satellites. The TRMM-based, near-real time Multi- satellite Precipitation Analysis (MPA) at the NASA Goddard Space Flight Center monitors rainfall over the global Tropics (http://trmm.gsfc.nasa.gov/).

3.1.1.4. Average rainfall over the study area

The average depth of rainfall over a specific area on a single storm, seasonal, or annual basis is required in many types of hydrologic problems. The simplest method of obtaining the average depth is to level arithmetically the gauged amounts in the area (Fig 3-8). This method yields good results in a flat country if the gauges are uniformly distributed and the individual gauge catches do not vary widely from the mean. Such limitations can be partially overcome if topographic influences and areal representativity are considered by the selection of gauge sites (LINSLEY, ET AL, 1982).

1- The THIESSEN method weighs each gauge in direct proportion to the area which it represents of the total basin without consideration of topography or other basin physical characteristics. The area represented by each gauge is assumed to be that which is closer to it than to any other gauge. The area of influence of each gauge is obtained by constructing polygons determined by drawing perpendicular bisectors to lines connecting the gauges as shown in (Fig 3-8b). The bisectors are the boundaries of the effective area for each gauge. The enclosed area is measured and converted to a percent value of total basin area. The polygon weighted rainfall is the product of gauge related rainfall and the associated polygon area in percent. The sum of these products is the basin average rainfall.

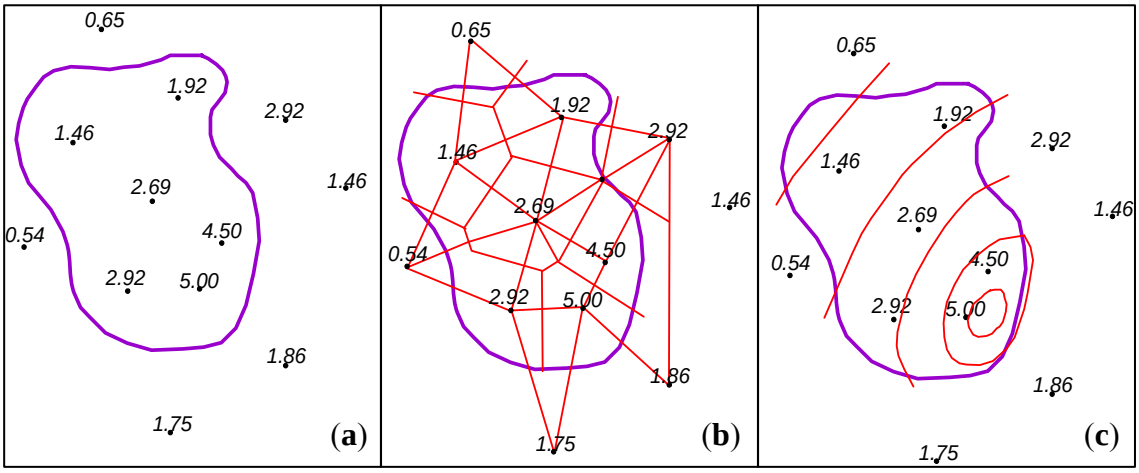

Fig (3-8) *areal averging of rainfall by (**a**) arithmetic method, (**b**) Thiessen method, and (**c**) isohyetal method, modified after Linsley et al 1982.*

The THIESSEN method is usually the best choice for prairie states during thunder storms, since elevation differences (topography) are insignificant and gauge density is inadequate to use other methods to define the areal pattern of the thunder storm cells. When analyzing several storm events having different gauges reporting each event, the THIESSEN method consumes more time than other techniques to be discussed.

2- The grid-point method averages the estimated rainfall at all points of a superimposed grid. This approach has certain advantages compared with the THIESSEN method but is easy to use with the aid of a computer. The reliability of the approach depends on the method used to estimate rainfall at the grid points.

3- Isohyetal method takes into consideration of topographic effects and other subjective informations about the meteorological patterns in the region. A rainfall-depth contour map is determined by tabulating gauge rainfall on a map of the region and constructing lines of equal rainfall called isohyets as shown in (Fig 3-8c, 3-9). Average depths are obtained by measuring the areas between adjacent isohyets (zones). Each increment of an area in percent of the total basin area is multiplied by the estimated rainfall depth for that area. This product for each zone is added up to obtain the basin average rainfall.

The Isohyetal method allows the input of judgment and experience by drawing the contour map. The accuracy is largely dependent on the skill of the person or the program used to draw the isohyets (Arc GIS program had been used in this study to draw isohyets), performing the analysis and the number of gauges. If simple linear interpolation between stations is used for drawing the contours, the results will be essentially the same as those obtained by the THIESSEN method.

The advantages of both the THIESSEN and Isohyetal methods can be combined where the area close to the gauge is defined by the polygons, but the rainfall over that area is defined by the contours from the Isohyetal method. This combination also eliminates the disadvantage of having to draw different polygon patterns when analyzing several different storm events with a variety of reporting gauges. Regardless of the technique selected for analysis of basin average rainfall, a regional map of areal distribution for the total of storm events is also produced.

Tab. (3-7) Annual rainfall amounts in El-Qaà plain area using Isohyetal method

Isohyetal mm	***Area km^2***	***%***	***Rainfall million m^3***	***%***
12.5	307.7	5.1	3.85	2.1
17.5	769.3	12.7	13.46	7.4
22.5	1428.8	23.5	32.15	17.6
27.5	868.3	14.3	23.88	13.1
32.5	967.2	15.9	31.43	17.2
37.5	472.6	7.8	17.72	9.7
42.5	505.6	8.3	21.49	11.8
47.5	307.7	5.1	14.62	8.0
52.5	329.7	5.4	17.31	9.5
57.5	120.9	2.0	6.95	3.8
Total	***6077.8***	***100.0***	***182.86***	***100.0***

- Source: Annual rainfall amounts and computed amounts using isohyetal method

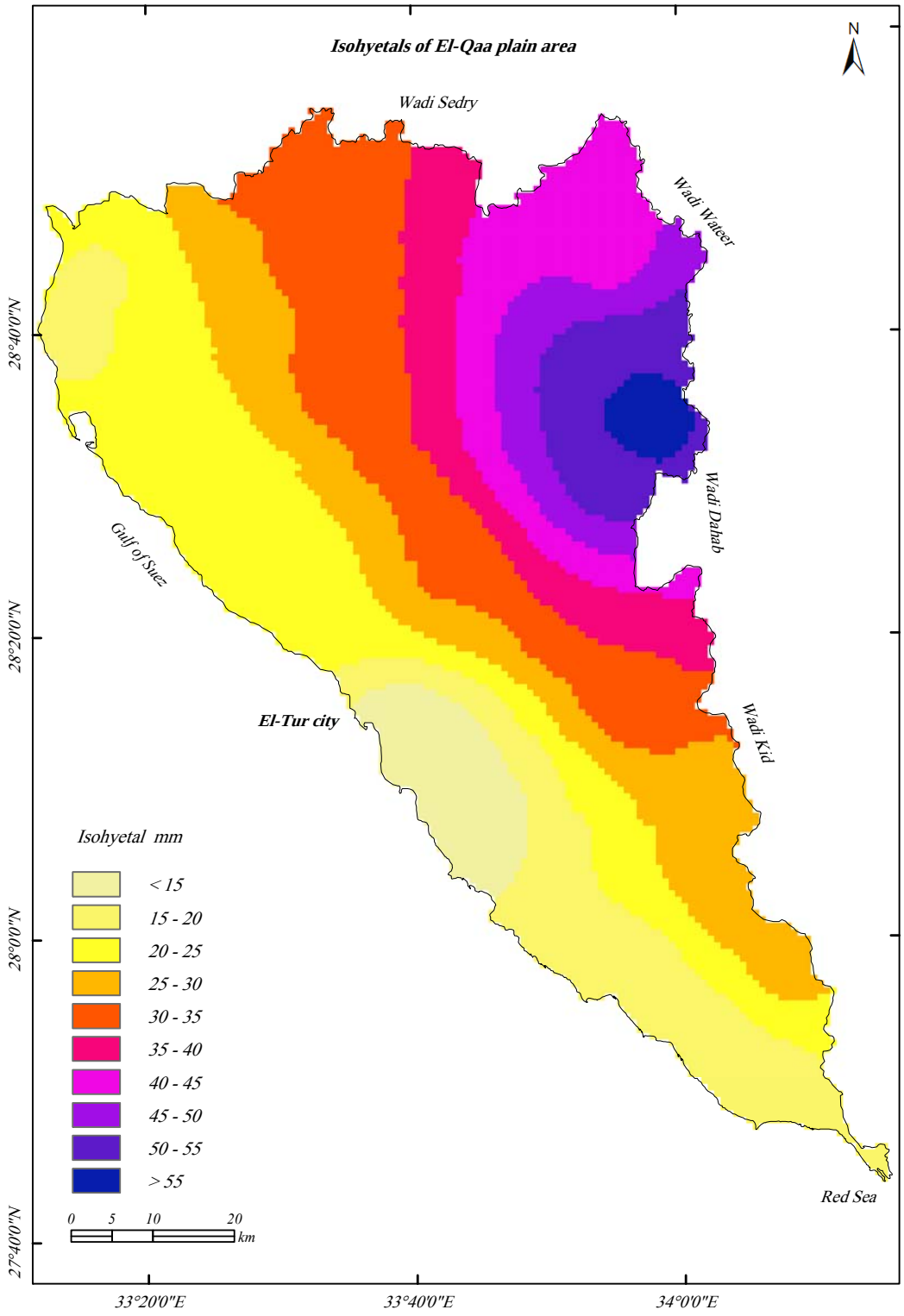

Fig (3-9) ***Isohyetals of El-Qaà plain area (annual amounts)***

Because of the Isohyetal method is considered the best method to compute the total amount of rainfall in areas with different relief like the study area, this method has been used to calculate the annual rainfall in El-Qaà plain area which can produce runoff, and, therefore, can be used to or develop the study area.

From (tab.3-7) and (fig 3-9) can be concluded that:

1- The total amount of rainfall in the study area has been computed using the isohyetal method and reaches to 182.86 million m^3/ year which can be considered a big amount in the arid area.

2- The relief plays an important role to increase the amount of rainfall, whereas, 23.5% of the total area lie between isohyetals 25 and 30 mm represented in the piedmont area.

3- 30.2% of the study area lie between the isohyetals 30 and 40mm and have approximately 55.31 millions m3 /year with ratio of 30.3% of total rainfall. This area is represented mostly in upper tributaries of the main Wadis i.e. Wadi Firan, Wadi Maier and Wadi Habran.

4- 12.5% of the study area has 21.3% of the amount of rainfall (annually more than 50mm). The amount of rainfall in this area reaches to 8.88 millions m^3/year that have been distributed in the eastern and north eastern are past of Wadi Firan and Wadi Habran.

3.1.1.5. Rainfall intensity - duration - frequency curve

Rainfall depth-duration-frequency relationships of high intensity rainfalls are needed for estimating floods in inadequately gauge - equipped streams, and for urban developments, drainage works for airports and water regulating structures on a small basis. In order to have reliable frequency relationships for a certain area, autographic point rainfall data over many years are needed (SENDIL, U., and SALIH, A., 1987). However, in many developing countries such data are either sometimes unavailable in some areas or insufficient in length because of war periods in these areas or no stations to record rainfall.

There are several methods that can be used to generate Rainfall Intensity – Duration - Frequency (IDF Curves). Primary GUMBEL Type 1 distribution methodology was selected to perform the flood or rainfall probability analysis. The Gumbel theory of distribution is relatively simple and uses only extreme events (maximum values or peak rainfalls).

Once the data have been sorted into the various areas of influence, curve development begins. IDF curves are used when storm information is needed to design a structure. In El-Qaà plain area, rainfall intensity-duration-frequency curves are used in conjunction with the Rational Method to calculate peak runoff from a particular watershed.

This area has sometimes extreme rainfall events and many years of data. Graphical representations have been developed to present the rainfall data in a usable format. Each graph has six curves on it, each one representing a different storm frequency. They usually represent the 2-, 5-, 10-, 25-, 50-, and 100-year storms. Rainfall intensity is on the x-axis and is measured in mm/day. Probability of a given rainfall is on the y-axis and is measured in %. The amount of rain produced by a particular storm is site specific.

When a particular rainfall is referred to as a one day, 100-yr storm, that means that the rain will last for one day (duration) and will only be equaled or exceeded once every one hundred years (frequency) in that particular area. Understanding the significance of each curve, it is then a simple matter to determine the amount of rainfall (intensity) for that particular area during that time period. For example:

1. *Select the 100-year IDF curve.*
2. *Find the probability of a given rainfall on the y-axis.*
3. *Determine where the curve and the graph line intersect, then follow it straight across to the x-axis to determine the amount of rain (*Fig 3-10*).*

Using only peak rainfall data to represent each year reduces the probability of error to less than 0.5 percent. The GUMBEL Method calculates the 2-, 5-, 10-, 25-, 50-, and 100-year return intervals for each duration period and requires several calculations.

Gumbel 1941 has suggested some equations to compute the probability of rainfall and runoff, return period of these values

1- The first equation to compute the probability of rainfall p^-

$$P^- = 1 - \frac{m}{n+1}$$

p^- *is probability of a given rainfall*

m *is the value order*

n *is the number of record years*

2- The second equation to compute Return period ***T***

$$T = \frac{1}{P^{-}} = 1 / \left(1 - \frac{m}{n+1}\right)$$

3- The third equation to compute the frequency curve

$$X_T = X_n - = \left(S_{n-1}(X) / S_n(Y) * \left(\bar{Y}_n Y_T\right)\right)$$

Where ***T*** is standard return period, ***X*** is the maximum of daily rainfall; ***Y*** is Logarithmic Constant, S_n is Reduced Standard deviation and Y_n is reduced mean.

Tab. (3-8) Rainfall probability, duration, frequency, and return period in the study area

rec. years	Annual rain	Daily rain	Sort desc. annu.	Sort desc. daily	return period	P	p^{-}	2 years	5 years	10 years	25 years	50 years	100 years
1934	64.8	48.4	121.5	76.2	***1.1***	***0.06***	***0.94***	***0.1***	***0.3***	***0.6***	***1.6***	***3.1***	***6.3***
1935	13.1	9.5	64.8	48.4	***1.1***	***0.13***	***0.88***	***0.3***	***0.6***	***1.3***	***3.1***	***6.3***	***12.5***
1936	18.6	17.2	62.2	18.2	***1.2***	***0.19***	***0.81***	***0.4***	***0.9***	***1.9***	***4.7***	***9.4***	***18.8***
1937	121.5	76.2	47.5	17.2	***1.3***	***0.25***	***0.75***	***0.5***	***1.3***	***2.5***	***6.3***	***12.5***	***25.0***
1979	5.3	3.2	39.4	12.9	***1.5***	***0.31***	***0.69***	***0.6***	***1.6***	***3.1***	***7.8***	***15.6***	***31.3***
1980	39.4	18.2	26.4	12.2	***1.6***	***0.38***	***0.63***	***0.8***	***1.9***	***3.8***	***9.4***	***18.8***	***37.5***
1981	18	12.2	23.3	11.2	***1.8***	***0.44***	***0.56***	***0.9***	***2.2***	***4.4***	***10.9***	***21.9***	***43.8***
1982	47.5	12.9	20.1	10.7	***2.0***	***0.50***	***0.50***	***1.0***	***2.5***	***5.0***	***12.5***	***25.0***	***50.0***
1983	20.1	4.4	18.6	9.5	***2.3***	***0.56***	***0.44***	***1.1***	***2.8***	***5.6***	***14.1***	***28.1***	***56.3***
1984	4.8	1.8	18.5	6.4	***2.7***	***0.63***	***0.38***	***1.3***	***3.1***	***6.3***	***15.6***	***31.3***	***62.5***
1985	6.2	1.6	18	4.4	***3.2***	***0.69***	***0.31***	***1.4***	***3.4***	***6.9***	***17.2***	***34.4***	***68.8***
1986	18.5	2.7	13.1	3.2	***4.0***	***0.75***	***0.25***	***1.5***	***3.8***	***7.5***	***18.8***	***37.5***	***75.0***
1987	23.3	6.4	6.2	2.7	***5.3***	***0.81***	***0.19***	***1.6***	***4.1***	***8.1***	***20.3***	***40.6***	***81.3***
1988	62.2	11.2	5.3	1.8	***8.0***	***0.88***	***0.13***	***1.8***	***4.4***	***8.8***	***21.9***	***43.8***	***87.5***
1989	26.4	10.7	4.8	1.6	***16.0***	***0.94***	***0.06***	***1.9***	***4.7***	***9.4***	***23.4***	***46.9***	***93.8***

- *Source: The archive of Meteorological authority, reports none published, and computed with researcher using GUMBEL method*

Many hydrological engineering planning, design, and management problems require a detailed knowledge of rainfall and flood event characteristics, such as flood peak, volume, and duration. Flood frequency analysis often uses the GUMBEL distribution to model flood peak values, which provides an assessment of flood events.

(Tab 3-8) and (Fig 3- 10) show that:

1- The rainfall estimates were computed for durations of one day and for return periods from 2 to 100 years. The return period of maximum rainfall in the study area during the record years (15 years) reaches to 1.1 and probability of the maximum rainfall (76.5 mm/ day) has been estimated 94% during the same period, but the frequency of maximum rainfall ranges between 0.1 in 2 years and 6.3 in 100 years.

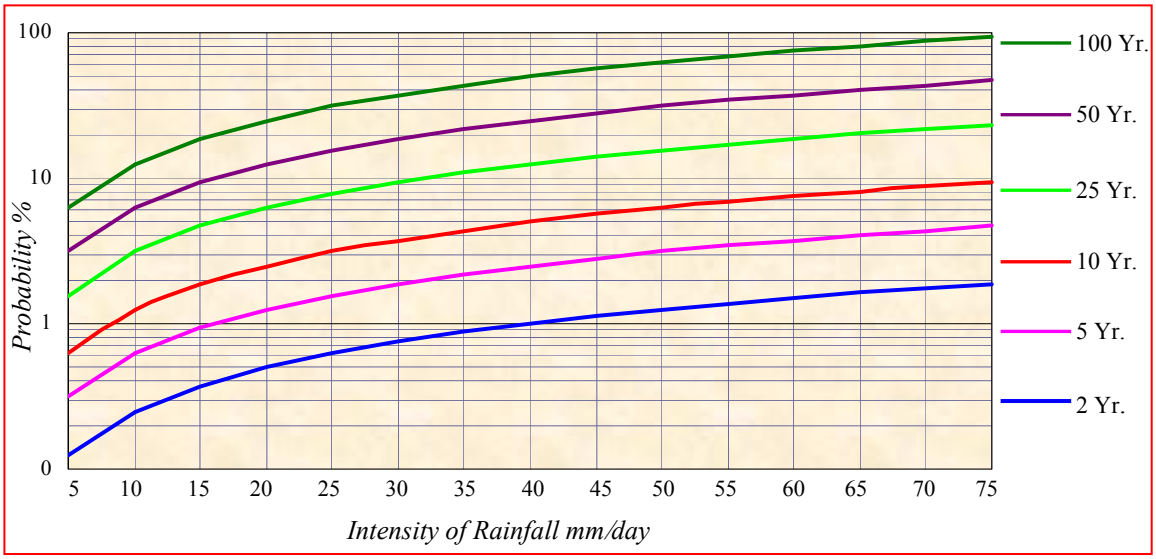

Fig (3-10) *Rainfall depth- frequency relationships in El-Qaà plain area of 2 to 100 years*

2- The return period of influence of amount of rainfall (from 10 to 20mm /day) is approximately 1.1, and the frequency ranged between 0.8 during 2 years and 37. 5 in 100 years, whereas the return period of the amount of rainfall (from 20 to 50mm/ day) reaches to 4.4, and the frequency ranges from 1.1 during 2 years and 12.5 in 100 years.

3- From previous analysis can be concluded that the study area perhaps had 6.3 times heavy rainfall (more than 70mm/day) through 100 years, 3.1 time through 50 years , and 0.1 time during 2 years. This amount can produce destroying flash floods which have a direct impact the human activity and infrastructure in the study area.

3.1.1.6. Rainfall – runoff relationships

The relationship between rainfall and runoff is one of the most important problems in applied geomorphology and hydrology. It is also one of the most difficult problems. The rainfall-runoff relationship quantifies the response function describing the behavior of a watershed. The response function is a result of numerous processes, complex and interdependent, that participate in the transformation of rainfall into runoff. The transformation process encompasses virtually the entire domain of hydrologic cycle. This all encompassing nature of the transformation process is largely responsible for the complexity underlying the rainfall-runoff relationship. The complexity is enhanced further by spatial and temporal variability of hydrometeorological conditions and watershed physiography as well as their interacting influences.

It is evident that there are three processes involved in a rainfall-runoff relationship: *rainfall process, transformation process* and *runoff process*. The quantification of this relationship depends on the characterization of the two former processes, namely, rainfall process and transformation process. Their description is the cornerstone of classifying models proposed to predicate the rainfall-runoff relationships (SINGH, V., and BIRSOY, Y., 1977).

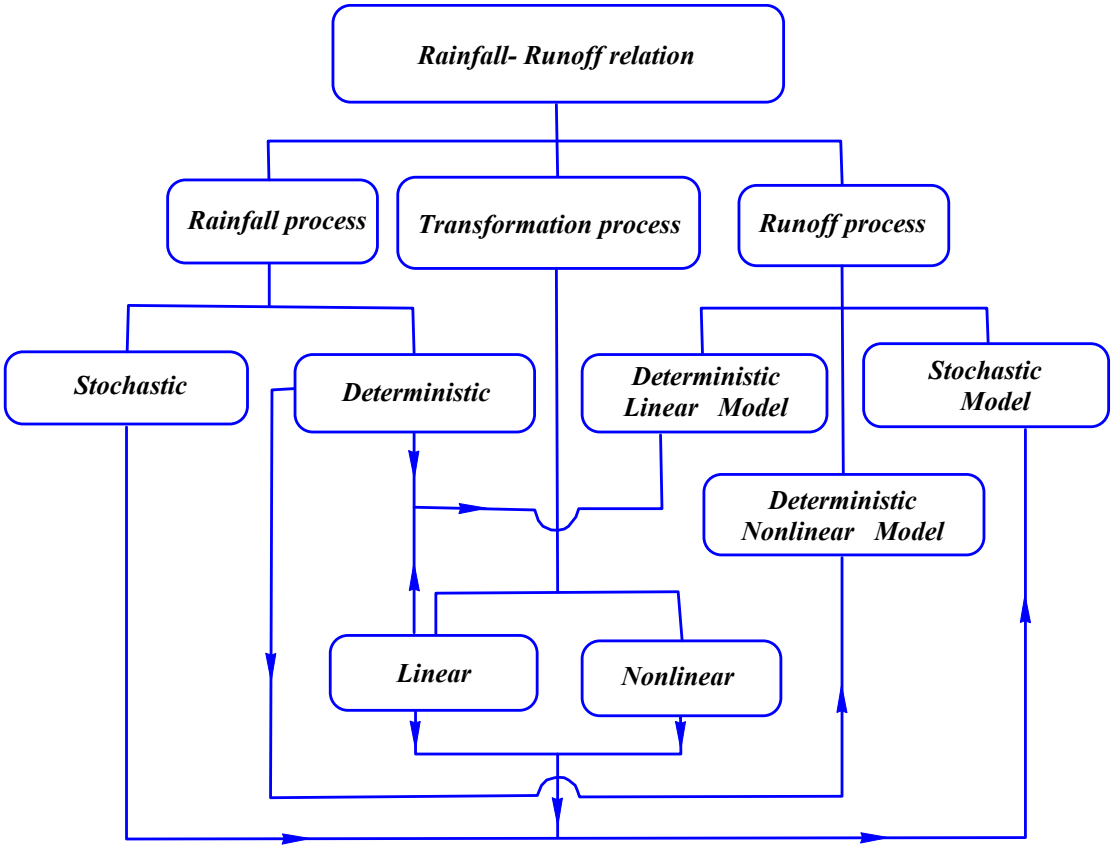

Fig (3-11) *(Rainfall- runoff relation), evolution of three broad, general classes of models for the runoff process, modified after* (SINGH, V., and BIRSOY, Y., 1977)

For example, if the rainfall process is completely known a priori, as is the case when dealing with an individual rainfall event, i.e., the rainfall process is deterministic then, with an assumed structure of the transformation process, the resulting model for the runoff process will be deterministic as well, and will be able to describe completely the runoff hydrograph due to that known rainfall episode. However, if the rainfall process is described by a set of statistical parameters or its structure is assumed to be stochastic, then, the resulting model of the runoff process will also be stochastic.

Therefore, SINGH, V., and BIRSOY, Y., 1977 had suggested an approach showing the evolution of three broad, general classes of models for the runoff process. This classification is merely illustrative and obviously not exhaustive (Fig 3-11).

Many researchers have examined temporal and spatial rainfall distributions, especially the distribution of extreme rainfall values. These studies are important for water resource and flood control management and for designing and planning various engineering projects (SALEH, A. 1989, SMITH 1992; PALMER et al 2002, and ASHOUR, M. 1994,). They concluded that rainfall generally increases with elevation, and mountain ranges can create leeward-side ‘‘rain shadows.’’ This implies some underlying mechanisms that play an important role in organizing rainfall systems in a mountainous region

Fig (3-12) shows an analysis of the rainfall-runoff relationship and, subsequently, an assessment of relevant runoff coefficients should best be based on actual, simultaneous measurements of both rainfall and runoff in the study area that have a strong direct relationship between rainfall and runoff. As explained above, the runoff coefficient from an individual rainstorm is defined as runoff divided by the corresponding rainfall both expressed as depth over catchments area (mm).

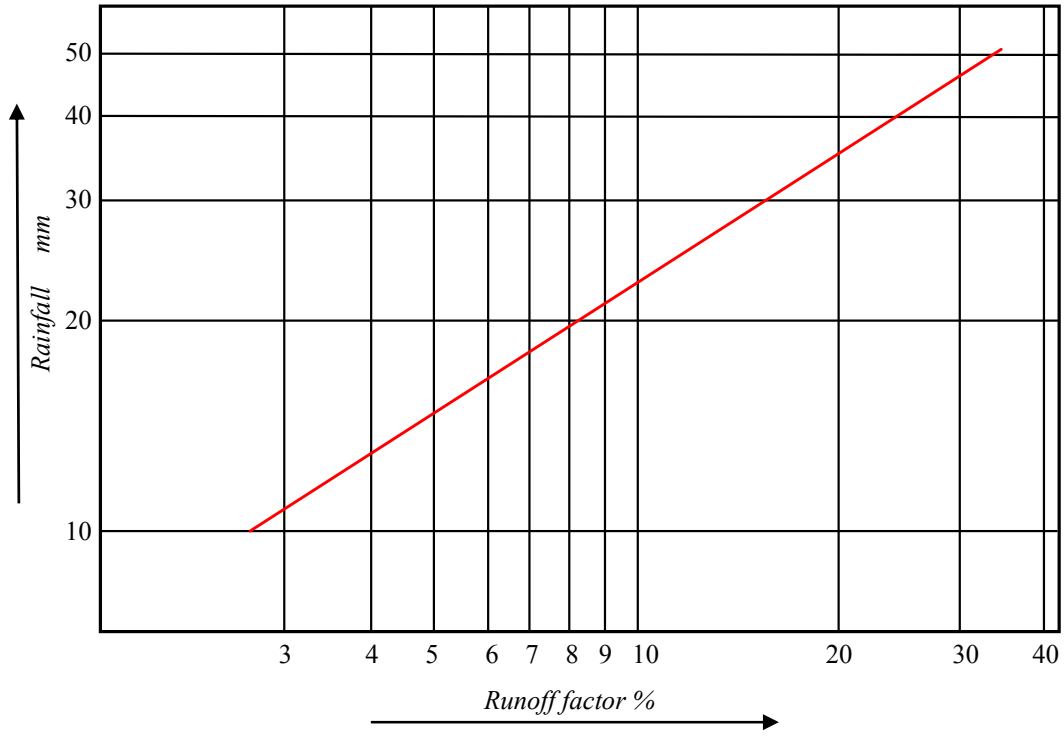

Fig *(3- 12) Rainfall-runoff relationships in El-Qaà plain area*

From previous discussed can be concluded that:

1- The number of rainy days during the months of December and February are normally higher than the rest of the year. Two major meteorological features are normally responsible for rainy conditions during that period; they are the Development of Barometric Lows of Cyprus, and the formation of wet Prevailing Westerlies (EL FANDI 1946).

2- The climate conditions lead to the formation of successive cold fronts advancing over the Mediterranean Sea and invading the northern parts of Egypt and Sinai. The rainfall intensities due to these storms decrease as the storms advance in-lands. Thus, although these types of stones may cause relatively more frequent and rather intense rainy conditions over the northern parts of Sinai, their effect over the central and the southern parts is rather limited.

3- The northward oscillations of the Sudan monsoon low and the passage of troughs of the upper westerlies are the two major types of meteorological conditions producing rain during spring and autumn Fig (3-1B). The storms leading to the formation of such rainy conditions are completely different from those producing rain during winter (EL FANDI 1948 & 1350).

4- The rainfall events that occur during autumn and spring are usually rare. However, their intensity and the extension of the rainy clouds formed by these types of storms are much larger than those produced by winter storms. Furthermore, the intensity of rainfall events due to these storms is usually higher over the southern parts of Egypt and Sinai. These storms have been responsible for most of the disastrous flash flood events observed over the southern parts of Egypt and Sinai. The two major types of these storms are described next with some details.

5- *The Northward Oscillations of the Sudan Monsoon Low*, rainy storms due to this type of meteorological conditions occur due to an actual extension of the Sudan Monsoon low towards the northern zones of the Red Sea. This low gives rise to an inflow of south east rather warm and humid currents into the eastern desert of Egypt and Sinai.

6- The northward oscillations coincide with the presence of another low with cold air ever the eastern parts of the Mediterranean as shown in Fig. (3-1B). When this happens, rapid lifting of these south easterly currents takes place over the front the eastern desert and southern Sinai causing severe thunder storms. The actual location of the surface over red sea and southern Sinai depends on the oscillation of the Sudan Monsoon low. Heavy rainfall due to this type of meteorological situation was reported eastern desert. The duration and areal extent of such conditions are rather large. Consequently, they are normally accompanied with flash floods. Most of the deadly floods that have already taken place in Wadi Watir of Sinai over the past few years were caused by such storms.

7- *The Passage of Troughs of the Upper Westerlies*, this form of rainy conditions is related to the upper winds at approximately three kilometers above mean sea level. During autumn and spring such winds changes their directions from being Westerlies to Easterlies and North Easterlies, and are accompanied with the formation of troughs notably over Upper Egypt and Sinai. These troughs set up centers of convergence that ultimately give rise to the development of cyclones. Such cyclones in turn draw into their circulation air masses of widely different physical properties. The convergence of such air masses does ultimately cause the formation of heavy thunderstorms. They are heavier in autumn than in spring. The duration of storm may last up to one day and is sufficient to cause a lot of damage. Moderate storms of this type occur once every year on the average (EL-FANDY 1950).

8- The rainfall depth at any location next year can be any value larger than zero. However, some values are more likely to occur than the others. Nevertheless, extremely high values are less likely to be exceeded than the relatively smaller values. Yet, only one sever storm is sufficient to cause a lot of flood damages. Therefore, in the design of many structures such as the spillway of a dam, and/or flood protection works it is essential to properly define the likelihood of occurrence for the extreme events in particular.

9- Extreme value analysis implies the use of available records, together with some theoretically sound extrapolation technique, to estimate the maximum possible rainfall depth anticipated within 10, 50, 75, 100, or any other number of years.

Such an analysis was conducted for the GMA (General meteorological authority) rainfall recording stations in southern Sinai. For each meteorological station the maximum daily rainfall depth recorded in each year was obtained. Thus, if thirty years of records were available, then thirty daily storms were selected (each storm is the maximum storm recorded during one of these years). These records were arranged in a descending order (HAAN, 1979). The results were plotted on GUMBEL probability Fig (3-10).

10- The return period of maximum rainfall in the study area during the record years (15 years) reaches to 1.1 and probability of the maximum rainfall (76.5 mm/ day) has been estimated 94% during the same period, but the frequency of maximum rainfall ranges between 0.1 in 2 years and 6.3 in 100 years.

11- The return period of influence of amount of rainfall (from 10 to 20mm /day) is approximately 1.1, and the frequency ranged between 0.8 during 2 years and 37. 5 in 100 years, whereas the return period of the amount of rainfall (from 20 to 50mm/ day) reaches to 4.4, and the frequency ranges from 1.1 during 2 years and 12.5 in 100 years.

12- The study area perhaps had 6.3 time's heavy rainfall (more than 70mm/day) through 100 years, 3.1 times through 50 years, and 0.1 times during 2 years. This amount can produce destroying flash floods which have a direct impact the human activity and infrastructure in the study area.

3.1.2. Surface losses estimation

In arid regions, water losses are usually high due to infiltration and evaporation from open surfaces. These losses are often neglected by many project planners. A theoretical analysis has been developed to modify the equation usually used to determine the water losses based on the ponding method, where the channel longitudinal slope was considered in the analysis (MOGHAZI, M. and ISMAIL, S., 1997**)**.

Initial losses occur in the sub-basins before runoff reaches the stream networks, whereas transmission losses occur as water is channeled through the valley network. Initial losses are largely related to infiltration, surface soil type, land use activities, evaporation, transpiration, interception, and surface depression storage.

The interception loss comprises two distinct elements. The first is the interception storage, i.e., the depth (or volume) retained in the foliage against the forces of wind and gravity. The second is the evaporation loss from the foliage surface, which takes place throughout the duration of the storm. The combination of these two processes leads to the following formula for estimating interception loss

3.1.2.1. Evaporation losses

Evaporation has been discussed in the first chapter as a climate element like distribution monthly average and the factors that influence on the evaporation, but in this chapter we describe the evaporation as an important influence factor on the runoff. It is focused from many sciences such as Hydrology, Botany, Geology, and Geomorphology especially in the arid zones. Evaporation is expressed as an evaporation rate in millimeters per day (mm/d). Evaporation rate is a function of several meteorological and environmental factors. Those important from a hydrologic viewpoint are net solar radiation, the saturation vapor pressure, the vapor pressure of the air, air and water surface temperatures, wind velocity, and atmospheric pressure.

The evaporation values in the study area have been differenced from one place to another owing to air temperature, altitude, wind speed, position, and local relief. Whereas the annual range of evaporation is measured at Ras Sudr for about 11.6 mm/day, 11 mm/day at Abu Rudeis, 9.9 mm/day at El-Tur and 17.9 mm/day at Sharm El-Sheikh. It is the result of the Gulf of Suez and wind speed in the study area (SALEM, 1993).

Generally, daily evaporation amount can be calculated using three ways. First way is direct evaporation estimation by pan experiments. Second way is indirect depending on meteorological data like PENMAN-MONTEITH model (PM model). There are some difficulties in these methods, such as: long measurement times, difficulties in measurement and, evaporation calculation equations are not universal. The third method is of Genetic Algorithm (GA) and Backpropagation Feedforward Neural Network (FFNN). They have been adapted to estimate daily evaporation amount for Lake Sapanca in Turkey.

In the study area, FFNN and GA models are considered the best methods to compute daily evaporation estimation depending on daily min. and max. temperature, wind speed, relative humidity, real solar period and maximum solar period. Evaporation amount is a function of solar radiation, temperature, wind speed, vapor pressure deficit, atmospheric pressure, and the surrounding environment. Evaporation, as a major component of the water cycle, is important in water resources development and management.

According (DOGAN, E. and DEMİR A. 2006) the Genetic algorithm application, first, evaporation amount of the study area function is determined by tried different functions. In this step, while appropriate function is selected, best function shown in equation 3 was determined according to Root of Mean Square Error (RMSE) by evaporation data used in training. The coefficients of the appropriate function have been determined by using genetic algorithm.

$$E = k + \sum_{i=1}^{6} Sin(p_i * x_i)$$

$$E=1.168+Sin(-0.25*x_1)+Sin(-0.11*x_2)+Sin(0.03*x_3)+Sin(0.52*x_4)+Sin(0.04*x_5)+Sin(0.57*x_6)$$

E = Measured evaporation, E (mm)

X_1 = Max. Temperature, T_{max} (°C)

X_2 = Min. Temperature, T_{min} (°C)

X_3 = Relative humidity, RH (%)

X_4 = Wind velocity, U (m/s)

X_5 = Daily solar period, N (hour)

X_6 = Astronomic solar period, N (hour)

K, P_i = Constants $_i$ = (1. 6)

Parameters best estimate

p1 = -0.25

p2 = -0.11

p3 = 0.03

p4 = 0.52

p5 = 0.04

p6 = 0.57

k = 1.168

3.1.2.1.1. The total amount of evaporation

The water amount of evaporation is very important to determining runoff hazard in the study area, especially during rainy months. Therefore, it is not necessary to compute these amounts in dry months. Because there is no measuring of evaporation amount during rain storm it can be depending on daily evaporation to compute the total amount, or, divide the daily value by 24 hour to define the amount of evaporation during a short rainy storm.

Tab (3-9) daily evaporation (mm/day) and total evaporation losses (millions m^3/day) in rainy months in El-Qaà plain area.

Station	Jan.	Feb.	Mar.	Oct.	Nov.	Dec.	Aver.
RasSudr	7.4	8.8	9.7	10.5	8	6.9	***8.1***
Abu Rudeis.	8	9	10.3	9.8	5.5	8.4	***8.5***
Nekhel	5.6	7.1	10.4	10.6	7.2	5.9	***7.8***
St. Catherine	5.7	6.9	9.1	10.7	6.9	6.2	***7.6***
El-Tur	7.2	8	9.5	8.2	7.5	7.3	***7.9***
Sh. El-Sheikh	11.1	13.2	14.7	16.4	13	11.7	***13.4***
Average	***7.5***	***8.8***	***10.8***	***11.0***	***8.0***	***7.7***	***8.9***
Water losses Million m^3	**45.58**	**53.49**	**65.64**	**66.86**	**48.62**	**46.80**	***54.09***

Tab (3-9) shows the average daily amount of evaporation mm/day at several stations during rainy months. These values range from one station to another in conformity with situation, altitude, and local relief. Sharm El-Sheikh station has a higher value of daily evaporation, 13.4mm/day, while St. Catherine station has a lower value, 7.6mm/day; the average of total area has reached 8.9mm/day.

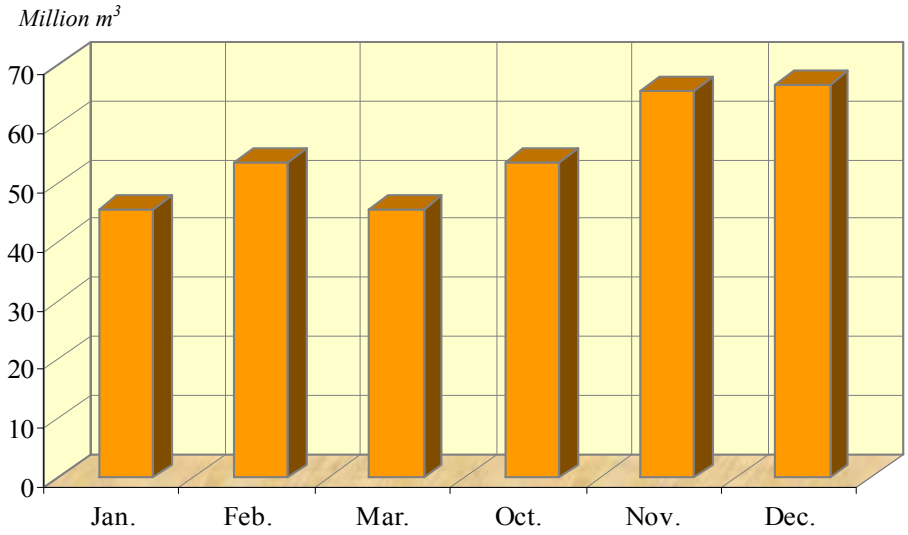

Fig (3- 13) *total evaporation losses million m^3/day in rainy months in El-Qaà plain area.*

Fig (3- 13) shows the total evaporation losses in rainy months in the study area. The values range from 45.58 millions m^3/day in January to 66.86 millions m^3/day in October, while the average of evaporation losses during rainy months reaches about 54.09 millions m^3/day. These amounts in one day often have a little influence to mitigate flash floods compared with the total amount of rainfall that reaches about 182 million m^3/year, which may be occur in one day or two hours, Whereas the evaporation during rain storm is lower than any time, therefore, the amount of evaporation at the time of rain is very small and its influence is also limited.

3.1.2.2. Infiltration losses

Infiltration is one of the main factors with influence on flash floods and their energy. Infiltration is the process by which precipitation is abstracted by seeping into the soil below the land surface. Once below the surface, the abstracted water moves either laterally, as interflow, into valleys or vertically, by percolation, into aquifers. The water stored in aquifers moves as groundwater flow, driven primarily by gravitational forces, eventually flowing into subsurface reaching the sea.

Infiltration is a complex process. It is described by either an instantaneous infiltration rate or an average infiltration rate, both measured in millimeters per hour. The total infiltration depth, in millimeters, is obtained by integrating the instantaneous infiltration rate over the storm duration. The average infiltration rate is obtained by dividing the total infiltration depth by the storm duration.

Infiltration rates vary widely, depending on the condition of the land surface (eventually crust), the type, extent, and density of vegetative cover; the physical properties of the soil, including grain size and gradation; the storm character, i.e., intensity and duration; the water temperature and the water quality, including chemical constituents and other impurities (PONCE, V. M. 1989).

A number of studies have addressed transmission losses in similar climatic (arid to semi-arid environments), hydrologic (ephemeral streams), and geologic settings (drainage network dissecting mountainous areas). BEN-ZVI (1996) estimated an infiltration loss rate of 7200 m^3/h/km in the Negev Desert, Israel. WALTERS (1990) proposed three regression equations, two of which relate transmission losses to upstream flow volume and channel length. The third equation includes the effect of channel width. His expressions provide reliable predictions for large floods (WALTERS, 1990).

SHARMA and MURTHY (1994) applied a similar approach for ephemeral streams in northwest India and developed similar but not identical expressions. Using a mass-water-balance approach, ABDULRAZZAK and SORMAN (1994) provided equations to derive transmission losses knowing inflow volume, active flow width, and antecedent-soil-moisture measurements. Their equations were based on an extensive database for an arid watershed (the Tabalah basin) in the southwestern region of the Kingdom of Saudi Arabia.

SHENTSIS et al. (1999) used data for the Nahal Tsin in Israel to develop a model that relates transmission losses to total inflow for a Wadi reach between hydrometric stations. Because of the obvious similarities between the climatic conditions and landforms of the Southern Sinai hills and those of the southwest hills of Saudi Arabia, and because some of the above-mentioned methods require knowledge of parameters that are unavailable for our study area, we adopted Walters' expressions to calculate transmission losses in the valleys of the El-Qaà plain area. Because of a lack of information on channel width along the ephemeral streams of the Southern Sinai and because the investigated floods were quite large, we adopted Walter's expression that relates transmission losses to the flow.

Transmission loss assessment in ephemeral streams of arid regions is difficult due to the transient nature of the surface and subsurface flow processes. However, simplified procedures based on the mass balance approach provide a reasonable estimate of the mean infiltration losses. If *TL* represents the cumulative volume of transmission loss, V_{UR} the cumulative upstream inflow volume, V_{DR} the cumulative downstream outflow volume and V_{TR} the tributary runoff contribution to the main channel, then it follows by mass balance that:

$$TL = V_{UR} - V_{DR} + V_{TR} \qquad (1)$$

The main difficulty in the assessment of transmission loss is the estimation of any tributary runoff contribution, a factor which has been ignored in the majority of studies (SHARP & SAXTON, 1962; JORDAN, 1977; LANE, 1983; and WALTERS, 1990) In this study, a runoff coefficient procedure based approximately on a Soil Conservation Service (SCS) formula is suggested for the estimation of tributary runoff. The procedure utilizes information collected on precipitation, runoff and estimated storage abstraction capacity for upstream as well as downstream and tributary areas. The upstream runoff coefficient *(CRU)* is estimated from its common definition and the SCS relationship:

$$C_{RU} = \frac{V_{UR}}{V_{UP}} = \frac{V_{UP}}{V_{US} + V_{UP}} \qquad (2)$$

Where V_{UP} and V_{UR} are the precipitation and runoff volumes for the upstream area and V_{US} is the upstream storage abstraction capacity. The tributary basins runoff coefficient, C_{RT}, for areas located between the upstream and downstream runoff stations, can be estimated by a similar relationship:

$$C_{RT} = \frac{V_{TR}}{V_{TP}} = \frac{V_{TP}}{V_{TS} + V_{TP}} \qquad (3)$$

Where V_{TP}, V_{TR} and V_{TS} represent the tributary precipitation, runoff, and storage abstraction capacity volumes, respectively, rearrangement of the terms in equation (3) produces an equation for the estimation of tributary runoff:

$$C_{TR} = C_{TR} V_{TP} = \left(\frac{V_{TP}}{V_{TS} + V_{TP}} \right) V_{TP} \qquad (4)$$

The assessment of tributary runoff requires the estimation of storage abstraction capacity, V_{TS}. However, the relationship between abstraction capacity of both upstream and tributary values to their respective areas provide a means for estimating abstraction capacity as follows:

$$V_{TS} = V_{TS} \frac{A_T}{A_U} \qquad (5)$$

Where A_U and A_T are the upstream and tributary basin areas, respectively. Tributary runoff (V_{TR}) estimation requires calculation of the upstream and tributary storage abstraction volumes, V_{US} and V_{TS}, using equations (2) and (5). The foregoing procedure was applied for the assessment of transmission loss in a typical Wadi channel using rainfall-runoff information.

(ABDULRAZZAK, M, and SORMAN, A, 1993) had concluded that the transmission loss can be estimated using tow equations as follows:

$$TL = 0.058 + 0.033(HxT)$$

$$TL = 0.079 + 0.0005(MFWxT)$$

Where TL is transmission losses, H_X is the duration of flow, and MFW is maximum flow width in km^2. But the results have variation from one region to another owing to outcrops lithology, and climate elements.

Infiltration losses of water in the study area has been related with some variables, i.e. local relief, slope angels, thickness of deposits and their humidity, time of rainstorm, and plant cover, in addition, kind of rock and its characteristics such as porosity (photo 3-4), permeability and structure (SALEM, A., 1989).

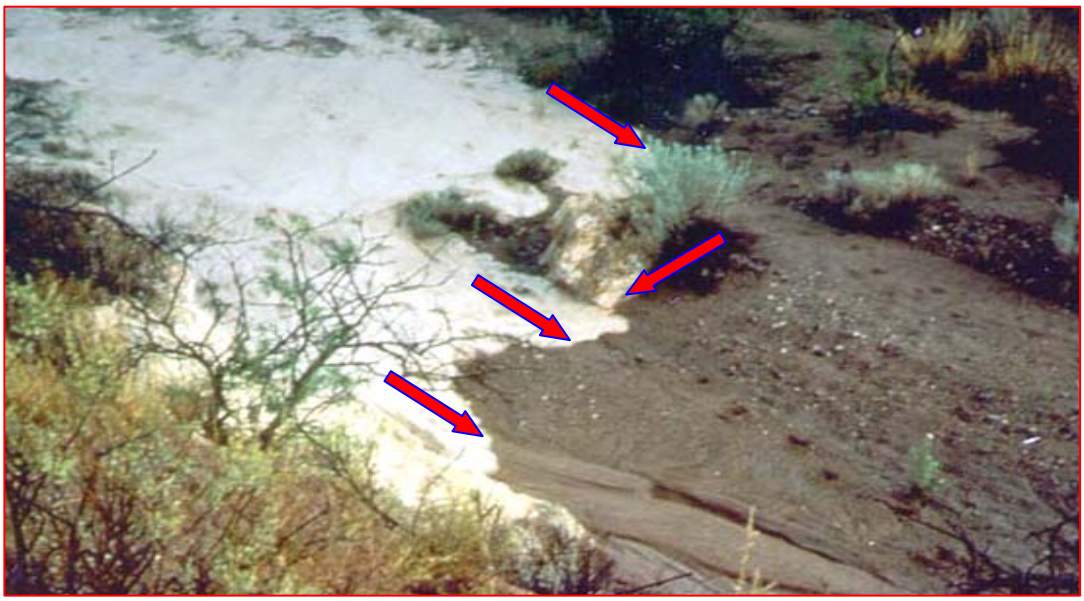

Photo (3-4) Channel transmission losses during runoff wave advancing over a dry streambed in Wadi Kid 1999 (Southern Sinai)

Chorley, J. 1973 had attained a classification to estimate infiltration losses range depending on outcrops of lithology and thickness of deposits. This method is considered the best to estimate the total water of infiltration losses in arid regions by porosity and permeability. The volume of water which can be held within the sediment is controlled by the porosity of material. Porosity may be defined as follow:

$$Porosity = \frac{volume\ of\ voids\ in\ a\ material}{Bulk\ volume\ of\ the\ material}$$

Porosity is usually expressed as a decimal fraction or as a percentage. For example, a rock specimen which contains pores or open spaces equal to one fourth of the total volume of the specimen would have a porosity of 25%. Naturally occurring geologic materials vary widely in porosity. Table (3-10) contains a list of representative porosity for various geologic materials. These values range between 0.0001- 1 % in granite rocks, 5- 25% in sandstone, and 30- 40% in alluvial sand and wadi deposits (CHORLEY, J., 1973). In the case of granular sediments, porosity is not directly affected by the grains, but is affected by the uniformity of size, the shape, and the packing characteristics of the grains (photo 3-5).

Photo (3-5) *shows the uniformity of size and the shape of the grains in Wadi Asla deposits.*

The spead by which water can penetrate sediments is a function of their permeability. The permeability of granular in the study area is greatly affected by size of grains as well as by their shape, packing, and uniformity of size. Permeability can be expressed by different ways. Table (3-10) gives approximate ranges of permeability for various geological materials in the study area; it will be described as a rate of discharge per unit area (e.g. m^3/day/km^2) under controlled hydraulic conditions.

Tab (3-10) Representative porosity, permeability, and infiltration losses amount of El-Qaà plain area.

Geologic material	***Area km²***	***%***	***Porosity (Void space) %***	***Permeability ranges*** *1000m^3/day/km^2*	***Infiltration losses million m^3***
Granite, Slate, Schist, Gneiss, Tuff	2598.5	42.8	0.0001 - 1	3.79	9.9
Volcanic	221.6	3.6	0.001 - 50	37.9	8.4
Clay, Silt, Shale, Sabkha	277.4	4.6	15 - 50	75.7	21.0
Sandstone	403.8	6.6	5 - 25	151.4	61.1
Limestone	282.7	4.7	0.1 - 10	1514	428
Alluvial sands, Wadi deposits	543.4	8.9	30 -40	15140	822.7
Alluvial fans (gravels and boulders)	1750.4	28.8	25 -35	151400	265,011
total	6077.8	100			266,362.1

- Source: modified after Chorley 1973, and the amounts of infiltration losses are computed by researcher

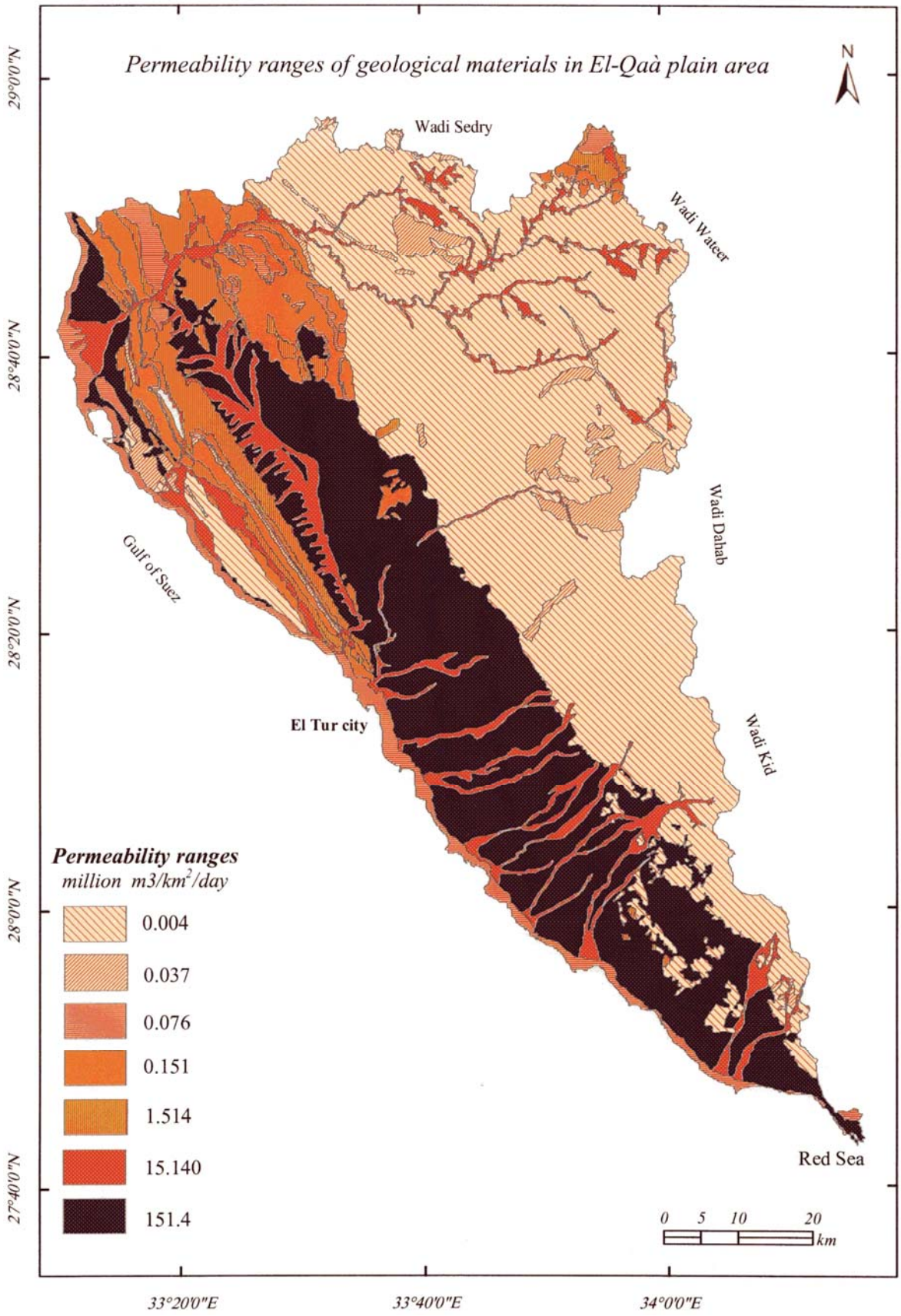

Fig (3-14) ***Permeability ranges of geological materials in El-Qaà plain area,*** *the source: Geological map of Sinai, scale 1: 250 000, 1994, Geological map of Egypt –digital map- scale 1: 250 000, 2003, modified by the researcher, and permeability ranges modified after CHORLEY, 1973.*

Fig (3-14) and Tab (3-10) show that:

1- The permeability is mostly related with outcrop lithology of the study area, whereas the lowest values of permeability were found in granite, slate, schist, volcanic, and gneiss rocks 3790 $m^3/day/km^2$. Due to these rocks which cover 46.4% of the study area especially in the mountain area which has rainfall more than the coastal area, the affect of permeability and infiltration in the eastern part of the study area is limited.

2- The values of permeability range between 0.076 to 151.4 million $m^3/day/km^2$ in the areas which are covered with sedimentary rocks and Wadi deposits, these materials cover about 24.8% of the total area; they are represent in the north east and the north west of the study area in Wadi Firan and Wadi El-Aawag. The effect of permeability and infiltration losses in these areas is higher than in the igneous rock area.

3- The alluvial fans (gravels and boulders) which cover about 28.8% of total area have the highest values of permeability in the study area 151.4 million $m^3/day/km^2$ if this amount of water wasfound. This value seems being very high, but it is related with the size and shape of grains and the thickness of these deposits. In addition, during the flash flood the permeability and infiltration is limited only at the bottom of wadis. Therefore, it is useful to compute the infiltration and rainfall for the basin areas which collect a lot of water during rainfall, and lose few amounts of this water by runoff.

3.1.2.2.1. The relationship between infiltration and runoff

During rainfall the first drops of water are intercepted by the leaves and stems of the vegetation. This is usually referred to as interception storage. As the rain continues water is reaching the ground surface and infiltrates into the soil until reaching a stage where the rate of rainfall (intensity) exceeds the infiltration capacity of the soil. Thereafter, surface puddles, ditches, and other depressions are filled (depression storage) after which runoff is generated.

Infiltration capacity depends on many factors such as soil type, moisture content, organic matter, plant cover, and season. Of the soil characteristics affecting infiltration, noncapillary porosity is perhaps the most important. Porosity determines storage capacity and also affects resistance to flow.

Thus, infiltration tends to increase with porosity. An increase in organic matter also results in increased infiltration capacity, largely because of a corresponding change in porosity

Although a distinction is made between infiltration and percolation, the gravity flows of water within the soil. The two phenomena are closely related because infiltration cannot continue unimpeded unless percolation removes infiltered water from the surface soil. The soil is permeated by noncapillary channels through which gravity water flows downward toward the groundwater, following the path of least resistance.

Capillary forces continuously divert gravity water into capillary-pore spaces, so that the quantity of gravity water passing successively lower horizons is steadily diminished. This leads to increasing resistance to gravity flow in the surface layer and a decreasing rate of infiltration when a storm progresses. The rate of infiltration in the early phases of a storm is less if the capillary pores are filled from a previous storm.

The maximum rate at which water can infiltrate the soil at a particular point under a given set of conditions is called the infiltration capacity. The actual infiltration rate f_i equals the infiltration capacity f_p only when the supply rate i_s, (rainfall intensity less than of retention) equals or exceeds f_p. Theoretical concepts presume that actual infiltration rates equal the supply rate when $i_s \leq f_p$ and are otherwise at the capacity rate Fig (3-15). The value of f_p is at a maximum f_0 at the beginning of a storm and approaches a low, constant rate f_c as the soil profile becomes saturated. The limiting value is controlled by subsoil permeability. (HORTON, 1937) found that infiltration-capacity curves approximate the form

$$f_p = f_c + (f_0 - f_c)e^{-kt} \qquad (1)$$

Where e is the napierian base, k is an empirical constant, and t is time from beginning of rainfall. The equation is applicable only when $i_s \geq f_p$ throughout the storm. (PHILIP, 1954) suggested the equation

$$f_p = \frac{bt^{-1/2}}{2} + a \qquad (2)$$

Integrating equation (2) with respect to time gives the cumulative infiltration f at time t as

$$f_p = bt^{1/2} + at \qquad (3)$$

In equations, (2) and (3), a and b are parameters to be determined experimentally. Other equations for infiltration have been suggested, both physically based.

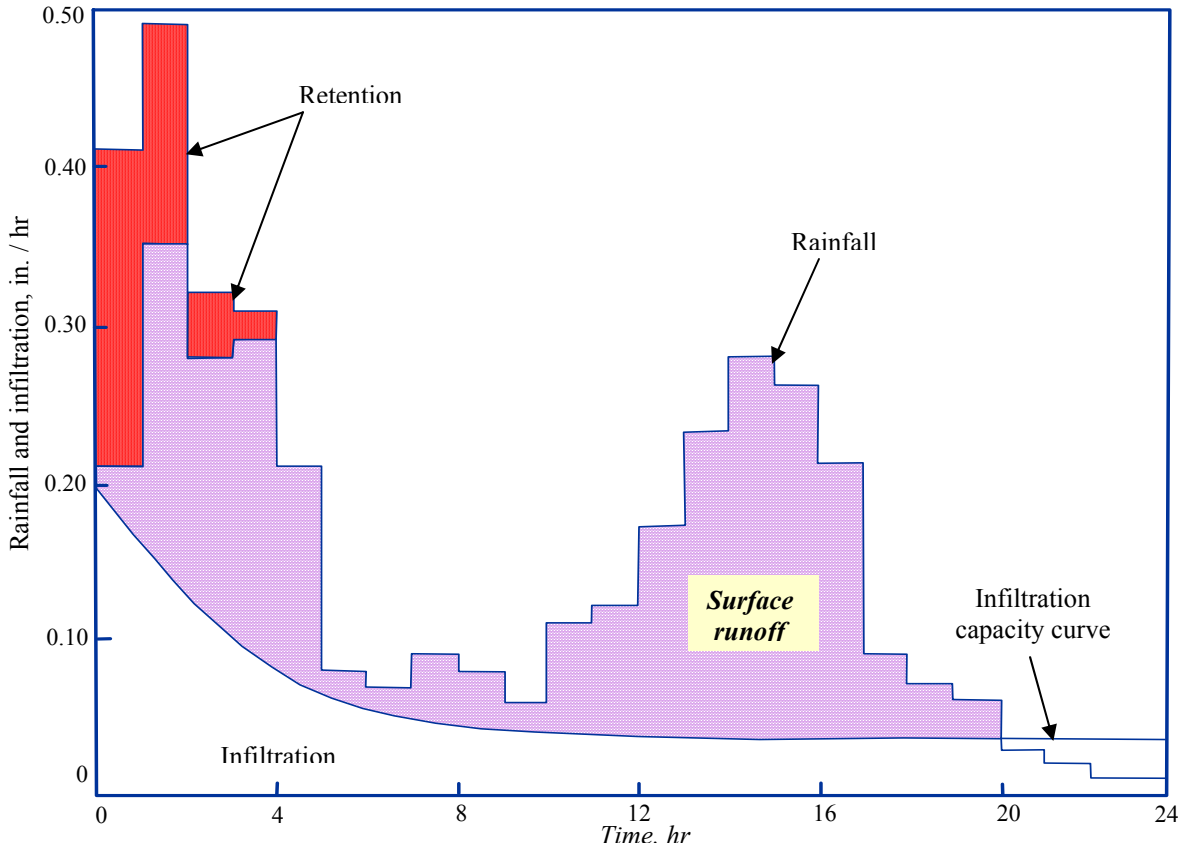

Fig (3-15) Schematic diagram illustrating relationship between rainfall, infiltration and runoff (modified after LINSLEY et al. 1982)

Infiltration capacity depends on many factors such as soil type, moisture content, organic matter, vegetative cover, and season. Of the soil characteristics affecting infiltration, noncapillary porosity is perhaps the most important. Porosity determines storage capacity and also affects resistance to flow. Thus, infiltration tends to increase with porosity. An increase in organic matter also results in increased infiltration capacity, largely because of a corresponding change in porosity

Fig (3-16) demonstrates the effect of initial moisture content and the variations to be expected from soil to soil. The effect of vegetation on infiltration capacity is difficult to determine, especially in Wadi bottoms in the study area, for it also influences interception. Nevertheless, vegetal cover does increase infiltration compared with barren soil because

- It retards surface flow, giving the water additional time to enter the soil.

-The root systems make the soil more pervious.

-The foliage shields the soil from raindrop impact and reduces rain packing of the surface soil.

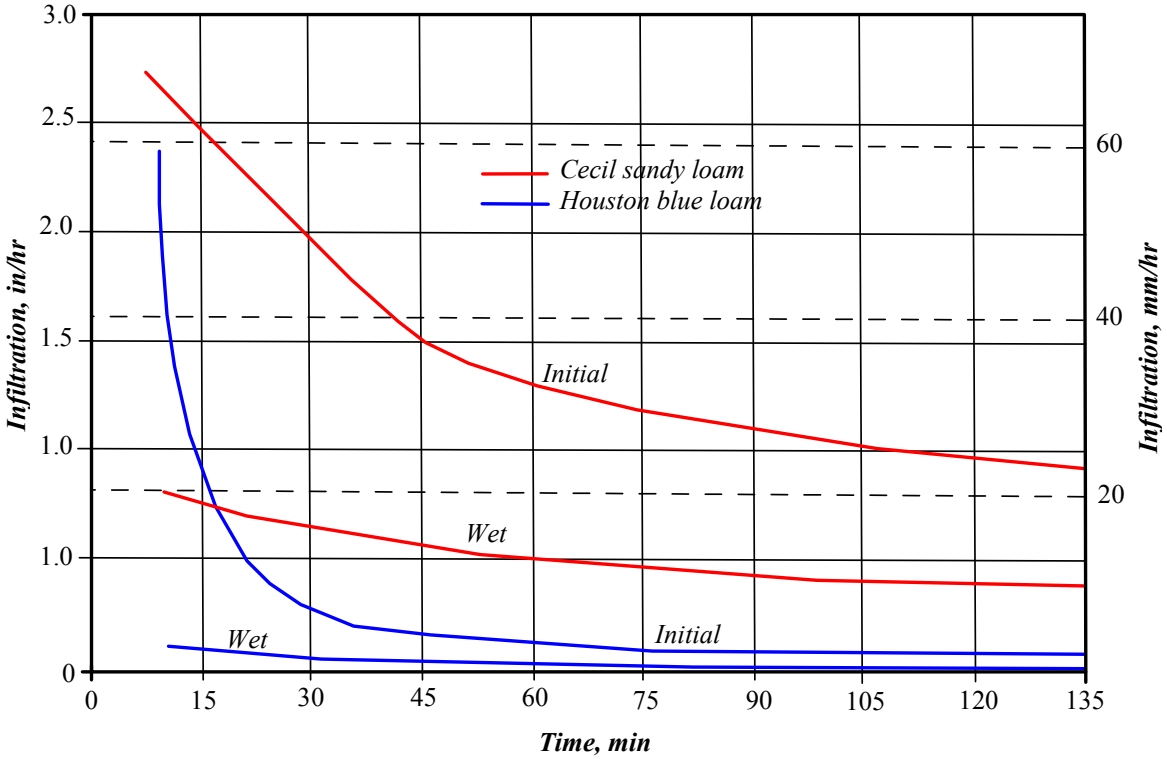

Fig (3-16) Comparative infiltration rates during initial and wet runs after LINSLEY et al. 1982)

Most data on infiltration rates are derived from infiltrometer tests. An infiltrometer is a tube or other boundary designed to isolate a section of soil. The effective area varies from less than 1000 cm^2 to several square meters. Although many of the earlier tests were made by flooding the infiltrometer, this method is no longer recommended and has been replaced by sprinkling techniques which can better simulate heavy and uniform rainfall (LINSLEY et al. 1982).

As it is impossible to measure directly the quantity of water penetrating the soil surface, infiltration is computed by assuming it to equal the difference between needed water applied and measured surface runoff. In addition to the difficulties inherent in simulating raindrop size and velocity of fall with sprinklers, experiments using artificial rainfall have other features tending to cause higher infiltration rates in tests than under natural conditions.

Finally, the process of runoff generation continues as long as the rainfall intensity exceeds the actual infiltration capacity of the soil but it stops as soon as the rate of rainfall drops below the actual rate of infiltration.

3.1.3. Basins and channel network

The interdependence of factors, the difficulties of quantifying and identifying them correctly, and the problems of establishing clear statistical relationships between variables have to be overcome in determining the controls of the flood peak. Interdependence is probably the major obstacle, because virtually all the controls are related in some way to one another. Hence the usual approach is to select as variables factors that on physical grounds are least likely to be interdependent. There are difficulties in quantifying some of the factors, such as vegetation or land use, while in many cases measurements of others are simply not available (e.g. infiltration rates and rainfall intensities).

Often the only material available besides flash flood records is what can be derived from map analyses or from aerial photographs and satellite images. This emphasizes the importance of combining quantitative geomorphology with hydrology: few of the morphometric properties that can be assessed have been shown by objective methods being important controls. Basin size, basin and channel slope, and various measurements of the drainage system can be determined from maps (chapter 2). These and similar factors have been demonstrated to be significant and have been incorporated into a range of "flood formula" by means of standard statistical methods producing expressions of the following type:

$$Qt = aX_1^b X_2^c X_3^d$$

Where $\boldsymbol{Q_t}$ = the T-year annual peak discharge;

a…..s = regression coefficients;

$\boldsymbol{X_1}$ etc = the factors controlling the flood peak.

3.1.3.1. Basin area

Other factors being equal, the larger the size of the basin, the greater the amount of rain it intercepts and the higher the peak discharge that results. This rather obvious conclusion has been the basis for a large number of flood formulae in the general form:

$$Q = CA^n \qquad \textit{LINSLEY et al. 1982}$$

Where $\boldsymbol{Q}$ = peak discharge;

A = basin area;

$\boldsymbol{C}$ = a constant that varies according to the land use or topography of the basin;

$\boldsymbol{n}$ = a constant that has a range from 0.2 to 0.9, depending on climate to some extent.

Tab (3-11) The area and the amount of rainfall in the main basins of the study area

Basins	Area km^2	Rainfall 1000 m^3	Basins	Area km^2	Rainfall 1000 m^3
El Akhdar	336.9	15160.5	**Ghowaitat**	75	1500.0
El Sheikh	348.6	17430.0	**Amlaha**	39.4	985.0
Rahba	206.8	8272.0	**Asla**	198	4950.0
Nesreen	84.6	3384.0	**Abu Garf**	53.9	1078.0
Firan (main wadi)	619.7	12394.0	**Moreikh**	22.6	452.0
Solave	316.1	15805	**Timan**	92.5	2312.5
Abyad	52.2	1305.0	**Sad**	44.3	886.0
Tughda	53.4	1068.0	**El Mahash**	137.5	3712.5
Apoura	46.1	922.0	**El Raboud**	46.6	1165.0
Gebah	53.8	1076.0	**Lethy**	47.3	1182.5
Waraqa	53	1166.0	**Eghshy**	144.7	3617.5
Habran	182.3	4922.1	**Mekhairad**	57.9	1447.5
Meiar	251	6777.0	**El Taalby**	69.2	1730.0
Aawag	928.4	18568.0	**Araba 1**	67	1340.0
Maaishya	70.3	1406.0	**Araba 2**	121	2420.0
Wagran	32.9	658.0	**Aat El gharby**	54.9	1372.5
Shadq	81	1620.0	**Khashaby**	17.6	352.0
Moreikh Shadq	38	760.0	**Abu Retmat**	37.4	935.0

- *Source: Rainfall amounts were computed using isohyetal method*

Tab (3-11) and Fig (3-18) show a forward relationship between basins area and the amount of rainfall, and sometimes runoff and peak flood, the larger basins area the more amount of rainfall. Whereas, the basins with large areas have higher amount of rainfall such as the tributaries of Wadi Firan (Akhdar and Sheikh), Wadi El-Aawag basin, and Wadi Asla, and small wadis have lower amount of rainfall which sometimes causes local runoff. It is obvious that the drainage area is perhaps the most important basin property. It determines the potential runoff volume, provided by a storm covering the whole area.

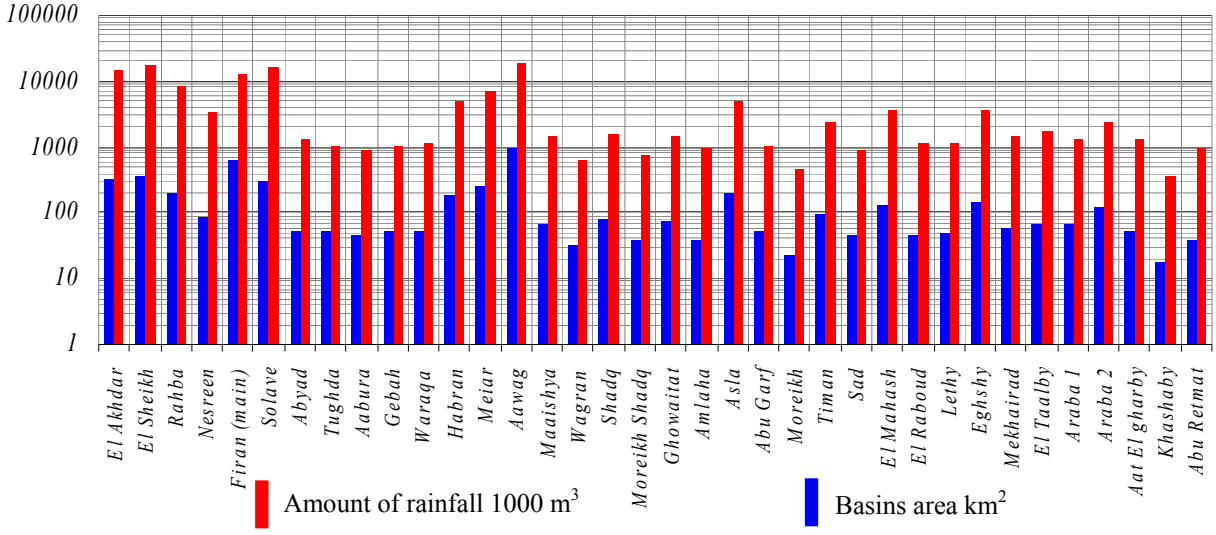

Fig (3-18) *The relationship between basins area and the amount of rainfall in El-Qaà plain area*

On the other hand, there is a number of other factors which are partly dependent on basin area and must be in some way accounted for by the constants in this type of relationship. For example, larger basins are usually less steep than smaller ones, and this applies to other factors, such as channel slope and rainfall intensity. As a consequence, when these additional characteristics of the basin are implicateted in the basin area we get in total the most meaningful results.

3.1.3.2. Basin shape

The shape, or outline form of a drainage basin, as it is projected upon the horizontal plane of a map is another factor affecting the stream discharging characteristics. As explained above, long narrow basins with high bifurcation ratios would be expected to have attenuated flood- discharge periods, whereas rotund basins of low bifurcation ratio would be expected to have sharply peaked flood discharge (STRAHLER, 1964). Circular basins produce larger floods than longitudinal watersheds if they are of similar sizes. This is obvious because a shorter time of accumulation of the flood is expected. Generally, the shape of basins is related with amount of discharge, velocity, peak of runoff and log time (SALEM, A. 1989).

It can be said that basin shape has obvious importance in influencing peak flow and other hydrograph characteristics, although it is a feature which is difficult to express numerically. However, a number of shape indices have been developed, some of the best known being the form factor and circularity ratio of MILLER 1953; STRAHLER 1964. The former is the ratio of average width to axial length of the basin (chapter 2)

This expression has a value of unity for a circular basin, while for two basins of the same size the flood potential would be considered largest for the one with the smallest circularity coefficient. The circularity ratio index and shape coefficient were employed in analyzing the flow from a number of Appalachian basins, but it was found to have a low correlation with peak discharge. On the other hand, in the same study, peak discharge was found to be highly correlated with the longest length of basin as measured from the head of the basin to the stream gauging station.

These indices of shape have been criticized on the grounds because they do not approach the ideal pear-shaped basin. It can be concluded that the different lag time between the basins plays an important role for occurring runoff or not.

3.1.3.3. Basin elevation

The altitudinal extent of the basin above the gauging station exercises direct and indirect control over the magnitude of runoff and flood peak in the study area. With basin slope and several additional factors, it determines the proportion of runoff, and indirectly it influences a number of other important controls, such as precipitation, temperature, vegetation and soil type. However, it is difficult to compute a single term which gives a meaningful measure of basin elevation. Indeed, several studies have shown the various indices that have been devised to have no significant relation to the size of the flood peak.

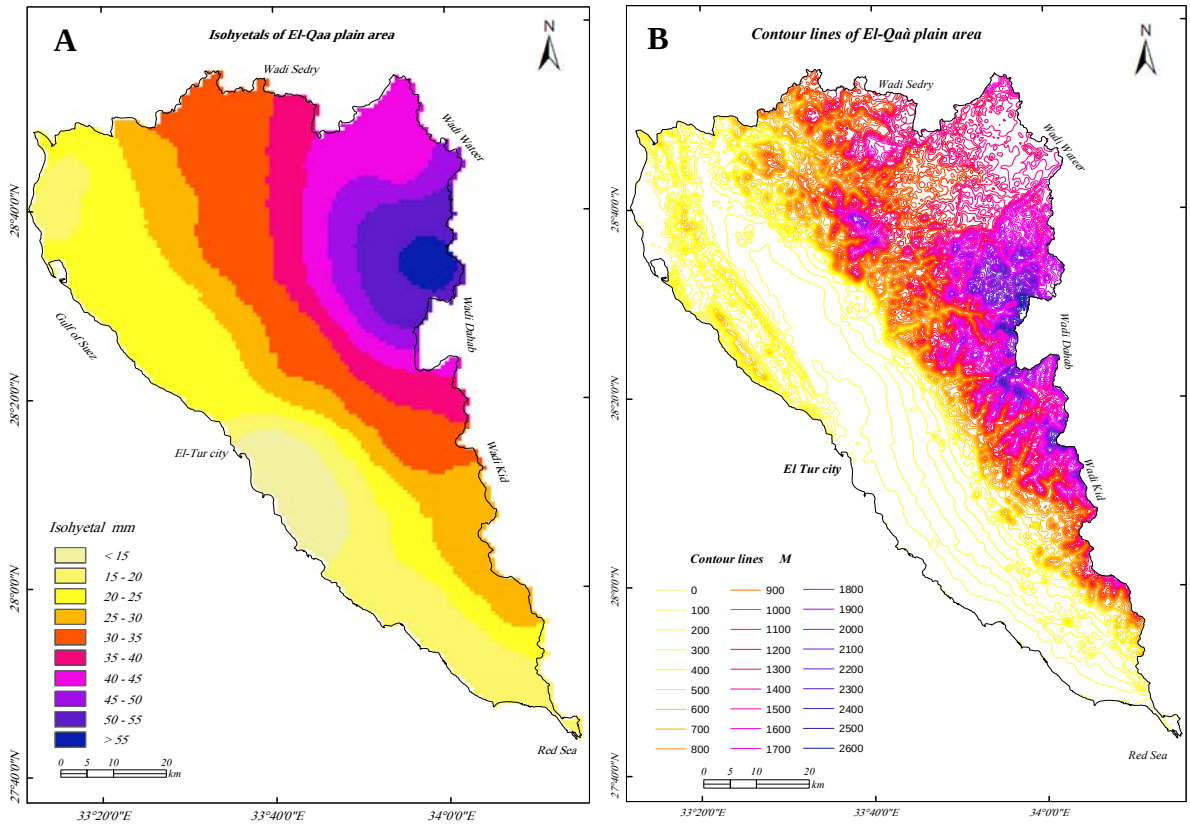

Fig (3-19) *A forward relationship between isohyetal* (**A**) *and contour lines* (**B**)

This occurrence of local saturation is related to topography, because water generally flows downhill, either on or below the surface. The most fundamental topographic property used in hydrology is contributing area. Contributing area is lying upslope of any point on a watershed or topographic surface. Contributing area may be concentrated as in distinct valleys, or dispersed as on smooth surfaces such as hillslopes. In the dispersed smooth surface case the area contributing to a point may be a line that theoretically has an area of zero. In such cases the contributing area concept is better defined as contributing area per unit contour width, in which case it is called specific catchment area (DAVID, G. 2003).

It can be noticed from fig (3-19) that the rainfall amounts are related with elevation and local relief in the study area. Whereas, the mountainous area has higher amounts such as: the values which more than 50 mm/ year are found in the areas above 2000 m, and the values between 25mm to 50mm are found in the areas which ranged between 500m to 2000m above sea level. Hence, the north eastern (Catherine area) is considered the highest level in the study area, and it has highest values of rainfall every year which cause mostly runoff and sometimes flash flood.

3.1.3.4. Basin slope

The slope is the rate of rise or fall against horizontal distance. It may be expressed as a ratio, decimal, fraction, percentage, or the tangent of the angle of inclination. The concept of measuring slopes from a topographic map is a familiar one for most professionals in the landscape planning/surveying professions. Slope is a measurement giving the steepness of ground surface. Slope is measured by calculating the tangent of the surface. The tangent is calculated by dividing the vertical change in elevation by the horizontal distance, or using SRTM image to compute slope degree by (DEM module).

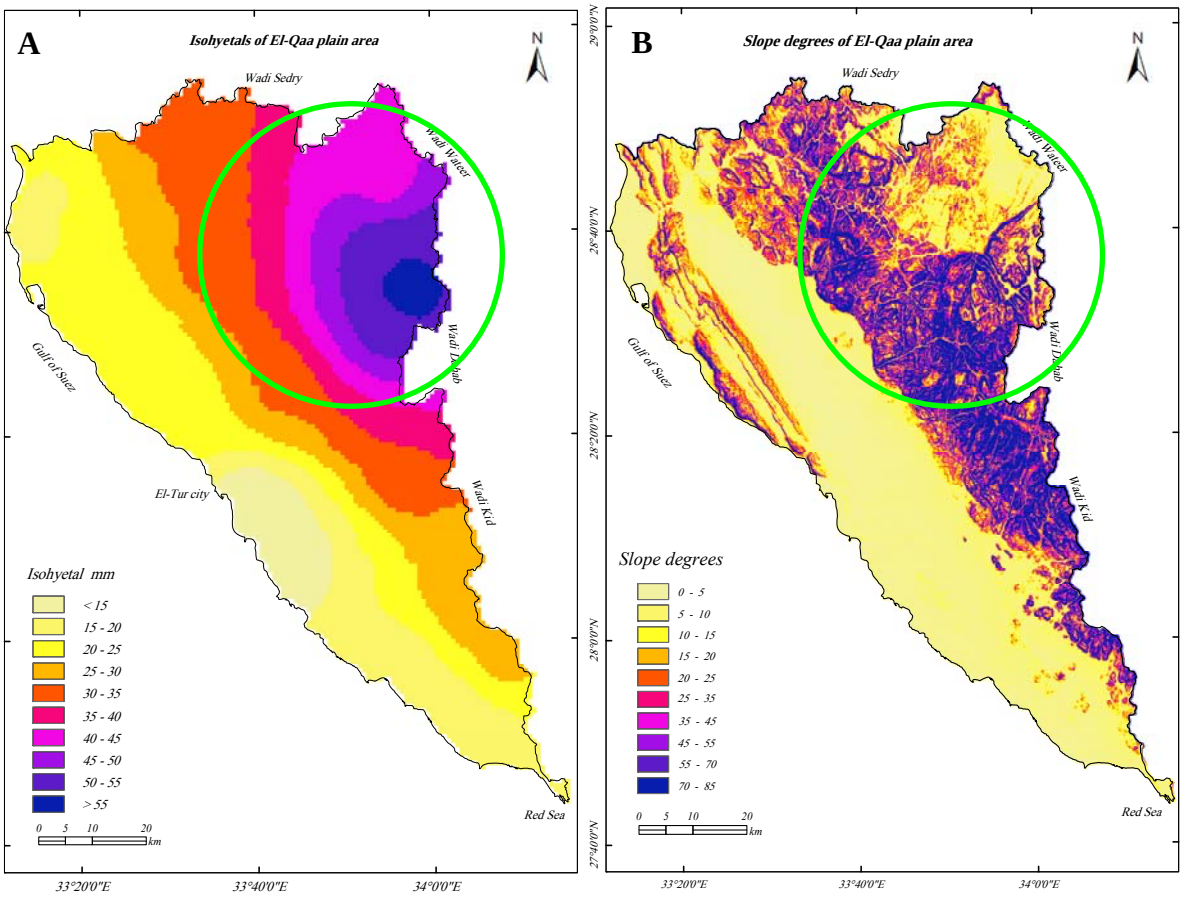

Fig (3-20) *Isohyetal* (**A**)*, slope degrees* (**B**) and their influence on runoff degree and peak flood in the study area, slope surface (DEM Module) were computed from SRTM image.

Local relief has also an important influence to determine the runoff volume; it is the elevation difference between two reference points. Maximum basin relief is the elevation difference between the highest point of the basin divide and the basin outlet. The principal watercourse (or main stream) is the central and largest watercourse of the catchment and the one conveying the runoff to the outlet. Relief ratio is the ratio of maximum catchment relief to the catchment's longest horizontal straight distance measured in a direction parallel to that of the principal watercourse. The relief ratio is a measure of the intensity of the erosional processes active in the catchment.

Slope, like elevation, is an obvious control of peak discharge, but again it is a factor which is difficult to interpret adequate. Some methods of slope assessment are extremely complicated and require measurement of length of all contours in a basin, or counting the number of intersections between contours and a grid overlay. Others are relatively simple, but the importance of these basin slope indices has been difficult to establish, whereas measurements of channel slope have been proved significant. It can be concluded from fig (3-20) that there is a direct influence from slope degrees and isoheytal on runoff and flood peak in the study area. Therefore, it will be easy to determine the dangerous areas in the study area depending on the data base of the other factors which are discussed.

3.1.3.5. The drainage network

The fundamental unit of study for fluvial processes is the drainage basin and watershed. A drainage basin is a portion of the Earth's surface that contains a main stream and its tributaries and is bounded by a drainage divide. The drainage divide represents the boundary between adjacent drainage basins and determines into which basin precipitation flows. The drainage network of basins constitutes the basic system for studies in climatic geomorphology. It is a basic system in which inputs of energy, both potential and kinetic, carry out work. Its variable components control the structure of the drainage system (IGNACIO & LUIS A, 1982).

Several characteristics of the flood hydrograph hinge on the efficiency of a basin's drainage system. A quick rise to a high peak is the mark of a well-developed network of short steep streams. Conversely, a minimal response to intense rain usually reflects an incipient channel system. How a particular basin relates to these extremes of development can be assessed in terms of linear aspects of the drainage network, the areal relationships of the system, and the various channel gradients,

Linear aspects of the channel system are expressed in terms of stream order, bifurcation ratio, stream length, and length of overland flow. These variables play an important role to control runoff and the flood peak. Whereas, the more stream orders and bifurcation ratio, the more amount of rainfall are cumulated during heavy rain, the more possibility of runoff. In addition are the other factors such as outcrop lithology, thickness of deposits, network slope, climate condition, and vegetation. More details about basin and network are found in the second chapter (morphometric analysis).

3.1.3.6. Climate factors

The magnitude of the flood is related to the rainfall that provokes it, coupled with the current storage capacity of the basin. There are difficulties in expressing this rainfall, because each storm is typified by a differing set of magnitude, duration, and intensity relationships, as well as those of frequency, distribution, and areal extent. The best way of avoiding these difficulties is to employ the basin's mean annual rainfall as an index of its flood susceptibility. This was the basis for a second part to the study of runoff in Britain, where the slope factor (***S***) was replaced by mean annual rainfall (***R***) to give:

$$Q_m = 0.009A^{0.85}R^{2.2}$$ *LINSLEY et al. 1982*

Where, **(Qm)** = the mean annual flood

(**A)** = the basin area

(R) = annual rainfall

However, this term is not a sufficiently realistic measure of the flood-producing rain, and several more likely ones have been determined. These include various intensity duration parameters and one of rainfall frequency. For example, in the New England study of floods, referred to previously, the intensity index showing the highest correlation with peak discharge proved to be the daily maximum rainfall of the same frequency as the flood. Further improvements could be made by the inclusion of factors indicative of antecedent conditions or the availability of storage, but such terms have rarely been employed.

Rainfall (Storm) Factors

The storm factors that influence the shape of the flood hydrograph, peakflow and the volume of runoff include: rainfall intensity, duration, and spatial distribution over the basin, direction of storm movement, and type of storm (AL-WESHAH R. 2002). These factors can be summarized as follows:

1- Rainfall intensity affects the amount of runoff and the peak flow rate. For a given rainfall duration, an increase in intensity will increase the peak discharge and the runoff volume, if the infiltration capacity of the soil is exceeded.

2- Rainfall duration affects the amounts of runoff, the peak flow rate and the duration of surface runoff. For a rainfall of given intensity, the rainfall duration determines, in part, the amount and timing of the peak flow.

3- The spatial distribution of rainfall can cause variations in hydrograph shape. If the center of the storm is close to the basin outlet, a rapid rise, sharp peak and rapid recession of the hydrograph is observed. If a larger amount of rainfall occurs in the upper reaches of a basin, the hydrograph exhibits a lower and delayed peak.

4- The direction of storm movement with respect to orientation of the basin can affect both the magnitude of the peak flow and the duration of surface runoff. Storm direction has the greatest effect on elongated basins. In these basins, storms that move upstream tend to produce lower peaks of a longer duration than storms that move downstream.

5- The type of storm is important because thunderstorms produce peak flows on small basins, whereas large cyclonic or frontal-type storms are generally dominant in producing major floods in larger basins.

It can be said that climate elements such as rainfall, temperature, air depressions, humidity, and winds are the main players to producing a flash flood in the study area. But maximum rainfall in one day and thunder storms in arid regions are considered the main elements to produce runoff.

3.1.3.7. Vegetation and land use

Indeed, vegetation factors have been employed as variables in assessing peak discharge in humid areas. Nevertheless, the information gained from these studies, which are as yet far from being complete, is of considerable interest and importance (PENMAN, 1963; SOPPCR and LULL, 1967) from the floods point of view and in terms of water resources. But natural vegetation in the study area is concentrated in wadis bottoms such as Wadi Firan and El-Aawag. These vegetations stripes are very small comparing with humid areas, and have a limited effect on runoff and the amount of rainfall by evapotranspiration.

3.2. Runoff generation mechanisms

The runoff mechanism different from one region to another interlocks many factors. Therefore, the hydrological behaviour of the soils in the arid areas concerning infiltration, soil water redistribution and runoff generation mechanisms does not fit the traditionally accepted models for humid environments (CASES, A. ET AL (2003). Mostly, the infiltration process and the runoff generation mechanisms in arid environments occur in a nonuniform way in space and time. Since the beginning of the 70s and more recently, research has demonstrated that Mediterranean slopes behave as a mosaic of runoff generation and infiltration patches (YAIR AND KLEIN, 1973; YAIR, 1983; YAIR AND LAVEE, 1985; YAIR AND ENZEL, 1987; LAVEE ET AL., 1998) depending enormously on the morphometric characteristics of the slopes, the lithology, the different development of the soils and the land uses in the past.

On one hand, a nonuniform pattern of runoff generation in the catchments characterised by a flux discontinuity due to a hydrological disconnection between the elements of the slopes takes place. The slopes behave like a mosaic of runoff and runon areas (sources and sinks) described by many authors in different parts of the Mediterranean Basin (LAVEE ET AL., 1998, AND YAIR, 1996). This point is out the existence of a systematic nonuniform pattern of contribution area to runoff after analyzing runoff generation mechanisms in arid areas of different lithologies. This pattern is caused by the local differences in soil infiltration capacity.

On the other hand, very frequently water under clusters of vegetation moves through preferential paths within the soil profile causing a nonuniform model of infiltration and water redistribution (BERGKAMP ET AL., 1996). The soil water normally content decreases progressively at deeper soil horizons during the infiltration process but this is not widely applicable in this type of environment.

Additionally, the research carried out on the spatial distribution of soil moisture at catchments scale (WESTERN ET AL., 1998; FITZJOHN ET AL., 1998) has resulted in interesting informations on mosaic-like soil moisture distribution, reflecting the different hydrological characteristics of the soils and the potential runoff and runon soil patches. Isolated degraded areas with low water retention capacities appear as potential sources for runoff whereas other isolated or well connected areas with deeper soils are able to retain more soil water and are able to behave as potential sink areas for runoff.

Fig (3-21) shows a cross section through a hillslope that represents in more detail the pathways infiltrated water may follow. It may flow through the matrix of the soil in the inter-granular pores and small structural voids. Infiltrated water may also flow through larger voids referred to as macropores. Macropores include pipes that are open passageways in the soil caused by decaying roots and burrowing animals. Macropores also include larger structural voids within the soil matrix that serve as preferential pathways for subsurface flow. The permeability of the soil matrix may differ between soil horizons and this may lead to the build up of a saturated wedge above a soil horizon interface. Water in these saturated wedges may flow laterally through the soil matrix, or enter macropores and be carried rapidly to the stream as subsurface stormflow in the form of interflow (DAVID, G. 2003).

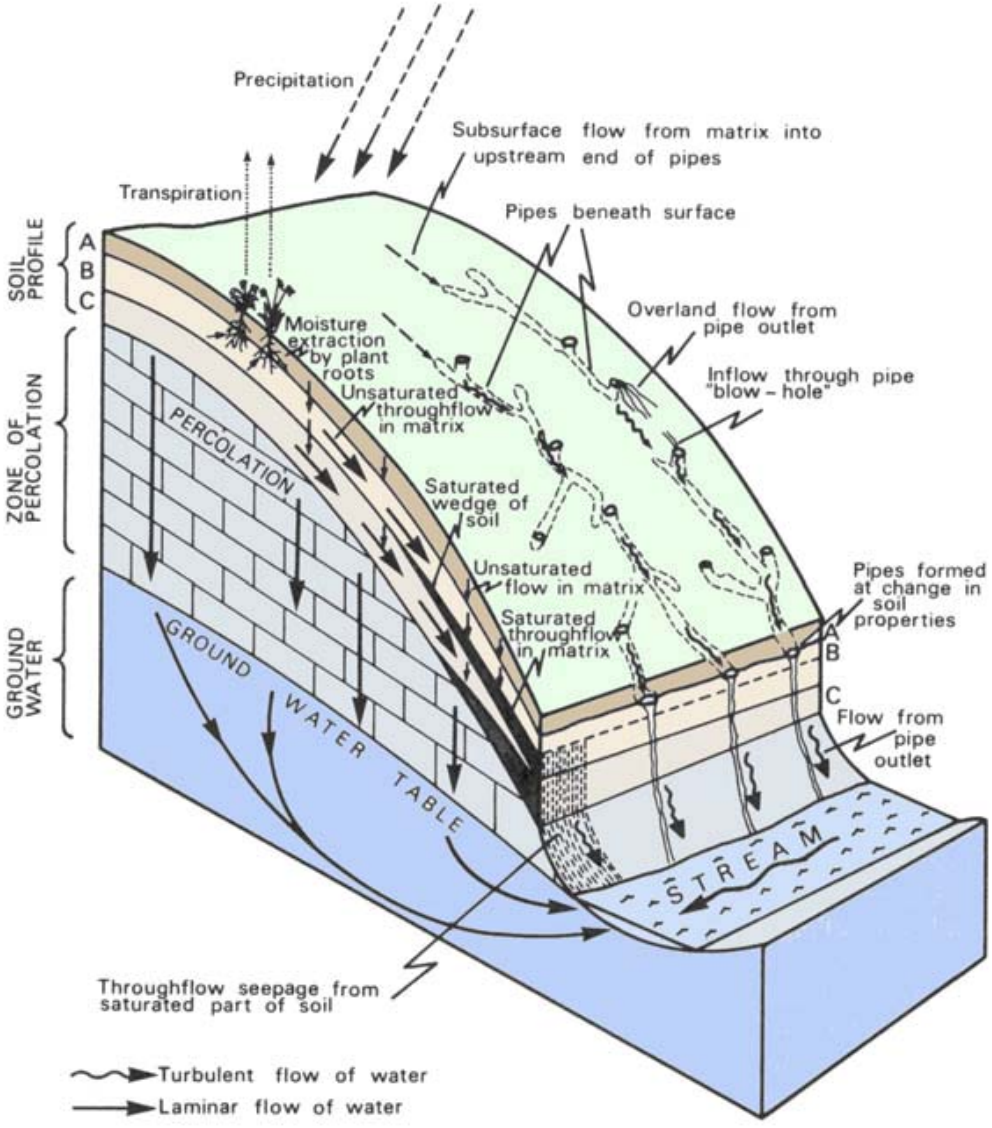

Fig (3-21) *Pathways followed by subsurface runoff on hillslopes, after KIRKBY, 1978*

In Fig (3-22a) the infiltration overland flow mechanism is illustrated. There is a maximum limiting rate at which a soil in a given condition can absorb surface water input. This was referred to by HORTON (1933), one of the founding fathers of quantitative hydrology, as the infiltration capacity of the soil, and hence this mechanism is also called HORTON overland flow. Infiltration capacity is also referred to as infiltrability. When surface water input exceeds infiltration capacity the excess water accumulates on the soil surface and fills small depressions. Water in depressions storage does not directly contribute to overland flow runoff; it either evaporates or infiltrates later. With continued surface water input, the depression storage capacity is filled, and water spills over to run down slope as an irregular sheet or to converge into rivulets of overland flow. The amount of water stored on the hillside in the process of flowing down slope is called surface detention.

The transition from depression storage to surface detention and overland flow is not sharp, because some depressions may fill and contribute to overland flow before others. Figure 7 illustrates the response, in terms of runoff from a hillside plot due to rainfall rate exceeding infiltration capacity with the filling of depression storage and increase in, and draining of, water in surface detention during a storm. Note, in Figure 7, that infiltration capacity declines during the storm, due to the pores being filled with water reducing the capillary forces by drawing water into pores.

Due to spatial variability of the soil properties affecting infiltration capacity and due to spatial variability of surface water inputs, infiltration runoff does not necessarily occur over a whole drainage basin during a storm or surface water input event.

BETSON (1964) pointed out that the area contributing to infiltrate runoff may only be a small portion of the watershed. This idea has become known as the partial-area concept of infiltration overland flow and is illustrated in Fig (3-22b).

Infiltration overland flow occurs anywhere when surface water input exceeds the infiltration capacity of the surface. This occurs most frequently in areas devoid of vegetation or possessing only a thin cover. Semi-arid rangelands and cultivated fields in regions with high rainfall intensity are such places where this process can be observed. It can also be seen where the soil has been compacted or topsoil removed. Infiltration overland flow is particularly obvious on paved urban areas.

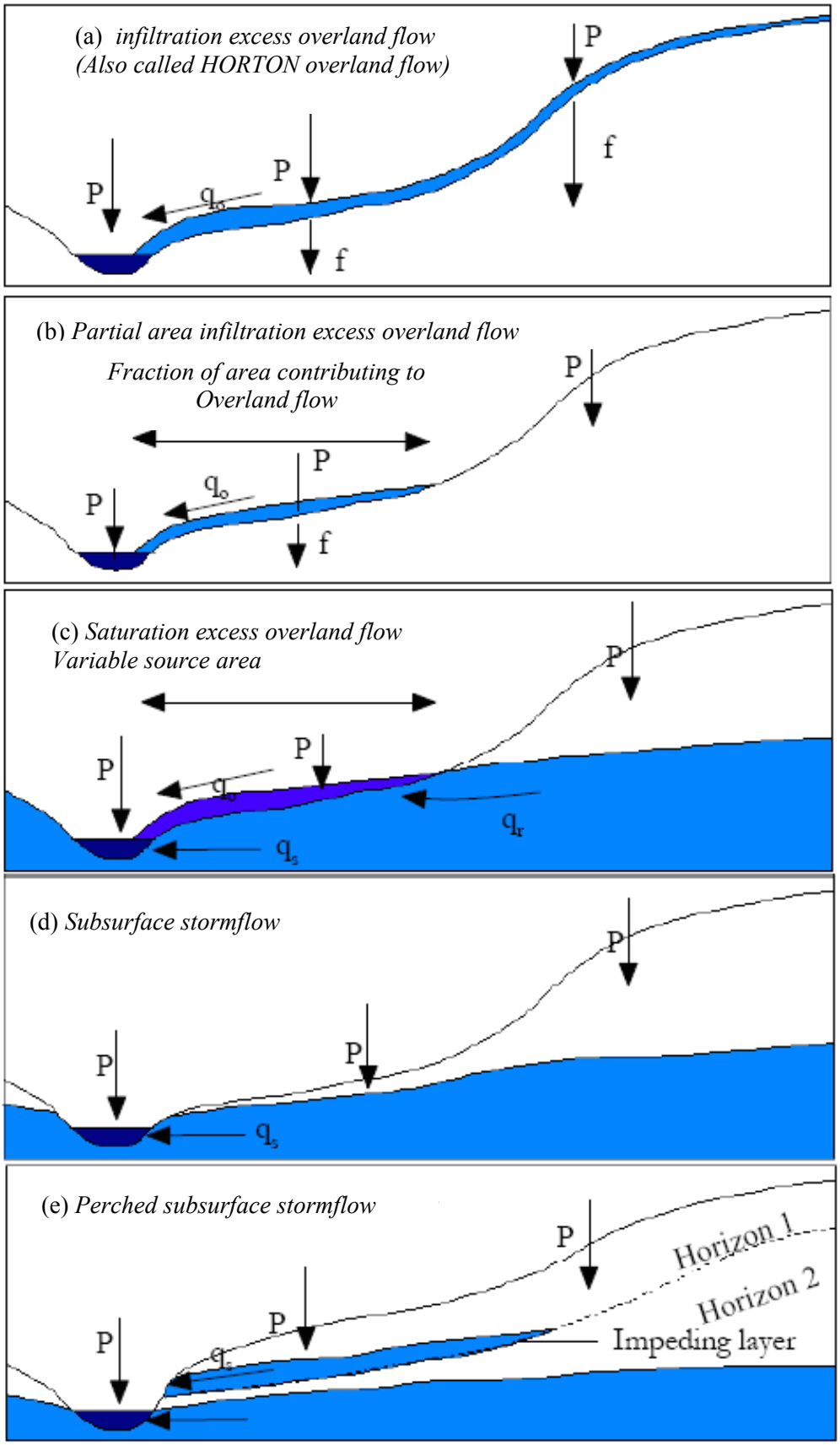

Fig (3-21) *Pathways followed by subsurface runoff on hillslopes* 3-22) *classification of runoff generation mechanisms (BEVEN, 2000)*

Some authors explain the runoff generation process as being a consequence only of the saturation of different soil layers even in arid conditions. For example, PUIGDEFA´ BREGAS ET AL. (1999), under arid conditions and in soils developed on mica-schist bedrock, found two main mechanisms of runoff generation related to the saturation of different soil layers:

- The first mechanism implies the saturation of the uppermost soil layer just after rainfall initiation. It disappears as soon as the progress of the wetting front develops a transmission zone that allows the drainage of the upper soil layer.
- The second mechanism requires the persistence of nearly saturated conditions in a shallow subsurface soil layer. It may occur in areas where permeability decreases with soil depth. This mechanism provides a long lasting saturation of the subsurface soil layer.

In this way, the effect of rainfall variability on the water content of the uppermost layer tends to be buffered, allowing overland flow to last for longer periods of time and to cover greater distances. PUIGDEFA´ BREGAS ET AL. (1999) point out that this mechanism is probably the most important for the creation of hydrological connections across hillslopes.

The next chapter will be focused to estimating runoff in the main basins of the study area using variation methods. They deal to determine runoff mechanisems in the study area, extreme event analysis, and maps of affected areas.

Chapter 4
Assessment of flood hazard

Many people in southern Sinai live near and above the dynamic, distributaries channel net works of alluvial fans where flood behavior is complex and poorly constrained. Most of these fans can be cultivated and used in other economic activities such as, industry, tourism, and new cities building. Alluvial fans may be divided into two process- based types: debris flow fans and stream flow fans, with important implications for flood hazards. Debris-flow fans are often more geomorphologically unstable than stream flow fans because their debris fills channels and triggers more frequent avulsions (NATIONAL RESEARCH COUNCIL, 1996). Debris flows have a relatively high viscosity, however, leading to localized flood risk on steep, proximal fan areas. Low relief fans of both types, however, can exhibit rapid channel changes that should be incorporated into flood hazard assessments.

Therefore, the assessment methods of flood hazard in El-Qaà plain area were chosen based on their historical flood complexity. The alluvial fans of the study area have moderate relief that results in complex flow patterns and rapid channel changes, especially in active wadis such as Wadi Maier, and Wadi Firan. In addition, the study area has most of hydrologic, geologic and geomorphic databases, including satellite images, DEM scale 1:50,000, geologic maps, topographic maps, paleo-flood records, and some reports for recent extreme floods. Hence, runoff can be estimated, and risk zones distributed in the study area by dissection and analysis the follow elements:

4.1. Runoff estimation *4.2. Extreme event analysis*

4.3. Risk zones map for El-Qaà plain area

4.1. Runoff estimation consists of two main elements as following:

4.1.1. Methods of runoff estimation *4.1.2. Variables of runoff*

The hydrologic system seems being black box model in which inputs are rainfall and watershed characteristics and the output is a runoff hydrograph, which is needed for hydraulic analysis and design. Because of the studies of runoff estimate in applied geography until now very little and to be limited on the hydrological and engineering studies, therefore, it is necessary showing the different methods which are used to estimate this phenomena with details to be a base to use in applied studies.

There are different methods and procedures available to estimate runoff from rainfall for individual storm events. The following factors should be considered before selecting the most suitable runoff calculation methods:

1. The desired objective of analysis: what do us actually need; a runoff volume, peak flow, or a runoff hydrograph?
2. Available data: long-term records of hydrologic data allow the application of statistical procedures (for example, frequency analysis, and duration) and/or the analysis of catchment response (for example, derivation of a unit hydrograph). The effectiveness of the analysis techniques is limited by the adequacy of available data series. Where data are limited or non-existent, methods based on regional analysis may be available.
3. The area and characteristics of the watershed: these factors affect the runoff process and generally govern the way in which runoff and peak flow occurs.
4. The importance of the study area and the project as well as the resources and time available for analysis: the resources and time available for the analysis govern mainly the depth and sophistication of the analysis.

AL-WESHAH, R. (2000) pointed out some methods for estimating peak flows which may be grouped on the basis of basins area as a guideline shown in Tab. (4-1). The most of main basins lie in the category two, three wadis in category three like Wadi El-Akhdar, Wadi El-Sheikh and Wadi Meiar, While last category contains two wadis, Wadi El Aawag and Wadi Firan.

Tab. (4-1) *Methods used for peak-flow analysis depending on the area of basins*

	Basin area (km^2)	***Basins No.***	***method commonly used***
1	Area < 2.5	-	*Infiltration approach, rational method*
2	2.5- 250	30 Basins	*Some empirical methods (e.g., Talbot); unit hydrograph; flood frequency analysis; flood peaks versus drainage area and catchment characteristics.*
3	250- 500	3 basins	*Unit hydrograph; flood frequency analysis; flood peak versus drainage area and catchment characteristics.*
4	Area > 500	2 basins	*Distributed modeling including flood routing; flood frequency analysis; flood peak versus drainage area and catchment characteristics.*

The commonly used methods are given below, in a sequence of increasing complexity. An important distinction is between methods based on rainfall in the study area and basins area, and other methods based on flow data and basins area.

4.1.1.1. Simple correlation method

The relationship between rainfall and the resulting peak runoff is complex and is influenced by the basins area and climate conditions. With adequate records of data, a simple correlation for the estimation of runoff can be investigated. One of the most common methods is to plot runoff (R) against rainfall (P) values. In humid areas, no simple relationship may emerge, due to effects of antecedent conditions, seasonality of vegetation, etc. However, for arid areas, such effects may be less important.

A common simple method is to fit a linear regression line between R and P and to accept the result if the correlation coefficient (**r**) is close to unity. The equation for straight-line regression between runoff **R** and rainfall **P** is

$$R = aP + b \qquad (1)$$

The values of the coefficient **a**, and **b** are given by the slope and intercept of the straight line equation, respectively (AL-WESHAH, R. 2000). The coefficient of correlation r represents the quality of fitting; the value of r lies between 0 and +1 as runoff can have only positive correlation with precipitation. A value of 0.8 or more indicates good correlation. However, the data should always be plotted for visual inspection, for example a non-linear relationship might give a better result as discussed below. It should be noted that localized rainfall and the effect of transmission losses can complicate this simple plot.

WHEATER and BROWN (1989) found for a small wadi in South West Saudi Arabia that the largest observed flow came from the smallest observed rainfall - an artefact of incomplete measurement of spatial rainfall and transmission losses.

For large catchments, it is common to have an exponential relationship such as:

$$R = c\ P\ m \qquad (2)$$

Where ***c*** and ***m*** are constants; in fact equation (2) can be reduced to a linear form by logarithm transformation. Many improvements of the above basic rainfall – runoff regression by considering additional parameters such as soil moisture or antecedent rainfall have been attempted. As noted above, antecedent rainfall influences the initial soil moisture and can have a strong effect on runoff generation.

4.1.1.2. Methods based on area

For situations where data are limited or non-existent, regional analysis must be used. The discharge of a given frequency can be expressed as a function of the drainage area and other catchment characteristics based on relationships for catchments which have similar climatic and hydrologic characteristics. Design flood formulae are generally based on a function of drainage area and possibly other parameters. Where area is the dominant explanatory variable, a general expression is used, of the form:

$$QT = C.\ A_m \qquad (3)$$

Where $\mathbf{Q_T}$ = design flood discharge of return period ***T*** years

A = area of a drainage basin

m = an exponent ranging from 0.4 to 0.7

C = a constant, which depends upon many factors such as topographic, climatic and other characteristics of a drainage basin, which affect the run-off.

The use of empirical formulae involves the determination of the area that contributes to the flow at the drainage structure site. The drainage area, expressed in square kilometers, is determined from survey or topographic maps. The value of **C** depends on many factors pertaining to a particular drainage area such as shape, size, slope, type of soil, surface infiltration, storage and land use. The factor **C** can be determined based on adequate historical data of flood events over different areas with similar characteristics. The value of **C** will be valid only for the region or drainage basin for which it has been determined. But in fact, flood records of most of the wadis in the Arab world are not available; therefore the use of empirical formulae mostly depends upon the experience of the hydrologist WHEATER and BROWN (1989).

4.1.1.3. The Talbot and modified Talbot formula

In Saudi Arabia, the Ministry of Communications (MOC) has developed a modified form of TALBOT formula, which is a special case of the area-based methods. The general form of the Modified Talbot formula, being used by MOC is:

$$Q_{25} = C.\ A_n \qquad (4)$$

Where Q_{25} = the 25-year return period flood flow.

A = drainage area in hectares

n = an exponent see Tab (4-2).

C = total or (composite) coefficient for runoff = C1 + C2 + C3

Tab. (4-2) *Modified form of Talbot formula used by MOC*

Drainage Area (Hectares)	***25-Year Frequency Flood Flow***
0 to 400 (small catchment area)	Q_{basic} *x S. F.*
400 to 1258	$0.837 \times C \times A^{3/4}$
1258 to 35944	$4.985\ C\ A^{1/2}$
Over 35944	$14.232\ C\ A^{2/5}$

Accordingly, the 50-year and 100-year flood events, which may be used for design of hydraulic structures, the following equations are adopted.

$$Q_{50} = 1.2\ Q_{25} \qquad (5)$$

$$Q_{100} = 1.4\ Q_{25} \qquad (6)$$

Where terms in Tab (4-2) are

Q_{basic} = basis peak flow derived from MOC curves based on catchment area;

A = drainage area in hectares;

S.F. = slope factor for drainage area given in MOC manual; and

C = total coefficient of runoff which is the sum of ***C1 + C2 + C3.***

Values of ***C1, C2*** and ***C3*** are derived from the guidelines given by MOC and based on the watershed characteristics.

Because of this equation is considered relatively general and don't contains many variables which have a direct affected on the runoff, such as geological sitting, climate elements, soil, vegetation cover, and slope. Hence, it can be difficult using this equation to estimate runoff amounts, and peakflow in the study area.

4.1.1.4. The regional regression method

More general, regional flood regression equations can be developed which include independent variables like area, precipitation intensity, catchment slope, soil and land use parameters. The general form of this equation for peak flow of return period T is given by

$$Q_T = a_1 A^{a2} E^{a3} P_T^{a4} S^{a5} M^{a6} \qquad (7)$$

Where Q_T is the peak flow of return period ***T,*** A is the catchment area, E is the catchment elevation above sea level, P is the storm precipitation (daily or annual), S is the catchment slope, M is a factor for soil and vegetative cover, and the coefficients ***a1*** through ***a6*** are regression coefficients derived from regional regression analysis.

The relationships have been developed for the arid and desert regions of the southwest area of the United States, by the USGS (e.g**.** BLAKEMORE et al., 1995), where area, mean elevation, mean annual precipitation, mean annual evaporation, as well as latitude and longitude were used as the explanatory variables.

Alternative approaches to regionalization of flood frequency evaluate the ratio of ***QT*** to an index such as the mean annual flood QBAR (the growth curve). A useful analysis of arid region data is given by FARQUHARSON et al., 1992. An advantage of this approach is that where just a few years of site-specific data are available, they can be used to estimate QBAR, and the regional data can be used to provide the growth curve.

4.1.1.5. The rational formula method

This method is based on the assumption that a steady uniform rainfall rate in time and space will produce maximum runoff when all parts of the watershed are contributing to outflow. This condition is given when the storm duration exceeds the time of concentration. It is used to calculate the surface runoff discharges generated from a design storm with a specific return period and a duration time equal to the time of concentration of the catchment. The method translates the rainfall to runoff using the following formula.

$$Q = \frac{C\,I\,A}{3\,6\,0} \qquad \textbf{(8)}$$

Where

Q = peak flow rate (maximum runoff), m^3/s

A = catchment area,

I = rainfall intensity, millimeters per hour.

C = runoff coefficient

Values of runoff coefficient ***C*** are given in most hydrology textbooks.

Due to assumptions regarding homogeneity of rainfall and equilibrium conditions at the time of peak flow, the rational method should not be used on areas larger than about 250 hectares (2.5 km^2) without subdividing the overall watershed into sub-basins and including the effect of routing through any drainage channels. Practically, it can be applied to the catchments with an area up to 500 hectares (5 km^2) for comparison purposes and validation of other methods.

Therefore, The Rational Formula method may be not suitable to estimate the maximum runoff (peak flow) in the study area, whereas total sub-basins area is more than 250 hectares (2.5 km^2), but can help to estimate runoff volume and peak runoff during rainy storm.

4.1.1.6. Soil conservation services (*SCS*) *method*

The (SCS) Soil Conservation Services now Natural Resources Conservation Service (*NRCS*) or Curve Number method calculates the volume of runoff given the input rainfall depth and the curve number (CN). This is a widely used method where data for site-specific analysis are not available. The relations are given by

$$Q = \frac{(p - \lambda s)^2}{\left[p + (p - \lambda)s\right]} \qquad \textit{All units in inches} \qquad \textbf{(9)}$$

$0 < \lambda < 0.4$, with a mean $\lambda = 0.2$

and $S = \frac{1000}{CN} - 10$

Where

Q = direct runoff depth

P = rainfall depth

S = potential retention

CN = the curve number, a value depending on hydrologic soil group and land use-land cover complex). The hydrologic soil groups, as defined by SCS soil scientists, are ***A, B, C,*** and ***D*** described earlier.

Antecedent moisture conditions are another parameter to affect the choice of the CN value. Three AMC conditions were developed by the SCS method, these are AMC I, AMC II, and AMC III. AMC I represents dry soil conditions; it yields the lowest runoff potential. AMC II represents average (normal) soil conditions; it yields the average (normal) runoff potential. AMC III represents wet soil conditions; it yields highest runoff potential.

According to the US Soil Conservation Service (SCS), the curve number for dry AMC denoted by CN (I) is related to the curve number of the normal average CN (II) as (CHOW et. al, 1988).

$$CN\,(I) = \frac{4.2CN\,(II)}{10 - 0.058\;CN\,(II)} \qquad \textbf{(10)}$$

Where CN (II) is the curve number for the normal AMC given preferably in hydrology, similarly, for wet conditions of antecedent moisture the curve number CN (III) is related to the average normal CN (II) as

$$CN\,(III) = \frac{23CN\,(II)}{10 + 0.13\;CN\,(II)} \qquad \textbf{(11)}$$

Peak flood calculations by the SCS method

The shape of the SCS flood hydrograph is standard and depends on the watershed area and the lag time of the basin. The lag time is about 0.6 times the time of concentration. The peak flow for one unit of rainfall excess is given by

$$Q_{peak} = \frac{2.08\;A}{T_R} \qquad \textbf{(12)}$$

Where

Q_{peak} = *the* peak discharge in (m^3/s)

A = the drainage area in (km^2)

T_R = the time of rise of the flood hydrograph which equals the lag time plus on-half of the storm duration in (hours).

The SCS flood hydrograph calculations are performed by many available computer software and package described in Appendix 6.A. While the method is simple and flexible, it is important that it is evaluated using data from the region; there is as yet little critical analysis of its performance in the region.

4.1.1.7. Unit hydrograph method

First proposed by SHERMAN in 1932, the unit hydrograph (UH) of a watershed is defined as a surface runoff hydrograph (SRH) resulting from a unit depth of excess rainfall (10mm) generated uniformly over the drainage area at a constant rate for the effective rainfall duration. The duration of the excess rainfall designate the duration of the UH, thus a 3h-UH is a SRH resulting from a one cm excess rainfall storm of 3h duration.

The UH is derived from the direct runoff hydrograph. In general, when analyzing a recorded flood hydrograph, the baseflow contribution should be subtracted from the total flow before deriving the UH. Likewise, when using the UH method to compute a design flow, a baseflow should be added to obtain the total design discharge.

However, in arid areas with ephemeral flows, baseflow may be non-existent. The following basic assumptions are used in developing the UH concept:

1- The excess rainfall has a constant intensity within the unit duration.
2- The excess rainfall is uniformly distributed throughout the whole drainage area.
3- The base time of the SRH (the duration of surface runoff) resulting from an excess rainfall of a given duration is constant.
4- The ordinates of the SRH of a common base time are directly proportional to the total amount of surface runoff represented by each hydrograph.
5- For a given watershed, the hydrograph of surface runoff resulting from a given excess rainfall reflects the unchanging characteristics of the watershed.

Assumption 4 implies that if the ordinates of the UH represent one inch of runoff, then a hydrograph representing two inches of runoff is obtained by simply multiplying each ordinate of the UH by 2. Where data on rainfall and runoff are available, site-specific unit hydrographs should be derived. Various methods are available, ranging from sophisticated time-series analysis methods to simple methods such as trial and error. A convenient code for a relatively simple matrix inversion method is given by BRUEN AND DOOGE (1984). Where data are not available, regional methods must be used.

U.S. SCS has examined many hydrographs nationwide and computed a standard dimensionless UH which has 37.5 percent of the volume under the rising limb. This volume has been determining the peak rate of runoff Qp expressed in m^3 per cm of runoff from a given drainage area. This factor is primarily a function of the time it takes for runoff to travel through the basin to the design point. Once this rate of runoff is determined, it can be multiplied by the amount of excess rainfall to produce a discharge. The versatility of this method is that it can account changes in watershed travel time, and subsequently Qp, which are caused by alterations in the hydraulic capacity of the stream, such as channel maintenance operations, flood control structures, etc.

The volume of runoff from a given amount of rainfall can also be adjusted to reflect changing land use within a watershed. This method is also suitable for ungaged watersheds. The advantage of this method is that it is straight forward to apply and the physical parameters are easily determined. This method should also be limited to watersheds with a drainage area of approximately (about 50 sq. km.) or less.

In general, a dimensionless unit hydrograph is developed for use in catchment areas, where the required data for unit hydrograph derivation are not available. The dimensionless data for the unit hydrograph is constructed from the available physiographical characteristics of the basin.

The previous discussion is considered very important to determine the suitable method which can be applied in the study area to estimate runoff volume and peakflow. The *Soil Conservation Services Method* (*SCS*) will be used in the study area to compute some variables such as curve number (CN) and time concentration (TC), and lag time. Equations of SCS are the best for arid areas because they have the most variables which are used to estimate runoff.

4.1.2. Variables of runoff

4.1.2.1. Runoff coefficient

The runoff coefficient coverage is used in the same way as the land use coverage, except that rather than defining a land use type a floating point runoff coefficient can be entered for each polygon. Composite runoff coefficients (C values for the rational method or CN values for the SCS method) can then be computed using the compute GIS attributes command in the calculators menu of the hydrologic modeling module using the following equation:

$$C = \left[\frac{D * \sqrt{(9.81 * p)}}{G} \right]^{(1-S)} \qquad \textbf{(13)}$$

Where ***C*** = runoff coefficient

D = drainage density km/km^2

P = the rainfall depth mm

S = the average land surface slope

G = an integer number representing the surface geology

G varies between 1.0 and 9.0; the value 1.0 is assigned to the basement rocks, and 9.0 for the most recent Quaternary deposits. G values are consistent with the nine classes used on the geological map (chapter one).

Tab. (4-3) *Runoff coefficient in the main basins of El-Qaà plain area*

Basin	Area km^2	Runoff Coe. (*C*)	Basin	Area km^2	Runoff Coe. (*C*)
El-Akhdar	336.9	**15.2**	**Moreikh Shadq**	38	**4.6**
El-Sheikh	348.6	**14.6**	**Ghowaitat**	75	**4.6**
Rahba	206.8	**12.8**	**Amlaha**	39.4	**5.9**
Nesreen	84.6	**12.9**	**Asla**	198	**7.8**
Firan (main wadi)	619.7	**10.1**	**Abu Garf**	53.9	**5.6**
Solave	316.1	**14.3**	**Moreikh**	22.6	**5.7**
Abyad	52.2	**7.7**	**Timan**	92.5	**5.8**
Tughda	53.4	**8.0**	**Sad**	44.3	**6.0**
Apoura	46.1	**6.8**	**El-Mahash**	137.5	**7.4**
Gebah	53.8	**4.7**	**El-Raboud**	46.6	**7.6**
Waraqa	53	**6.0**	**Lethy**	47.3	**8.6**
Habran	182.3	**9.7**	**Eghshy**	144.7	**8.0**
Meiar	251	**6.3**	**Mekhairad**	57.9	**6.7**
Aawag	928.4	**4.9**	**El-Taalby**	69.2	**6.3**
Maaishya	70.3	**8.0**	**Araba 1**	67	**7.6**
Wagran	32.9	**4.9**	**Araba 2**	121	**8.0**
Shadq	81	**5.3**	**Aat El-Gharby**	54.9	**7.7**

- Source: DEM model, topographic map scale 1:50000, and Egyptian meteorological authority.

It can be noticed from Tab. (3-4) and Fig (4-1) that:

1- The values of runoff coefficient in the main basin in the study area range between 4.9 and 15.2 owing to local factors.

2- The first category has values < 5 and contains the small basins such as Wadi Gebah, Wadi Wagran, Wadi Moreikh Shadq, and Wadi El-Aawag. The area of basins in this category has a direct affect on runoff coefficient, but in Wadi El-Aawag basin, the lithology factor is considered the major factor.

3- The second and third categories which ranged between 7 and 11 contain most of basins in the study area. The determine factor in these basins is considered as basins area, but in Wadi Habran, Wadi Asla, and El-Mahash basin had affected more by slope and drainage density.

4- The last category has high values and concentrates in the big basins such as Wadi El Akgdar, Wadi El-Sheikh, and Wadi Solave which are tributaries of Wadi Firan. These basins are characterized by relatively steep slopes, and their outcrop lithology are igneous and metamorphic rocks which have a direct affect to increase the runoff coefficient values. In addition, these basins had high values of drainage density, and usually have had rainfall more than others because the affect of altitude factor.

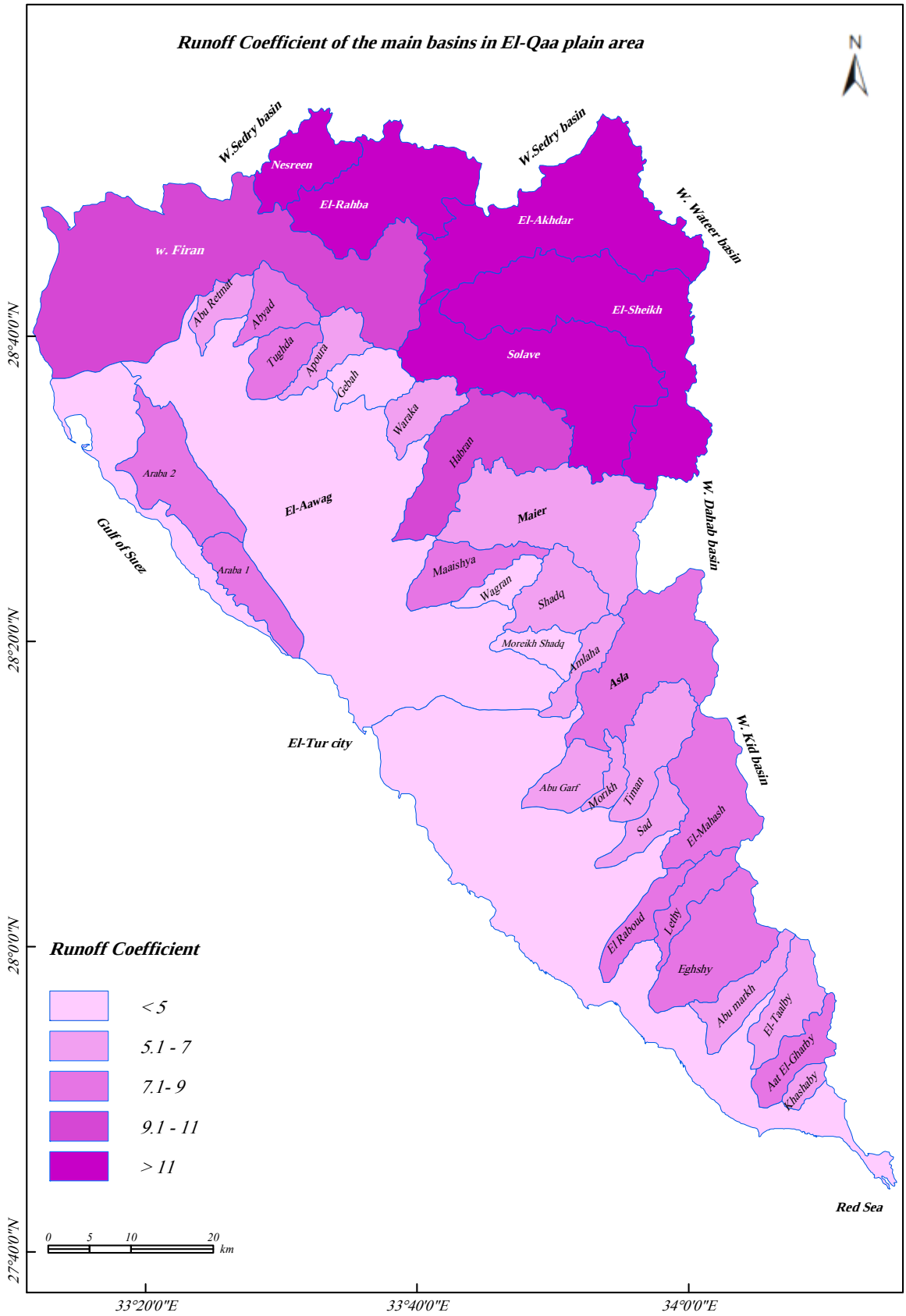

Fig (4-1) *Runoff coefficient in the main basins of El-Qaà plain area depending on basins area, drainage density, slope, rainfall depth, and geological surface setting*

4.1.2.2. Lag time

Wadi basin lag time (T_{LAG}), defined as the elapsed time between the occurrence of the centroids of the effective rainfall intensity pattern and the storm runoff hydrograph, is an important factor in determining the time to peak and the peak value of the instantaneous unit hydrograph (BANASIK, K., et al 2005). The lag time between rainfall excess and runoff at the plot or basins area is a critical parameter in runoff routing models (BOYD & BUFILL, 1989). Variable lag time implies basin nonlinearity. However, there are some examples suggesting that basin linearity is approached during extreme flood events (BATES & PILGRIM, 1986).

Basin lag time (T_{LAG}) is also an important hydrological parameter because it is directly related to the time of concentration. The latter is needed to use the rational method for estimating peak flood discharge. The lag time, like the time of concentration, is often determined as a power function involving the ratio of a characteristic length and the square root of the basin slope (WATT & CHOW, 1985), although the rainfall excess rate has been included recently in the estimators of the lag time (LOUKAS & QUICK, 1996).

To determine heavy rainfall as a function of time can be problematic because infiltration characteristics have to be assumed and the temporal distribution of rainfall excess will depend on the particular infiltration equation adopted. Another practical difficulty with the lag time defined using the mass centre of rainfall excess is the uncertainty in the runoff rate to which this lag time should be related (YU, B., et al 2000).

The lag time (T_{LAG}) determined using field data at the plot scale can be used to validate the relationship between the hydrological lag time and runoff rate, and estimate the effective roughness coefficient for natural storm events. In addition, the lag time can be used to quantify the storage effect on runoff rate, whereas the larger the lag time, the greater the attenuation of the runoff rate. Vegetative cover not only increases the amount of infiltration but also reduces the flow velocity, lengthens the lag time, and increases the storage effect on runoff rate. Even if the amount of runoff is the same with different surface treatments, one factor reducing the rate of soil loss would be the reduced runoff rate (YU, B., et al 2000). Lag time can be defined using National Resources Conservation Service (NRCS) equation as the following:

$$T_{lag} = \frac{2.587 * L^{0.8} \left(\frac{1000}{CN} - 9 \right)^{0.7}}{1900 * H^{0.5}} \qquad \textbf{(14)}$$

Where T_{lag} = Lag time (hr).

L = hydraulic watershed length (m).

CN = hydrologic area – weighted curve number.

H = average watershed land slope (%).

Tab (4-4) *Lag time in the main basins of the study area using* (NRCS) *equation.*

Basins	Lag time T_{lag}(hr)	Basins	Lag time T_{lag}(hr)
El-Akhdar	**13.4**	*Ghowaitat*	**1.67**
El-Sheikh	**6.31**	*Amlaha*	**1.97**
Rahba	**2.85**	*Asla*	**2.51**
Nesreen	**12.1**	*Abu Garf*	**7.43**
Firan (main wadi)	**10.88**	*Moreikh*	**2.48**
Solave	**6.89**	*Timan*	**4.58**
Abyad	**4.89**	*Sad*	**3.83**
Tughda	**11.2**	*El-Mahash*	**2.3**
Apoura	**7.93**	*El-Raboud*	**2.97**
Gebah	**3.19**	*Lethy*	**3.19**
Waraqa	**5.05**	*Eghshy*	**3.09**
Habran	**3.71**	*Mekhairad*	**4.02**
Meiar	**2.05**	*El-Taalby*	**4.38**
Aawag	**2.44**	*Araba 1*	**7.83**
Maaishya	**6.52**	*Araba 2*	**5.82**
Wagran	**4.55**	*Aat El-Gharby*	**4.62**
Shadq	**8.70**	*Khashaby*	**11.89**
Moreikh Shadq	**7.3**	*Abu Retmat*	**8.28**

- Source: All variables were computed depending on data base of the study area using equation (14)

From Tab (4-4) and Fig (4-2) can be noticed that:

- The lag time ranged between 1.97 (hr) in Wadi Amlaha and 13.4 (hr) in Wadi El-Akhdar with average 5.6 (hr).
- There are several factors playing an important role to control in Lag time such as lithology, shape, slope and area of basin, besides length of watershed and drainage density of these Wadis.
- It can be concluded depending on tab. (4-4) that runoff during heavy rainfall can be expected in the study area. Whereas, runoff may be occur during heavy rainfall in Wadi Firan in the period ranged between 3 and 4 hours, in Wadi El-Aawag after nearly 3 hours, and in Wadi Meiar runoff may be coming after 2 hours. Generally, it can be said that the tributaries of Wadi Firan are more dangerous than others because they often have more rainfall the infiltration of which is very small.

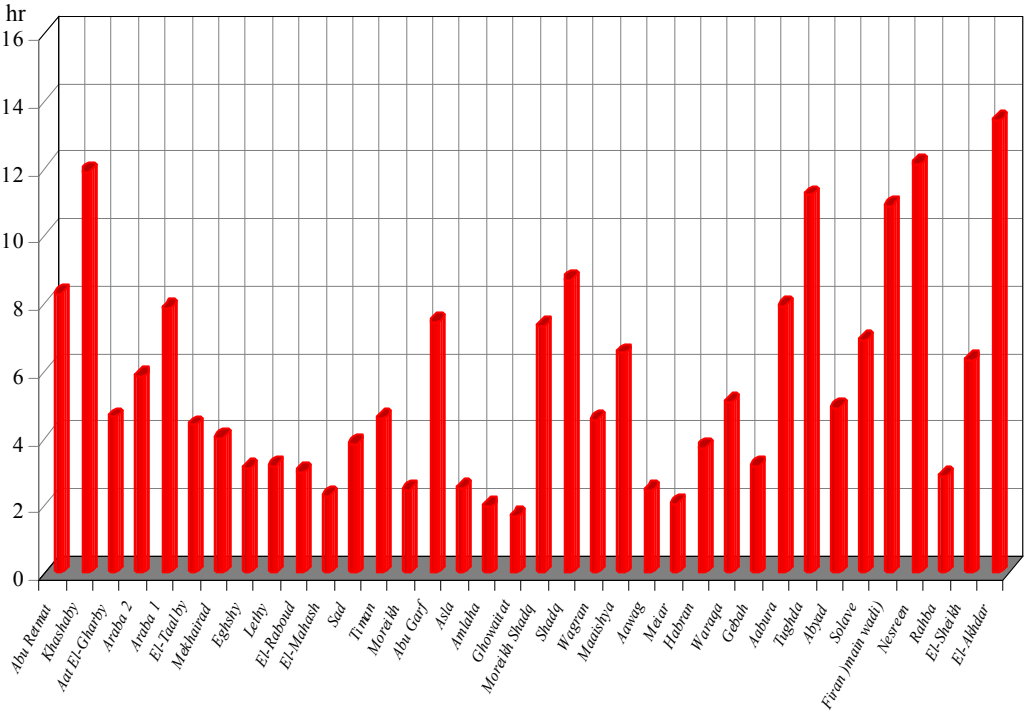

Figs (4-2) *Lag time in the main basins of El-Qaà plain area using equations (14)*

4.1.2.3. Time of concentration

This is a time parameter which is related to other watershed characteristics such as slope, length, and area. The time of concentration (Tc) is defined as the time needed for a drop of water to moving from the most distant point in the watershed to the design point downstream. It includes both time for overland flow and time for channel flow. Many empirical equations are available to calculate Tc (EL-WESHAH, R., 2000). Attention should be paid to the system of units and to the limitations of each method. In order to determine the time of concentration using the KIRPICH / RAMSER formula you need to calculate the drainage length (L) and the distance weighted channel slope (S).

$$Tc = 0.0195L^{0.77} * S^{-0.385} \qquad \textbf{(15)}$$

Where ***Tc*** = Time of concentration (min) ***L*** = Length of main wadis (m)

S = distance weighted channel slope (m/m)

To evaluate the weighted channel slope, a *DEM* of the study area must be created by means of Contour Interpolation (chapter 3). This DEM is needed for investigating the height in the drainage area. Once found the height for two points along the Wadi and the distance between them, it is possible to compute the weighted channel slope to calculate the time of concentration using equation (15).

Tab (4-5) The time of concentration of runoff in the main basins of the study area

Basins	**Length** L (m)	**Slope** S (m/m)	**Tc** (hr)	**Basins**	**Length** L (m)	**Slope** S (m/m)	**Tc** (hr)
El-Akhdar	39196	0.017	**5.4**	**Ghowaitat**	7050	0.201	**0.6**
El-Sheikh	50000	0.038	**4.8**	**Amlaha**	14350	0.155	**1.1**
Rahba	23820	0.045	**2.5**	**Asla**	27420	0.082	**2.2**
Nesreen	15087	0.043	**1.8**	**Abu Garf**	11860	0.08	**1.2**
Firan (main	55077	0.019	**6.7**	**Moreikh**	9935	0.1	**0.9**
Solave	36400	0.043	**3.6**	**Timan**	19517	0.113	**1.5**
Abyad	9880	0.086	**1.0**	**Sad**	14430	0.094	**1.3**
Tughda	11880	0.046	**1.5**	**El-Mahash**	19430	0.104	**1.6**
Apoura	12280	0.09	**1.2**	**El-Raboud**	16690	0.048	**1.9**
Gebah	9500	0.195	**0.7**	**Lethy**	15320	0.055	**1.7**
Waraqa	10640	0.166	**0.8**	**Eghshy**	20540	0.046	**2.2**
Habran	28480	0.067	**2.5**	**Mekhairad**	16730	0.06	**1.7**
Meiar	28416	0.088	**2.2**	**El-Taalby**	16045	0.089	**1.4**
Aawag	55612	0.004	**12.3**	**Araba 1**	18580	0.017	**3.0**
Maaishya	18550	0.045	**2.1**	**Araba 2**	15790	0.027	**2.2**
Wagran	9630	0.18	**0.7**	**Aat El-Gharby**	15250	0.056	**1.6**
Shadq	10980	0.159	**0.9**	**Khashaby**	6430	0.061	**0.8**
Moreikh Shadq	10010	0.142	**0.8**	**Abu Retmat**	10717	0.07	**1.2**

- Source: All variables were computed depending on data base of the study area using equation (15)

The time of concentration of runoff in the main wadis in the study area depends first on length of Wadi channel, and slope, and secondly on some factors such as lithology of surface cover and the thickness of deposits. From tab (4-5), and fig (4-3) is pointed out that there are 4 categories of wadis owing to the time of concentration as following:

- First category consists of about 9 of main basins such as Wadi Moreikh 0.9 (hr), and Wadi Gebah 0.7 (hr) with characteristic small areas, and the time of concentration of them is less than 60 minutes; this means that runoff of these basins arrives in about one hour. Because of their small areas. They have small volumes of runoff during rainy storms; therefore, these basins often have local dangerous runoff.

- Time of concentration of runoff in the second category ranging between 60 to 120 minutes and containing about 14 of main basins. There are Wadi Nesreen 1.8 (hr), Wadi Timan 1.5 (hr), and Wadi El-Taalby 1.4 (hr) which have relatively big area, steep slope, little infiltration, and during rainy storm have sometimes a big amount of rainfall. Therefore, it can be concluded that the big basins in the second category may be have sometimes dangerous during runoff.

- The time of concentration for the third category ranges between 120 to 180 minutes; it contains 7 of main basins such as Wadi Asla 2.2 (hr), Wadi Habran 2.5 (hr), and Wadi Meiar 2.2 (hr) which are considered being active wadis in the study area and more dangerous than others wadis in the same category. This may be owing to local slope, area, and length of main channel. The previous field work has demonstrated also that the three previous basins until now are active during runoff.
- The last category consists of basins which have time concentration of runoff more than 3 hours; it contains all big basins such as Wadi El-Akhdar 5.4 (hr), Wadi El-Sheikh 4.8 (hr), Wadi Solave 3.6 (hr), and Wadi El-Aawag basin 12.3(hr). All wadis in this category except Wadi El-Aawag are considered more dangerous during runoff especially Wadi El-Sheikh and Wadi Solav which are the upper tributaries of Wadi Firan. While Wadi El-Aawag basin has little chance to occurring runoff except when the water or some tributaries are added to it, at that time may be Wadi El-Aawag basin will more dangerous than others basin, like in March 1991.
- The time of concentration of Wadi El-Aawag basin is relatively high 12.3 (hr) as a result of basin setting characterized by low slope, wide channel, and big thickness of deposits.

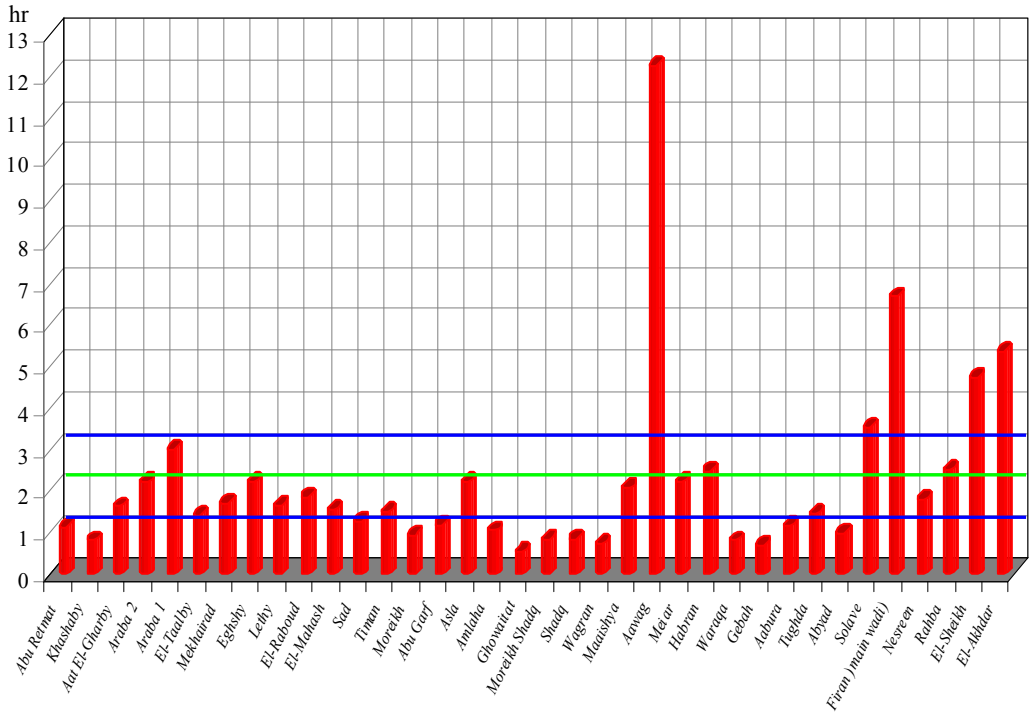

Figs (4-3) *The time of concentration of runoff in the main basins of El-Qaà plain area, the values were calculated using KIRPICH / RAMSER equation (15).*

4.1.2.4. Runoff volume

A storm event is generally characterized by its size and the frequency of its occurrence. The size of the storm is the total precipitation that occurs within a specified time. How often this storm size is likely to repeat is called the frequency. For instance, the total rainfall resulting of a single 24 hour duration storm once every ten years is called the 10-year storm and has a 10% chance of occurring in any given year. A 2-year storm has a 50% chance; a 25-year storm has a 4% chance; a 100-year storm has a 1% chance (http://www .state.nj.us/dep/waters hedmgt)

The peak discharge resulting from a given rainfall is particularly influenced by the rainfall distribution, which describes the variation of the rainfall intensity during the storm duration. A rainfall may have been evenly distributed over the 24 hour period or the majority of it may have come in just a few hours, which is typical. These two scenarios present entirely different types of rainfall distributions and peak discharges.

Major factors which affect the runoff volume and associated peak discharge are the rainfall duration and intensity, soil types in the watershed, type of natural or man made cover on the soil, and the time of concentration. Time of concentration is the time required for runoff water to travel from the hydraulically most distant point in a watershed to the point of analysis at the lower end of the watershed.

- High intensity rainfall of shorter duration will produce a higher peak discharge than a larger rainfall that is distributed over a longer duration.

- Porous soils that infiltrate rapidly produce less runoff than soils that restrict infiltration.

- Soils that do not infiltrate may be naturally tight, or may have become compacted by activities of man.

- Conversely, impermeable areas such as pavement and rooftops intercept the rainfall, preventing infiltration, and increase runoff volumes and velocities.

The following set of equations can be used to estimate surface runoff in the study area. Basically, the following form of the rational equation was used:

$$V = R * C * A * P \qquad \textbf{(16)}$$

$$R = 1.05 - 0.0053\sqrt{A} \qquad \textbf{(17)}$$

Where ***V*** is the surface runoff volume, ***P*** is the total rainfall depth, ***C*** is runoff coefficient, ***A*** is the basin area upstream the point of interest, and ***R*** is the reduction factor that depends on basin area (HELWA, M., 1993).

Tab. (4-6) *Runoff volume in the main basins of El-Qaà plain area*

Basins	**(A) km^2**	**P (mm)**	**R**	**C**	*** V *1000* m^3 (4 hour)**	****V*1000* m^3 (4 hour)**
El-Akhdar	336.9	45	0.95	15.2	**2195.44**	**2299.68**
El-Sheikh	348.6	50	0.95	14.6	**2420.20**	**2548.8**
Rahba	206.8	40	0.97	12.8	**1031.06**	**1055.52**
Nesreen	84.6	40	1	12.9	**437.08**	**434.88**
Firan (main wadi)	619.7	20	0.92	10.1	**1149.23**	**1251.36**
Solave	316.1	50	0.96	14.3	**2160.15**	**2262.24**
Abyad	52.2	25	1.01	7.7	**101.66**	**99.36**
Tughda	53.4	20	1.01	8	**86.40**	**84.96**
Apoura	46.1	20	1.01	6.8	**63.57**	**63.36**
Gebah	53.8	20	1.01	4.7	**51.13**	**50.4**
Waraqa	53	22	1.01	6	**70.76**	**70.56**
Habran	182.3	27	0.98	9.7	**467.15**	**478.08**
Meiar	251	27	0.97	6.3	**412.45**	**424.8**
Aawag	928.4	20	0.89	7.3	**1204.34**	**1346.4**
Maaishya	70.3	20	1.01	8	**113.11**	**112.32**
Wagran	32.9	20	1.02	4.9	**32.87**	**31.68**
Shadq	81	20	1	5.3	**86.06**	**86.4**
Moreikh Shadq	38	20	1.02	4.6	**35.57**	**34.56**
Ghowaitat	75	20	1	4.6	**69.28**	**69.12**
Amlaha	39.4	25	1.02	5.9	**59.09**	**57.6**
Asla	198	25	0.98	7.8	**376.61**	**384.48**
Abu Garf	53.9	20	1.01	5.6	**61.04**	**60.48**
Moreikh	22.6	20	1.02	5.7	**26.40**	**25.92**
Timan	92.5	25	1	5.8	**133.99**	**133.92**
Sad	44.3	20	1.01	6	**53.94**	**53.28**
El-Mahash	137.5	27	0.99	7.4	**271.39**	**275.04**
El-Raboud	46.6	25	1.01	7.6	**89.76**	**87.84**
Lethy	47.3	25	1.01	8.6	**103.07**	**102.24**
Eghshy	144.7	25	0.99	8	**285.42**	**288**
Mekhairad	57.9	25	1.01	6.7	**97.92**	**96.48**
El-Taalby	69.2	25	1.01	6.3	**109.63**	**109.44**
Araba 1	67	20	1.01	7.6	**102.51**	**102.24**
Araba 2	121	20	0.99	8	**191.99**	**192.96**
Aat El-Gharby	54.9	25	1.01	7.7	**106.82**	**105.12**
Khashaby	17.6	20	1.03	6.8	**24.60**	**24.48**
Abu Retmat	37.4	25	1.02	6.4	**60.89**	**60.48**
Total					**14342.61**	**14964.48**

- Source: All variables were computed by researcher depending on data base of the study area, and runoff volume has been estimated using equations (8) and (16) **.*

Several techniques have been available for the estimation of runoff volume and peak discharge. Some of the common methods are:

1. The graphical peak discharge method: This method was developed from hydrograph analysis using TR-20. It calculates peak discharge using an assumed hydrograph and a thorough evaluation of the soils, slope, and surface cover characteristics of the watershed. This method is useful in homogenous watersheds and is recommended in the design of soil erosion and sediment control structures. This method was applied in the study area to determine the peak runoff and runoff volume.

2. The USDA-NRCS TR-20 model is a rainfall runoff simulation model which uses a storm hydrograph and CN combined with channel features to determine runoff volumes as well as unit hydrographs to estimate peak rates of discharge. The dimensionless unit hydrographs from sub basins within the watershed can be routed through stream reaches and impoundments. The TR-20 method may be used to analyze the impact of development and detention basins on downstream areas. The parameters needed in this method include total rainfall, rainfall distribution, CN, travel time and drainage area. It considered one of the best methods to estimate runoff volume, because it depends on many variables which control runoff; these variables are used to estimation CN (curve number) values using previous equations (9, 10, and 11).

It can be concluding from Tab (4-6) and Fig (4-4) that:

- Runoff volume in the different basins in the study area has been influenced by basins area, altitude, rainfall amount, and the thickness of deposits. Whereas, some basins have approximately the same conditions such as area (Wadi Sad basin 44.3 km^2, and Wadi lethy basin 47.3 km^2), basin shape, and rainfall amount, but they have different values of runoff amount 53.8, and 102.24 (1000 m^3) respectively. We think that local relief, outcrop lithology, and runoff coefficient in the previous basins were of important influence to variation runoff volume.

- Wadi Firan basin has the biggest runoff volume in the study area 9852.28 (thousand m^3) about 65.8% of total runoff volume in the study area. This amount is distributed on five main tributaries Wadi El-Akhdar basin 2299.68, Wadi El-Sheikh basin 2548.8, Wadi Rahba basin 1055.52, Wadi Solave basin 2262.24, Wadi Nesreen basin 434.88, and the main Wadi basin 1251.36.

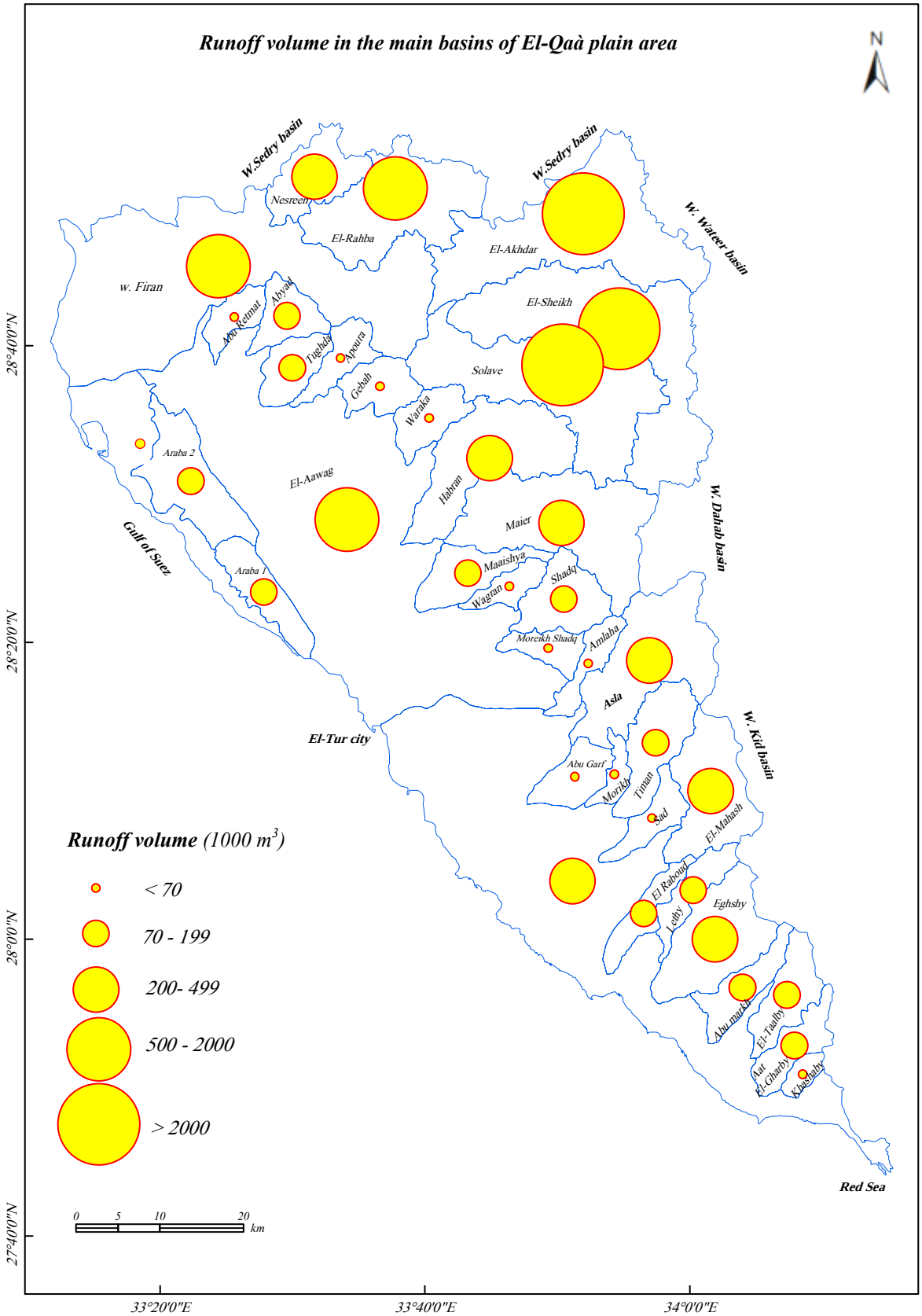

Fig (4-4) *Runoff volume* (m^3) *during four hours in the main basins of El-Qaà plain area depending on basins area, drainage density, slope, rainfall depth, and geological surface setting using equations (8) and (16)*

- The three upper tributaries of Wadi Firan basin have rainfall amount more than others. They are characterized with steep slopes, and mostly developed in igneous rocks. Therefore, Wadi El-Sheikh, Wadi Solave, and Wadi El-Akhdar are considered relatively dangerous areas during rainy storm and runoff more than other tributaries in Wadi Firan.

- Wadi El-Aawag basin is ranging in the second order after Wadi Firan, whereas it has 3012.43 (1000 m^3) for about 20.1% of runoff volume in El-Qaà plain area. This amount is distributed in several basins, the most important are Wadi El Aawag (main area) 1346.4 (1000 m^3), and two main tributaries of Wadi El-Aawag, Wadi Habran and Wadi Meiar with basin areas of 474.08, and 424.8 (1000 m^3) respectively.

- Because of the main part of Wadi El-Aawag basin has been covered by alluvial and wadi deposits originating from Wadi Meiar, and Wadi Habran basins developed in igneous rockstheir influence is predominant, they are considered more dangerous than Wadi El-Aawag during runoff, except some rare events of widespread heavy rainfall when the amounts of both Wadis are added to the amount of Wadi El-Aawag producing severe flash floods.

- The last three categories range between 24480 (m^3) in Wadi Khashaby to 384480 (m^3) in Wad Asla. There are 15 basins in these categories, but Wadi Asla basin, Wadi El-Mahash basin 275040 m^3, and Wadi Eghshy basin 288000 m^3 have a relative influence because of these basins have also higher values of runoff volume during floods in the southern part of the study area, and have also a relatively steep slope which has a direct affect on peak runoff hence runoff volume.

- Finally, it can be said that runoff volume is different from one basin to another, resulting of variation of some affect factors like geological and structure settings, morphological setting, basin shape, drainage density, thickness and kind of deposits, as well as some climatic elements such as temperature, relative humidity, wind speed, and rainfall amount. In addition, time factor is considered an important influence on runoff volume i.e. season of rainfall, the time of rainfall (day or night), duration, time of concentration, and lag time of every basin.

4.1.2.5. Peak runoff (Q_r)

A peak runoff (Q_r) is defined as the maximum instantaneous flow that results from an individual storm. According to the theory of rational formula, peak runoff is a function of the average rainfall intensity during the time of concentration (ABU FARAH MD., ET AL 2005). Peak discharge is the peak rate of surface runoff from a drainage area for a given rainfall. There are some factors having direct influence on runoff volume and peak runoff, in the same time is used to calculate them.

The time of concentration is one of the important factors affecting instantaneous discharge. This is so because the runoff reaching the outlet of the basin will, at first, only summarize the precipitaation in the immediate vicinity of the outlet, but, later on, water from further and further up the basin will reach the outlet (GHAYOOR, H., 1991). After a period of time, depending on the time of concentration, runoff from all points within the basin will contribute to the basin's discharge at the outlet. Thus, if the rainfall duration is less than the time of concentration, it does not have very much influence on the peak discharge; but it could be an effective factor on runoff-peaks for durations of more than the time of concentration. Therefore, this factor was used as an influencing factor in the study area.

There are two main methods to calculate peak runoff, the SCS triangular hydrograph approach (USA-SCS, 1972) to estimate peak flow utilities by triangular approximation of a runoff unit hydrograph, and the rational formula method which characterizes by consideration of the entire drainage area as a single unit, estimation of flow at the most downstream point only, and the assumption that rainfall is uniformly distributed over the drainage area (www.itc.nl/ilwis/applications/application11.asp). Therefore, the rational formula equation is considered the best method to estimate peak runoff in the study area considering the basins of the study area as individual morphological units.

$$Q = \frac{C\,I\,A}{3\,6\,0} \qquad \textbf{(17)}$$

Where

Q = peak flow rate (maximum runoff), m^3/s

A = catchment area,

I = rainfall intensity, millimeters per hour.

C = runoff coefficient

Values of runoff coefficient ***C*** are given in most hydrology textbooks.

Tab. (4-7) *Maximum runoff* (m^3/s) *in the main basins of the study area depending on rational formula method*

Basins	**Runoff Coeffic. (C)**	**Max. rainfall I** (mm/h)	**Runoff (Q)** m^3 / s	***Basins***	**Runoff Coeffic. (C)**	**Max. rainfall I** (mm/h)	**Runoff (Q)** m^3 / s
El-Akhdar	15.2	11.3	***159.7***	***Ghowaitat***	4.6	5.0	***4.8***
El-Sheikh	14.6	12.5	***177.0***	***Amlaha***	5.9	6.3	***4.0***
Rahba	12.8	10.0	***73.3***	***Asla***	7.8	6.3	***26.7***
Nesreen	12.9	10.0	***30.2***	***Abu Garf***	5.6	5.0	***4.2***
Firan (main	10.1	5.0	***86.9***	***Moreikh***	5.7	5.0	***1.8***
Solave	14.3	12.5	***157.1***	***Timan***	5.8	6.3	***9.3***
Abyad	7.7	6.3	***6.9***	***Sad***	6.0	5.0	***3.7***
Tughda	8.0	5.0	***5.9***	***El-Mahash***	7.4	6.8	***19.1***
Apoura	6.8	5.0	***4.4***	***El-Raboud***	7.6	6.3	***6.1***
Gebah	4.7	5.0	***3.5***	***Lethy***	8.6	6.3	***7.1***
Waraqa	6.0	5.5	***4.9***	***Eghshy***	8.0	6.3	***20.0***
Habran	9.7	6.8	***33.2***	***Mekhairad***	6.7	6.3	***6.7***
Meiar	6.3	6.8	***29.5***	***El-Taalby***	6.3	6.3	***7.6***
Aawag	7.3	5.0	***93.5***	***Araba 1***	7.6	5.0	***7.1***
Maaishya	8.0	5.0	***7.8***	***Araba 2***	8.0	5.0	***13.4***
Wagran	4.9	5.0	***2.2***	***Aat El-Gharby***	7.7	6.3	***7.3***
Shadq	5.3	5.0	***6.0***	***Khashaby***	6.8	5.0	***1.7***
Moreikh Shadq	4.6	5.0	***2.4***	***Abu Retmat***	6.4	6.3	***4.2***

- Source: All variables were computed depending on data base of the study area using equation (17)

Tab (4-7) and Fig (4-5) pointed that:

- The peak runoff values in the study area have varied from one basin to another owing to several affected factors. The average peak runoff values ranges between (1.8 m^3/s) in Wadi Moreikh and (177 m^3/s) in Wadi El-Sheikh. In the present study, the values have been distributed in 5 categories to classify the basins depending on values (m^3/s).
- The higher category has values more than 150 m^3/s, and contains Wadi El-Akgdar 159.7 (m^3/s), Wadi El-Sheikh 177 (m^3/s), and Wadi Solave 157.1 (m^3/s) which are the upper tributaries of Wadi Firan. Because of these wadis are characterized by a relatively large area, steep slope, surface cover of igneous and metamorphic rocks, high altitude and little thickness of deposits, they are considered more dangerous during runoff than other wadis in the study area.
- Wadi Firan 86.9 m^3/s (main wadi) and Wadi El-Aawag 93.5 m^3 /s came in the second order as alone Wadis, but they can be considered very dangerous during runoff because they have several dangerous tributaries which add more water to them. Consequently the values of peak runoff for both Wadis are mostly varying and related with runoff volume, time of concentration, lag time and duration.

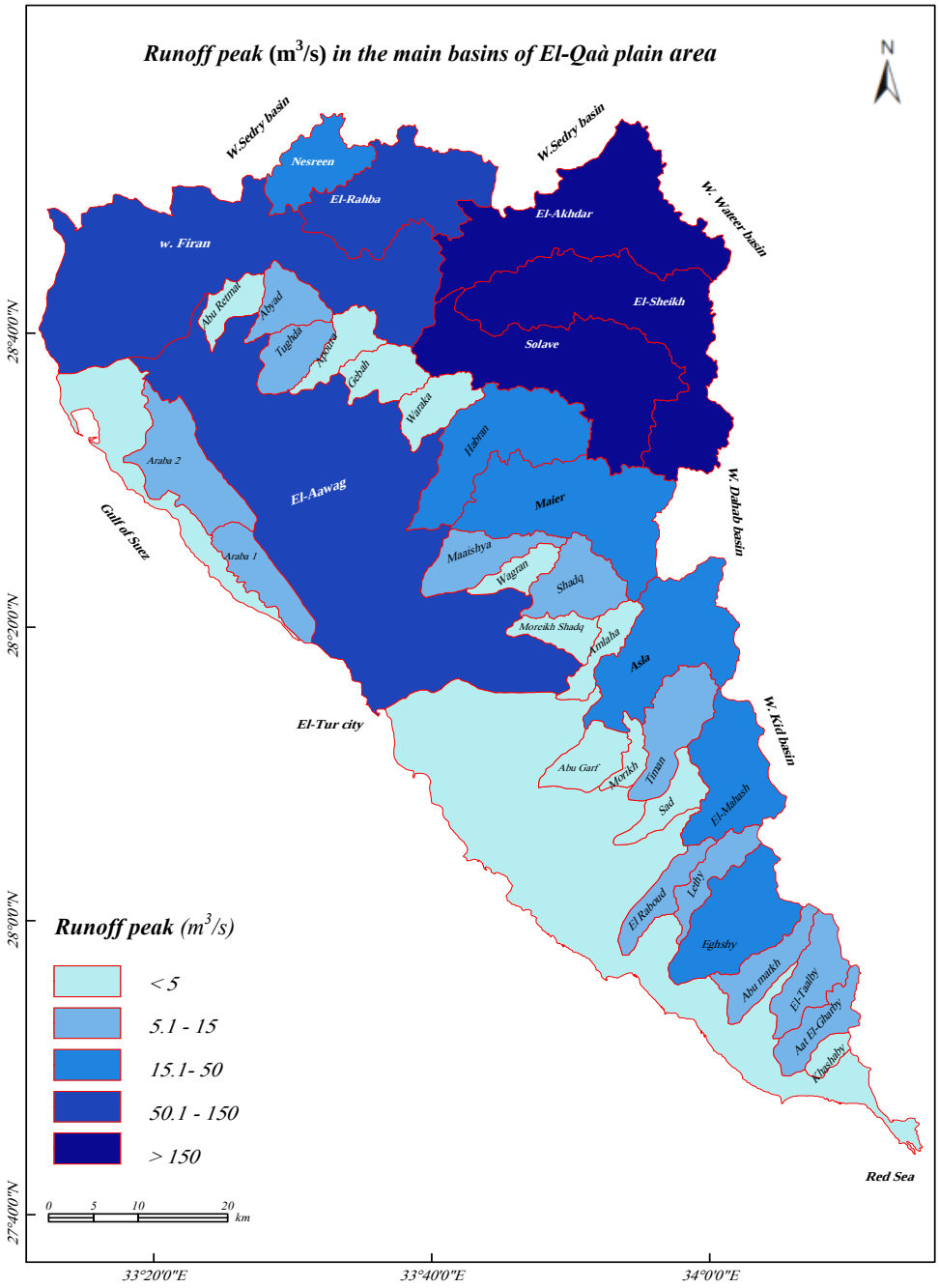

Fig (4-5) *Runoff peak* (m^3/s) *in the main basins of El-Qaà plain area depending on basins area, drainage density, slope, rainfall depth, and geological surface setting using equation (17)*

However, there are many climatic factors with direct influence on peak runoff, such as type of precipitation, rainfall intensity, rainfall amount, rainfall duration, distribution of rainfall over the drainage basin, direction of storm movement, antecedent precipitation and resulting soil moisture, other meteorological and climatic conditions that affect evaporation, such as temperature, wind, relative humidity and season etc (ABU FARAH MD., ET AL 2005). In addition geological and morphological factors have been direct influence on volume and peak runoff.

4.1.2.6. Frequency analysis of flash flood

Flash floods are characterized as quick floods usually difficult to forecast and cause, therefore huge damage. They are also events with a high rate of flood rise or peak discharge. In any given region, such floods may not occur every year but yet may occur several times in any specific year because of the randomness and variation in the conditions which promote their formation (UNESCO, 1999).

Selection of flash flood data series

The two main approaches to flood frequency analysis are peaks-over threshold and annual maxima. The first technique uses only those peaks which exceed a given threshold while the second selects the highest peak in each year of record; following on from the definition outlined above, the first approach is the most suitable for the selection of flash flood data.

In general, all peaks over a given threshold may be selected to form a flood peak series but we need to select flash floods only. The threshold is determined on the basis of the rate of flood rise and the predetermined flood peak (but note that if the rate of flood rise is small and not particularly sudden, flash floods will not differ significantly from normal floods). (Arshad M Sheikh 1994) has defined an index for flash flood magnitude, FFMI. FFMI is calculated from the standard deviation of the logarithms of annual maximum discharge, as follows:

$$FFMI = X^2 / N - 1$$

Where

$X = X_m - M$

X_m = logarithm of annual maximum discharge

M = logarithm of mean annual discharge

N = number of years of record

However, as we carry out flood frequency analysis using a peaks-over threshold time series, some of the intervals may be surplus for annual values required in engineering design which requires translating frequency intervals into annual values, as follows:

$$P = \frac{s}{n} p^{-}$$

Where

P = annual frequency

P^{-} = frequency calculated by peaks over threshold

s = number of peaks over threshold

n = number of years of record

For some regions where flash floods occur frequently, a better method of selection of the sample series is the annual maxima approach because of better sample independence. Since the floods which occur in any one river basin may have different causes, there is also the question of how to divide flood types according to their origins.

Types of frequency curve

There has been relatively few study of different types of curves in flood frequency analysis and choosing which type of frequency curve to work with will depend on experience and custom. The Pearson Type II analysis, for example, is used extensively in China, while the Log-Pearson Type III is used in the USA. The Flood Studies Report (vol. I, NERC 1975) used goodness of fit indices computed for seven distributions of data from 35 long-term stations. These were extreme value Type I (GUMBEL), gamma, lognormal, general extreme value (JENKINSON), Pearson Type 3, log gamma and Log-Pearson Type III. This report recommends the general extreme value (GEV) distribution.

There were few data available for analyzing flash flood flow frequencies in the past. ZHOU LUCHAO studied flash flood frequency curves in arid zones in 1992 and recommended GUMBEL distribution curves for general use because the GUMBEL distribution has just two parameters, whereas the shape of Pearson Type III curves depends on three parameters which, although giving somewhat more flexibility but are harder to fit for the short flood peak series generally available for arid zones.

If there are no historic floods available within the series (like the study area), it is difficult to obtain a close fit. But it is nessesary to focus the frequency analysis of events on rainfall data in the study area which is considered the main reason generating flash floods. Therefore, GUMBEL method has been used in the previous chapter to showing the frequency analysis of events with the amount of rainfall.

4.2. Extreme event analysis

Due to the importance of flash floods in the study area because they have direct effect on all economic activities and the infrastructure it is necessary to study their occurance. They relate often with high amounts of rainfall in the period between autumn and spring (more than 10mm) which leads normally to runoff, it also necessary to know the number of rainy storms, and their duration (EL-HUSAINY, S. 1987). here, it will be focused on the extreme event analysis of flash floods which occured in the study area to know the frequency analysis and probability. So their danger and use for irrigation purposes can be estimated.

Because for the study area until now exist only some meteorological reports of rainfall amounts, temperature, wind, and humidity, but no archive about the realy floods, the extreme events should be computed on the base of the influencing amount of rainfall, especially the maximum rainfall occurring in one day. Therefore, the statement is as follows: maximume rainy days are such with extreme runoff (Tab 4-8).

Tab (4- 8) *showing the highest amount of rainfall in one day*

Station		Mar.	Apr.	Mai.	Aug.	Oct.	Nov.	Dec.	St.Dev
ST. Catherine	*mm*	***18.2***	***12.9***	***37.1***	***14.5***	***20.2***	***11.6***	***15.8***	10.5
	Day	**20/80**	**8.82**	**27/97**	**27/99**	**17/97**	**9/82**	**26/80**	-
EL-Tur	*mm*	8.2	0.2	0.0	0.0	4.0	***18.6***	***11.6***	6.2
	Day	22/91	21/93	0.0	0.0	16/86	**2/94**	**17/85**	-
Sh. El-Sheikh	*mm*	***10.3***	0.3	4.2	0.0	7.1	***48.3***	3.0	14.1
	Day	**9/89**	23/92	10/98	0.0	16/87	**17/96**	17/85	-

- *Source: The archive of Meteorological authority, reports none published.*

(Tab 4-8) shows that there are about 11 times of runoff during the period between 1980 and 2000 (20 years) at different locations in the study area considering the values of rainfall which exceed 10mm/day. It has been also noticed that 7 events were recorded in Catherine station which lies in upper Wadi Firan basin. Therefore, Wadi Firan basin is considered the maximum dangerous basin in the study area. Consequently, it is possible to calculate the runoff volume in the study area during the previous 11 events depending on the maximum rainfall in one day over parts of the study area to determine the different volumes of runoff. In addition it can be given a classification of the degree of dangerrish of the main basins in the study area.

Tab (4-9) *Extreme event values of runoff volume in the main basins of SW- Sinai depending on maximum rainfall in one day during the period between 1980 to 2000 (1000 m^3).*

Basins	20 Mar.80	26 Dec.80	8 Apr.82	9 Nov.82	9 Mar.89	2 Nov.94	17 Nov.96	27 Mai.97	17 Oct.97	Average
El-Akhdar	876	769	628	564	501	905	2350	1805	983	***1042***
El-Sheikh	870	764	624	561	498	899	2335	1794	977	***1036***
Rahba	462	406	331	298	264	478	1240	953	519	***550***
Nesreen	196	172	141	127	112	203	527	405	220	***234***
Firan (main wadi)	1036	910	743	668	593	1071	2781	2136	1163	***1233***
Solave	781	686	560	503	447	807	2096	1610	877	***930***
Abyad	73	64	52	47	42	76	196	151	82	***87***
Tughda	78	68	56	50	44	80	208	160	87	***92***
Apoura	57	50	41	37	33	59	153	117	64	***68***
Gebah	46	40	33	30	26	48	123	95	52	***55***
Waraqa	58	51	41	37	33	60	155	119	65	***69***
Habran	312	274	224	201	178	322	837	643	350	***371***
Meiar	276	242	198	178	158	285	741	569	310	***329***
Aawag	1086	953	778	700	621	1122	2913	2238	1218	***1292***
Maaishya	102	90	73	66	59	106	274	211	115	***122***
Wagran	30	26	21	19	17	31	79	61	33	***35***
Shadq	77	68	55	50	44	80	207	159	87	***92***
Moreikh Shadq	32	28	23	21	18	33	86	66	36	***38***
Ghowaitat	62	55	45	40	36	64	167	128	70	***74***
Amlaha	43	37	31	28	24	44	115	88	48	***51***
Asla	272	239	195	176	156	282	731	562	306	***324***
Abu Garf	55	48	39	35	31	57	147	113	62	***65***
Moreikh	24	21	17	15	14	24	63	49	27	***28***
Timan	97	85	69	62	55	100	259	199	108	***115***
Sad	48	42	35	31	28	50	130	100	54	***58***
El-Mahash	181	159	130	117	104	187	487	374	203	***216***
El-Raboud	64	57	46	41	37	67	173	133	72	***77***
Lethy	74	65	53	48	42	76	198	152	83	***88***
Eghshy	206	181	148	133	118	213	554	425	232	***246***
Mekhairad	71	62	51	45	40	73	189	145	79	***84***
El-Taalby	79	70	57	51	45	82	213	163	89	***94***
Araba 1	93	81	66	60	53	96	248	191	104	***110***
Araba 2	173	151	124	111	99	178	463	356	194	***205***
Aat El-Gharby	77	67	55	50	44	79	206	158	86	***91***
Khashaby	22	19	16	14	13	23	60	46	25	***26***
Abu Retmat	44	39	31	28	25	45	118	91	49	***52***
Total	**8133**	**7139**	**5829**	**5241**	**4654**	**8404**	**21824**	**16763**	**9127**	**9679**

- Source: All values were computed by researcher depending on climate data of the study area, and runoff volume has been estimated using Equation (16).

According to maximum rainfall amount more than 10mm/day, it can be estimated extreme event values of flash floods in the main basins of the study area. It can be noticed from Tab (4-8) that:

1- Runoff mostly occurred in the study area in the years of 1980, 1982, 1985, 1989, 1994, 1991, 1996, 1997 and 2004 owing to maximum rainfall in one day more than 10mm. In addition some information from Bedouins (local population) to confirm that the runoff has occurred in the years of March 1991 (big flood) and November 2004, whereas both March and November have about 67% of total runoff number in the study area and the other months (October, December, January and February) have 33%.

2- Runoff volume has varied from one basin to another dependent on the basins area, rainfall amount, and other morphometric parameters. These are the increase of basins area, the increase runoff volume, but peak runoff, lag time, and time of concentration with regard to other influencing factors besides the area.

3- Wadi El-Aawag basin and Wadi Firan have had the biggest amounts of water during the previous floods owing to the total area of them. Those of Wadi Firan basin are dangerous more than other wadis because it has four main direct tributaries which have also high amounts of water at every runoff. If the four tributaries of Wadi Firan have runoff in the same time and the water of them was cumulated, it is resulting proably a big catastrophe in the area. Consequently, it could be necessary to stop the accumulation of water resulting of these tributaries to mitigate hazard in Wadi Firan

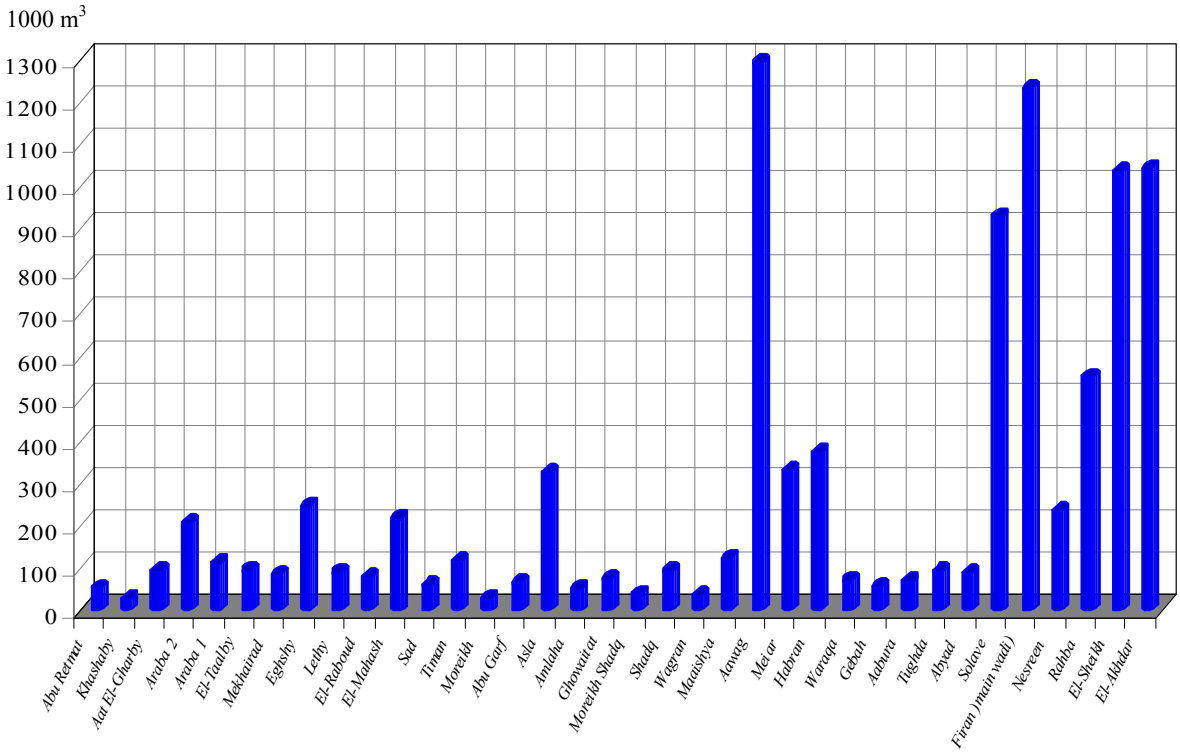

Fig (4-6) *Extreme events of runoff volume in the main basins of the study area (1000 m^3)*

4.3. Map of affected area

Flash floods in arid zones are regarded being one of the most devastating natural hazards in the world causing large amounts of deaths and property damage (CEOS 2003). As extreme hydrological phenomena, floods can influence many aspects of human life due to their destructive effects and the significant expenses of mitigation efforts. Drainage basins are the fundamental units of the fluvial landscape and a great amount of research has focused on their geometric characteristics, including the tyopology of the stream networks, and quantitative description of drainage texture, pattern, shape, and relief characteristics (ABRAHAMS 1984). In some studies, the characteristics of basin morphometry have been used to predict or describe geomorphic processes such as prediction of flood peaks, assessment of sediment yields and estimation of erosion rates (BAUMGARDNER 1987; GARDINER 1990).

Morphometric studies involve evaluations of streams through the measurement of various stream properties. Evaluation of morphometric parameters necessitates the analysis of various drainage parameters such as ordering of the various streams, measurement of basin area and perimeter, length of drainage channels, drainage density, stream frequency, bifurcation ratio, texture ratio, basin relief, ruggedness number and time of concentration (CHAPTER 2). The application of geomorphic principles to flood potential has led to a noteworthy amount of research attempting to identify relationships between basin morphometry and stream flooding (PATTON 1988; OZDEMIR AND BIRD, 2008).

Identification of drainage networks within basins or subbasins can be achieved using traditional methods such as field observations and topographic maps or alternatively with advanced methods using remote sensing and DEMs (VERSTAPPEN 1983; MARK 1983; O'CALLAGHAN AND MARK 1984; RINALDO ET AL. 1998; MACKA 2001; MAIDMENT 2002; OZDEMIR AND BIRD, 2008).

Extracting drainage networks from DEMs is based on the gravity; the water will flow from higher to lower elevation using the steepest descent and it is assumed that there is no interception, evapotranspiration and loss to groundwater. Automated extraction methods are the most efficient when DEM cell size is significantly smaller than the watershed dimensions. With a coarse resolution, the variability of the surface may not be adequately captured. Furthermore, depressions, flat areas and flow blockages create errors in defining surface drainage paths from DEMs (GARBRECH AND STARKS 1995; MARTZ AND

GARBRECHT 1998). A number of methods has been developed for solving these difficulties (BAND 1986; JENSON AND DOMINGUE 1988; MARTZ AND DE JONG 1988; FREEMAN 1991; MARTZ AND GARBRECHT 1998; OZDEMIR AND BIRD, 2008).

The study area was divided into sub-basins such as Wadi Firan, Wadi El-Aawag. The drainage networks of the sub-basins were extracted from two sources: topographic maps and a contour based DEM. The drainage network obtained from the topographic maps was created from topographic maps using manual digitizing of the blue lines in GIS. The drainage network extracted from the DEM represents and includes all the exterior links alongside the blue lines in the sub-basins. It was extracted from a DEM, generated from the contours of 10 m intervals and 5m in flat areas, using the hydrology toolset in Arc GIS program (OZDEMIR AND BIRD, 2008). The accurate wadis network is dependent on the scale of DEMs, whereas the large scale of DEMs leads to accurate wadi network.

Because of the surface of El-Qaà plain is relatively flat composed of many alluvial fans the main channels of wadis above it are wide. Therefore, it is very difficult to determine the main channel of wadis by using the topographic network especially in flat areas. The importance of the main channels is high because they are considered the main source of flash floods in the study area. Consequently, it is necessary to identify the position of the main channel on each alluvial fan using DEMs method which is developed by (GARBRECH AND STARKS 1995; MARTZ, GARBRECHT 1998 AND OZDEMIR, 2008) to avoid the consequences of flash floods along these channels.

The precision of the DEM affects the accuracy of the extracted drainage networks. The 10-m resolution DEM used in this application provided good results for hilly areas of the basin (OZDEMIR AND BIRD, 2008). However, inadequate results were obtained for the floodplain area of the basin. After creating the DEM, errors such as sinks and peaks were removed in order to eliminate discontinuities in the drainage network.

Flow direction was calculated for each pixel using the filled DEM, i.e. the direction in which water will flow out of the pixel to one of the eight surrounding pixels. This concept is called the eight-direction pour point model (FAIRFIELD AND LEYMARIE 1991). There are several variants of the model, but the simplest, and the one used in ArcGIS, allows water from a given cell to flow into only one adjacent cell, along the direction of steepest descent (Fig 4-7).

Accoring to OZDEMIR AND BIRD 2008, the flow accumulation was calculated from the flow direction grid. To each pixel was assigned a value equal to the number of pixels drained through a given pixel in the flow accumulation. The drainage network was extracted by considering the pixels greater than a threshold of 75 using the raster calculator. Contour simulation was adopted for the drainage extraction and 75 pixels were established by arial-and-error approach as a minimum accumulation threshold value in headward areas (MARK 1983). MOAWAD 2008 had concluded that the best drainage network can be extracted by considering the pixels greater than a threshold of 10 pixels dependence on SRTM image resolution 90m.

The extracted drainage network in the floodplain area was modified manually due to insufficient DEM resolution (Fig 4-7). In El-Qaà plain area, it can be getting over this problem by using only ERDAS imagine program to convert the image from format *.img to format *.grid.

Actually, the morphometric parameters within drainage networks derived from both topographic maps and DEMs should be considered in order to determine their differences. This means different values for morphometric parameters will result depending on the source used to identify the drainage network and therefore this will affect the outcome of the subbasins influence on the main channel (OZDEMIR AND BIRD, 2008).

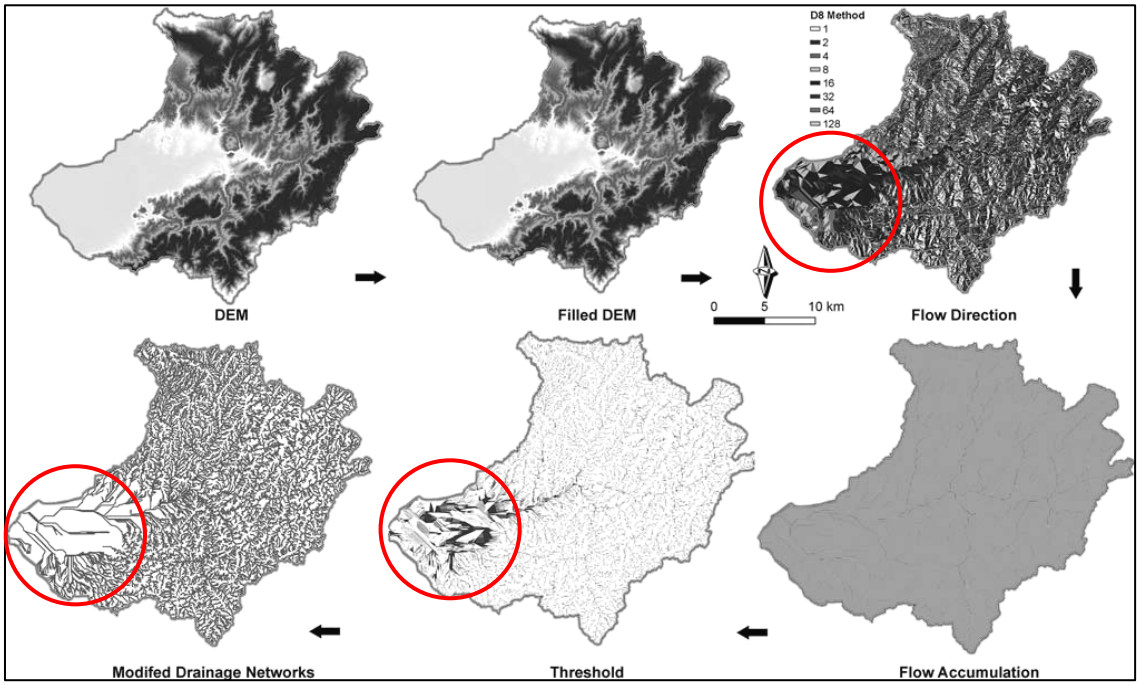

Fig (4-7) *Extracting the drainage network from DEM (must be modifing the network manually) after OZDEMIR & BIRD, 2008*

To understand the influence of the sub-basins to flooding on the main channel, morphometric parameters of drainage networks must be considered along with their hydrological characteristics. Geographic information systems (GIS) provide a broad range of tools for determining the area affected by flash floods and for forecasting areas that are likely to be flooded during runoff. When spatial data are used in an information system, one tends to speak of a spatial information system. The spatial data has a physical dimension and geographic location. There are stored in the digital data base of the GIS, such as a digital elevation model (DEM) which can be used to predict the future flood events.

The GIS data base may also contain agriculture, socio-economic, communication, population and infrastructural data. They can be used, in conjunction with the flooding data to adopt an evacuation strategy, rehabilitation planning and damage assessment in case of a critical flood situation. In one hand, there must be showing morphological features and the local relief of main basins which is important to control the runoff degrees and the distribution of the affected areas. On the other hand, it can be created the map of the affected area using sub-basins depending on their data base as following:

4.3.1. Wadi Firan basin

Wadi Firan Baisn represents the largest drainage basin of the study area that covers about 1918.5 km². The trunk channel of Wadi Firan extends generally from east to west about 148 km in accordance with the main geologic structures and rock contacts and attaining the 7^{th} order (Fig 4-8A). The wadi consists of five main tributaries as following:

4.3.1.1. Wadi El-Sheikh in Catherine mountainous drains the south east area of Wadi Firan; it covers about 348.6 km² and characterizes relatively high slopes which range between 7º to 1º. The trunk channel has 6^{th} order (Fig 4-8A). It includes several mountainous peaks such as Catherine Mountain 2614m, Al-Monagah Mountain 1854m, Mousa Mountain 2285m, Al-Sofsafa Mountain 2145m and Abdu-Allah Mountain 1551m (Fig 4-8B). Flash floods in Wadi El-Sheikh are classified as high floods ($177m^3/s$) in the upper parts of Firan basin. The affected areas of Wadi El-Sheikh are distributed in the main channel which the more the narrow channel the more the hazard of flash flood.It increases in the Gabal Abdu Allah area, Taleat El-Qadreen area, Sahab and El-Tarfa villages which lie in the main channel of Wadi El-Sheikh (Fig 4-8A and photo 4-1).

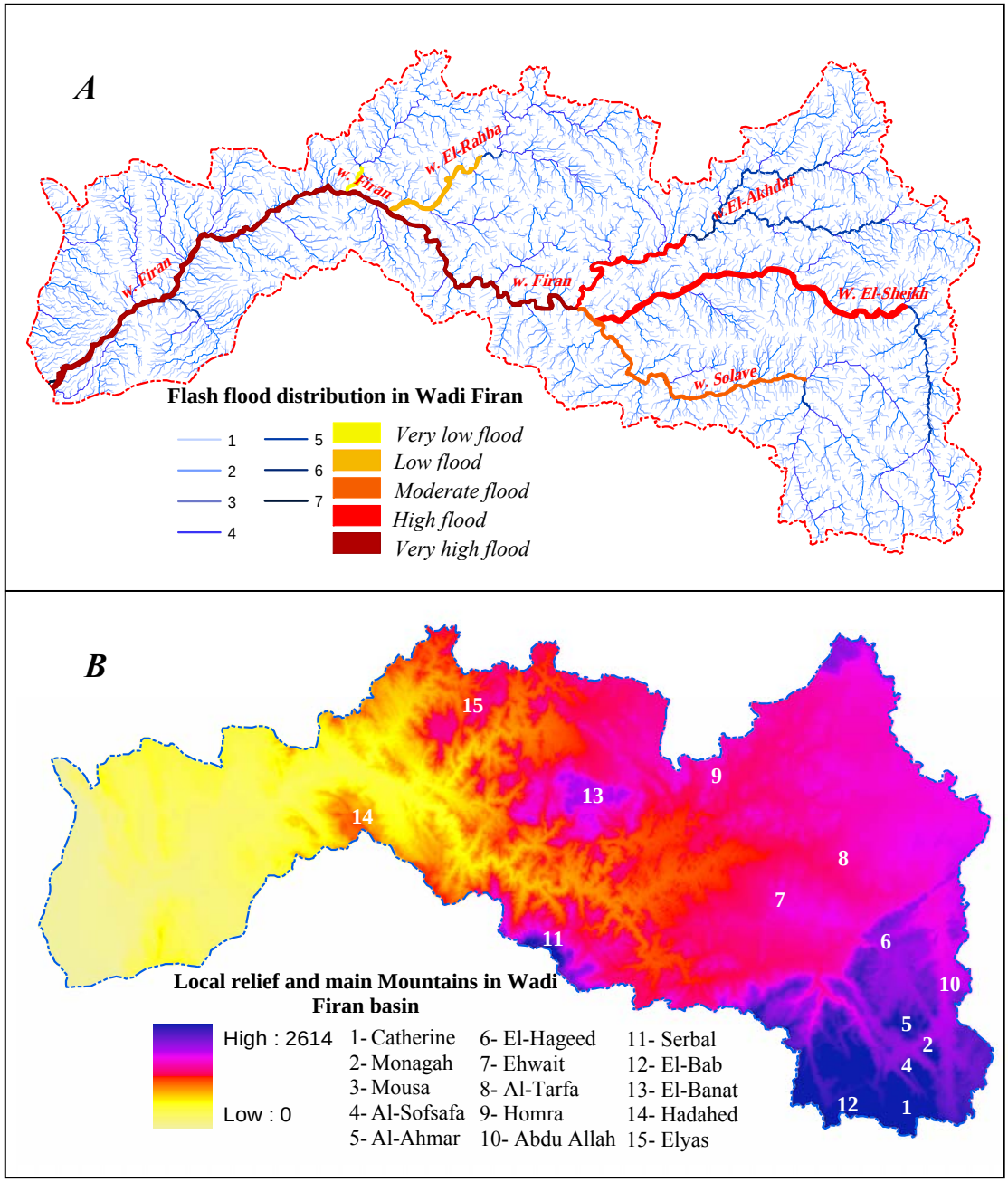

Fig (4-8) *Flash flood distribution of Wadi Firan basin (A), and local relief of the basin (B)*

4.3.1.2.Wadi El-Akhdar drains from the north east of Wadi firan basin; it is covered mostly by igneous rocks and characterized mostly by medium slopes which ranging between 4º to 1º. The basin has an area of about 336.9 km^2 and the trunk channel has 6th order. The basin is surrounded and contained some peaks such as Naqb Sheity, Homra Mountain and El-Samar Mountain (Fig 4-8B). Depending on the local relief, the slope and width of the main channel and the amount of water resulting by the flood, flash floods in the basin may be classified as moderate to high floods (159.7m^3/s) especially in the wide parts of the main channel in the

Wadi and sometimes high floods especially in the narrow channel of last 10 km near outlet of the Wadi (Fig 4-8A). The main affected ares in El-Akhdar basin are distributed around the main channel of Wadi El-Akhdar photo (4-2), Wadi Hemait and Rowis El-Anerg area (Fig 4-8B).

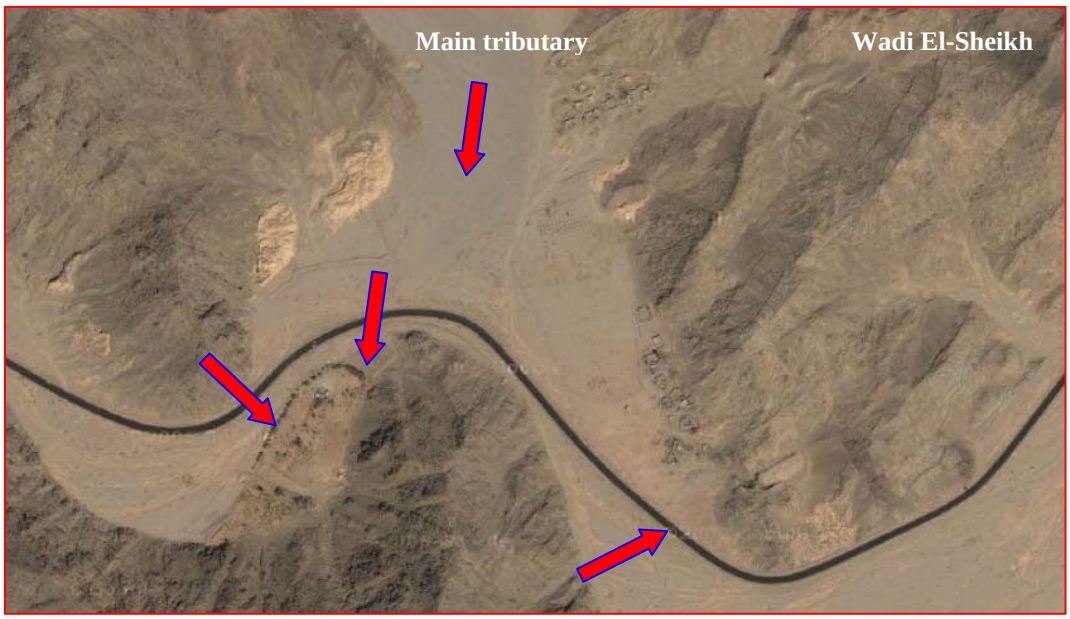

Photo (4-1) *An affected area of the main channel in Wadi El-Sheikh*

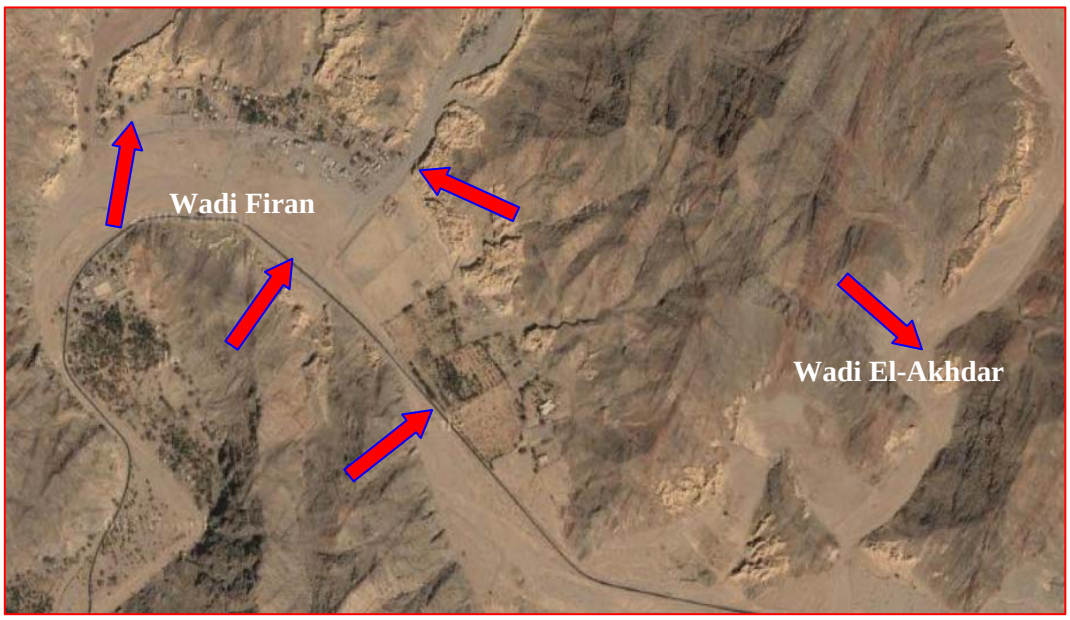

Photo (4-2) *The affected areas of the main channel in Wadi El-Akhdar (outlet) and Wadi Firan*

4.3.1.3.*Wadi Solav basin* (316.1 km) represents one of the largest tributaries of the hydrological system of Wadi Firan. The streams of the trunk channels attain 6th order in Wadi Solave which drains from the higher area in Wadi Firan (2614m) and is covered by igneous rocks.

The slope of Wadi Solav ranges between 6º in the upper tributaries near Catherine area and Al-Sofsafa Mountain to 1.5º in the part near the major channel of Wadi Firan. The basin is surrounded by some peaks such as Catherine Mountain 2614m, El-Bab Mountain 2234m, Ehwait Mountain 1860m and El-Hageed Mountain 1720m (Fig 4-8B). The affected areas in Wadi Solav are concentrated along the main channel of the Wadi and its main tributaries such as Wadi Demshy, Wadi El-Safha, and Wadi Dhisa (Fig 3-8A and photo 4-3). The flood hazard in Wadi Solave is classified as moderate flood (157.1m^3/s) depending on runoff duration, frequency and rainfall amounts.

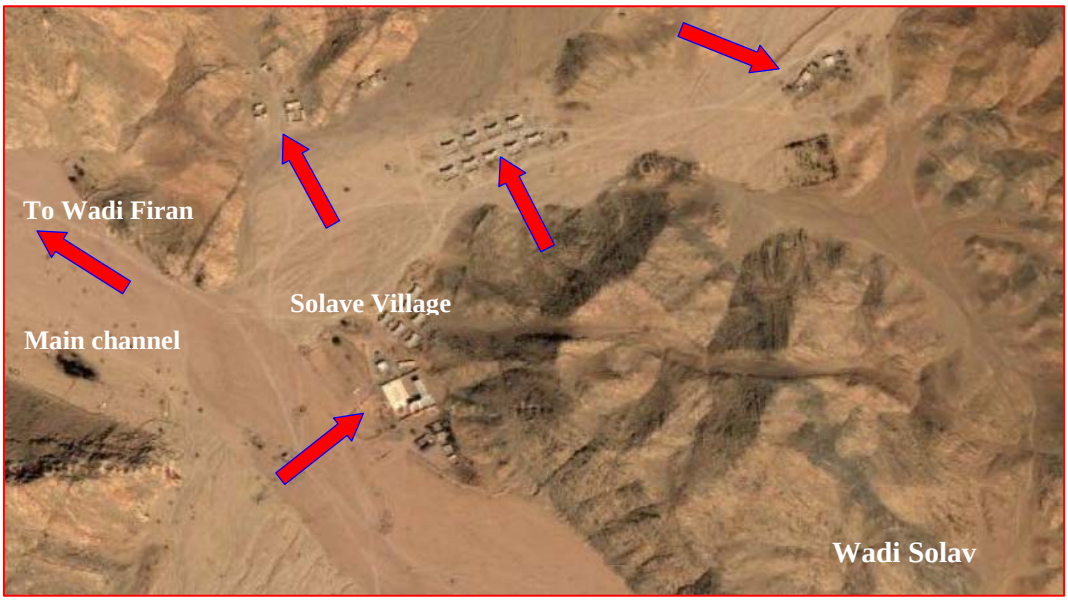

Photo (4-3) *An affected area of the main channel in Wadi Solav* (Solave village)

4.3.1.4. Wadi El-Rahba basin (206.8 km) has 5th order of trunk channel. It drains from the north of Wadi Firan and is covered mostly of igneous and metamorphic rocks. The slope of the main channel ranges between 3º in the upper part and 1º in the outlet area near the main channel of Wadi Firan. The basin area contains some peaks such as El-Banat Mountain 1510m, Elyas mountain1115m and Dub El-Bohaira 1260m (Fig 4-8B). Flash flood hazard in the basin concentrates at 15 km of the main channel toward Wadi Firan and can be classified as low flood (73m^3/s). The affected areas are Um El-Maqsour village and Elyas village (photo 4-4) and some cultivated areas around the main channel (Fig 4-8A).

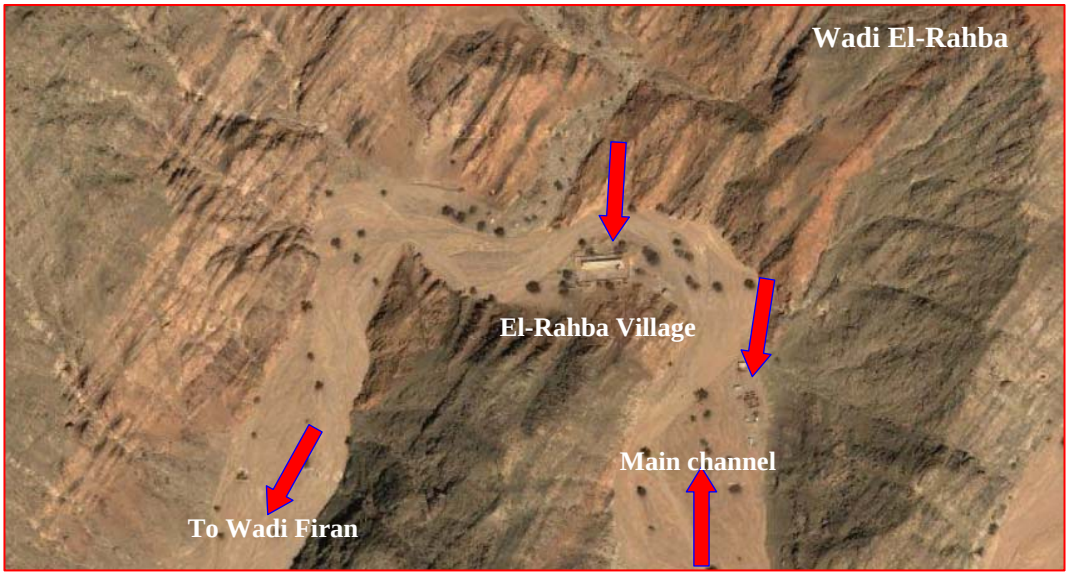

Photo (4-4) *An affected area of the main channel in Wadi El-Rahba* (Elyas village)

4.3.1.4. ***Wadi Firan (main Wadi)*** has 7th order of trunk channel; the flash floods in the main Wadi have been classified as the highest floods in the study area (Fig 4-8A). The tributaries of the main channel of Wadi Firan drain from the high mountainous area, therefore, during runoff they have large amounts of water which sometimes arrive to the main stream of the Wadi. At that time the flash flood becomes very strong and may destroy most of infrastructure in the main channel such as the highway to St. Catherine and some Bedouin villages.

The basin area has some peaks such as Serbal Mountain 2070m, El-Ahmar Mountain 1325m, Sarbeel Mountain 1770m and Hadahed Mountain 425m (Fig 4-8B). The slope of Wadi Firan ranges among steep slopes containing the upper tributaries higher than 1600m (Wadi El-Sheikh and most of Wadi Solav), and moderate slopes in the tributaries between 1600m to 1000m containing Wadi El-Akhdar and Wadi El-Rahba. Low slopes are typic for tributaries which lie in the area below 1000m as well the main stream.

Fig (4-9) point the longitudinal profile of Wadi Firan, showing the correlation between degree flash flood intensity. Consequently, it can be concluded that the upper tributaries of Wadi Firan have more dangerous, floods after heavy rainfall, as well as the main stream. Its water accumulation results from runoff of the higher tributaries.

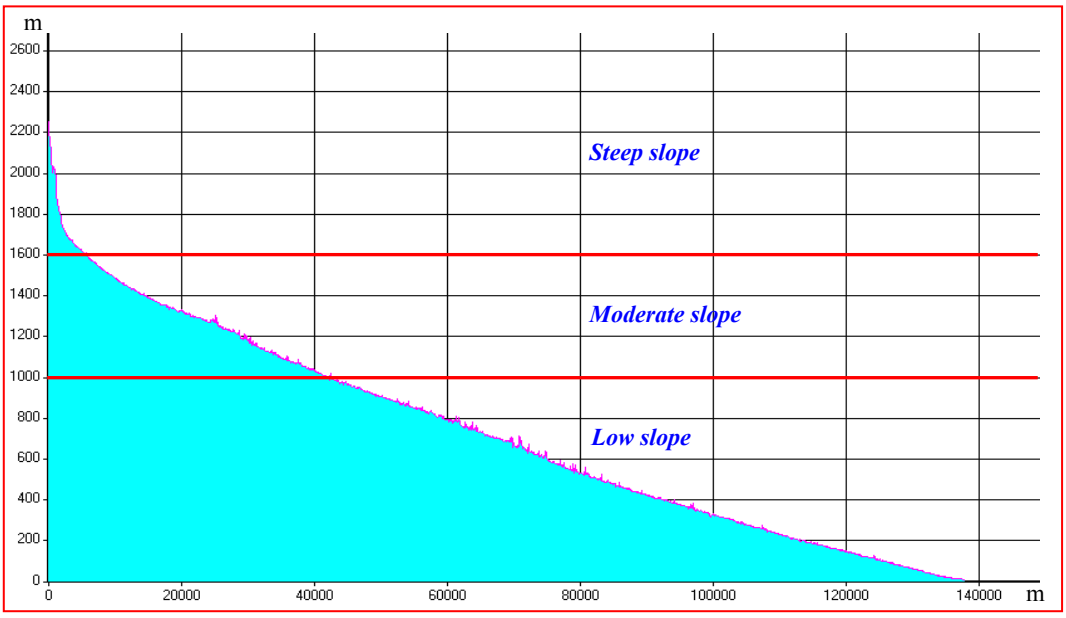

Fig (4-9) *The longitudinal profile of Wadi Firan basin dependening on DEM Image*

The affected areas in the main basin of Wadi Firan are distributed along the main channel especially Firan village and the oil region which lies close to Firan delta. The oil region in Wadi Firan usually is severely attacked by floods as well as the infrastructure such as roads, pipes and tanks. Therefore, the government has begun to build a high wall to shift the main stream from southern to northern part of the delta (photo 4-5). The effects of this wall will be discussed in the next chapter as hazard mitigation.

Photo (4-5) *Flashfloods hazard and its effects on the oil region above Wadi Firan Delta*

4.3.2. Wadi El-Aawag basin

Wadi El-Aawag Baisn is considered the largest basin in the study area occupying about 1982 km². The trunk channel of Wadi El-Aawag extends generally from north and north east to south west about 61.5 km in accordance with the main geologic structures and rock contacts and attains the 7th order (Fig 4-10A). The wadi consists of nine main tributaries from north to south as following:

4.3.2.1. Wadi Abyad basin is a small tributary of Wadi El-Aawag (52.2km^2) covered by sedimentary rocks which are characterized by high infiltration. It drains from Abu Taryfia Mountain (760m) in the north east of the main basin (Fig. 4-10B); the trunk channel of Wadi Abyad has 5th order. The floods in Wadi Abyad are classified as very low floods (8m^3/s) owing to the small area which has a small amount of water during rainfall. The affected area by floods in Wadi Abyad is very limited along the main channel (Fig 4-10A).

4.3.2.2. Wadi Tughda basin is considered also as one of the small tributaries of Wadi Aawag (53.4km^2). It drains from the El-Ttor Mountain (1083m) and has 5th order. Because of the small area of the basin, it has very low floods (7m^3/s) during runoff whereas the affected area is also limited along the main channel (Fig 4-10A).

4.3.2.3. Wadi Apoura basin occupies about 46.1 km^2 and the trunk stream has 6th order. The wadi drains the southen part of Apoura Mountain (1286m) and El-Ttor Mountain (1083m) which are mostly covered by sedimentary rocks. Consequently, the flash floods resulting from Wadi Apoura are known as very low floods (7m^3/s). The alluvial fan of Wadi Apoura is built up by of thick alluvial deposits where infiltrates most of water during runoff. So, the flood is often unable reach the main channel of Wadi El-Aawag and the influenced area is strictly limited to the main channel of Wadi Apoura (Fig 4-10A).

4.3.2.4. Wadi Gebah basin has 6th order and occupies about 53.8 km^2 and drains from Al-Gous Mountain (1129m) in the north east of Wadi El-Aawag. According to basin area, the alluvial fan area of the wadi and the flood water during runoff it can be concluded that the flash flood in Wadi Gebah basin is very low (6m^3/s). Depending on the new stream network which was extracted from SRTM image it is possible to determe the main stream of Wadi Gebah above El-Qaà plain which is considered as the affected area by flash flood (Fig 4-10A).

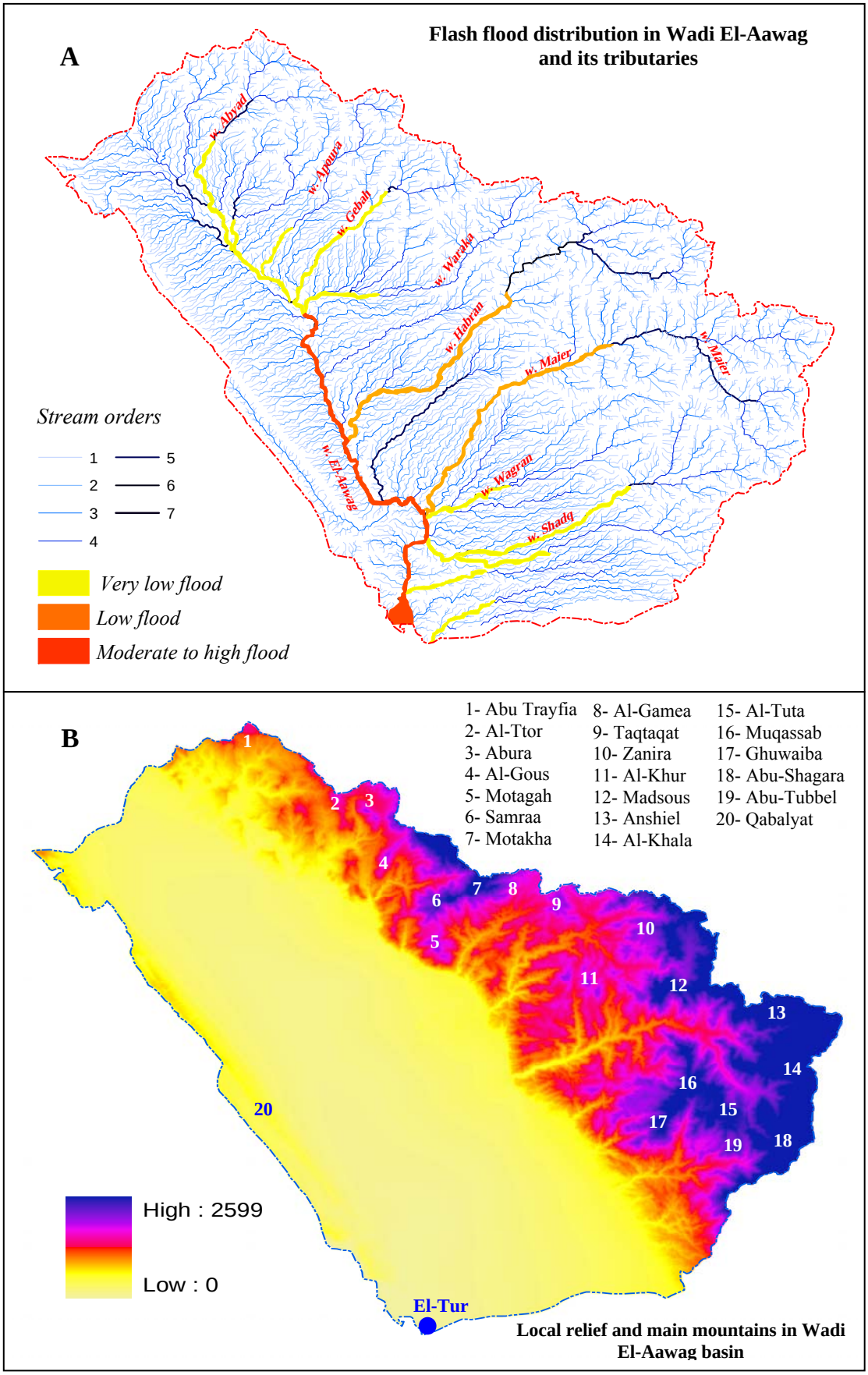

Fig (4-10) *Flash flood distribution of Wadi El-Aaag basin (A), and local relief of it (B)*

4.3.2.5. Wadi Waraqa basin is one of the tributaries of Wadi El-Aawag occupying about 53km^2. The trunk channel has 6th order and the main stream attains about 16.5km (Fig 4-10A). Wadi Waraqa drains some peaks such as Motagah Mountain 1303m, Samraa Mountain 1670m, Motakha Mountain 1624m and Al-Gamea Mountain 1624m (Fig 4-10B). According to the maximum runoff, the flash flood of Wadi Waraqa is very low, and the affected area is concentrated around the main channel on El-Qaà plain (Fig 4-10A).

4.3.2.6. Wadi Habran basin is one of the main tributaries of Wadi El-Aawag basin and has 6th order of trunk channel which attains about 16.5km. Wadi Habran basin occupies about 182.3km^2 and is mostly coverd by igneous rocks especially old granite. The basin is surrounded by some mountains such as El-Khur Mountain 1256m, Taqtaqat Mountain 1550m and Zanira Mountain 1917m. The local relief distance of the basin is about 1750m (Fig 4-10B); therefore the main stream slope is relatively high ranging between 5º in mountain area and 1.5º in the fan area. The flood of Wadi Habran is classified as low to moderate flood (35m^3/s). The affected areas are distributed in Habran Village, Sail* Habran village (photo 4-6) and along the main stream of Wadi Habran in the El-Qaà plain (Fig 4-10A).

Photo (4-6) *The affected area of Wadi Habran* (Habran village and the main channel)

* ***Sail*** *means in Arabic, the area which is usually affected by flash flood such as Sail Habran and Sail Meiar. These are usually covered by granss vegetation and therefore, important for the herds of Bedouins .*

4.3.2.7. Wadi Meiar basin has 6th order trunk stream and occupies about 251 km^2; it has a huge alluvial fan (39.5 km^2). It is considered one of the most active tributaries of Wadi El-Aawag which drains relatively high peaks such as Madsous Mountain 2023m, Anshiel Mountain 2186, El-Khala Mountain 2555m, Al-Tuta Mountain 1805, and Ghuwaiba Mountain 1245m (Fig 4-10B). According to DEM image and field work, Wadi Meiar is a dangerous basin during flash flood although it has low to moderate classification of flash flood (32m^3/s). Consequently, it can be said that the local relief, the lithological outcrop and slope of the main channel have been played the major role to change the low and moderate flood of Wadi Meiar to high flood. The affected areas of the basin are distributed also in the outlet of the main channel, Meiar village, and around the main channel above El-Qaà plain (Fig 4-10A).

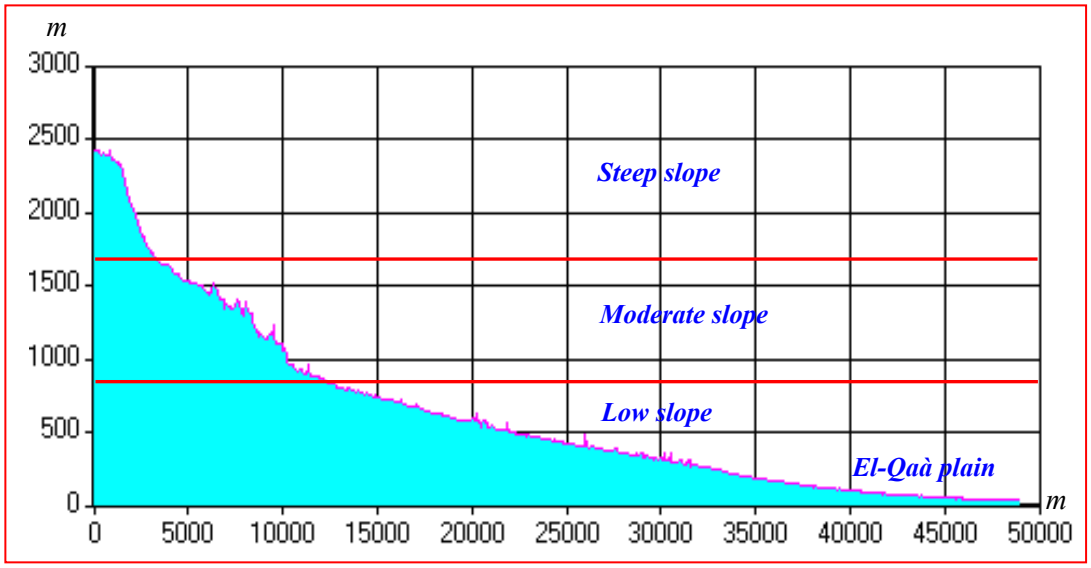

Fig (4-11) *Longitudinal profile of main channel of Wadi Meiar dependening on DEM Image*

Fig (4-11) points out the longitudinal profile of the main channel of Wadi Meiar. The profile can be divided into three parts, the upper part lies higher than 1650m characterized by steep slopes (more than 30º), while the middle part lies between 850m to 1650m with slopes ranging between 15º to 30º (moderate slope). The lower part lies between the outlet and the alluvial fan area with slopes ranging between 3º to 10º (low slope). Slope degree and violence of flash flood are corresponding. Consequently, it can be concluded that the upper tributaries of Wadi Meiar become dangerous, if they get heavy rainfall, but the main stream down valley is also dangerous especially in the outlet area.Here, the maximum of water can be expected.

4.3.2.8. Wadi Shadq basin is one of the southern tributaries of Wadi El-Aawag basin and occupies about 81 km^2. The trunk channel of Wadi Shadq has 5^{th} order and attains about 23km (Fig 4-10A). Wadi Waraqa drains Abu-Shagara Mountain 2343m and Abu-Tubbal Mountain 1821m (Fig 4-10B), whereas the slope of main channel ranges between 5º in mountainous area and 1.5º in the plain area. The flood of the wadi is classified as very low flood ($7m^3/s$), and the affected areas are concentrated around the main channel especially in the outlet area and the area near El-Tur city.

4.3.2.9. Wadi El-Aawag **(main wadi)** has 7^{th} order of trunk channel; the flash flood in the main Wadi has been classified moderate to high flood $160m^3/s$ (Fig 4-10A). The eastern tributaries of the main channel of Wadi El-Aawag such as Wadi Habran and Wadi Meiar drain from the high mountain area. During runoff the tributaries of Wadi El-Aawag have relatively large amounts of water which sometimes arrives at the main stream. Thereupon, the flood may become high and destroying infrastructure in the main channel such as the highway to Sharm El-Sheikh and El-Wadi village which lies around the main channel. It several times destroyed by floods (photo 4-7).

The main channel of Wadi El-Aawag runs from north to south along the highway Suez- Sharm El-Sheikh which is considered one of the important roads in South Sinai sometimes destroyed by flash flood of Wadi El-Aawag. The main channel slope of Wadi El-Aawag is low and ranges between 4º in the north to 1º in the south near the mouth of Wadi.

Photo (4-7) *El-Wadi village lies in and around the main channel of Wadi El-Aawag*

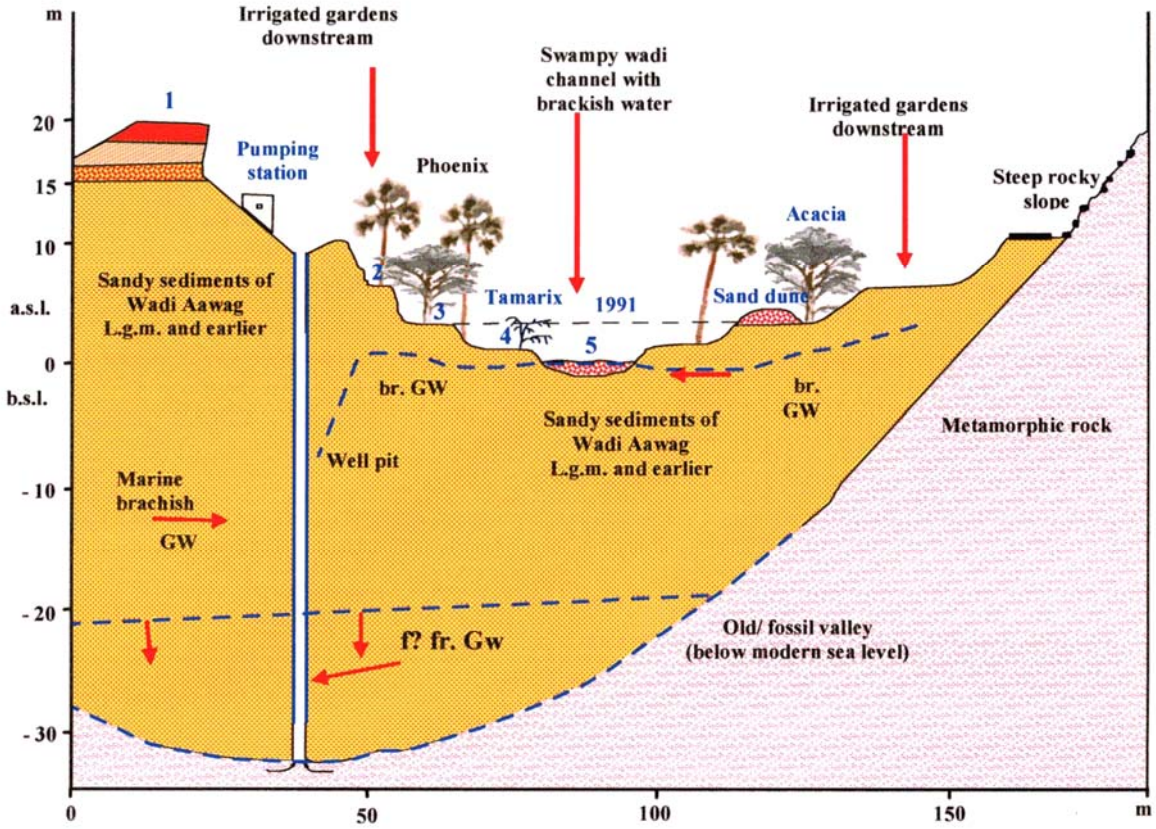

Fig (4-12) *Cross section of Wadi El-Aawag near El-Tur 6km east of the Gulf of Suez*

Wadi El-Aawag basin is considered one of the important basins in southern Sinai because the flood of the wadi affects directly on the strategic highway Suez- Sharm El-Sheikh and El-Tur city. Therefore, it should be known the geomorphological characteristics of the main stream in the cross section Fig (4-12) showing the following details:

1. Sandy high terrace (19m) of Wadi El-Aawag with calcareous crust on top corresponding with the 24 m high fossil Gulf terrace (middle to young Pleistocene).
2. Sandy lower terrace (5.5m) as typic for Wadi El-Aawag (early Holocene) corresponding with the 6m high fossile gulf terrace (young Pleistocene).
3. Recent sandy- silty terrace corresponding with the 3m- high flood in March 1991.

4+5, Modern sandy- silty- clayey wadi channel locally covered by a thin salt crust (gypsum in higher positions).

GW, groundwater

f? fr, Gw, Presumably fossil and abundant fresh groundwater of Wadi El-Aawag explored since 30 years from a 40m deep well pit of a pumping station. Today it is probably overused for field irrigation and fresh water providing for El-Tur and partly Sharm El-Sheikh.

Mar, br. GW, Marine brackish groundwater actually advancing from Gulf of Suez (distance 6km)

Br. GW, Modern slightly brackish superficial groundwater of Wadi El-Aawag

a. s. l, above sea level (related to the Gulf of Suez)

b. s. l, below sea level

4.3.3. Wadi Asla basin

Wadi Asla basin is considered one of the main basins in the study area; it has 5th order of trunk channel and occupies about 601.1km^2. The main stream runs in northeast to southwest direction toward Suez Gulf and attains about 29.8 km in length. Wadi Asla drains some peaks such as Um Shumer Mountain 2580m, Amlaha Mountain 1801m, Romhan Mountain 2392m, Sheikh El-Arab Mountain 1681m, El-Shabat Mountain 2438m, and Moreikh Mountain 829m (Fig 4-15B).

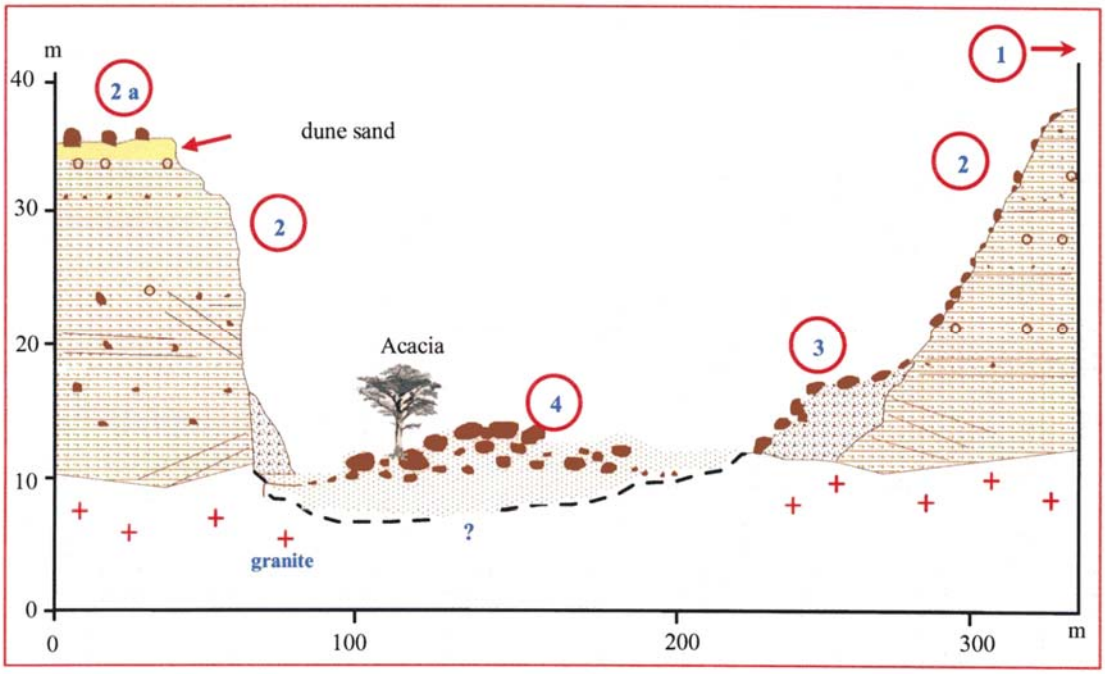

Fig (4-13) *cross section of the main channel of Wadi Asla in the outlet area*

According to field work, it can be focus the change in the main channel of Wadi Asla using cross section in the outlet area which shows the effect of flood on wadi terraces and wadi bottom Fig (4-13) and Fig (4- 14) as following:

1. High terrace (see overview- Fig 4-14)

2. Low terrace, grey- brown, homogeneous sediment of sand, granite grus and gravel, $CaCO_3$ cemented terrace.

2a is Erosional surface fossilized by dune sand.

3. Subrecent cobble and boulder terrace

4. Modern wadi bed with a big boulders alluvial fan, formed in March 1991 by a catastrophic flash flood, 4- 5 m high, today the wadi bed is dry (March 2007)

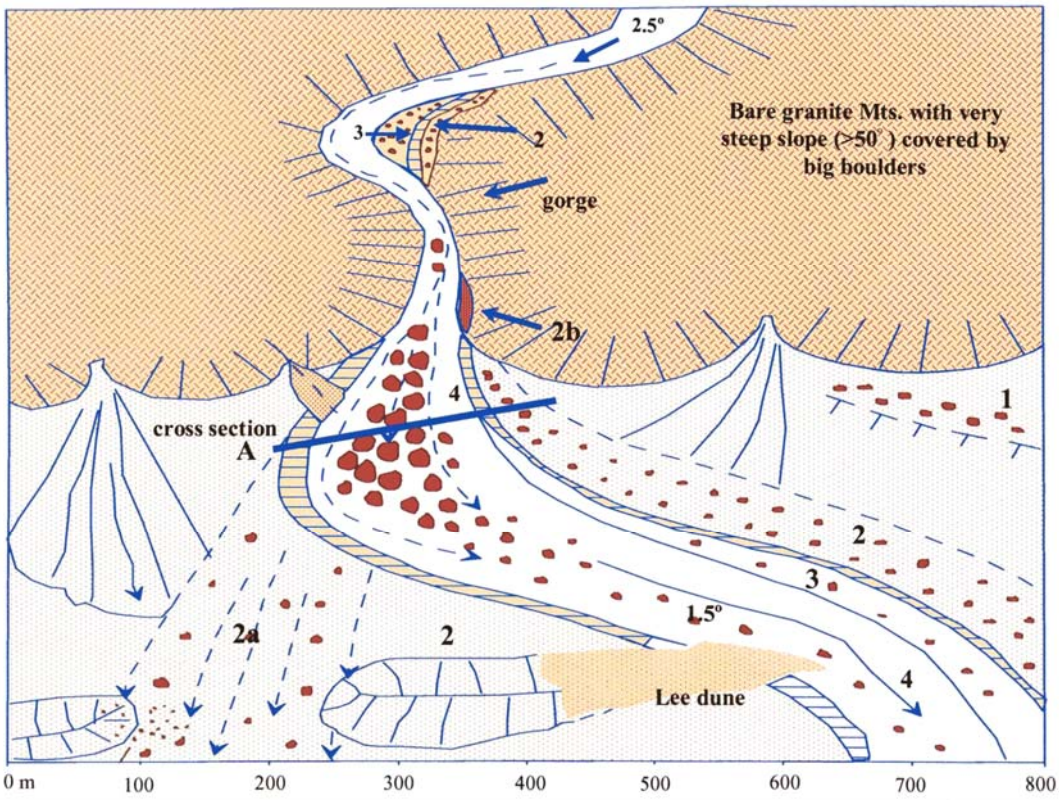

Fig (4-14) *Wadi Asla (SW- Sinai): Overview showing the outlet area with flash flood influence*

1. Well- rounded cobbles, high terrace (ca. 40 m)
2. Well- rounded cobbles and gravel on top; fluvial, well- bedded sediment of granite grus and gravel below, low terrace (24 m)

2a. Fossil alluvial fan representing an erosional surface of low terrace

2b. Travertine- like sediment on a steep granite slope (6 m)

3. Subrecent cobble and boulder terrace (5m)

4. Modern wadi bed, formed by a flash flood 4-5 m high in 1991

The flash flood of Wadi Asla area is classified as low to moderate flood ($30m^3/s$) compared with other large basins (Fig 4-15A), while the flood in Wadi Amlaha is classified very low flood ($6m^3/s$). The main channel of Wadi Asla in the mountainous and outlet area is narrow (about 50m) with the consequence that the moderate flood may be converted to high flood which strong effects on wadi bottom and low terrace which is attaced by lateral erosion in the outlet area (Fig 4-14).

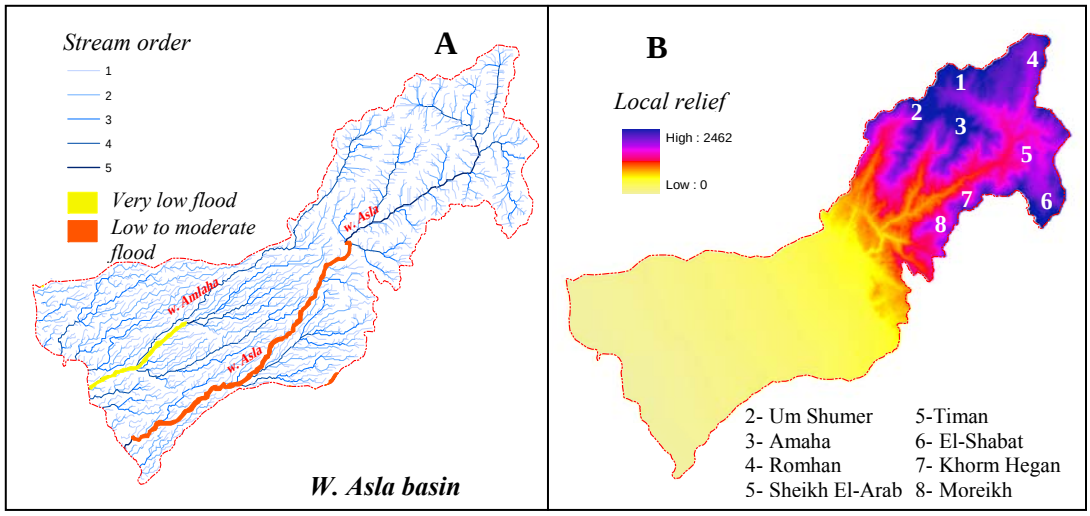

Fig (4-15) *flash flood distribution of Wadi Asla basin (A), and local relief of it (B)*

The flood influenced areas of Wadi Asla and Wadi Amlaha basins are are limited at and around the bottoms of wadis, Amlaha village (Fig 4-15A), and the highway Suez- Sharm El-Sheikh.

4.3.4. Wadi Timan basin

Wadi Timan basin is one of the main basins in the study area and occupies about 399 km^2. The trunk channel of Wadi Timan has 5th order and the tributaries drain from northeast to southwest. The basin contains some peaks such as Khurm Hegan Mountain 1734m, Moreikh Mountain 829m, Um Sayed Mountain 660m, and El-Rethoum Mountain 696m (Fig 4-18B). Wadi Moreikh is considered the north east tributary of Wadi Timan which drains Moreikh Mountain. Wadi Moreikh is a gorge deeply incised into the Precambrian granite. Nowadays floods partly reach the Gulf of Suez. In former days they didn't as indicated by large alluvial fans which now are cut by the modern flood events.

Although Wadi Moreikh is a small basin (about 22.9 km^2), and the trunk channel has 4th order compared with other basins in the study area, it contains important sediment deposits which have been described before by RÖGNER ET AL (2004) in the Wadi Firan. These deposits in Wadi Moreikh have been studied and OSL dated to determine the sedimentation conditions in the past and to get a chrono- strtigraphy (chapter 1). Therefore, it should be studied morphological setting of Wadi Moreikh is presented in detail by cross section (Fig 4-16) and longitudinal profile (Fig 4-17).

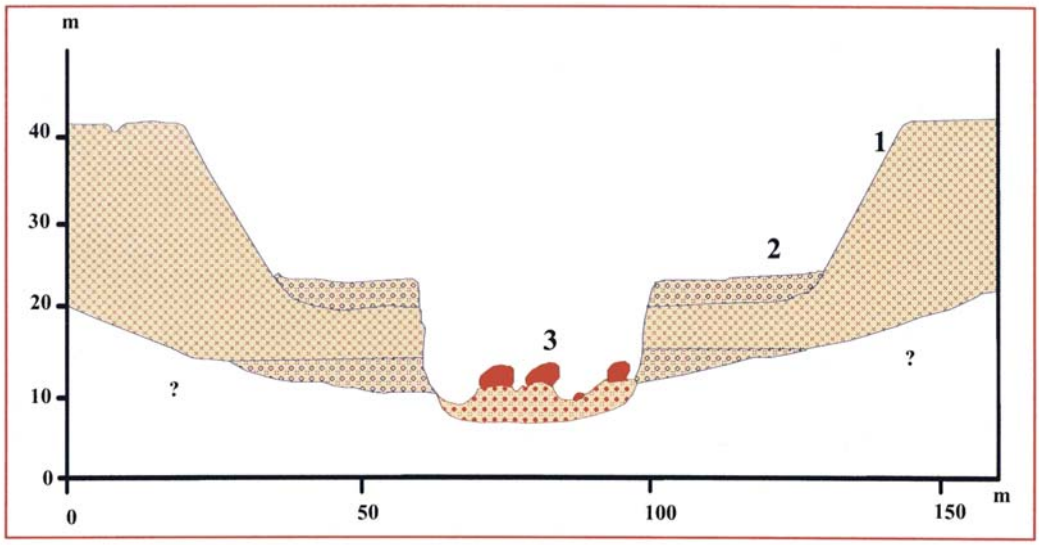

Fig (4-16) Wadi Moreikh (SW Sinai): Cross profile (A2) near the outlet

The cross profile of the main channel of Wadi Moreikh has been taken during the field work 2007. Fig (4-16) and (4-17) show:

1- Fluvial, well- bedded sediment of granite grus and removed dune sand, high terrace (Pre- L.g.m.) forming a thick alluvial cone at the wadi outlet.

2- Fluvial, well- bedded sediment of granite grus, angular gravel and dune sand in the central part, low terrace (Early Holocene).

3- Modern dry wadi bed with sand, gravel and big granite boulders.

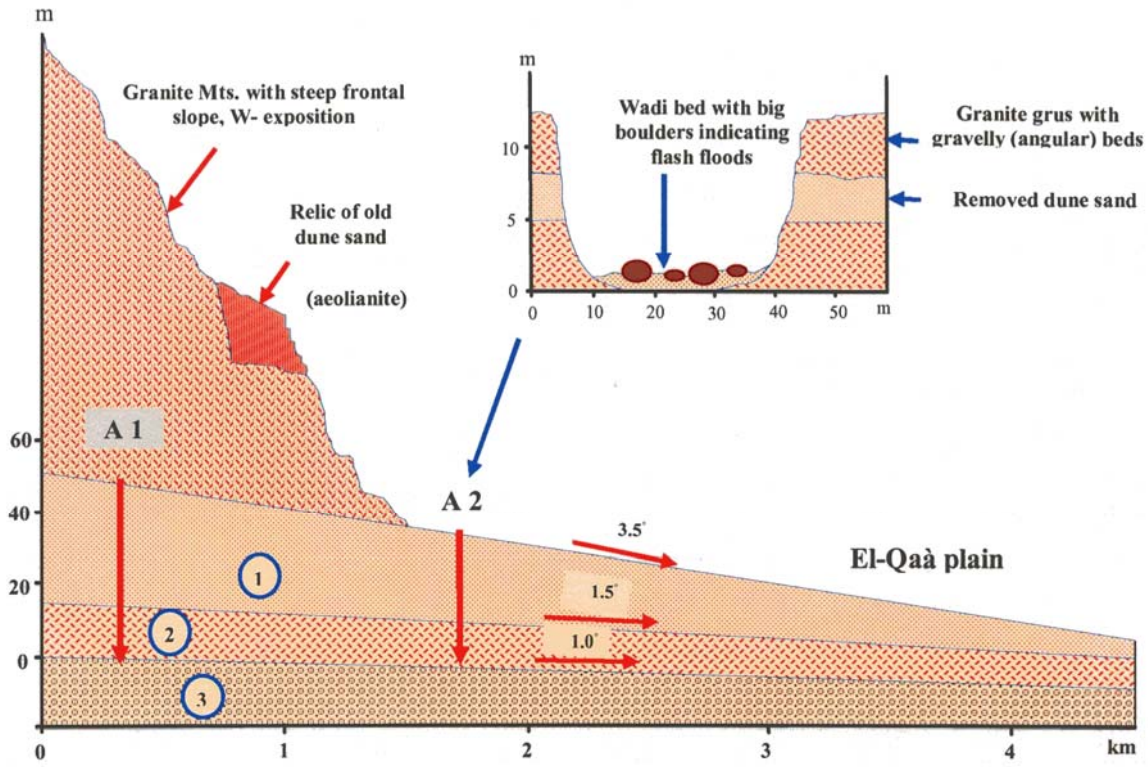

Fig (4-17) Wadi Moreikh (SW- Sinai): Longitudinal profile

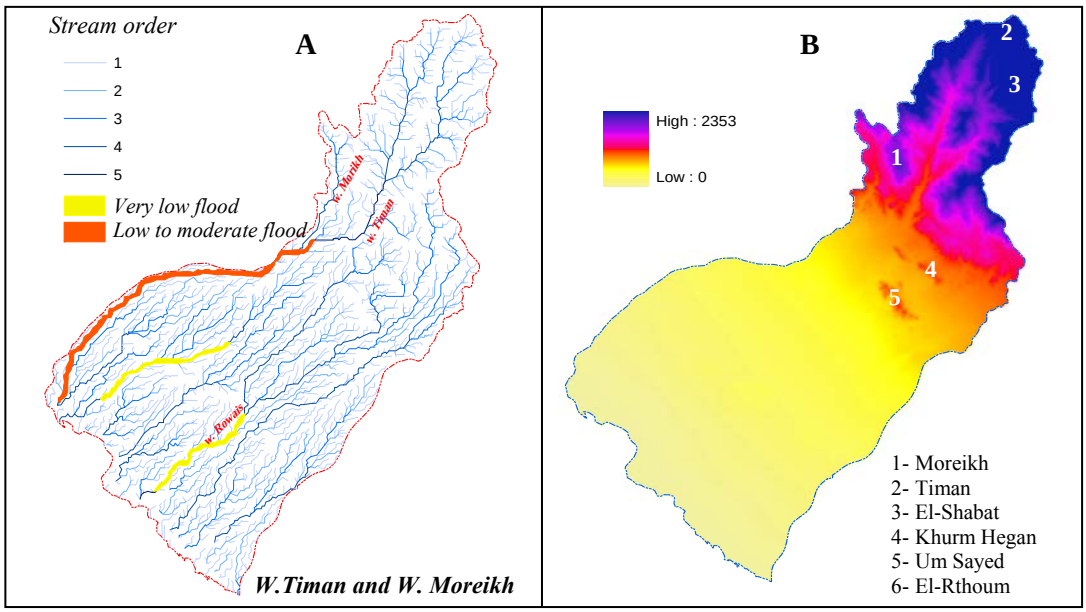

Fig (4-18) *Flash flood distribution of Wadi Timan basin (A), and local relief of the basin (B)*

According to (Fig 4-18A), the flash floods of Wadi Timan basin are classified as low to moderate flood (18 m^3/s) and the affected areas are following the main channel; especially its narrow segments are threated. The flood hazard increases where the highway crosses the main channel of Wadi Timan (photo 4-8) and around Timan Bedouin village. The flash flood in Wadi Rowis is very low and the values range between 3 to 5m^3/s.

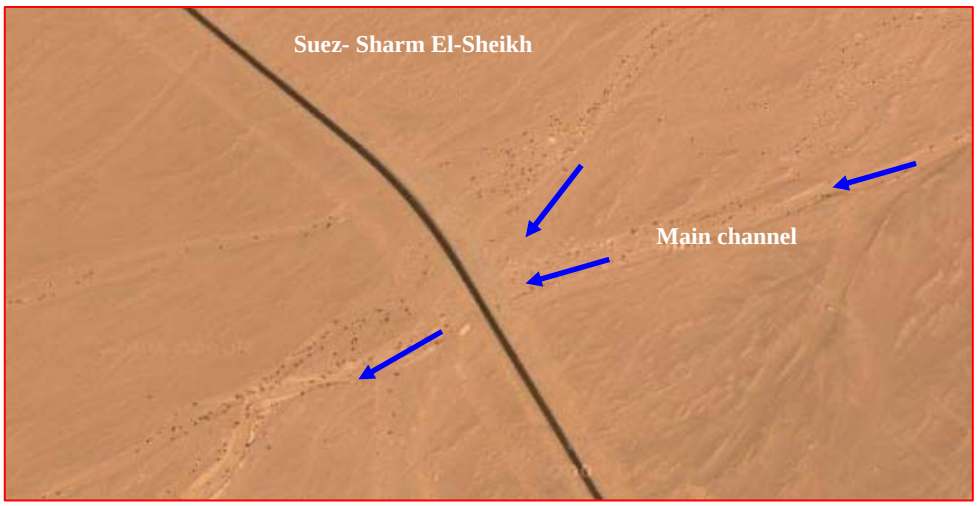

Photo (4-8) *The effects of flash flood of Wadi Timan the highway Suez- Sharm El-Sheikh*

4.3.5. Wadi El-Mahash basin occupies about 329.7 km^2; it is characterized by a relatively high slope ranging between 7º in the mountainous area and 2º on alluvial fan. The trunk channel has 6th order (Fig 4-19A). The basin includes some mountainous peaks such as El-Shabat Mountain 2438m, Sabbah Mountain 2274m, Abu Hamat Mountain 1692m, El-Raboud Mountain 894m, El-Mahash Mountain 524m, and Hansour El-Raboud

Mountain 752m (Fig 4-19B). Flash floods in Wadi El-Mahash are classified as low food in alluvial fan area to moderate flood in the mountain area (25m^3/s).

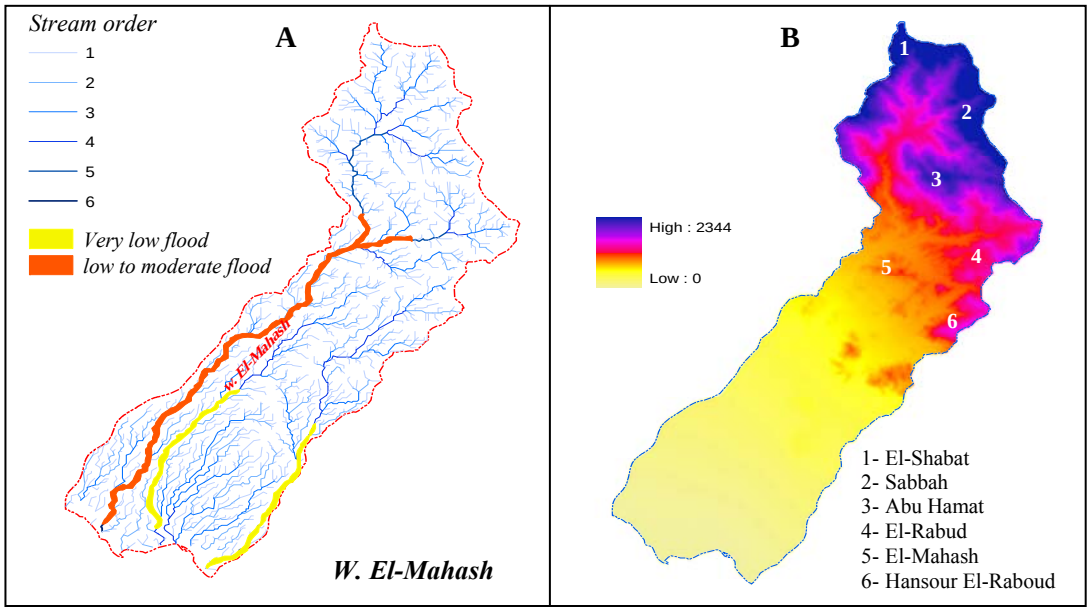

Fig (4-19) *Flash flood distribution of Wadi Timan basin (A), and local relief of the basin (B)*

The affected areas by flash flood of Wadi El-Mahash are distributed along the main channel and in the outlet area (photo 4-9). Although the flash floods in Wadi El-Mahash are classified as low to moderate flood the outlet area indicates high fluvial moreover, groundwater should be available because of several big and green acacia trees growing in the active channels.

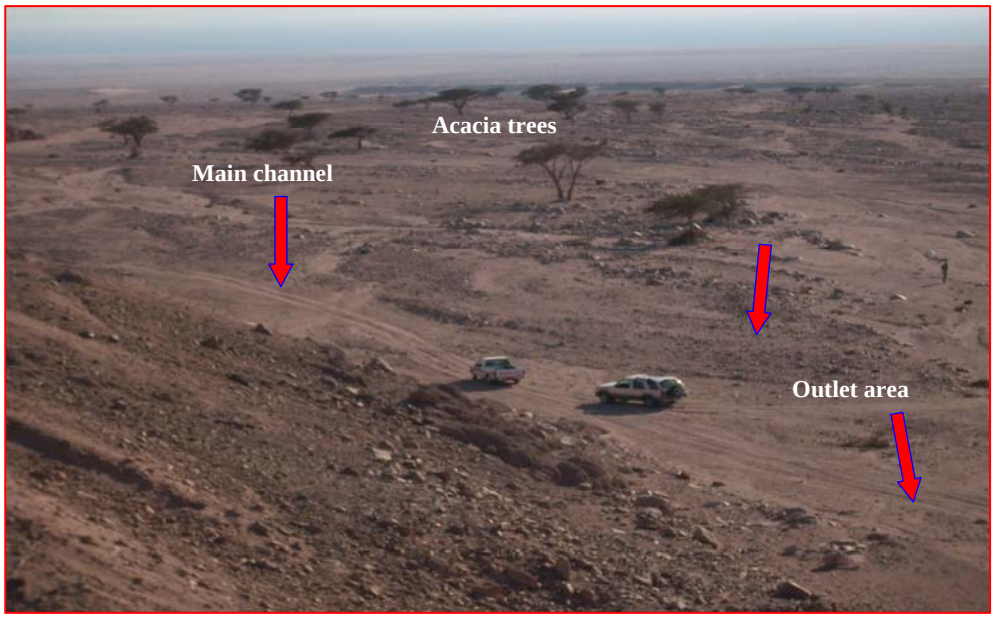

Photo (4-9) *The morphological effects of flash flood on the outlet area of Wadi El-Mahash basin*

4.3.6. Wadi Eghshy basin

Wadi Eghshy basin is one of the main basins in the study area, it occupies about 163.7 km^2 and the tributaries drain El-Nadouh Mountain 1324m, El-Homayrat Mountain 325m, and Al-Masraeya Mountain 477m. The trunk channel has 5^{th} order and attains about 20.2km. The slope of Wadi Eghshy is relatively high about 7º in the northeast of the basin near El-Nadouh Mountain, but is moderate to low in the outlet area.

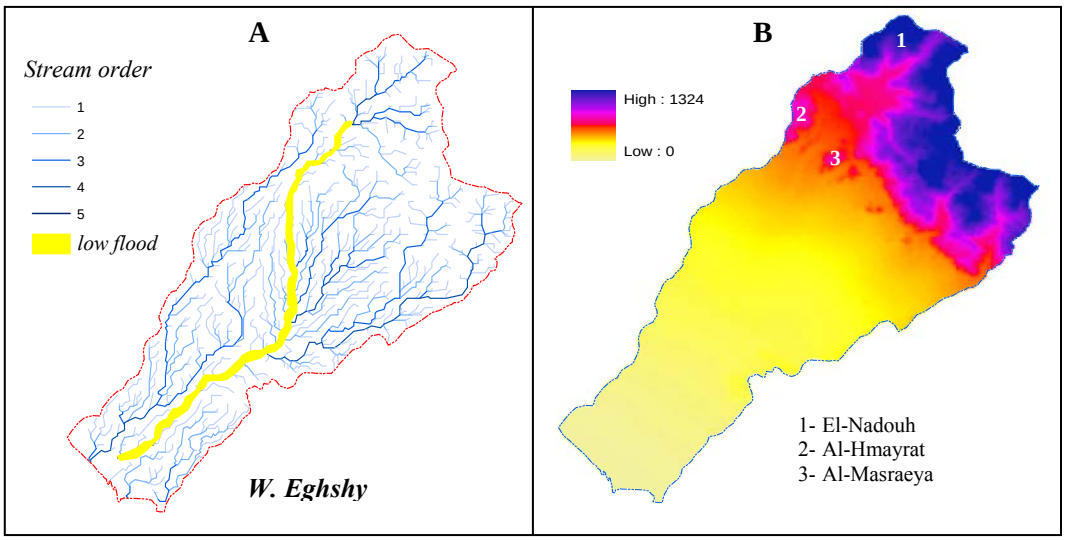

Fig (4-20) *Flash flood distribution of Wadi Eghshy basin (A), and local relief of the basin (B)*

The flash flood of Wadi Eghshy is classified low flood (25m^3/s) and distributed along the main stream (Fig 4-20A). It may be converted to moderate flood in the narrow parts of the channel photo (4-10).

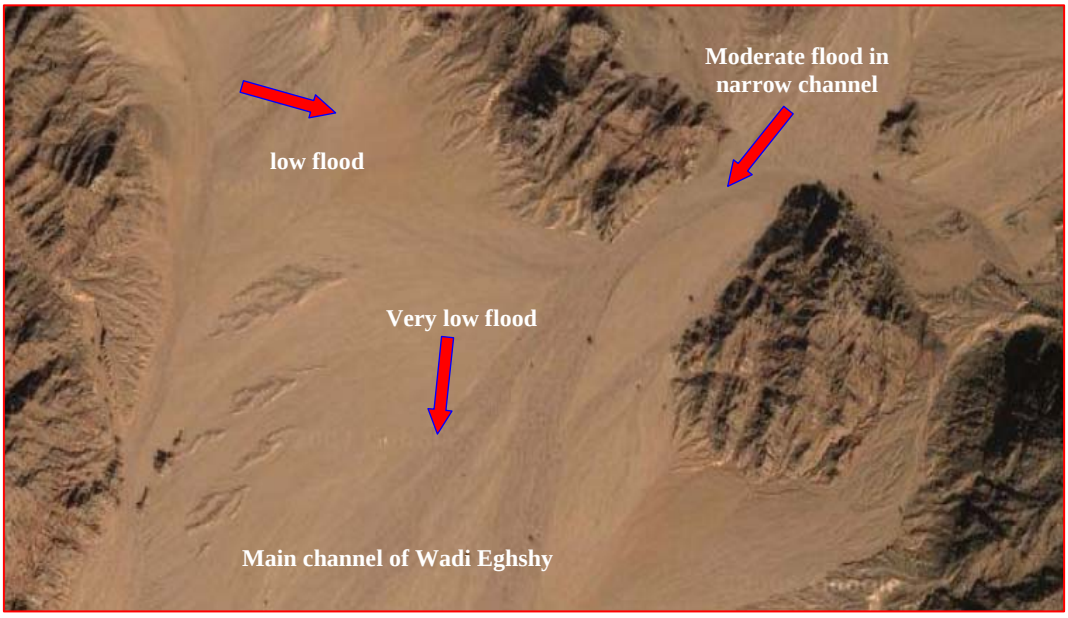

Photo (4-10) *Variation of flash floods in the main channel of Wadi Eghshy*

4.3.7. Wadi Abu Markh basin

Wadi Abu Markh basin occupies about 88km^2 and characterized by a relatively high slope ranging between 5º in the mountainous area and 1.5º in the plain. The trunk channel has 5th order (Fig 4-21A). The tributaries of Wadis Abu Markh and Um Markh drain Sahraa Mountain (1502m) in the northeast and El-Masraeya Mountain (477m) in the north of the basin (Fig 4-21B). Flash floods of both Wadis are classified as low flood in alluvial fan area to moderate flood in the mountain area (20m^3/s), but this low floods are concentrated along the main streams of Wadi Abu Markh and Wadi Um Markh. They affect directly on the highway Suez- Sharm El-Sheikh.

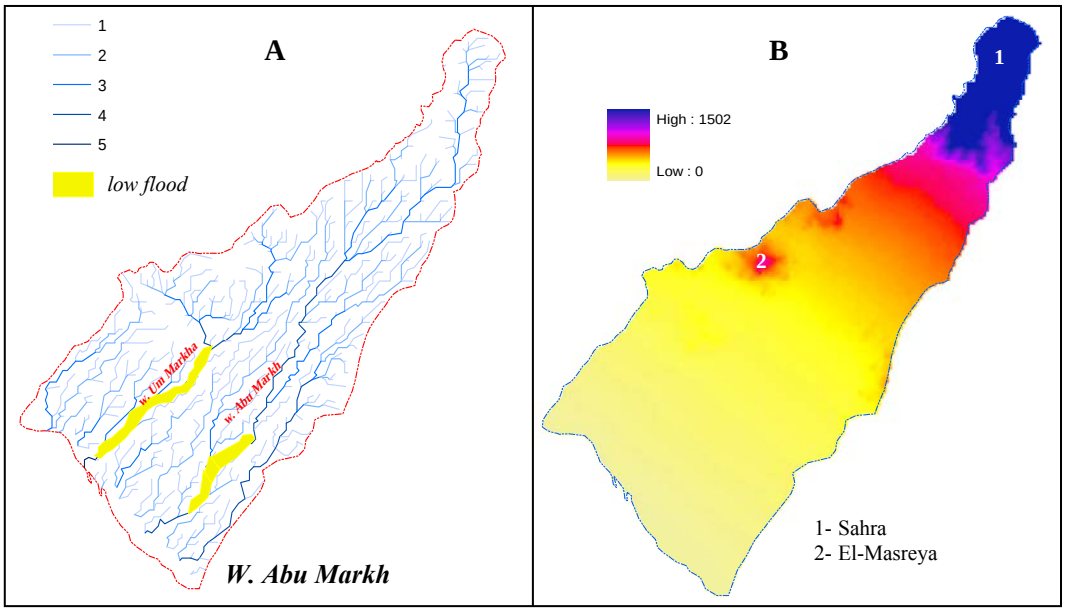

Fig (4-21) *Flash flood distribution of Wadi Abu Markh basin (A), and local relief of the basin (B)*

4.3.8. Wadi El-Taalby basin

Wadi El-Taalby is a small basin in the study area which occupies about 139.8 km^2. The tributaries of Wadi El-Taalby drain Sahara Mountain and Khashaby Mountain 1430m (Fig 4-22B); the trunk channel has 5th order and attains about 15.2km toward Suez Gulf (Fig 4-22A). The slope of Wadi El-Taalby ranges between 8º in the mountainous area and 3º in the alluvial fan. The flash flood in Wadi El-Taalby is classified very low to low (14m^3/s) concentrated along the main channel which crosses the highway near Sharm El-Sheikh.

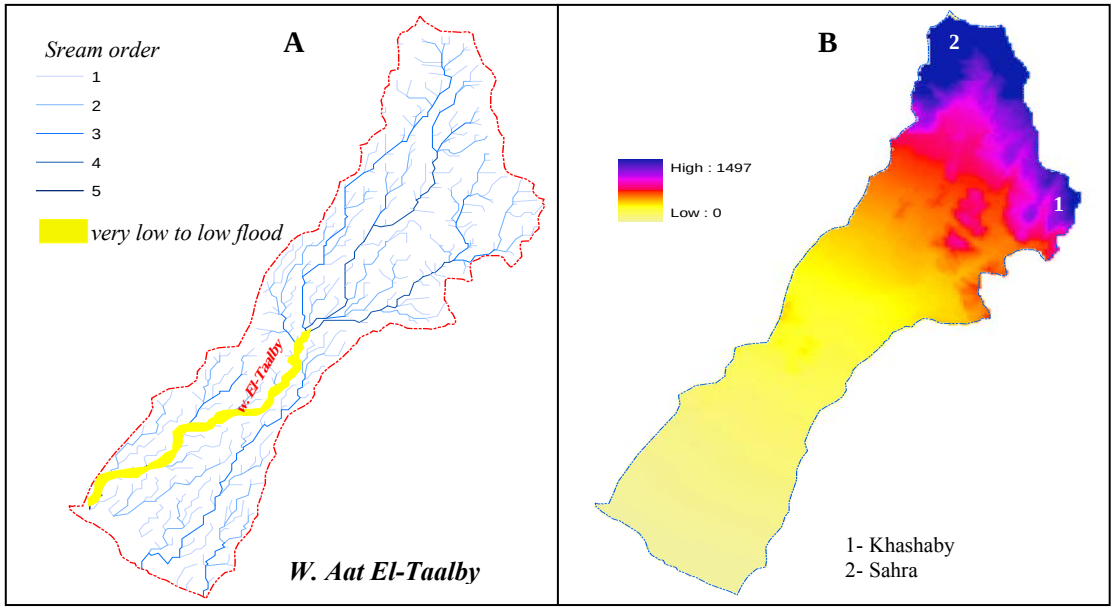

Fig (4-22) *Flash flood distribution of Wadi El-Taalby basin (A), and local relief of the basin (B)*

4.3.9. Wadi Aat El-gharby basin

Wadi Aat El-Gharby basin is one of the main basins in the study area which occupies about 117.8 km^2. The surface slopes of Aat basin range between 7º in the mountainous area and 3º in the pediment area. Wadi Aat El-Gharby drains Aat Mountain (1033m) and Khashaby Mountain 1430m (Fig 4-23B); the trunk channel has 5th order and attains about 12.5km (Fig 4-23A). The flash flood in the basin is classified very low to low (16m^3/s) and limited along the main channel. Sometimes it has affected on the main road near Sharm El-Sheikh.

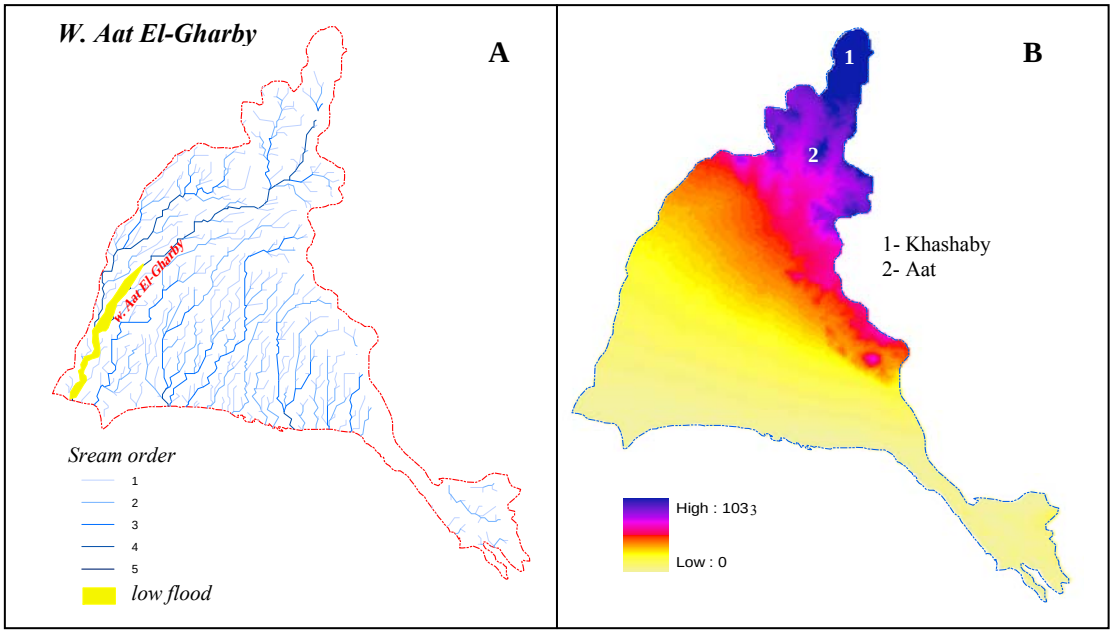

Fig (4-23) *Fash flood distribution of Wadi Aat El-Gharby basin (A), and local relief of the basin (B)*

4.4. Risk zone map of El-Qaà plain area

Flood risk maps have been prepared from satellite data for more than a decade by hydrologists and geographers all over the world. These are considered static techniques because they characterize the area at a particular point in time. While a dynamic long term flood history is desirable, such static techniques are capable of yielding useful information for flood hazard assessment, especially in the diagnostic and preliminary stages of an integrated development planning study (*http://www.oas.org/dsd/publications/Unit/oea66e/ch08.htm*). In the absence of information from dynamic techniques, it is possible to estimate the probability of a flood event occurrence when information from static techniques is combined with historical flood observations, disaster reports, and basic natural resource information, particularly hydrologic data.

Flood risk zone maps have been prepared for several communities in the South Sinai province most prone to flooding. The flood risk zone maps identify areas that are likely to be flooded once at any time. These areas are designated floodways, and governments are advised that their zoning regulations should prohibit settlement building in these areas (*www.heritage. nf.ca/environment/ floods.html*). *The flood risk zone map for El-Qaà plain area (Fig 4-24) shows that:*

- The flash floods are concentrated predominate along the main channels especially in the mountainous area of the investigated basins which are characterized by steep slope and narrow channel; the risk in these areas is strongly limited at the main streams. By contrast, some basins such as Wadi Firan and Wadi El-Aawag basin have wideness channels and contain some large valleys with broad valley bottoms with Bedouin villages and cultivated areas. Consequently, these cultivated areas and villages often have been destroyed during flash floods.
- Wadi Firan basin with the villages (El-Tarfa and Firan villages) is considered the more dangerous. The flash flood of it is classified as high because of the same classification in the three main tributaries. Along a 50km distance of of Wadi Firan toward Suez Gulf, the flash flood with of the main channel is classified as very high.
- Wadi El-Aawag basin has also high flood during runoff especially in the last 30 km of the main stream toward the outlet area, while the main tributaries of it such as Wadi Habran and Wadi Meiar basins have moderate floods. The affected areas are limited along the main channels sometimes attacking the Bedouin villages in El-Qaà plain.

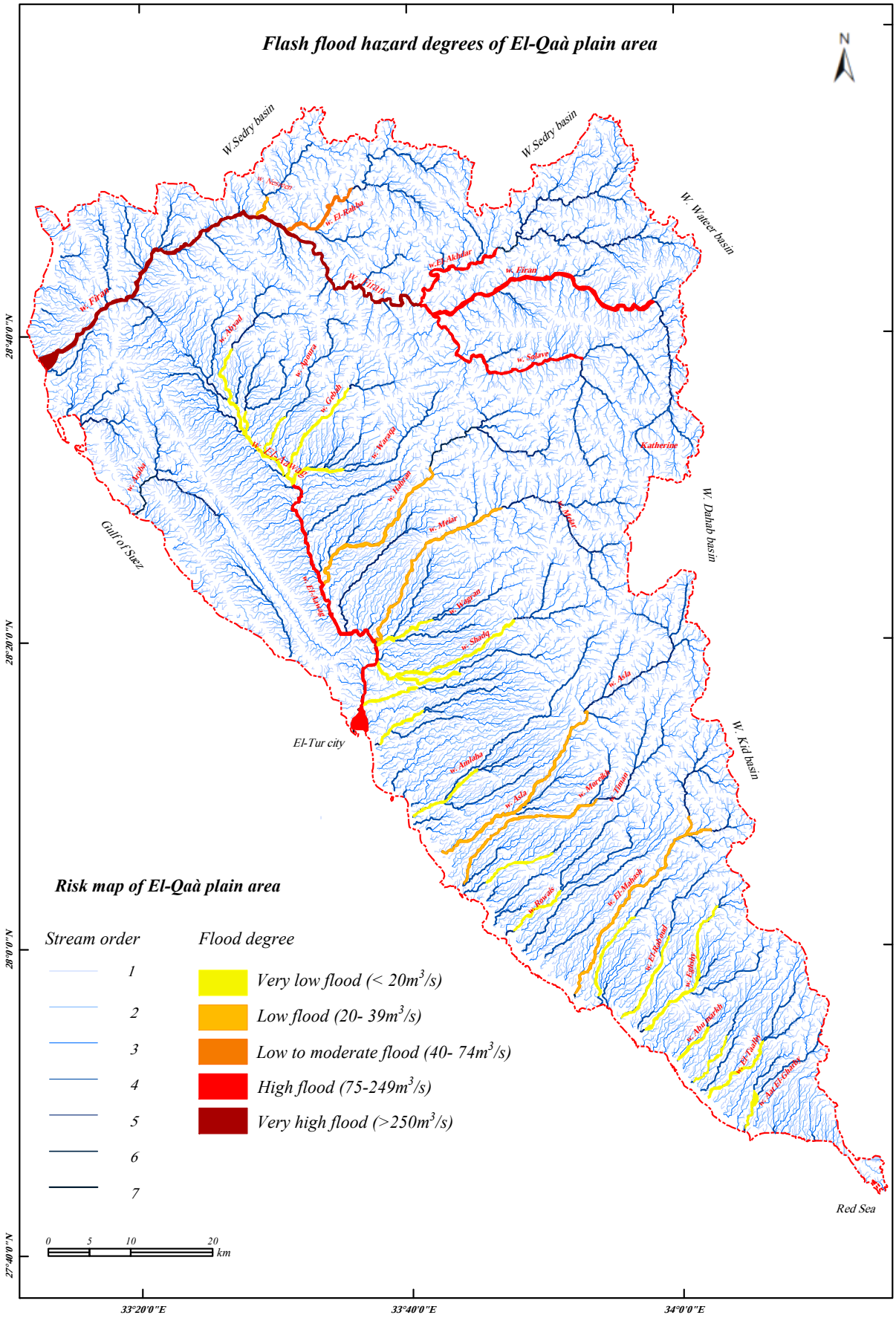

Fig (4-24) *Risk zones map and flash flood hazard degrees of El-Qaà plain area*

Chapter 5

Hazard mitigation and the development of the study area

Depending on the previous discussions of physical settings of El-Qaá plain area, the hydrological analysis of the probabilities of runoff and its danger, and developing the risk map of flash floods in the study area, it can be pointed out this chapter the requirements for the development of the study area represented by the main resources such as population, water resources, settlements and roads. The methods of flash flood prediction and mitigation to make development perspectives for the study area are also discussed,

5.1. Development aspects

5.2. Flash flood prediction

5.3. Methods of flash flood mitigation

5.4. Development perspectives for the study area.

5.1. Development aspects of El-Qaá plain area.

5.1.1. Population

The population is considered the major factor to develop the study area. The greatest number of Egyptian Bedouins lives in Sinai. They are usually living from fishing and grazing but the access as to natural resources reduces with the expansion of tourism and urbanization they can no longer depend on these traditional activities. There are some 12 tribes, which reresent the oldest population in Sinai .The members of each tribe range from 500 to 12000 individually. Five of them inhabit in southern Sinai, named Al Jabaliyah, Al Olayqat, Al Farowsha, Al Badarah and the tour dwellers Al Tawarah.

The total population of the study area was at 9,514 persons in 1986 and at 19,825 persons in 1996 with a big growth rate of about 10%, while it was at 42,713 persons in 2006. The increase of the total population in the study area especially in El-Tur city is corresponding with the local migration from Nile Delta region. The Egyptian government has suggested that El-Qaá plain should be one of the attractive areas for development.

Fig (5-1) shows the distribution of population in the study area 1996, about 50% has concentrated in El-Tur city; this is the capital of southern Sinai and has about 70% of services such as electric, education and economy. St. Catherine city is also an attractive touristic city; it has about 10% of total population, besides some Bedouin villages such as Solave, El-Naby Saleh, and El-Tarfa.

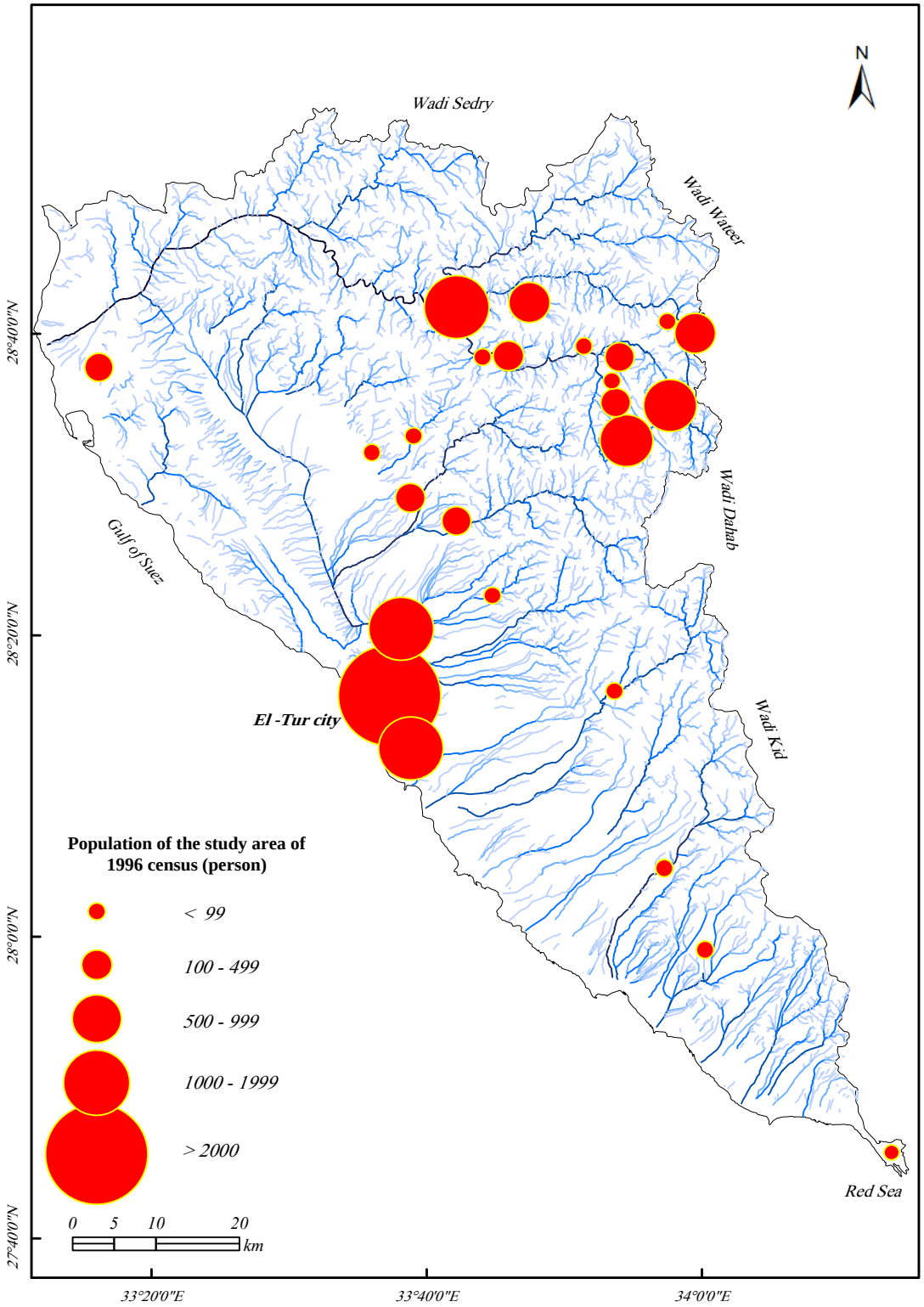

Fig (5-1) *Population distribution for 1996 census of the study area*

There are some small villages distributed above El-Qaá plain such as Habran, Sail Habran, Sail Meiar, Apoura and Timan, most of these villages in 1996 counting lie in the second category ranging between 100 to 499 persons.

Tab. (5-1) *Population numbers of the study area during 1986 and 1996 censuses*

Region	population 1986	population 1996	Region	population 1986	population 1996
El-Tur city	3250	10603	***Nesreen***	85	86
Wadi El-Tur	727	1356	***Maktab***	151	179
Al-Gebail	844	1502	***Wadi El-Ttor***	146	119
El-Sheikh Mousa	0	35	***St. Cathrine***	347	754
El-Qaá plain	81	0	***Abu Saila***	174	271
Sail Habran	15	53	***El-Esbaia***	340	228
Sail Meiar	271	374	***El-Rahba***	111	127
Oraik	0	104	***El-Sheikh Awad***	138	79
Wadi Aboura	26	0	***El-Sheikh Mohsen***	29	49
Wadi Mosaid	34	49	***El-Trafa***	455	411
Wadi Timan	16	20	***Wadi El-Arbeen***	409	559
Wagran	23	0	***El-Naby Saleh***	147	320
Wadi Hofra	0	33	***Wadi El-Akhdar***	148	129
Firan	633	996	***Bir El-Zaytuna***	33	158
Abu Garad	49	32	***Bir Haroun***	0	40
Al barima	43	19	***El-Zaraneeq***	0	65
Elyans	66	139	***Wadi Amlaha***	160	159
Um El-qosur	126	277	***Wadi Sahab***	322	287
Bir Solav	245	249	***Ras Mohamed***	0	4

Source: Central Agency for Public Mobilization and Statistics

Tab (5-1) points out that some Bedouin villages of the study area had some residents at 1986 census, while no population at 1996 census was registered in Wadi Apoura, Wagran, due to the traditions of Bedouins who move between different valleys, depending on the presence of grass. During the last decade, the population of the study area especially of El-Tur and St. Catherine cities has a serious increase resulting mainly from the migration of overpopulated areas in the delta and the special activities of the Government to develop the region.

Southern Sinai is considered a hopeful region; it can not be made a clear future projection of population increasing because it depends not only from the normal population growth but also from the local and regional migration. Therefore, it is necessary to find and to determine the best areas for settlement building depending on the economic and other factors such as protected areas from flash floods, water resources, soils, and the infrastructure.

Eventually, it can be concluded that more than 50% of population of the study area are Bedouins. While the majority of inhabitants are Bedouins, their status has changed towards urban inhabitants with increasing urbanization and settlement. The urban population of the study area was counted about 54% of total population at 1996 census and grew at 9.9% per annum between the two censuses, which was higher than the total population growths of 6.5%, whereas, the rural population grew at 3.7% per annum on average.

The population density of the study area was 1.9 persons per km^2 in 1996 census. The density of Egypt was 59.4 persons per km^2 in the same year, so the southern Sinai governate was scarcer than the country. An average density of both El-Tur and St. Catherine cities was 255.5 persons per km^2 (JICA, 1999).

5.1.2. Highways and tracks

There are two highways and several tracks in the study area. The first highway Suez- Sharm El-Sheikh extends about 162km and starts from the delta toward El-Tur city and Sharm El-Sheikh. The highway is considered being the important road in Southern Sinai due to the increasing importance of Sharm El-Sheikh city. It is often attacked by flash floods especially in the parts crossing the main channels of Wadi Firan and Wadi El-Aawag (Fig 5-2), and additionally other crosses between the highway and the main wadis in the study area.

The second highway in the study area extends about 125km toward St. Catherine along the main channel of Wadi Firan (Fig 5-2). It is considered one of the most dangerous roads in Egypt; it is often attacked and destroyed by flash floods especially along the last 50km toward Suez Gulf. It will be focused in details in the part of hazard mitigation with GPS points of dangerous places.

Moreover, there are several tracks in the study area which are usually used by Bedouins for economic activities such as cultivation and mining. The tracks in the mountain area are limited by the main channels of wadis and are considered as short connection roads between different tribes in the study area. (Fig 5-2) shows that most of the tracks are concentrated in El-Qaá plain especially north of El-Tur city where some Bedouin villages such as Sail Habran and Sail Meiar are. These tracks have an important role to develop the study area and it is necessary to select some of them for road constructing in the future.

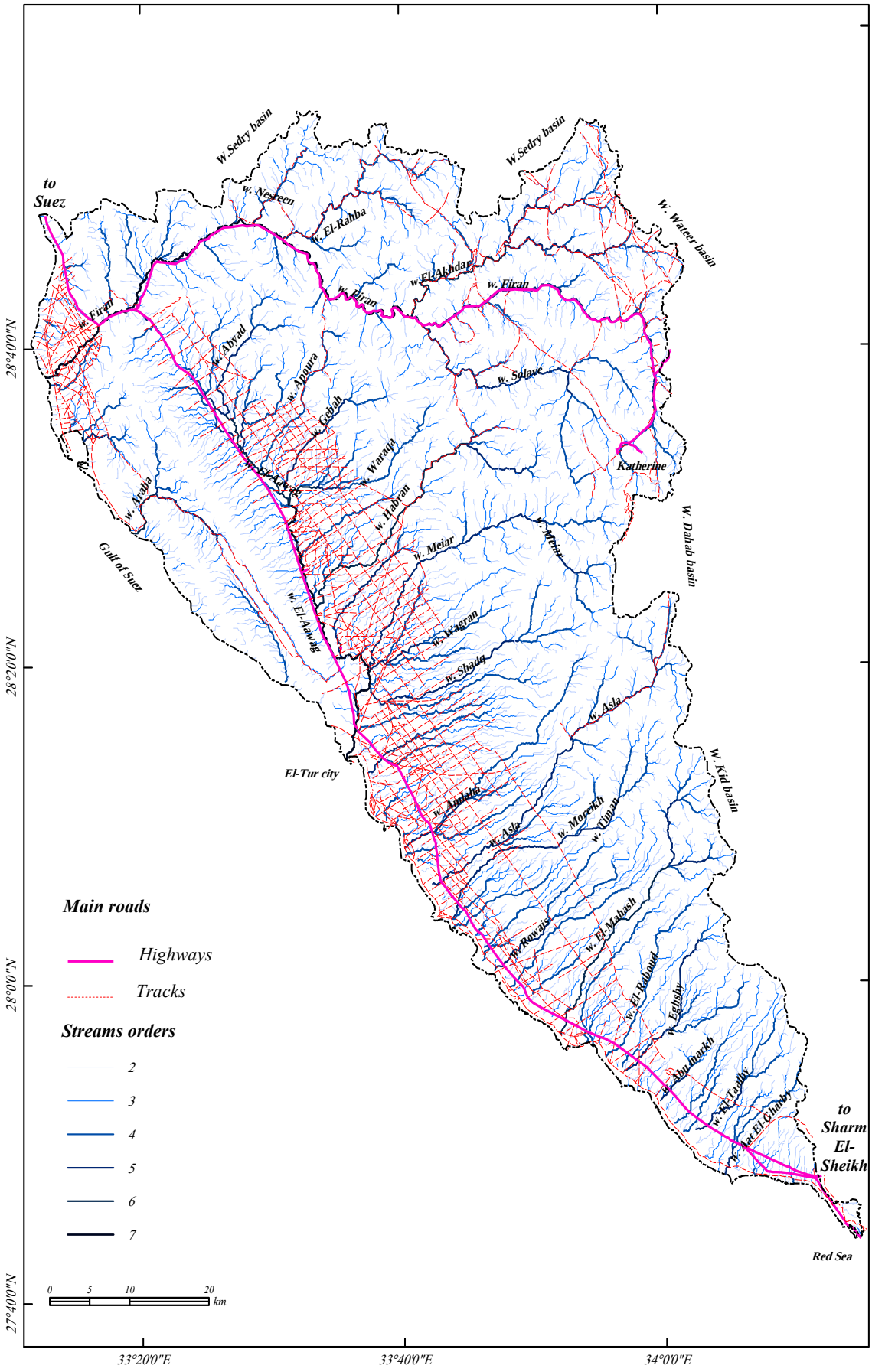

Fig (5-2) *The main roads and tracks of the study area.*

5.1.3. Water resources

The groundwater resources of southern Sinai are a reflection of the ancient to recent hydrologic cycle (Abdallh, A. et al, 1995). They are manifested by different depositional regimes and structure patterns with variability of the palaeo-to-recent climatic conditions. Because the study area is considered as an attractive area for investment, there have been maids several hydrological studies to determine the amount, quality and the depth of groundwater in El-Qaá plain area.

El-Qaá plain is the most representative Quaternary sedimentary basin in South Sinai. The plain is bounded in the east by the uplifted Precambrian basement rocks, in the northern half of the west part by Musa Mountain and in the southern half by the Suez Gulf. El-Qaá plain rankes as the high priority development area in South Sinai. The groundwater in the Quaternary aquifers is considerably exploited for the water demand of domestic water use n El-Tur and Sharm El-Sheikh, and irrigation use in the plain.

Thick Quaternary deposits cover El-Qaá plain overlying the older formations for the Tertiary, Mesozoic, Paleozoic and Precambrian. The Quaternary deposits are called as El-Tur group and consist mainly of sand and gravel with clay beds. JICA, 1999 had divided El-Qaá plain into two areas by inferred faults running through Wadi Asla. Geological data are rich in the north of El-Qaá plain, but it is scarce in the south.

According to Japan International Cooperation Agency (JICA 1999), the Aquifers in El-Qaá plain extend in two areas from the northern part of the plain toward the east of El-Tur and to the mountain feet about 22km east of El-Tur. The first aquifer occupies a limited area in Wadi El-Aawag basin near El-Tur and El-Wadi village. The second is the main aquifer and widespread in El-Qaá plain; it is distributed in the wide area between 10km from the entrance o the highway to the north-west in the plain. The aquifer is about 60 km in length with about 10km of width. Therefore, the main aquifer occupies about 678km2. The bottom of the main aquifer varies in arrange from -20m ASL to than -100m ASL. This fact reveals that most of wells are exploiting groundwater in the second aquifer (Fig 5-3).

JICA 1999 had used the Trasient- Electrmagatic (TEM) Survey and detected another aquifer near the outlet of Wadi Timan and concluded that few fresh groundwaters was found in the southern part of El-Qaá plain in the past, especially in Wadi Asla and Wadi Timan by two wells located about 5km inland from the coast.

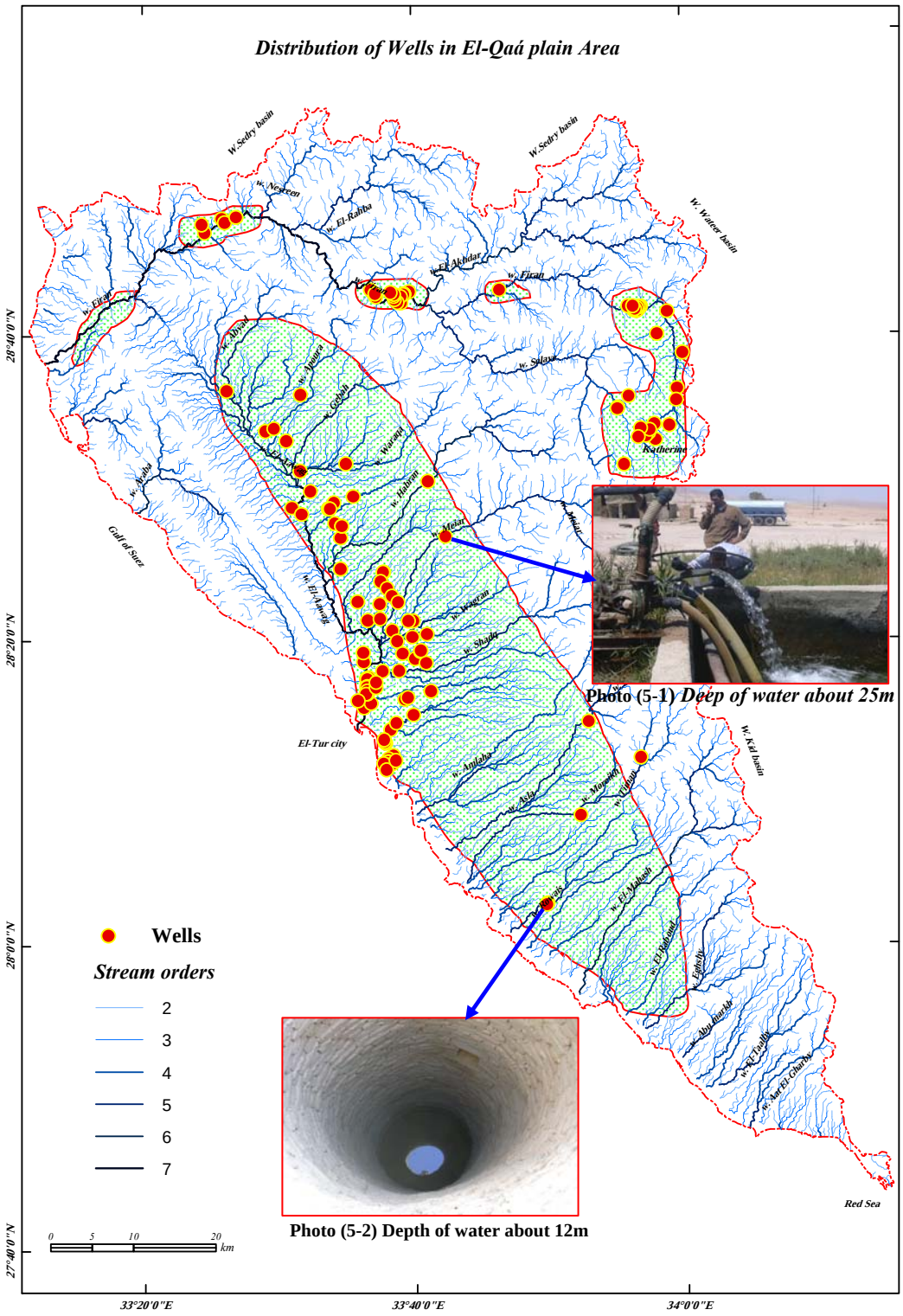

Photo (5-1) *Deep of water about 25m*

Photo (5-2) Depth of water about 12m

Fig (5-3) *Distribution of wells and Quaternary aquifers in the study area*

Fig (5-3) shows the distribution of wells in the study area. Wells are concentrated in two main areas: The first area is El-Qaá plain north of El-Tur city which has been pointed by JICA and has about 65% of wells, while the second groundwater area is Catherine. EL-SHAMY et al (1992) concluded that Catherine area

is one of main aquifers characterized by high joints densities; it stores huge quantities of rain water. The units comprise fewer fractures and retard the download movement of the overlying stored water into the local aquifers which exist as fault zones, alluvial deposits and areas behind basic dykes.

Relatively deep, wide wells are proposed to be drilled in the monzonite rocks of hilly terrain to discharge more water from such aquifer. Moreover, wide horizontal wells may be constructed along the contact between the elevated regional aquifer, of Catherine volcanics and medium grained granites as well as underlying aquifer units of the coarse granites. Groundwater from such wells is transported to St. Catherine village by gravity (SHAMY et al, 1992).

Based on the observation during field work and according to Water Resources Research Institute (WRRI), it can be concluded that water level is 25m a.s.l, in the center of El-Qaá plain (photo 5-1) and 5m a.s.l, near El-Tur city (photo 5-3), while water level in El-Wadi village ranges from 5.2 to 13.9m a.s.l, from 1.1 to 13.6 m a.s.l, in south of El-Tur (photo 5-2).

Photo (5-3) *Water level is **3.5**m deep in a well of the delta of Wadi El-Aawag north of El-Tur.*

The standard volume of the main aquifer of El-Qaá plain is approximately 83.6×10^9 m^3. Therefore, total groundwater storage is estimated at 12.5×10^9 m^3 in the northern part of El-Qaá plain. While the total increases of groundwater storage during the mentioned period (1994 to 1996) is calculated as 36.6×10^6 m^3. In addition, annual extraction of groundwater is estimated as 3.4×10^6 m^3. Therefore, the total recharge amount is estimated as 40×10^6 m^3/year (JICA 1999).

5.2. Flash flood prediction

Extreme events often exert a disproportionately large effect on the environment, much larger than those associated with the more commonplace typical events, and they are mostly associated with risks affecting humans. The extremes of rainfall result in a variety of hazardous phenomena ranging from intense drought through to mega- and super-flooding events (HERSCHY, 2002) and associated consequential problems. In arid regions such as the study area, flooding represents a major hazard to human health and well-being as well as to the infrastructure of the societies dwelling in such regions. In such environments, a major concern is flash flooding, events that may develop within a very short period of time (FOODY, M, et al 2004).

Flash floods are a major threat to human life and infrastructures. Unfortunately, there is often a lack of data of key hydrological processes in arid areas (GHEITH and SULTAN, 2002). This fact limits the ability to understand the flooding process and use this knowledge to minimize its threat to human health and well-being. The lack of understanding sometimes compounds problems of flooding, with settlements, roads and other structures inappropriately located and designed relatively to the flood risk. The ability to predict sites mostly prone to flooding would help mitigate future damage and substantially aid regional development.

In recent years, the required information on regional hydrological properties can be derived from satellite remote sensing (ENGMAN and GURNEY, 1991; FOODY et al., 2004) such as evapotranspiration which is strongly correlated with the basic state variables that control the remotely sensed response of a surface. The estimation is, however, difficult and often limited by technical problems. These expensive methods are not found in all countries.

On the other hand, remote sensing techniques can be also used to estimate key hydrological variables indirectly. Frequently, land cover is used as an intermediary between the remotely sensed imagery and desired hydrological variables; i.e. there was used unsupervision classification for ETM images in El-Qaá plain area to determine the land cover of plant (chapter 1). Land cover has a strong influence on key hydrological variables such as infiltration, interception and evaporation and is typically the dominant variable determining the remotely sensed response of a site.

Consequently, land cover maps derived from remotely sensed data have often been used to estimate a range of hydrological variables for the parameterization of hydrological models (STORCK et al., 1998; SU, 2000, FOODY et al., 2004). These models may be used to predict the response of a site to a precipitation event. In particular, the models may be used to predict the storm hydrograph that may help in identifying locations sensitive to flood hazards.

5.2.1. Methods of flood prediction

There are two main methods to predict flash flood:

5.2.1.1. The first method is used in the absence of detailed data, especially on rainfall and ground surface properties for the site. The only feasible means of predicting sites sensitive to flooding was to adopt a modeling approach supported by acquisition of data on land cover and associated hydrological variables. Given the spatial variability in rainfall and basin hydrological properties, a spatially distributed rather than lumped model was required.

The hydrologic modeling system (HMS) has been developed by the Hydrologic Engineering Center of the US Army Corps of Engineers., It was used to model the rainfall-runoff processes of the basin and predict the hydrograph at locations within it. Model parameters, outlined below, were determined with the CRWR-PrePro system (OLIVERA AND MAIDMENT, 1999). CRWR-PrePro extracts topographic, topologic and hydrological information from digital elevation data. The model is an integration of HEC-HMS and HEC-RAS in a GIS environment. A number of flood related studies have shown that these models provide accurate and useful results.

The hydrologic model was generated with the help of the HEC-Geo HMS (USACE, 2003) using DEM of the region. Using terrain data in the form of a DEM, HEC-Geo HMS, and an extension of GIS Arc View creates HMS input files in the form of stream network, sub-basin boundaries, connectivity of various hydrologic elements etc. through a series of steps collectively known as terrain pre-processing and basin processing. The physical representation of watersheds or basins and rivers was configured in the basin model. Hydrologic elements were connected in a network to simulate runoff processes. Then it was supplemented by following models:

1. Models that compute runoff volume (loss rate): The Curve Number (CN) of the U.S. Dept. of Agriculture, Natural Resources Conservation Service (NRCS) (formerly Soil Conservation Service, SCS) known as SCS CN was used to predict the runoff properties for surface based on the hydrologic soil group and ground cover (US SCS, 1986). One weighted CN for each sub-basin was computed (Chapter 4).

2. Models of direct runoff (transform): Transformation of excess precipitation into surface runoff was accomplished using SCS Unit Hydrograph (Fig 5-4A).

3. Models of base flow: Base flow can be an important parameter in flood studies because it defines a minimum wadi depth over which additional runoff accumulates. Models that neglect base flow may under estimate water levels and therefore fail to identify inundated reaches (KNEBL ET AL., 2005). In this study constant monthly values were used for base flow computations (Fig 5-4B).

4. Meteorological model (precipitation): The inverse distance method addresses dynamic data problems. The method was originally designed for application in real time forecasting systems. It can use recording gages that report on regular interval and gages that only report daily total precipitation. Because it was designed for real time forecasting, it has the ability to automatically switch from using close gages to using more distant gages when the closer gages stop reporting data (Fig 4-4C).

5.2.1.1. The second method had been used by CLARK who is one of the main advantages of using GIS for flood management as its creation of potential to further analyze the visualization of flooding for estimating probable flood damage (CLARK, 1998). The knowledge of the catchment's characteristic, spatial and temporal stream flow and rainfall distributions are crucial for setting up a hydrologic model and its calibration. Therefore, it could be known details of Geographic Information System (GIS) for the main basins in the study area which had analyzed during previous chapters. It comprised the following layers:

1. Contour lines of the relief (interval 5- 10m); Digital Elevation Model (DEM)

2. Stream network (chapter 2)

3. Stream flow and precipitation measuring stations (chapter 3)

4. Administrative boundaries, settlements and roads (present chapter)

5. Land cover (chapter 1)

6. Geological map, Soil map etc. (chapter 1)

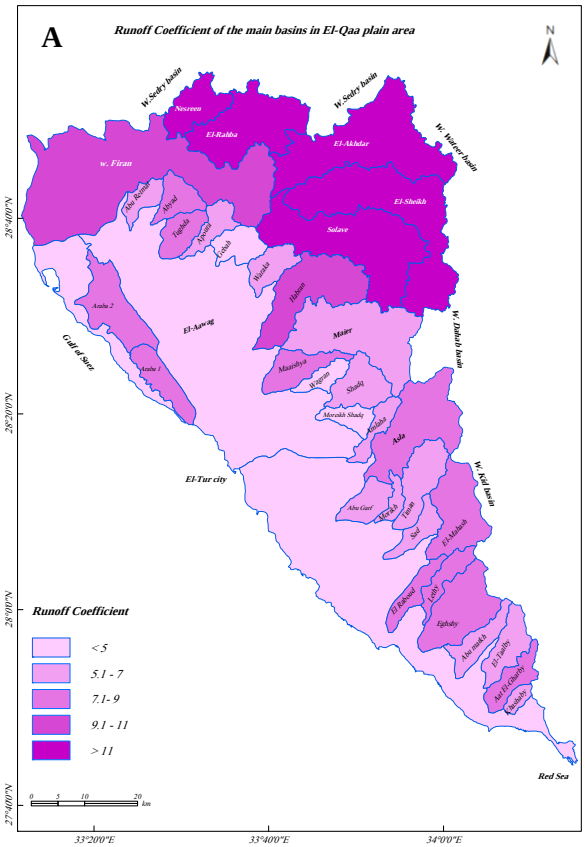

Runoff coefficient in the main basins of El-Qaà plain area

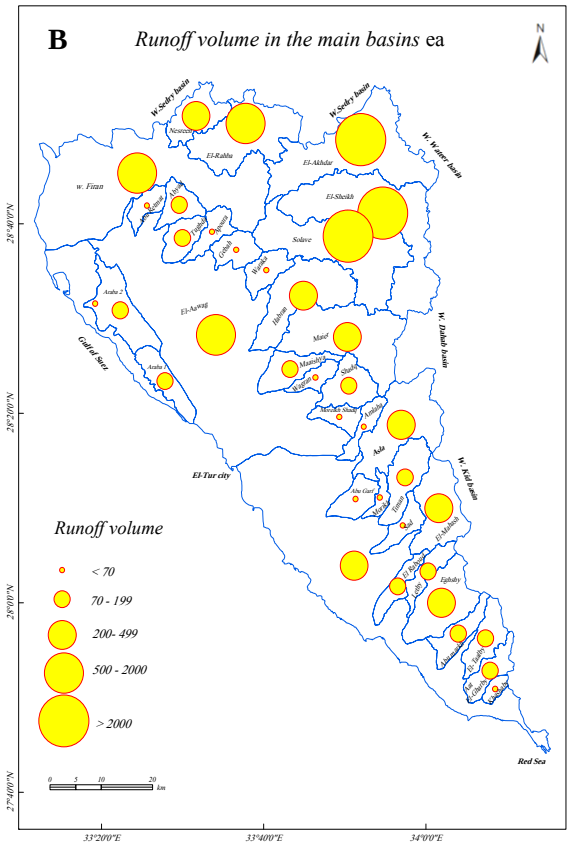

Runoff volume (m^3) *during four hours in the main basins*

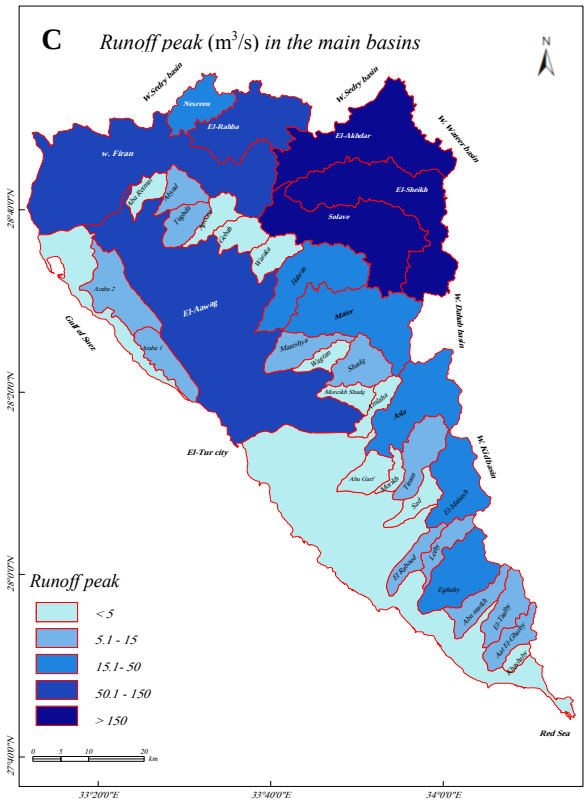

Runoff peak (m^3/s) *in the main basins of El-Qaà plain area*

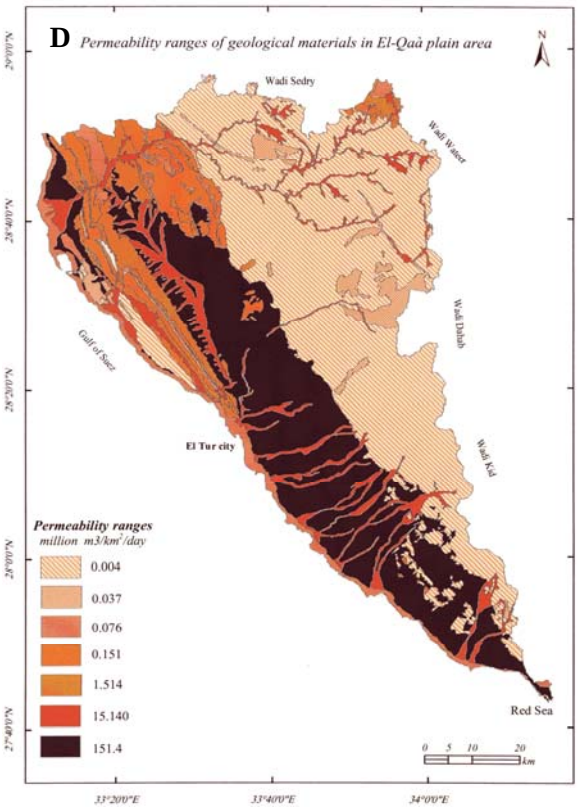

Permeability ranges of geological materials in El-Qaà plain area

Fig (5-4) *Flood prediction depending on hydrological aspects such as runoff coefficient, runoff volume, runoff peak, as well as permeability and (SCS) and (HMS) models*

(Fig 5-4) and previous analyses of flash flood prediction in the study area show that:

1. The peak runoff values in the study area have varied from one basin to another owing to several affected factors. The average peak runoff values ranges between 1.8 (m^3/s) in Wadi Moreikh and 177 (m^3/s) in Wadi El-Sheikh.
2. The higher category has values more than 150 m^3/s, and contains Wadi El-Akgdar 159.7 (m^3/s), Wadi El-Sheikh 177 (m^3/s), and Wadi Solave 157.1 (m^3/s) which are the upper tributaries of Wadi Firan.
3. Wadi Firan 86.9 (m^3/s) (main wadi) and Wadi El-Aawag 93.5 (m^3/s) came in the second order as single Wadis, but they can be considered very dangerous during runoff because they have several dangerous tributaries which add more water to them.
4. The rainfall-runoff model predicted the peak discharge, based on point gauge data, fairly accurately. Hence the methodology could be considered valid for application in peak flow computation for flood forecasting.
5. Flash flood maps were prepared for various return periods and are corresponding to main basins in the study areas they were computed in chapter 4.
6. These maps can be used in conjunction with the predicted peak flows for flood forecasting, awareness raising, development planning, emergency services and post disaster rehabilitation aimed at reducing flood damages and economic impacts in future.
7. Finally. It has been demonstrated that the location of sites particularly at risk from large peak flows associated with flash flooding may be predicted using a hydrological model in which key parameters were derived from conventional topographic maps, field survey and a land cover map derived from satellite remote sensing.

5.3. Flash flood mitigation

Alot of measures are being used to control or mitigate flood effects some of which are not properly designed or implemented often caused by intensive and severe floods. The construction of unsuitable and unwell-designed structures such as bridges, flood walls, groins and dikes as well as human interferences may have significant effects on flooding or flood exaggeration. The effects may be imposed through changing of cross sections, flow velocity, storage area, flow level and extension. Mostly of focussed are mitigation measures in the upstream side of the catchment areas, which are physically distant from the monuments' site.

5.3.1. Control aspects of flash flood mitigation in arid regions

5.3.1.1. Afforestation of the watershed

Afforestation could be undertaken at selected areas in the two upstream watersheds of the main channel of Wadi Firan (photo 5-4) and the outlet area of Wadi El-Aawag (photo 5-5). The analysis investigates good afforestation practices according to the definition of the SCS (1986). The afforestation conditions affect the infiltration-runoff process in the catchment, as reflected hydrologically by the CN value (chapter 4). Accordingly, the weighted average of CN values for the main basin in the study area ranged between 12 in Wadi Ghowaitat and 76 in Wadi Solav; the values are related to the outcrop lithology of the study area.

The flood peak and volume are estimated in the main basins and their tributaries in El-Qaá plain area, the values range between 2.2m^3/s in Wadi Wagran to 177m^3/s in Wadi El-Sheikh. Afforestation reduceds the flood peak especially in the main channel of Wadi Firan and the mouth of Wadi El-Aawag by 7–15%. Similar reduction in the range of 7–15% was noted for flood volumes.

Photo (5-4) *Afforestation of the main channel of Wadi Firan by palm trees*

Photo (5-5) "*Afforestation" of the outlet area of Wadi El-Aawag by phragmites*

5.3.1.2. Terracing, check dams

According to AL-WESHAH, and EL-KHOURY, Terracing and constructing of check dams involve construction of dry-stone walls and gabions, which follow the contour lines and intercept overland flow lines. Check dams are gabion structures that are constructed a few meters high across the wadi bed. Terracing activities are usually accompanied by afforestation schemes. Terracing and check dams have three fold interconnected effects, namely:

1. Increasing the time of concentration (T_c) for the sub-basin. This will decrease the sensitivity of the watershed to short duration but high intensity storms, making it less vulnerable to more frequent flood events. The value of T_c depends on the spacing, configuration, and height of terracing. From a practical point of view, compared to existing T_c, it was found that T_c values (and thus lag time values) can be increased by about 30% for the terraced catchments.

2. Decreasing values of the Curve Number (CN) for afforested terraced catchments. Values of CN are reduced by land conservation practices such as terraced catchments. Terracing allows for greater infiltration and abstraction during a storm event.

3. Providing additional shallow storage, which in turn increases the T_c. Storage provided by terraces and check dams may attenuate the hydrograph and delay the per- peak time. The effect of terracing and check dam storage is already considered in the reduced values for CN and increased values for T_c. Therefore, the storage effect of check dams and terracing was not considered as an additional potential benefit (chapter four).

5.3.1.3. Storage/detention dams

Storing flood water in reservoirs and detention basins behind dams is another alternative for flood mitigation and control. The topography of the catchments in Wadi Firan, Wadi Meiar, and Wadi El-Aawag seems to allow the construction of these reservoirs to mitigate the hazard.

5.3. Mitigation methods of flash flood hazard

Although, the government had built some culverts crossing (photo 5-6) and bridges (photo 5-7) to mitigate and protect the economic activities in the study area, these tools until now are not able to protect the study area. The construction of unsuitable and unwell designed structures such as bridges, flood walls, groins and dike as well as human interferences may have significant effects on flooding or flood exaggeration. During the filed work, it could be recorded using GPS some dangerous points along the main channel of the main basins such as Wadi Firan and Wadi El-Aawag, in addition, some points along the highway to Sharm El-Sheikh city.

Photo (5-6) *Culverts of the highway Suez- Sharm El-Sheikh*

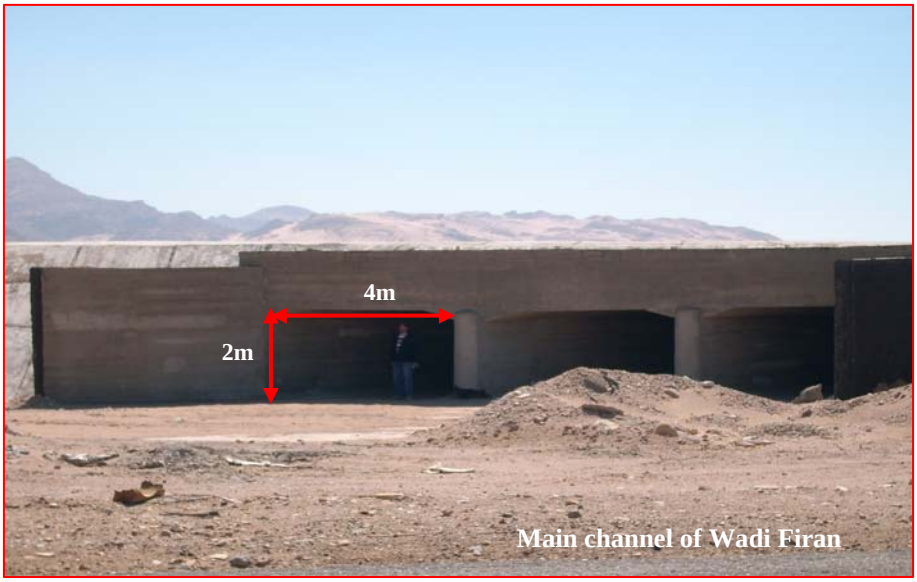

Photo (5-7) *Construction of diversion for the main channel of Wadi Firan above the delta*

There are several engineering methods to mitigate flash floods such as construction of dams, extension and raising of wadi interceptor guard dam, construction of diversion channel for interceptor guard dam, wadi protection works requiring resectioning, levee construction, reconstruction of bridges with increased waterway and construction of bridges in place of existing Irish crossings (EL-HAKAMANI, A., 2006).

5.3.1. Bridges crossing

Normally, bridge construction causes the least amount of disturbance to the stream bed and banks when compared to the other types of crossings. They can also be quickly removed and reused. According to U.S. Army Corps of Engineers, the designer must also be aware that such structures are subject to the rules and regulations for in-stream modifications as following:

- Structures may be designed in various configurations. However, the materials used to construct the bridge must be able to resist the anticipated loading of the construction traffic.
- The waterway crossing shall be at right angles to the stream. Where approach conditions dictate, the crossing may vary 15 degrees from a line drawn perpendicular to the center line of the stream at the intended crossing location.
- The centerline of both roadway approaches shall coincide with the crossing alignment centerline for a minimum distance of 15m from each bank of the waterway being crossed. If physical or right-of-way restraints preclude the 15m minimum, a shorter distance may be provided. All fill materials associated with the roadway approach should be limited to a maximum height of 60 cm above the existing floodplain elevation.

In the study area, the bridges are limited to crossing the highways with the largest basin channels which usually have large values of peak runoff, large amount of runoff volume, steep slopes, narrow streams, and a few thicknesses of deposits. The bridges are distributed in the study area as following:

- Wadi Firan basin has most bridges crossing the main channel and their main tributaries such as Wadi Solave which has a peak runoff of 157.1 m^3/s, Wadi El-Akhdar 159.7 m^3/s, Wadi El-Raha 73.3 m^3/s, and Wadi Nesreen 30.2 m^3/s. All these tributaries have a direct effect on the highway toward St. Catherine city. Therefore, it was necessary to construct these bridges to protect it (Fig 5-5).

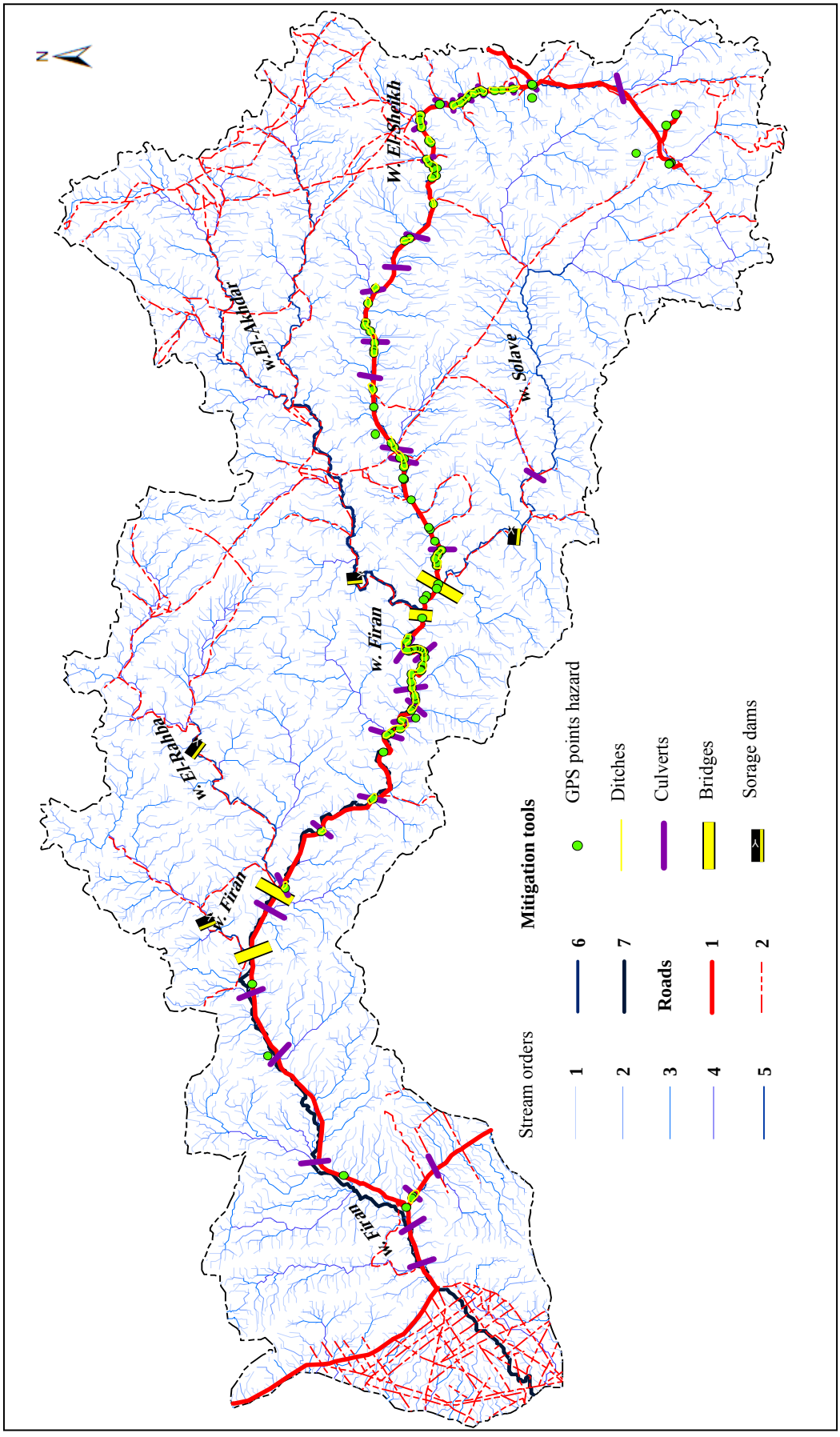

Fig (5- 5) *Suggestion methods to mitigate flash flood hazard in Wadi Firan basin*

- Wadi El-Aawag basin has two suggestion bridges along the main channel; the first bridge is crossing between the main channel and the main channel of Wadi Meiar near El-Wadi village, the second bridge is crossing between the main channel of Wadi El-Aawag and the highway Suez- Sharm El-Sheikh (Fig 5-6).

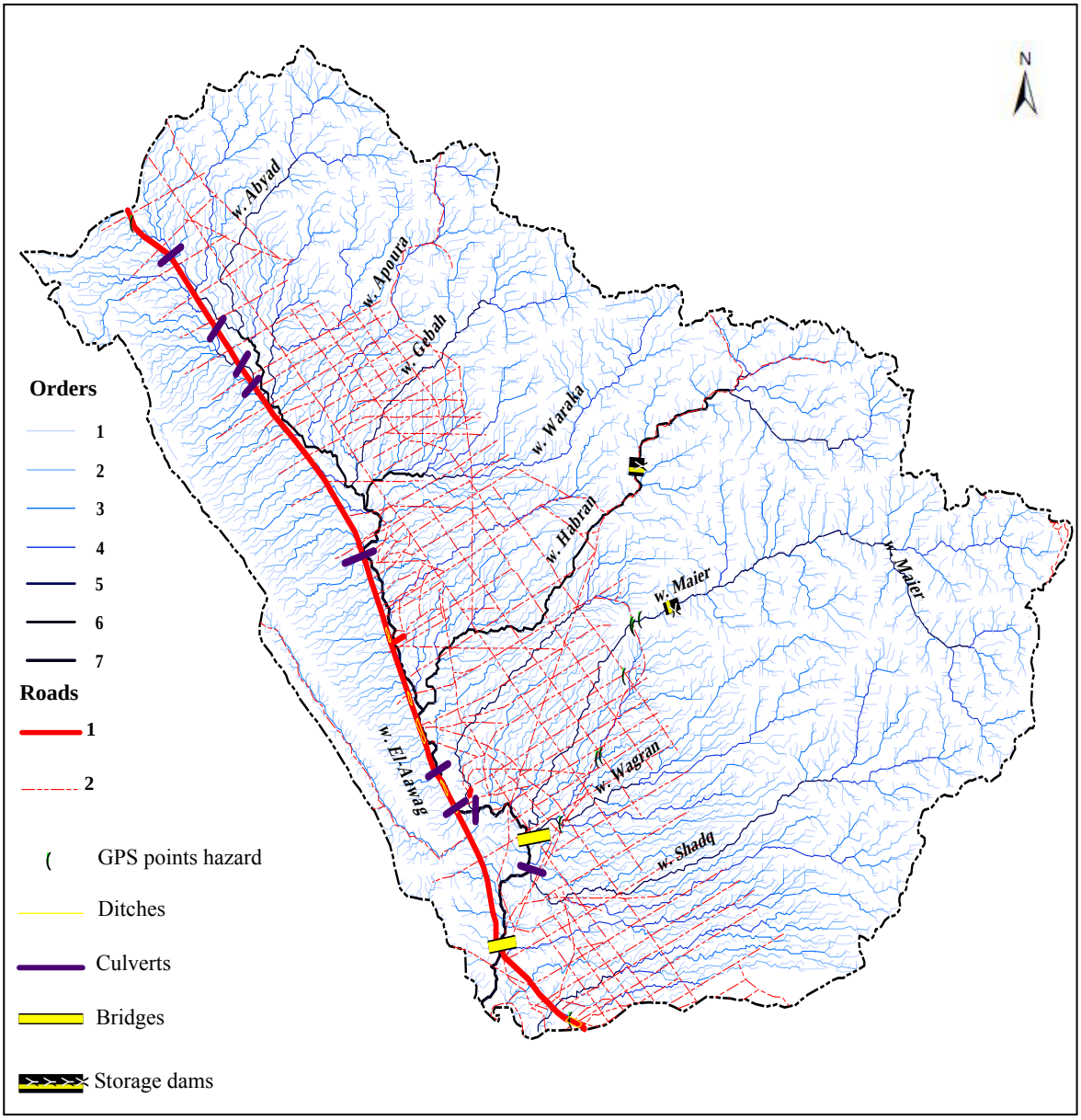

Fig (5-6) *Suggestion methods to mitigate flash flood hazard in Wadi El-Aawag basin*

- The southern part of the study area contains some active wadis such as Wadi Asla, Wadi Timan and Wadi El-Mahah. They have direct effect on the highway to Sharm. Therefore, mitigation of flash floods along the highway requires constructing three bridges crossing between the main channels of these wadis and the main road (Fig 5-7).

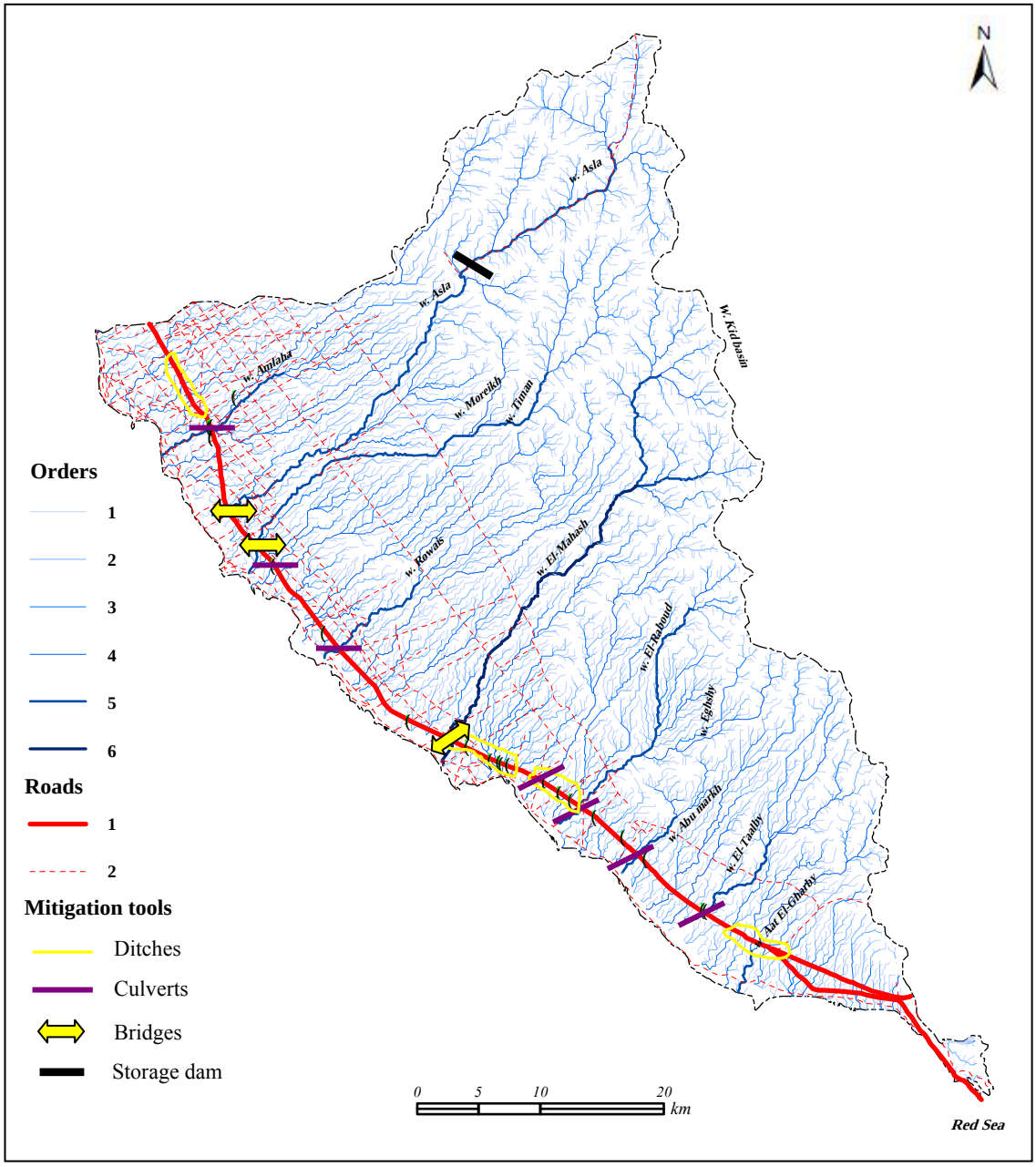

Fig (5-7) *Suggestion methods to mitigate flash flood hazard in southern study area*

5.3.2. Culvert crossing

Culvert crossing is a structure consisting of stone and sections of circular pipe, pipe arches, or oval pipes of reinforced concrete, corrugated metal, or structural plate which are used to convey flowing water through the crossings. Culverts are used where the channel is too wide for normal bridge construction or the anticipated loading of construction vehicles may prove unsafe for single span bridges. According to U.S. Army Corps of Engineers, the designer must also be aware that such structures are subject to the rules and regulations for in-stream modifications as following:

- Where culverts are installed, 7.5 to 15cm coarse aggregate or larger will be used to form the crossing. The depth of stone cover over the culvert shall be equal to one-half the diameter of the culvert or 30cm, whichever is greater.
- Multiple culverts may be used in place of one large culvert if they have equivalent capacity. The minimum-sized culvert that may be used is about 50cm.
- All culverts shall be strong enough to support their cross sectioned area under maximum expected loads.
- The length of the culvert shall be adequate to extend the full width of the crossing, including side slopes.
- The slope of the culvert shall be at least 1.2º.
- The temporary waterway crossing shall be at right angles to the stream. Where approach conditions dictate, the crossing may vary 15º from a line drawn perpendicular to the centerline of the stream at the intended crossing location.

The suggestion culvert crossings are located in the study area at the crosses between the main tributary channels and the roads. As St. Catherine highway runs along the main channel of Wadi Firan, so, it has most of suggestion culverts whereas most channels of its tributaries are rectangular with the road (Fig 5-5). The other culverts are distributed along the highway toward Sharm El-Sheikh such as Wadi El-Aawag especially at the crosses between the main channel and the road (Fig 5-6), such as Wadi Amlaq Wadi Eghshi, and Wadi Aat El-Ghary (Fig 5-7).

5.3.3. Storage dams

Based on available topographic, contour, DEM, drainage network, structure, outcrop lithology, and field work observation of the study area, it could be determined a number of locations which possible sites for constructing storage dams. However, a detailed field survey to check the exact location, storage volume, and outlet type of these dams would be require to confirm the feasibility and costs.

Wadi Firan basin has four suggested narrow places to construct storage dams in the main channels of its tributaries such as Wadi El-Akhdar, Wadi Solav, Wadi El-Raha, and Wadi Nesreen (Fig 5-5). Wadi El-Aawag contains two suggestion dams in Wadi Habran and Wadi Meiar (Fig 5-6), while another dam can be constructed in Wadi Asla (Fig 5-7). These dams could help to mitigate flash floods in the study area and improve the groundwater resources as well.

5.3.4. Ditches and roads dam

The Ditches are considered one of the main tools using to mitigate flash foods and help to drain the water far from the road; they are constructed along the highways, and distributed in the study area along St. Catherine highway in Wadi Firan and Sharm El-Sheikh highway in Wadi El-Aawag and other wadis (photo 5-8).

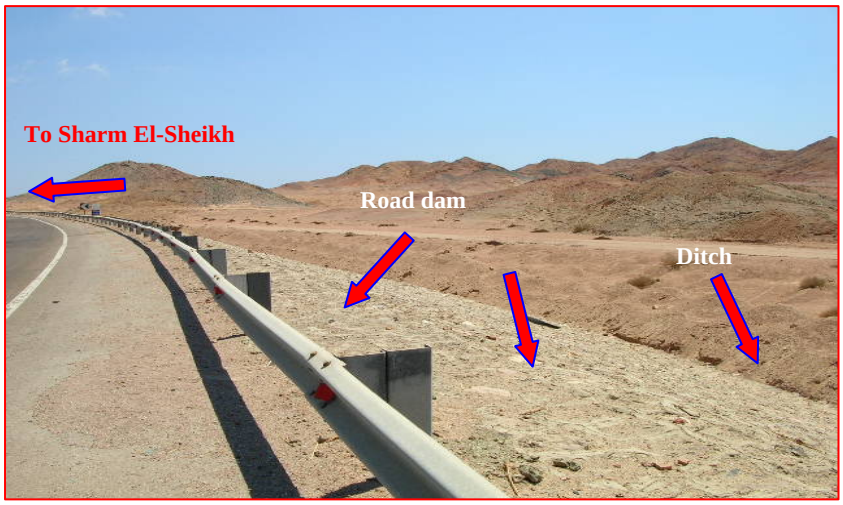

Photo (5-8) *Ditches and road dam of Suez- Sharm El-Sheikh Highway*

5.3.5. Construction of diversion channel

Construction of diversion channel is considered an important tool to protect strategic places which lie in the flood channel and deltas, the Egyptian Government used this tool to protect the Oil center above the delta of Wadi Firan (photos 5-9). The diversion channel tools of the main channel of Wadi Firan may be not effectire, especially during high flash flood; it is obvious that the wall which was constructed to change the channel may be destroyed by a high flood. Therefore, the best method may be the deeping of the main channel of Wadi Firan upstream of the delta.

Photo (5-9) *Construction of diversion the main channel of Wadi Firan*

5.4. Development perspective of El-Qaá plain area

South Sinai is an attractive area for tourism development due to its natural environmental conditions and remoteness which attract nature lovers. The seclusion of Sinai as a Peninsula offers a safer area for tourists who were being targeted in Upper Egypt by terrorists. A number of urban, economic, tourism and environmental development policies contributed to changes in Sinai during the last few years after many years of being in seclusion (Ali, D., 1998).

The government envisioned a way to address population increase by absorbing the excess population in non-rural economic activities (such as industry, mining, and tourism) away from arable lands in new towns and urban centers. The solution may be to create urban settlements in the desert. Sinai is considered one of these proposed regions. However, Sinai means a challenge for urban development due to its remoteness and isolation from the Nile Valley. The cost of modernizing and providing basic infrastructure for development in this region would be a heavy burden for an already indebted Egypt.

Depending on the previous discussions, it could be shown that El-Qaá plain is considered an attractive area, it extends about 150 km from north to south and the wide ranges between 7 to 25 km from east to west. The slope ranges between 4º in the pediment area to less than1º in the flat and coast area. The study area has development requirements such as soils, groundwater, roads, and flash flood hazard mitigation. Therefore, it could be suggested a perspective to develop the study area as following:

5.4.1. Agriculture development

The study area has already some spots of cultivated areas distributed in Wadi Firan basin photo (5-10), Wadi El-Aawag basin photo (5-11), and the delta of Wadi Asla. There is a large area for cultivation in El-Qaá plain of about 803.2 km^2 which can be distributed in the wide channel and the delta of Wadi Firan of 47.1 km^2, the areas between the main channels of tributaries of Wadi El-Aawag above El-Qaá plain of 505.2 km^2, and the southern basins having a bout 256.9 km^2 (Fig 5-8).

Although, the study area has several water resources such as groundwater, springs (5-12) and flood water, it must be using a new method (photo 5-11) to irrigate these areas to keep the storage of groundwater which is necessary for cultivation. In addition, it could be also used the Nile water by extending a big pipe to El-Qaá plain.

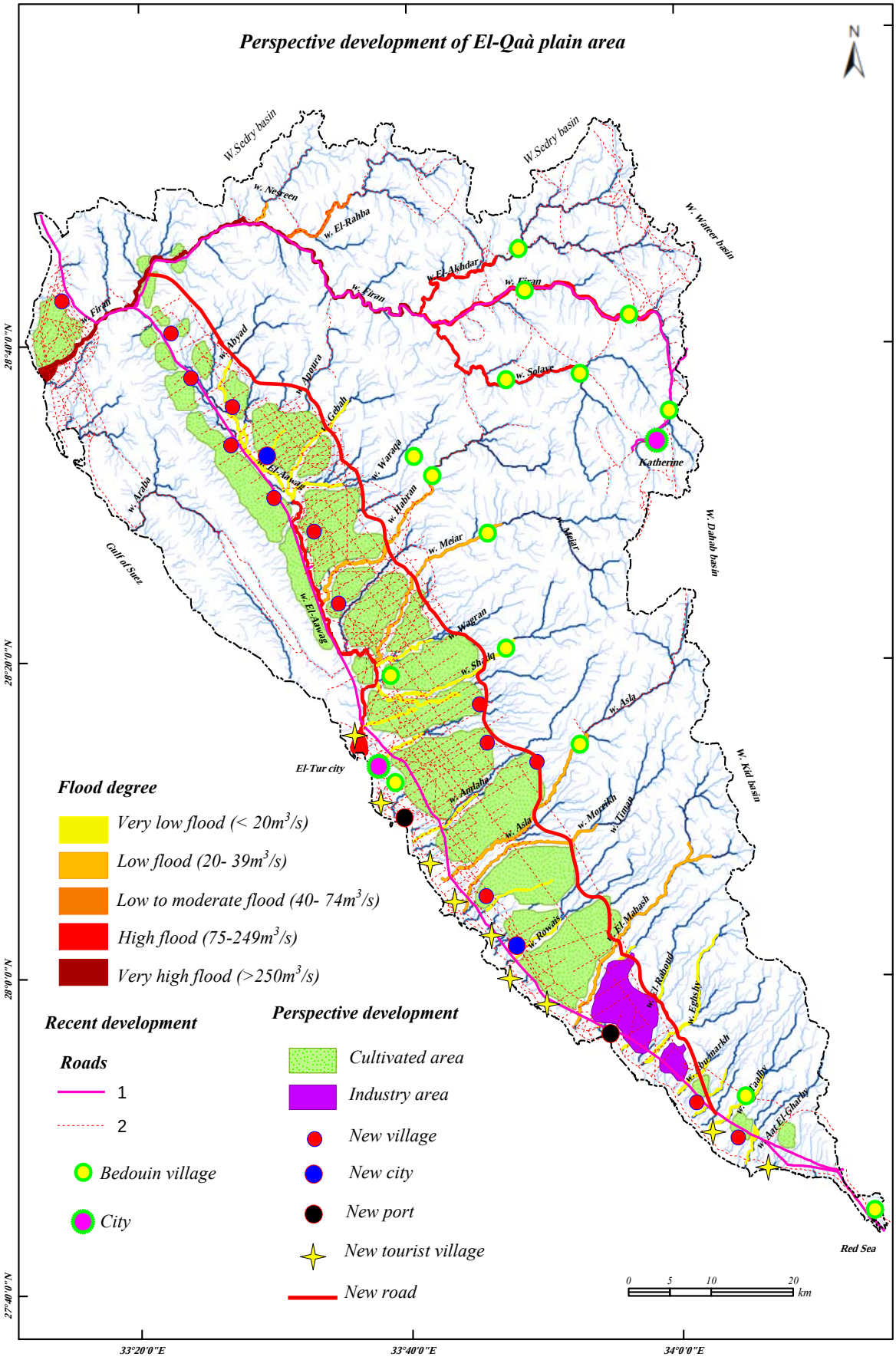

Fig (5-8) Flood hazard and perspective development in El-Qaa plain area

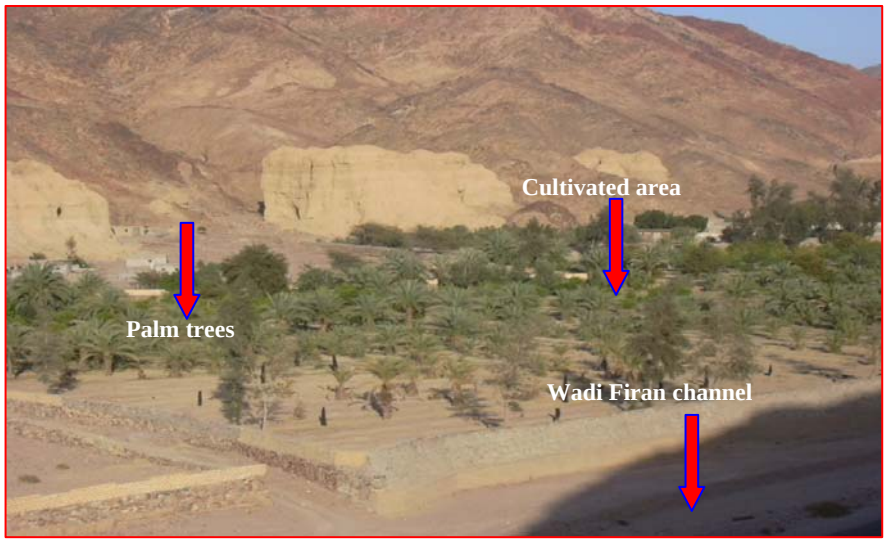

Photo (5-10) Cultivated area in the main channel of Wadi Firan

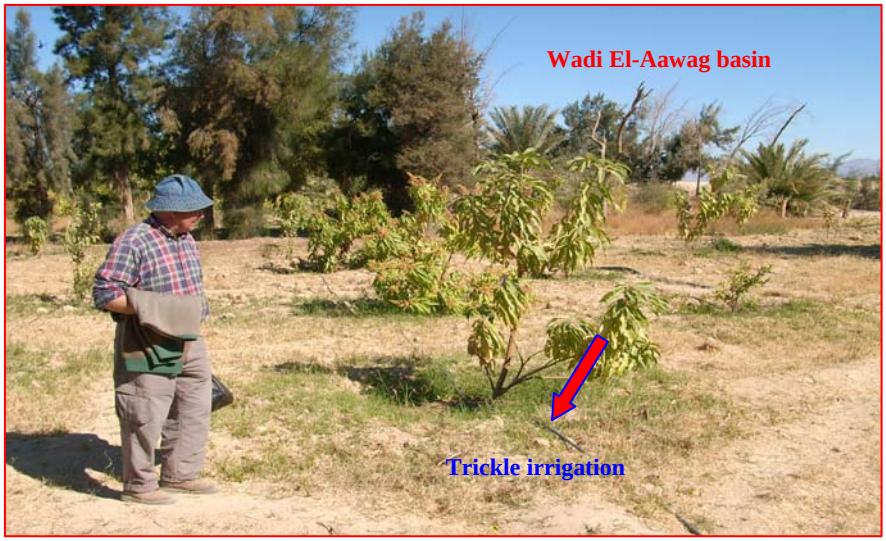

Photo (5-11) Trickle irrigation in cultivated area of Wadi El-Aawag

Photo (5-12) Using spring water for irrigation in Ayoun Musa area

5.4.2. Settlement development

El-Qaá plain could be an attractive area for the population in southern Sinai, it represents a large area for rural development, and these are big reserves of groundwater and several tracks which can be transformed in good roads. The dangerous flash floods can be larged avoid. Therefore, depending on the previous discussions about El-Qaá plain, it could be suggested a perspective for new villages, cities, and ports in the study area (Fig 5-8). The settlement perspective of El-Qaá plain is concentrated along the highway Suez-Sharm El-Sheikh containing 14 new villages, two new cities, two ports, and a proposed new road along the contour line of 100m a.s.l. to create a good communication among new villages and cities (Fig 5-8).

The position of new cities is selected by functional aspects, i.e. to service all villages. The position of the first city should be in the middle between Firan crossing and El-Tur city, and that of the second city about 35 km South of El-Tur. The two new ports should being constructed at places without coral reef and not to far new industrial zones.

5.4.3. Industrial development

The industry in the study area should depend firstly on the local resources such as agricultural products, petro-chemical industry and mining. Based on the observations during field work, the soil of southern El-Qaá plain can not cultivated whereas it is characterized by rocky surfaces. Therefore, this could be a suitable place to construct an industrial center to serve the whole area (Fig 5-8). In addition, this area is closed to a new projected exportation port in Ras Gara.

5.4.4. Tourism development

The study area has several requirements of tourism; the coast with several types of Coral reef is considered an attractive area for diving. The touristic development depends on spectacular natural resources like marine life, safari, and diving at coral reefs along the Suez Gulf. The Tourism on the Gulf of Suez coast could be progressed rapidly with other economic activities if the government makes a politic decision. These could be constructed several tourist centers distributed along the coast especially south of El-Tur city towards Sharm El-Sheikh (Fig 5-8).

Conclusions

Physical setting

1. The igneous and volcanic rocks cover nearly 2629.21 km² at about 43.3 % of the study area, where as the metamorphic rocks cover about 179.41 km², which is nearly 3% of the total area and the sedimentary rocks expand on the surface for 791.49 km² at about 12.9%. But recent deposits cover 2468.49 km² nearly at 40.8%; they are distributed on deltas and alluvial fans, terraces, wadi deposits and sabkhas.

2. Clay deposit (< 0.002mm) ratios have more variations between the main basins of the study area; very low clay ratios were found in the basins which drain from igneous and metamorphic rocks. The ratio of clay represent 1.12 % of total sample o.k. of Wadi Asla, 1.27% in Wadi Amlaq, 1.48% in sample 1 of Wadi El-Taalby 1, and 1.36 in sample1 of Wadi Meiar.

3. Silt deposits (0.002- 0.063mm) in the study area have a low ratio which contain categories fU, mU, and gU. The total ratios of these categories have been recorded as low in basins such as Wadi El-Taalby 4.9%, Wadi Aat El-Gharby 3.4%, and Wadi Asla 3.54% of total weight of samples, whereas the average of silt ratios of all samples in Wadi Meiar, and Wadi El-Aawag has represented about 20.1%, and 23.6% respectively.

4. Sand deposits (0.063- 2.0mm) represent highest ratios of weight samples in the study area. Sand deposits form about 93% of Wadi El-Taalby samples, 94% of Wadi Amlaq samples, 92% of Wadi Asla samples, 56.7% of Wadi El-Aawag samples, and 72.6% of Wadi Meiar samples. Consequently, it can be said that the deposits of the study area consist of mostly coarse deposits which had probably kept a big amount of paleoflood water and can be considered it as big ground water storage.

5. The samples have nearly the same ratios of $CaCl_2$ calcium chloride which range between 7.22% in Wadi El-Taalby to 8.13% in Wadi El-Aawag, but the ratios of calcium carbonate $CaCO_3$ range within 0.0% of some samples in Wadi Asla and Wadi Meiar, 23.45 % in the samples2 of Wadi Aat El-Gharby, and 40.87% in the samples 4 of Wadi El-Aawag.

6. OSL dating has evidenced that the age of alluvial deposits which are found in the small Wadi Moreikh ranges between 24.7-40 ka, and the study area during this period had influenced by humid and semi humid climate. Whereas, through earlier Thermo-luminescence (TL) dating**,** RÖGNER, ET AL 2004 concluded that the layered silts of the wadis of central Sinai are alluvial loesses. They contain Miocene foraminifera, which originate from the center of the Ataqua anticline in the Gulf of Suez, where loose Miocene globigerina marls formed outcrops at the surface 20-27 ka ago.

7. July is considered the month with the highest temperature during the year, while the daily mean temperature has recorded for about 37.2˚C at Sharm El-Sheikh, 35.5˚C at Ras Sudr, 35.4˚C at Nekhel and 32.9˚C in Abu Rudeis.

8. January has the lowest temperature at St. Catherine with mean value 0.5˚C, 0.7˚C at Nekhel, 8.4˚C at Ras Sudr and 9.9˚C at El-Tur, while the lowest mean of temperature in December is recorded at Nekhel with 0.9˚C and 1.8˚C at St. Catherine.

9. The mean of evaporation in the high altitude area of St. Catherine area (2000-2650m) increases, whereas the annual range is recorded at about 11.6 mm/day. The July is considered being the month with highest evaporation and lowest relative humidity, with regard to wind speed, especially of Al-khamasin wind

10. Relative humidity has increased at the coastal stations more than at inland stations such as Ras Sudr station 58%, Abu Rudeis 56% and El-Tur 59% especially in summer season due to the evaporation increasing.

11. the average wind speed is about 5-20 knot/h. Maximum speed has been recorded at El-Tur to 20 knot/h in June, 19 knot/h in August and September, but, at St. Catherine maximum speed has recorded in October and November to 18 knot/h. Relative high speed is reported in summer during June and July along the Gulf of Suez at El-Tur and Abu Rudeis stations, while the minima speed has measured to 4 knot/h in February at Ras Sudr and St. Catherine stations.

12. ETM image analysis and field work show that the soils especially in northern part of El-Qaá plain are derived from several common rocks of different igneous, metamorphic and sedimentary origins, whereas in northern extremities of the plain in the area of country hills, wadis are cutting through the three types of major common rocks.

13. Plants in the study area are restricted to microenvironments (as in wadis, channels and depressions) where runoff water collects and provides sufficient moisture for plant growth.

Drainage basin analysis

14. The total stream lengths of the basins in the study area reach 15621.6 km. The streams of the first order occupy 63.4%, of the second order 19.6%, of the third order 8.6%, and the seventh order 0.6%. On the other hand, there is an obvious increment in the total length of high tributary streams (1^{st}, 2^{nd} and 3^{rd} 81.6%) and an obvious decrease in the total of the streams of higher order.

15. the values of drainage density in the main basins of study area range between 1.7km/km^2 for Wadi Timan basin and 2.9km/km^2 in Wadi Firan basin with average 2.4km/km^2 of total study area. The relative increase of drainage density in Wadi Firan basin is related to the morphology of basin surface which is characterized by rugged relief and steep slopes especially in the upper part of the basin.

16. There is a strong positive relationship between drainage density (**Dd**), slopes of streams (0.97), and texture ratios (0.64). Finally, the relation is positive and strong between texture radios and slops (0.82).

17. The relation is negative and strong between the stream orders (**u**) and each of stream numbers like length, drainage density, and slope while it is positive between the orders and stream length (0.75), as well as the area of these orders (0.90). This means that, the more the number of streams, the more the area of basins and their lengths and widths.

18. The geomorphological stage has played a significant role to the occurrence of some consequent drainage patterns such as dendritic parallel pattern, whereas, the dendritic (first) drainage pattern is considered a preamble to form the parallel drainage pattern (second) with prescription. This means that the stage has played a main role to change types of drainage patterns.

19. The relationship between the basins area and orders is a strong direct proportion which ranges between 0.910 in Wadi Aat El-gharby basin and 0.786 in Wadi Asla

basin. This means that whenever the order was increasing the average area of stream order increased directly.

20. The area has a strong positive relation with each stream number (0.99), basin width (0.98), texture ratio (095), basin perimeter, and basin length, but this relation is negative between the area and drainage density (-0.69). Whereas, the more the basin area is extended the more drainage density is decreasing.

21. Structure geology has played the main role by changing the shape of basins, especially in the southern basin of the study area which is mostly covered by metamorphic and igneous rocks, whereas the hydrologic and climatic conditions in this area are strongly limited. But north basins (Araba, El-Aawag) have been affected by hydrologic and climatic conditions compared with structure condition (faults, joints and folds) and geomorphological stage.

22. Wadi Firan basin registers the lowest relief ratio among all other basins (33.3m/km), followed by Wadi Araba basin (46.5m/km), then Wadi El-Aawag basin (57.4m/km), whereas Wadi Abu Markh basin registers the highest ratio in relief (77.8m/km).

23. The value of relative relief increases gradually, it reaches 27m/km in Wadi Abu Markh. This means that basins with large areas underwent a faster progress in erosve actions than the basins with small areas.

24. The hypsometric curve shows that all basins in the study area are within the mature stage according to Strahler's classification (1952), whereas all values are less than 40%. Wadi Aat El-Gharby basin has the lowest value of stable mass (14%) and 86% of basin surface are eroded, followed by El-taalby basin (16%), while the stable mass of Wadi Firan basin reaches to 37%.

25. Alluvial fans ranges from a few 2.1 to 69.3 km^2 with an average value exceeding 18.5 km^2. The largest mapped fans are Firan (69.3 km^2) and Habran (58.5 km^2). Fan length, measured along the steepest gradient (i.e., at right angle to contour lines), from the apex to the distal boundary contacting the external plain, varies from Hadahid with 1.8 km to Habran with 11.4 km. Within the mapped features, altitude ranges from sea level at Araba W fan to 520 m at Timan fan.

26. The fans with high average topographic gradients exhibit small total relief but high values of relative relief. These fans are small (Hadahid). On the contrary, alluvial fans with high values of total relief (with the exception of Firan) show low values of topographic gradient and a large areal extent (i.e. Habran).

Rainfall and Losses

27. Orographic rainfall is the main type of rainfall which occurs when masses of air pushed by wind encounter sizeable objects or land formations they cannot pass, such as high mountains (hence its name of orographic rainfall).

28. The Red Sea Trough extends from equatorial eastern Africa towards Sinai, northwards along the Red Sea, and is accompanied by widespread rainfall. it is characterized by southerly winds over Sinai at the 500 hPa level. This parameter is the most powerful predictor for major floods and crucial for activation of the frequent Red Sea Trough at the surface.

29. The relief plays an important role to increase the number of thunder storm days in the study area which ranges between 1.8 days in St. Catherine station (1350m), 1.4 days in Nekhel (460m), and one day in El-Tur station.

30. The amount of rainfall decreases from west toward east, while, the annually average of rainfall during observation years in Ras Sudr station has reached 14.4mm, Abu-rudeis staion 16.4mm, El-Tur Station 7.8mm, and Sharm El-Sheikh station 23.8mm, but the amounts of rainfall in Nekhel and St. Catherine stations have reached 37.9mm and 64.3mm consecutively.

31. December is considered having the highest rainfall in most stations of south Sinai during the year, where the monthly rainfall has recorded for about 6.7mm in Abu Rudeis, 2.7mm in El-Tur, and 23.4mm in Sharm El-Sheikh.

32. The highest rainfall in autumn season is recorded to 25.2mm and 11.3 mm which represent 39.2 %, 29.8% of total rainfall respectively in St. Catherine and Nekhel stations, whereas, the highest rainfall in spring season is recorded to 28.8mm, and 4.8mm respectively, this represents 44.8%, and 33.3% of total rainfall in St. Catherine and Nekhel stations.

33. The rainy days number in the upland stations is higher than those of coastal stations. Nekhel and St. Catherine as upland stations reach 20.8 days, and 33.4

days respectively, whereas the coastal stations El-Tur and Abu Rudeis only reach 5 and 9.6 days consecutively.

34. The rainy storms can be followed to forecasting flash floods from satellite images to avoid the flood hazards; this method can be used to calibrate rainfall estimates from other satellites. The TRMM-based, near-real time Multi- satellite Precipitation Analysis (MPA) at the NASA Goddard Space Flight Center monitors rainfall over the global Tropics.

35. The total amount of rainfall in the study area has been computed using the isohyetal method and reaches to 182.86 million m^3/ year,

36. The return period of maximum rainfall in the study area during the record period (15 years) reaches to 1.1 and probability of the maximum rainfall (76.5 mm/ day) has been estimated at 94% during the same period, but the frequency of maximum rainfall ranges between 0.1 in 2 years and 6.3 in 100 years.

37. The return period of influence of amount of rainfall (from 10 to 20mm /day) is approximately 1.1, and the frequency ranges between 0.8 during 2 years and 37. 5 in 100 years, whereas the return period of the amount of rainfall (from 20 to 50mm/ day) reaches to 4.4, and the frequency ranges from 1.1 during 2 years and 12.5 in 100 years.

38. The average daily amounts of evaporation values range from one station to another in conformity with situation, altitude, and local relief. Sharm El-Sheikh station has a higher value of daily evaporation, 13.4mm/day, while St. Catherine station has a lower value, 7.6mm/day; the average of total area has reached 8.9mm/day.

39. The total evaporation losses in rainy months in the study area ranges from 45.58 millions m^3/day in January to 66.86 millions m^3/day in October, while the average of evaporation losses during rainy months reaches about 54.09 millions m^3/day.

40. Infiltration losses of water in the study area has been related with some variables, i.e. local relief, slope angels, thickness of deposits and their humidity, time of rainstorm, and plant cover, in addition, kind of rock and its characteristics such as porosity, permeability and structure.

41. The permeability is mostly related with outcrop lithology of the study area, whereas the lowest values of permeability were found in granite, slate, schist, volcanic, and gneiss rocks to 3790 m^3/day/km^2, and the areas which are covered with sedimentary rocks have permeability values between 0.076 to 151.4 million m^3/day/km^2. Whereas, the alluvial fans (gravels and boulders) which cover about 28.8% of total area have the highest values of permeability in the study area 151.4 million m^3/day/ km^2.

Assessment of flood hazard

42. The *Soil Conservation Services Method* (*SCS*) was used to compute some variables such as curve number (CN) and time concentration (TC), and lag time. Equations of SCS are the best for arid areas because they have the most variables which are used to estimate runoff.

43. The values of runoff coefficient in the main basin in the study area range between 4.9 and 15.2 owing to local factors. High values of runoff coefficient (> 11) have related to the large basins such as Wadi El Akgdar, Wadi El-Sheikh, and Wadi Solave which are tributaries of Wadi Firan.

44. The lag time ranged between 1.97 (hr) in Wadi Amlaha and 13.4 (hr) in Wadi El-Akhdar with average 5.6 (hr). Whereas, runoff may occur during heavy rainfall in Wadi Firan in the period ranging between 3 and 4 hours, in Wadi El-Aawag after nearly 3 hours, and in Wadi Meiar runoff may be coming after 2 hours.

45. Time of concentration of runoff in the study area ranges between 0.7 (hr) in Wadi Gebah to 12.0 (hr) in Wadi El-Aawag. Whereas, the basins which have time concentration of runoff more than 3 hours contain all big basins such as Wadi El-Akhdar 5.4 (hr), Wadi El-Sheikh 4.8 (hr), Wadi Solave 3.6 (hr), and Wadi El-Aawag basin 12.3(hr). All wadis in this category except Wadi El-Aawag are considered more dangerous during runoff especially Wadi El-Sheikh and Wadi Solav which are the upper tributaries of Wadi Firan.

46. Runoff volume in the different basins in the study area has been influenced by basins area, altitude, rainfall amount, and the thickness of deposits. Wadi Firan basin has the biggest runoff volume in the study area 9.9 (million m^3) which is about 65.8% of total runoff volume in the study area, and Wadi El-Aawag has about 3 (million m^3) for about 20.1% of runoff volume in El-Qaà plain area.

47. The average peak of runoff values ranges between 1.8 m^3/s in Wadi Moreikh, and 177 m^3/s in Wadi El-Sheikh. The higher category has values more than 150 m^3/s, and includes Wadi El-Akgdar 159.7 (m^3/s), Wadi El-Sheikh 177 (m^3/s), and Wadi Solave 157.1 (m^3/s) which are the upper tributaries of Wadi Firan.

48. According to extreme event analysis (more than 10mm) and some information from Bedouins (local population), runoff had often occurred in the study area in the years of 1980, 1982, 1985, 1989, 1991,1994, 1996, 1997 and 2004. Bedouins reported runoff occurred in March 1991 (big flood) and November 2004. Consequently, it can be considered that both March and November have about 67% of total runoff number in the study area with dangerous effects.

50. The extracted drainage network in the floodplain area was modified manually due to insufficient DEM resolution. In El-Qaà plain area, it could be getting over this problem by using ERDAS imagine program to convert the image from format *.img to format *.grid. Consequently, it could be determining the actually channels of the main basins especially above the plain area which has been influenced by flash floods.

Risk zone map

51. The flash floods are concentrated predominately along the main channels especially in the mountainous area of the investigated basins which are characterized by steep slope and narrow channel; the risk in these areas is strongly limited at the main streams. By contrast, some basins such as Wadi Firan and Wadi El-Aawag basin have wide channels and contain some large valleys with broad valley bottoms where Bedouin villages and cultivated areasare found. Consequently, these cultivated areas and villages often have been destroyed during flash floods.

52. Wadi Firan basin with the villages (El-Tarfa and Firan villages) is considered as the more dangerous. The flash flood of it is classified as high resulting from the same classification in the three main tributaries. Along a 50km distance of Wadi Firan toward Suez Gulf, the flash flood width of the main channel is classified as very high.

53. Wadi El-Aawag basin has also high floods during runoff especially along the last 30 km of the main stream toward the outlet area, while the main tributaries of it

such as Wadi Habran and Wadi Meiar basins have moderate floods. The affected areas are limited along the main channels sometimes attacking the Bedouin villages in El-Qaà plain.

Flood hazard mitigation and development of the area

54. The total population of the study area was at 9,514 persons in 1986 and at 19,825 persons in 1996 with a big growth rate of about 10%, while it was at 42,713 persons in 2006. The increase of the total population in the study area especially in El-Tur city is corresponding with the local migration from Nile Delta region.

55. There are two highways and several tracks in the study area which are often attacked by flash floods especially in the parts crossing the main channels of Wadi Firan and Wadi El-Aawag, and additionally other crosses between the highway and the main wadis in the study area.

56. El-Qaá plain has a big amount of groundwater, the level of which is 25m a.s.l, in the center of El-Qaá plain and 5m a.s.l, near El-Tur city, while water level in El-Wadi village ranges from 5.2 to 13.9m a.s.l, from 1.1 to 13.6 m a.s.l, in south of El-Tur.

57. The standard volume of the main aquifer of El-Qaá plain is approximately 83.6×10^9 m^3. Therefore, total groundwater storage is estimated at 12.5×10^9 m^3 in the northern part of El-Qaá plain. While the totals increase of groundwater storage during the mentioned period (1994 to 1996) is calculated to 36.6×10^6 m^3. In addition, annual extraction of groundwater is estimated to 3.4×10^6 m^3.

58. It has been demonstrated that the location of sites particularly at risk from threatened by large peak flows associated with flash flooding may be predicted using a hydrological model in which key parameters were derived from conventional topographic maps, field survey and a land cover map derived from satellite remote sensing.

59. The afforestation conditions affect the infiltration-runoff process in the catchment, as reflected hydrologically by the CN value. Accordingly, the weighted average of CN values for the main basin in the study area ranged between 12 in Wadi Ghowaitat and 76 in Wadi Solav, the values are related to the outcrop lithology of the study area.

60. Storing flood water in reservoirs and detention basins behind dams is another alternative for flood mitigation and control. The topography of the catchments in Wadi Firan, Wadi Meiar, and Wadi El-Aawag seems to allow the construction of these reservoirs to mitigate the hazard.

61. Wadi Firan basin has most bridges crossing between the main channel and their main tributaries such as Wadi Solave which has a peak runoff of 157.1 m^3/s, Wadi El-Akhdar of 159.7 m^3/s, Wadi El-Raha of 73.3 m^3/s, and Wadi Nesreen of 30.2 m^3/s. all these tributaries have a direct effect on the highway toward St. Catherine city.

62. The suggestion Culvert crossings are distributed in the study area in the crosses between the main tributaries channels and the roads. Because St. Catherine highway runs along the main channel of Wadi Firan, it has most of suggestion culverts whereas most channels of its tributaries are rectangular with the road.

63. Based on available topographic, contour, DEM, drainage network, structure, outcrop lithology, and field work observations of the study area, it could be determining a number of locations are possible sites for constructing storage dams. Wadi Firan basin has four favorable narrow places to construct storage dams in the main channels of its tributaries such as Wadi El-Akhdar, Wadi Solav, Wadi El-Raha, and Wadi Nesreen. Wadi El-Aawag contains two suggestion dams in Wadi Habran and Wadi Meiar.

64. The diversen channel tools of the main channel of Wadi Firan may be not effectual tools, especially during high flash flood; it is quite probable that the wall which was constructed to change the channel may be destroyed by high flood. Therefore, the best method may be deeping the main channel of Wadi Firan above the delta to Suez Gulf.

65. There is a large area prone to cultivating in El-Qaá plain of about 803.2 km^2 which is distributed in the wide channel and the delta of Wadi Firan at about 47.1 km^2, the areas between the main channels of tributaries of Wadi El-Aawag above El-Qaá plain at 505.2 km^2, and the southern basins have about 256.9 km^2.

66. The settlement perspective of El-Qaá plain is often distributed along the highway Suez- Sharm El-Sheikh and contains 14 new villages, two new cities,

two ports, and a new suggestion road along the contour line of 100m to allow a good communication among new villages and cities.

67. Tourism development on the Gulf of Suez coast could be growing rapidly with other economic activities if the government has a politic decision. It can be constructed many tourist centers which are distributed along the coast especially southern El-Tur city.

References

- ABDALLAH, A., ABU KHADRAH, A (1976): Remarks on the geomorphology of the Sinai Peninsula and its associated rocks. Egypt, Colloquium on the Geology of the Aegean Region, Athens, Vol. 1: 509-516.
- ABDALLAH, A., ELKIKI, M., ABOU KHADRAH, A., AND EL REFEAI, A. (1995): Paleohydrogeology of southern Sinai, Egypt, Sedimentology of Egypt, vol.3, p. 95-110.
- ABDALLAH, A., ET AL (1995): Paleohydrology og southern Sinai, Egypt, Sedimentology of Egypt, Vol. 3, P. 95-110.
- ABDEL AAL, M. (1995): Environmental Geological studies on the Gulf of Aqaba coastal region, Egypt. PhD. Thesis (Environmental geology). Geology, Dept., Fac. Science, Mansoura University
- ABDEL TAWAB, S. (1989): Engineering Geology of some areas in The Greater Cairo, PhD. Thesis, Geology, Dept., Fac., Science, Ain Shams University.
- ABDEL-HADY, ET AL (1991): Contribution of Landsat data (MSS) to soil survey: application to the soil of southwestern Sinai (Egypt), Int. J. Remote sensing, Vol. 12, No. 5, PP. 1053-1061.
- ABDEL-HADY, ET AL (1995): Land capability classification of Sinai Peninsula, National Authority for Remote Sensing and Space Sciences, Cairo, Egypt.
- ABDEL-MAGUID, A., FAYED, L. AND MOSTAFA, M. (1998): Geotechnical and environmental hayards in desert new cities: A case study of El Minia El Gedida site, Egypt, Kluwer Academic Publishers. Netherlands, natural hazards 17: 47-67.
- ABDEL-MEGUID, A., ET AL (1998): Geotechnical and Environmental hazards in desert new cities: A case study of El Minia El Gedida site, Egypt, natural hazards 17: 47-67.
- ABDULRAZZAK M. J., SORMAN A. U. (1993): Infiltration recharge through wadi beds in arid regions. Hydrol Sci J 38(3):173–186.
- ABDULRAZZAK, M. J., SORMAN, A. U. (1994): Transmission losses from ephemeral streams in arid region, J. Irrig. Drain. Engrg, ASCE, 120, 669-675.
- ABRAHAMS (1984): Channel networks: a geomorphological perspective. Water Resour Res, 20:161–168
- ABU FARAH MD., ET AL (2005): Effects of Forest Thinning on Direct Runoff and Peak Runoff Properties in a Small Mountainous Watershed in Kochi Prefecture, Japan, Pakistan Journal of Biological Sciences 8 (2): 259-266
- ADEDIRAN, A.O., PARCHARIDIS, I., POSCOLIERI, M., AND PAVLOPOULOS, K. (2004): Computer-assisted discrimination of morphological units on north-central Crete (Greece) by applying multivariate statistics to local relief gradients. Geomorphology 58, 357–370.

- AKL, M.T. (1994): An approach to the morphometric analysis of wadi Tayyibah drainage basin through using geographic information systems (GIS), Menoufia University, Faculty of Arts Journal, vol.19, pp.91-146.
- AL DESOKY, T. (1995): The climate characterized which go together with flash flood in ASHMAWY, M., SWEDAN, A. ABDEL FATAH, T. (2000): Flash flood hazards of drainage basins of Sinai Peninsula, Egypt, Annals Geol. Survey., Egypt, V. xxxIII, pp.467-489.
- AL SALEH, M., KING, S. (1991): Alluvium thickness and stream orders relationships in wadi Al-Khanagah basin, central Saudi Arabia, GeoJournal 24.4, Kluwer Academic Publishers, pp.421-426.
- ALI, D., (1998): Case Study of Development of the Peripheral Coastal Area Of South Sinai in Relation to its Bedouin Community, Master of Urban and Regional Planning, Blacksburg, Virginia
- ALPERT, P. NEEMAN, B.U. (1992): Cold small-scale cyclones over the Eastern Mediterranean: Tellus, v. 44A, p. 173–179.
- ALPERT, P., SHAFIR, H., (1989): 'Physical Model to Complement Rainfall Normals over a Complex Terrain', J. Hydrol. 110, 51–62.
- AL-WESHAH R. (2002): Rainfall- Runoff analysis and modiling in Wadi systems, Department of Civil Engineering, University of Jordan, Amman, Jordan
- ASHOUR, M. (2002): Flash flood in Egypt- A case study of Durunka village – upper Egypt, Soc., geog. Egypt, vol. 75.
- BAKER, V.R. (1977): Stream-channel response to floods, with examples from Central Texas. Geological Society of Amerika, Bulletin 88, 1057-1071.
- BALL, J. (1916): The geography and geology of west central Sinai, Egypt. Survey Dept., Cairo.
- BANASIK, K., ET AL (2005): An investigation of lag times for rainfall–runoff– sediment yield events in small river basins, Hydrological Sciences–Journal–des Sciences Hydrologiques, 50
- BAND L. (1986): Topographic partition of watersheds with digital elevation models. Water Resour Res 22(1):15–24
- BARRON, T. (1907): The topography and geology of the peninsula of Sinai: Western portion. Geol. Survey. Egypt.
- BARROW, A. P., LETTENMEIER, D. P. (1994): 'Dynamic Modelling of Orographically-Induced Precipitation', Rev. Geophys. 32, 265–284.
- BASIST, A., BELL, G. D., AND MEENTEMEYER, V. (1994): 'Statistical Relationships between Topography and Precipitation Patterns', J. Climate 7(9), 1305–1315.

- BATES, B. C., PILGRIM, D. H. (1986): Simple models for non-linear runoff routing. Civil Engng Trans., IE Aust. CE28 (4), 284-291
- BAUMGARDNER (1987): Morphometric studies of subhumid and semiarid drainage basin, Texas Panhandle and Northeastern New Mexico. Austin Univ Texas Bur Econ Geol Rept Invest 163:66
- BEAUMONT, P. (1972): Alluvial fans along the foothills of the Elburz Mountains, Iran. Paleogeography, Paleoclimate, Paleoecol. 12: 251-273.
- BEN-YVI, A. (1996): Quantitative prediction of runoff events. In: A.S. Issar and S.D. Resnick, Editors, Runoff, Infiltration, and Subsurface Flow of Water in Arid and Semi-Arid Regions vol. 21, Water Science and Technology Library, Kluwer Academic Publishers, Norwel, Massachusetts (1996), pp. 121–130.
- BERGKAMP, G., CAMMERAAT, L.H., AND MARTI´NEZ, J. (1996): Water movement and vegetation patterns on shrubland and a abandoned field in two desertification threatened areas in Spain. Earth Surface Processes and Landforms 21, 1073– 109
- BETSON, R. P. (1964): (What Is Watershed Runoff?) Journal of Geophysical Research, 68: 1541-1552.
- BEVEN, K. J. (2000): Rainfall Runoff Modelling. The Primer, John Wiley, Chichester.
- BONACCI, O., ET AL (2006): Karst flash flood: an example from the Dinaric karst (Croatia), Nat. Hazards Earth Syst. Sci., 6, 195–203.
- BOYD, M. J., BUFILL, M. C. (1989): Determining runoff routing model parameters without rainfall data. J. Hydrol. 108, 281-294
- BULL, W.B. (1962): Relations on alluvial-fan size and slope to drainage-basin size and lithology in western Fresno County, California. U.S., Geol. Surv. Prof. Pap., 450B: 51-53.
- BULL, W.B. (1964): Geomorphology of segmented alluvial fans in western Fresno County, California. U.S., Geol. Surv. Prof. Pap., 352E: 89-129.
- BULL, W.B., (1977): The alluvial fan environment. Prog. Phys. Geogr., 1: 222-270.
- CARLSTON, C. W. (1963): 'Drainage density and stream flow', USGS Professional Paper, 422-C, 1–8.
- CASES, A. ET AL (2003): Runoff generation, sediment movement and soil water behaviour on calcareous (limestone) slopes of some Mediterranean environments in southeast Spain, ElSEVIER, Geomorphology 50 (2003) 269–291
- CEOS (2003): The use of earth observing satellites for hazard support: assessments and scenarios. Final Report of the CEOS Disaster Management Support Group (DMSG), November

- CHORLEY, R. J., MORGAN, M. A. (1962): 'Comparison of morphometric features, Unaka Mountains, Tennessee and North Carolina, Dartmoor, England', Geological Society of America Bulletin, 73, 17–34.
- CHORLEY, R.J. (1957) Climate and morphometry. J. Geol. 65.
- CHURCH, M.A., MARK, D.M. (1980): On size and scale in geomorphology. Prog. Phys., Geogr., 4: 342-390.
- CLARK M. J., (1998): Putting Water in its Place: A Perspective on GIS in Hydrology and Water Management, Hydrological Processes 12, pp. 823-834, John Wilwy & Sons Ltd.
- COOKE, G., WARRAN, A. (1973): Geomorphology in deserts, Batsford, London 394 pp.
- COTTON, C. A. (1964): 'The control of drainage density', New Zealand Journal of Geology and Geophysics, 7, 348–352.
- DALE, F., CRAIG, R., AND JERRY, R. (1995): Process geomorphology, Wisconsin New York.
- DANIN, A. (1978): Plant species diversity and ecological districts of the Sinai desert. Vegetation 36, 83–93.
- DANIN, A. (1983): Desert Vegetation of Israel and Sinai, Cana Publishing House, Jerusalem, pp 148.
- DAVID, G. (2003): Rainfall- Runoff Processes, Utah State University.
- DAVID, L. ET AL (2000): Revision of the rainfall intensity duration curves for commonwealth of Kentucky, Lexington.
- DAYAN, U., ABRAMSKI, R. (1983): Heavy rain in the Middle East related to unusual jet stream properties: Bulletin of the American Meteorological Society, v. 64, p. 1138–1140.
- DAYAN, U., MORIN, E. (2006): Flash flood–producing rainstorms over the Dead Sea, Geological Society of America,
- DAYAN, U., ZIV, B., MARGALIT, A., MORIN, E., AND SHARON, D. (2001): A severe autumn storm over the Middle-East: Synoptic and mesoscale convection analysis: Theoretical and Applied Climatology, v. 69, p. 103–122.
- DAYAN, U., ZIV, B., MARGALIT, A., MORIN, E., AND SHARON, D. (2001): A severe autumn storm over the Middle-East: Synoptic and mesoscale convection analysis: Theoretical and Applied Climatology, v. 69, p. 103–122.
- DEHN, M., GÄRTNER, H., AND DIKAU, R. (2001): Principles of semantic modeling of landform structures. Comput. Geosci. 27 (8), 1005– 1010
- DOGAN, E., DEMİR A. (2006): Evaporation Amount Calculation of Sapanca Lake by Using Genetic Algorithm and Neural Networks, Proceedings of 5th International Symposium on Intelligent Manufacturing Systems, May 29-31, 2006: 1239-1250
- DOMENICO, P., A. SCHWARTZ, F., W. (1990): Physical and chemical hydrogeology, John Wiley & Sons, New York.

- DOORNKAMP, J. C., KING, C., A. (1971): Numerical analysis in Geomorphology: An introduction, London.
- EDMUND, P. (1999): Floods, Applied geography, principles and practice, Michael, Routledge, London, Part 1 Chapter 7, pp.95-108.
- EL BARODI, M. (1986): The hydrological balance of Wadi Fatma Basin, (in Arabic). Geogr. .Soc. of Kuwait, 88
- EL BAZ, F. HIMIDA, I. MITSAH, MISSAK, R. AND ABDEL MOGHEETH, S. (1995): Dam site selection criteria for flash flood control in Wadi wateer, south Sinai, Egypt Geol. Surv. Egypt.
- EL GHAYAWI, M. KORANY, E. AND FAIAD, B. (2000): Hydrogeological evaluation of the quaternary aquifer in the delta of Wadi El-Atfihy, eastern desert, Egypt, annals Geol. Surv. Egypt, V.xxxIII, pp. 883-900.
- EL MASRY, N. ET AL (1992): Reconsideration of the geologic evolution of Saint Catherine ring dyke, south Sinai, Geol. Sinai Develop., Ismailia, Egypt, pp. 229-238.
- EL NAHRY, A., SALEH, A. (2003): Influence of flash floods on terrain and soils of El-Qaà plain, south Sinai, Egypt, National Authority for remote sensing and space sciences, Cairo, Egypt.
- EL RAKAIBY, M. (1991): Drainage basins and flash flood hazard in selected parts of Egypt, Geog .Soc. of Egypt.
- EL SHAMY, I. (1995): The control of flood, Geogr. Soc. of Egypt, (in Arabic)
- EL SHAMY, I., EL RAYES, A. (1992): Hydrogeologic assessment of Saint Catherine area , south Sinai, Geol. Sinai Develop., Ismailia, Egypt, pp. 71-76.
- EL SHAZLY, E., EL RAKAIBY, M., AND EL KASSAS, I. (1983): Groundwater investigation in Wadi Araba area eastern desert of Egypt, using landsat imagery, Symposium on Remote Sensing of Environment, Ann Arbor, Michigan.
- EL-GHAREEB, R., SHABANA, M.A. (1990): Vegetation-environment relationships in the bed of Wadi El-Sheikh of southern Sinai. Vegetatio 90, 145–157.
- EL-HAKAMANI, A. (2006): Flood Control Project in Salalah, Oman, Technical Coordinator, Dhofar Municipality, P.O., Box: 50, P.C.: 211, Salalah, Oman
- ENGMAN, E.T., GURNEY, R.J., (1991): Remote Sensing in Hydrology. Chapman and Hall, London.
- FARIS, M., EL DEEB, W., AND MANDUR, M. (2000): Biostratigraphy of some Upper Cretaceous / Lower Eocene successions in southwest Sinai, Egypt, Annals Geol. Surv. Egypt, V.xxxIII, pp.135-161
- FITZJOHN C., TERNAN, J.L., AND WILLIAMS A.G. (1998): Soil moisture variability in a semi-arid gully catchment: implications for runoff and erosion control. Catena 32, 55–70.

- FOODY, G., GHONEIM, E., ARNELL, N., (2004): Prediction locations sensitive to flash flooding in an arid environment, Journal of hydrology, 292, pp. 48-58.
- FREEMAN T. (1991): Calculating catchment area with divergent flow based on a regular grid. Comput Geosci 17(3):413–422
- GARBRECH J., STARKS P. (1995): Note on the use of USGS Level 1.75- minute DEM coverages for landscape drainage analyses. Photogrammetric Eng Remote Sensing 61(5):519–522
- GARDINER, V. (1975): Drainage basin morphometry. British Geomorphology Research Group, Technical BULL., No. 14. pp. 3-15.
- GARDINER, V., (1990): Drainage basin morphometry. In: Goudie AS (ed) Geomorphological techniques. Unwin Hyman, London, pp 71–81
- GARFUNKEL, Z., BARTOV, Y. (1977): The tectonic of the Suez rift, Geol. Surv. Israel, Bull, no. 71, 44 p.
- GEOLOGICAL SURVEY OF EGYPT (1994): Geological Map of Sinai, Arab Republic of Egypt (sheet No.1) scale 1:250000, Ministry of Industry and Mineral Resources.
- GHEITH, H., SULTAN, M., (2002): Construction of a hydrologic model for estimating Wadi runoff and groundwater recharge in the Eastern Desert, Egypt. Journal of Hydrology 263, 36–55.
- GOLDREICH, Y. (2003): The climate of Israel: Observation, research and application: London, Kluwer Academic Press, 270 p.
- GOUDIE, A. ET AL (1993): Desert geomorphology, Clazs Limited, London.
- GREGOR, E., TUCKER R. L. (1998): Hillslope processes, drainage density, and landscape morphology, water resources research, vol. 34, No. 10, pp. 2751-2764.
- GREGORY, K. J., GARDINER, V. (1975): Drainage density and climate', Z. Geomorph., 19, 287–298
- GREGORY, K. J., WALLING, D. E. (1973): Drainage Basin Form and Process, Arnold, London, 456 pp.
- GRÜN, R. (2001): Trapped charge dating (ESR, TL, OSL). In Brothwell, D. R. & Pollard, A .M. (eds.): Handbook of Archaeological Sciences. Chichester, John Wiley &Sons, 47-62.
- GRUNERT, J. (1977): Untersuchungsmethoden und Aussagewerte von Flußterrassen arider Gebirge, Mitteilung der Basler Afrika Bibliographien Communications from the Basel Afrika Bibliography, Vol.19.
- GRUNERT, J., BAUMHAUER R. and VÖLKEL J. (1991): Lacustrine sediments and Holocene climates in the southern Sahara: the example of paleolakes in the Grand Erg of Bilma (Zoo Baba and Dibella, eastern Niger). - Journal of African Earth Sciences 12, 1/2, S. 133-146.

- GRUNERT, J., MEYER, B. (1990): Starkegen und Wadiabkommen auf der Nordabdachung des Hoggar-gebirges anfang März 1988, Berliner Geographische Studien, Band 30 Seit 169-192.
- GUMBEL, E. J. (1941): "Probability-interpretation of the observed return-periods of floods," Trans. Am. Geophysical Union, pp. 836-850.
- GUMBEL, E. J. (1941): "The return period of flood flows," Annals of Math. Stat., Vol. 12, pp. 163-190.
- HADIDI, M. N., KOSINOVA. J., AND CHRTECK, J. (1970): Weed flora of southern Sinai. Biologia 1969: 367-381
- HAIDEN, T., KERSCHBAUM, M., KAHLIG, P., AND NOBLIS, F. (1992) 'A Refined Model of the Influence of Orography on the Mesoscale Distribution of Extreme Precipitation', Hydrology Sci. J. 37, 417–427.
- HAMMAD, M. ET AL (1998): Morphology and Mineralogy of El Qaa plain soil –South Sinai, El -Azhar journal of agriculture research, Cairo, Egypt, pp. 196-215.
- HARVEY, A.M. (1984): Debris flows and fluvial deposits in Spanish Quaternary alluvial fans: implications for fan morphology. In: E.H. Koster et al. (Editors), Gravels and Conglomerates. Can. Soc. Pet. Geol. Mem., 10: 123-132.
- HARVEY, A.M. (1988): Controls of alluvial fans development: the alluvial fans of the Sierra de Carrascoy, Murcia, and Spain. Catena Suppl., 13: 123-137.
- HARVEY, A.M. (1990): Factors Influencing Quaternary Alluvial Fan Development in Southeast Spain. In: A.H. Rachocki and M. Church (Editors), Alluvial Fans: A Field Approach. Wiley, pp. 247-269.
- HASHEM, S., EL RAKAIBY. M. (1991): Geomorphology of Sinai Peninsula from landsat satellite images and its potential for landsat, Geog. Soc. of Egypt
- HASSAN, A. ET AL (1982): Encyclopedia of Sinai, (in Arabic). Cairo, Egypt.
- HERSCHY, R., (2002): The world's maximum observed floods. In: Snorasson, A., Finnsdottir, H.P., Moss, M. (Eds.), The Extremes of the Extremes: Extraordinary Floods, 271. IAHS Publication 271, International Association of Hydrological Sciences, Wallington, pp. 355–360.
- HIRSHBOECK, K. (1999): Hydrology of fl oods and droughts—climate and fl oods; National Water Summary 1988–89; Floods and Droughts: Hydrology: U.S: Geological Survey Water-Supply Paper 2375, p. 67–88.
- HOOKE, R.L. (1968): Steady-state relationships on arid region alluvial fans in closed basins. Am. J. Sci., 266: 609-629.
- HORTON, R. E. (1937): Determination of infiltration Capacity for large Drainage basins, Tranc. Am. Geophy. Union, vol. 24, pt. 2, pp. 476-480.

- HORTON, R. E. (1945): Erosional development of stream and their drainage basin: Hydrological approach to quantitative morphology: Bull, Geophys. Soc. Am., v. 56, p. 275–370.
- HORTON, R.E. (1933): The role of infiltration in the hydrological cycle. Trans. Am. Geophys. Union, 14: 446-460
- HOSNY, H. (1989): These of synthetic apparent resistively for solving geoelect. Problems in Cairo – Alexandria desert road, geological survey, Egypt, pp. 281-284.
- IGNACIO, R., LUIS, A. (1982): The dependence of drainage density on climate and geomorphology, Hydrological Sciences – Journal. des Sciences Hydrologiques, 27, 2, 6/1982
- IMESON, A.C., LAVEE, H., CALVO, A., AND CERDA`, A. (1998): The erosional response of calcareous soil along a climatological gradient in Southeast Spain, Geomorphology 24, 3 – 16.
- ISSAWI, B., JUX, W. (1982): Contribution to the stratigraphy of the Paleozoic rocks in Egypt, Geol. Surv. Egypt.
- JABAN INTERNATIONAL COOPERATION AGENCY, (JICA) (1999): South Sinai groundwater resources study in the Arab Republic of Egypt, main report, pacific consultations international, Tokyo in association with sandy consultation. Tokyo.
- JENSON S, DOMINGUE J. (1988): Extracting topographic structure from digital elevation data for geographic information system analysis. Photogrammetric Eng Remote Sens 54:1593–1600
- KAFAFY, A. ET AL (1993): Palaeomagnetic results for some dykes from the Eastern Desert and Sinai. Egypt, J. Geol., 37-1, pp. 233-247.
- KAHANA, R., ZIV, B., DAYAN, U., AND ENZEL, Y. (2004): Atmospheric predictors for major fl oods in the Negev Desert, Israel: International Journal of Climatology, v. 24, p. 1137–1147.
- KAHANA, R., ZIV, B., ENZEL, Y., AND DAYAN, U. (2002): Synoptic climatology of major floods in the Negev Desert, Israel: International Journal of Climatology, v. 22, p. 867–882.
- KASSAB, A. S. OBAIDALLA, N. A. (2001): Integrated biostratigraphy and inter-regional correlation of the Cenomanian-Turonian deposits of Wadi Firan, Sinai, Egypt, Cretaceous Research 22, pp 105-114.
- KASSAS, M. (1966): Plant life in deserts. In: Hills, E.S. (Ed.), Arid Lands, Methuen, London/UNESCO, Paris, pp 461.
- KATRA, I. ET AL (2007): Rainfall distribution around shrubs: Eco-geomorphic implications for arid hillslopes. Geomorphology doi: 10.1016/j. geomorph. 2007 .05.16
- KIRKBY, M. J., ED. (1978): Hillslope Hydrology.

- KNEBL, M.R., YANG, Z. L., HUTCHISON, K., MAIDMENT, D.R., (2005): Regional Scale Flood Modeling using NEXRAD Rainfall, GIS, and HEC-HMS/RAS: Accase study for the San Antonio River Basin Summer 2002 storm event, Journal of Environmental Management 75 pp. 325–336.
- KOSTASCHUK, R.A., MACDONALD, G.M., AND PUTNAM, P.E. (1986): Depositional process and alluvial fan-drainage basin morpho-metric relationships near Banff, Alberta, Canada. Earth Surf, Process. Landforms, 11: 471-484.
- KOUKI, P. (2006): Environmental change and human history in the Jabal Harûn area, Jordan, Dissertation for the degree of Licentiate of PhilosophyDepartment of Cultural Studies, Archaeology, University of Helsinki.
- KRICHAK, S.O., ALPERT, P., AND KRISHNAMURTI, T.N. (1997a): Interaction of topography and tropogpheric flow-A possible generator for the Red Sea Trough: Meteorology and Atmospheric Physics, v. 63, p. 149–158.
- KUSKY, T., EL BAZ F. (2000): Neotectonics and fluvial geomorphology of the northern Sinai Peninsula, Journal of African Earth Sciences, vol. 31, No. 2 pp. 213-238.
- KUSS, J. (1992): Facies and Stratigraphy of Cretaceous Limestones from Northeast Egypt, Sinai, and Southern Jordan, Geology of the Arab world, Cairo University, pp. 283-301.
- LAVEE, H., IMESON, A.C., AND SARAH, P. (1998): The impact of climate change on geomorphology and desertification along a Mediterranean arid transect. Land Degradation and Development 9, 407– 422.
- LECCE, S.A. (1990): The alluvial fan problem. In: A.H. Rachocki and M. Church (Editors), Alluvial Fans: A Field Approach. Wiley, pp. 3-24.
- LEOPOLD, L. B., WOLMAN M. G., AND MILLER, J. P. (1964): Fluvial processes in geomorphology, W. H. Freeman, San Francisco, 522 p.
- LIN, X. (1999): Flash floods in arid and semi-arid zones, IHP-V Technical Documents in Hydrology, no. 23.
- LINSLEY, R. ET AL (1982): Hydrology for engineers, McGraw- Hill, New York.
- LOUKAS, A., QUICK, M. C. (1996) Physically-based estimation of lag time for forested mountainous watersheds, Hydro. Sci. 41 (1) 1-19
- MACKA Z (2001): Determination of texture of topography from large scale contour maps. Geografski Vestnik 73(2):53–62
- MADDOX, R.A. (1980): Mesoscale convective complexes: Bulletin of the American Meteorological Society, v. 61, p. 1374–1387.
- MADDUMA BANDARA, C. M. (1974): 'Drainage density and effective precipitation', Journal of Hydrology, 21, 187–190.
- MAIDMENT (2002) ArcHydro GIS for water resources. Esri Press, California

- MARK, D. (1983): Relation between field-surveyed channel network and map-based geomorphometric measures, Inez Kentucky. Ann Assoc Am Geographers 73(3):358–372
- MARKHAM, C. (1970): Seasonal of Precipitation in the United States, Annals of the Association of American Geography, Vol. 60, No. 3, PP. 593-597.
- MARTI´NEZ-MENA, M., ALBALADEJO, J., AND CASTILLO, V.M. (1998): Factors influencing surface runoff generation in a Mediterranean semiari environment: Chicamo watershed, SE Spain. Hydrological Processes 12, 741–754.
- MARTZ, GARBRECHT J (1998): The threatment of flat areas and closed depression in automated drainage analysis of raster digital elevation models. Hydrol Process 12:843–855
- MELTON, M. A. (1958b): Correlation structure of morphometric properties of drainage systems and their controlling agents, Journal of Geology 66 442–60.
- MELTON, M.A. (1965): The geomorphic and paleoclimatic significance of alluvial deposits is southern Arizona. J. Geol., 73: 1-38.
- MESA, L. M. (2006): Morphometric analysis of a subtropical Andean basin (Tucuman, Argentina), environ Geol, 50: pp. 1235-1242
- MILLS, N.H. (1982): Piedmont-cover deposits on the Dellwood quadrangle, Great Smoky Mountains, North Carolina, U.S.A.: Morphometry. Z. Geomorphol. N.F., 26: 163-178.
- MINA, M., ATTALA, R., SAAD, B., AND SHATYA F. (1993): Groundwater exploration in the basement rocks of Saint Catherine area southern Sinai, Egypt, 30 Years Cooper, PP 461-473.
- MOGLEN, G. E., ET AL (1998): On the sensitivity of drainage density to climate change, Water Resour. Res., 34, 855–862.
- MONOD, TH. (1954): Mode contracted diffuse de la vegetation Saharienne. In: Cloudsley Thompson, J.L. (Ed.), Biology of Desert, Institute of Biology, London, pp 224.
- MONTGOMERY, D. R., DIETRICH, W. E. (1989): Source areas, drainage density, and channel initiation, Water Resour. Res., 25, 1907–1918.
- MONTGOMERY, D. R., DIETRICH, W. E. (1994a): Landscape dissection and drainage area-slope thresholds, in Process Models and Theoretical Geomorphology, edited by M. J. Kirkby, pp. 221–246, John Wiley, New York.
- MOORE, I.D., NIEBER, J. L. (1989): Landscape assessment of soil erosion and non-point source pollution, J. Minn. Acad. Sci. 55, 18– 24.
- MOORE, I.D., TURNER, A.K., WILSON, J.P., JENSON, S.K., AND BAND, L.E. (1993b): GIS and land–surface–subsurface process modeling. In: Goodchild, M.F., Parks, B.O., Steyaert, L.T. (Eds.), Environmental Modeling with GIS. Oxford University Press, New York, pp. 196– 230.

- MORISAWA, M. E. (1957): Accuracy of determination of stream lengths from topographic maps. Ame, geophys, Union Trans., 88, 1, 86-88, Washington
- MORISAWA, M.E. (1962): Quantitative geomorphology of some watersheds in the Appalachian plateau, Geol. Soc. Amer. Bull., 78, 9, 1025--1046, Burlington.
- MOSTAFA, A., EL RAEY, A. (1993): Structure characteristics of the Suez rift margins, Geol., Rundsch, 82, pp. 101-109.
- MOUSTAFA, A. EL RAEY, A. (1993): Structure characteristics of the Suez rift margins, Geol. Rundsch. 82: pp.101-109.
- MOUSTAFA, A.M. (1992): Structure setting of the Sidri- Firan area, eastern side of the Suez rift, MERC, Ain Shams Univ., Earth Sci., Ser., V.6, p.44-50.
- NAGIB, M. (1970): Precipitation in the U.A.R. in relation to different synoptic pattern, Meteo, Bull, Vol., 2
- NAGUIB, N. (2000): Mineralogische und geochemische Untersuchungen an einem Schwemmlöss-Profil in der Oase Firan, Sinai (Ägypten). - Dipl.-Arbeit, Fak. f. Bio-u. Geowissenschaften, Univ. Karlsruhe.
- NEAL, J.T. (1975): Playa surface features as indicators of environment. In Neal, J.T. (Td.), Playa and Dried lakes, Benchmark papers in Geology, Halsted press, p 363.
- NIR, D. (1974): Lacustrine / fluviatile sediments in Firan and Tarfat el Kudrein. - Z. f. Geomorphologie N.F. Suppl. Bd. 22, 32-34.
- NOWEIR, A. EL SHISHTAWY, A. (1996): Structure setting and stratigraphy of the area east of El-Qaà plain, southwestern Sinai, Egypt, J. Geol., 40-1, pp. 1-22.
- O'CALLAGHAN J, MARK (1984): The extraction of drainage networks from digital elevation data. Comput Vis Graph Image Process 28:323–344
- OGUCHI, T. (1997): Drainage density and relative relief in humid steep mountains with frequent slope failure, Earth Surface Processes Landforms, 22, 107–120.
- OHMORI, H. (1978): Relief structure of the Japanese mountains and their stages in geomorphic development. Bull. Dep. Geogr. Univ. Tokyo, 10: 31-85.
- OLIVERA, F., MAIDMENT, D.R., (1999): GIS tools for HMS modeling support. In: Maidment, D.R., Djokic, D. (Eds.), Hydrologic and Hydraulic Modelling Support, ESRI Press, Redlands, CA.
- OZDEMIR, H. BIRD, D. (2008): Evaluation of morphometric parameters of drainage networks derived from topographic maps and DEM in point of floods, Environ Geol DOI 10.1007/s00254-008-1235-y.
- PATTON T.L. (1988): Drainage basin morphometry and floods. In: Baker VR, Kochel RC, Patton PC (eds) Flood geomorphology. Wiley, USA, pp 51–65

- PATTON, T.L. (1982): Surface studies of normal fault geometries in the pre-Miocene stratigraphy west central Sinai Peninsula, 6th Egypt Gen. Petrol. Corp. Expl. Seminar, Cairo, p. 437-452.
- PETER, R.B. (2000): Playa, playa lake, Sabkha: proposed definitions for old terms, journal of Arid Environments, vol. 45, pp 1-7.
- PHILIP, J. R. (1954): An Infiltration Equation with physical Significance, Soil Sci., vol. 77, p. 153.
- PIKE, R.J. (2002): A Bibliography of Terrain Modeling (Geomorphometry), the Quantitative Representation of Topography-Supplement 4.0.Open-File Report 02-465, U.S. Geological Survey.
- PIKE, R.J., DIKAU, R. (1995): Advances in geomorphometry. Z. Geomorph., N.F. Suppl. Bd. 101, 238.
- PONCE, V. M. (1989): Engineering Hydrology, Principles and Practices. Prentice-Hall, Englewood Cliffs, New Jersey
- PUIGDEFA´BREGAS, J., SOLE, A., GUTIERREZ, L., DEL BARRIO, G., AND BOER, M. (1999): Scales and processes of water and sediment redistribution in drylands: results from the Rambla Honda field site in Southeast Spain, Earth-Science Reviews 48, 39– 70.
- RINALDO A, RODRI´GUEZ-ITURBE I, AND RIGON R (1998): Channel networks. In: Jeanloz R, Albee AL, Burke KC (eds) Annual review of earth and planetary sciences, vol 26. Annual Reviews, Palo Alto, pp 289–327
- RÖGNER K., SMYKATZ-KLOSS, W. (1998): The fine-grained loess-like sediments of the Wadi Firan, Sinai, Egypt: Possibilities of palaeoclimatic interpretations? In- Al-sharhan, A.S., Glennie, K.W., Whittle, G.L. & Kendall, C.G.StC. (Eds): Quaternary Deserts and Climatic Change, Balkema, Rotterdam, pp. 209-211.
- RÖGNER K., SMYKATZ-KLOSS, W. AND ZÖHLER, L. (1999): Oberpleistozäne paläoklimatische Veränderungen imZentral-Sinai(Ägypten).-Erdkunde Bd, 33, 220- 230.
- RÖGNER, K., KNABE, K., ROSCHER, B., SMYKATZ-KLOSS, W., AND ZÖLLER, L. (2004): Alluvial loess in the central Sinai: Occurrence, origin, and palaeoclimatological consideration. Palaeoecology of Quaternary Drylands, Springer- Berlin Heidelberg, Germany, pp. 79-99.
- RÖGNER, K., SMYKATZ-KLOSS, W. (1991 a): The deposition of aeolian sediments in lacustrine and fluvial environments of Central Sinai (Egypt), Catena Suppl. 20, 75- 91.
- RÖGNER, K., SMYKATZ-KLOSS, W. (1991 b): Fluviale Geomorphodynamik im Zentralen Sinai wahrend des jüngeren Quartärs, Freiburger Geograph. Hefte 33, 209-221.
- RÖGNER, K. SMYKATZ-KLOSS, W. (1993): The fine-grained sediments'^ Wadi Firan (Sinai, Egypt): Origin and sedimentology. - Z. f. Geomorphologie N.F., Suppl.-Bd. 88, 123- 139.

- RUHE, R. V. (1952): 'Topographic discontinuities of the Des Moines Lobe', American Journal of Science, 250, 46–56
- SAID, R. (1962): the geology of Egypt, Elsevier Pub. Co., Amsterdam, 377p.
- SALEH, A. S., ET AL (1990): Report on Southern Sinai Field Trip for Risk Evaluation of Flash Floods, Remote Sensing Center, Cairo, pp.1-21.
- SALEH, A., S. (1985): Wadi El Arish basin; a geomorphological study (in Arabic). Ph D. Thesis, Geogr. Dept., Fac. Arts., Cairo Univ., Cairo
- SALEH, A., S. (1989): Natural hazards on the eastern sector of Nuweiba- Tunnel national highway, Sinai; a geomorphological study (in Arabic). Bull. Soc. Geog. Egypt., Tom. 62, pp. 143-176.
- SALEM, A., ET AL (1990): report on southern Sinai fild trip for risk evaluation of flash floods, institute for water resources development- South Sinai office.
- SCHECK, A. (1979): Fluvial Processes and Settlement in Arid Environments, Akademische Verlagsgesellschaft, Wiesbaden, GeoJournal 3.4 351-360.
- SCHEIDEGGER A. (1965): Statistical law of stream numbers. Journ. Geology, 74, 17-37.
- SCHROEDER, M. (1991): Fractals, Chaos, and Power Laws, Minutes from an Infinite Paradise. Freeman and Co. Pub., New York, 429 pp.
- SCHUMM S.A. (1956): Evolution of drainage systems and slopes in badlands at Perth Amboy, New Jersey. Geol. Soc. Am.Bull.67:597–646
- SCHUMM S.A. (1963): Sinuosity of alluvial rivers on the Great Plains. Geol. Soc. Am. Bull. 74:1089–1100
- SCHUMM, S.A. (1973): Geomorphic thresholds and complex response of drainage systems. In: Morisawa, M. (Ed.), Fluvial Geomorphology. New York State Univ. Pub. Geomorph, Binghamton, pp. 299– 310.
- SENDIL U., SALIH, A. (1987): Rainfall frequency studies for central Saudi Arabia, Baton Rauge, Louisiana, pp. 315-326.
- SHARMA, K.D., MURTHY, J.S.R. AND DHIR, R.P. (1994): Stream flow routing in the Indian arid zone, Hydrological Processes, 8: 27– 43.
- SHATA, A. (1960): The geology of Sinai Peninsula, The encyclopedia of Sinai, The Supreme Council of Sci., The government Press, Cairo.
- SHATA, A. (1992): Watershed management, development of potential water resources and desertification control in Sinai, Geol. Sinai Develop., Ismailia, Egypt, pp. 273-280.
- SHAY-EL Y., ALPERT P. (1991): A diagnostic study of winter diabatic heating in the Mediterranean in relation to cyclones: Quarterly Journal of the Royal Meteorological Society, v. 117, p. 715–747.

- SHENDI, E., GERIESH, M. (1998): Landfills as a tool for controlling the environmental pollution of the National protectorates, (Saint Catherine area as a case study). Conf. Geol. Sinai Develop., pp. 65-81.
- SHENTSIS, I., MEIROVICH, L., BEN-ZVI, A., AND ROSENTHAL, E. (1999): Assessment of transmission losses and groundwater recharge from runoff events in a wadi under shortage of data on lateral inflow, Negev, Israel. Hydrological Processes, 13: 1649-1663.
- SHERIEF, Y., SH. (1999): Wadi Baba basin, geomorphological study, (MSc), Zagazig University, Faculty of Arts, Geography department.
- SHERVE, R. (1966): Statistical law of stream numbers, Jour., Geology, 74, 17-37.
- SMITH, K. G. (1950): "Standards for grading texture of erosional topography," American Journal of Science, 248: 655-668.
- SMITH, K., WARD, R. (1998): Floods – physical processes and human impacts, John Wiley and Sons, Chichester.
- SMYKATZ-KLOSS W; KNABE, K. & RÖGNER, K, (1997): The geo^mical development of (semi-) andic so.ls as a tool for the reconstruction of palaeoclimatic chanses- a case study for the Wadi Firan, Sinai, Egypt. - Zbl. GeoL Paläontol. 1, 41-57
- SMYKATZ-KLOSS, W.; KNABE, K.; RÖGNER, K.; HÜTTL, C. & ZÖLLER, L. (1998): Palaeoclimatic changes in central Sinai, Palaeoecology of Africa 25, 143 155.
- SMYKATZ-KLOSS, W.; ROSCHER, B, KNABE, K.; RÖGNER, K. &ZÖLLER, L. (1999/2000): Wüstenforschung und Paläokhmatologie im zentralen Sinai. - Chemie d.Erde 59, 245-258.
- SOLIMAN, H., K. (1972): World Survey of Climatology, climate of the United Arab Republic, College Station, Texas (U.S.A.), Volume 10 pp. 79-92.
- SOLIMAN, H., K. (1978): Climate of Egypt, the Egyptian meteorological authority, Cairo.
- SOLIMAN, H., K. (1991): Report on the 19th-23rd October, 1990 flash flood of south Sinai, Remote Sensing Center, Cairo, pp.1-6.
- STEIN, U., ALPERT, P. (1993): 'Factor Separation in Numerical Simulations', J. Atmos. Sci. 50, 2107–2115.
- STORCK, P., BOWLING, L., WETHERBEE, P., LETTENMAIER, D., (1998): Application of a GIS-based distributed hydrology model for prediction of forest harvest effects on peak stream flow in the Pacific Northwest. Hydrological Processes 12, 889–904.
- STRAHLER A. N. (1952): "Hypsometric (area-altitude) analysis of erosional topography," Geological Society American Bulletin, 63: 1117-1142.
- STRAHLER A. N. (1964): Quantitative geomorphology of drainage basin and channel networks. In: Chow VT (Ed) Handbook of applied hydrology. McGraw Hill Book Co., New York, pp. 4–76.

- SU, Z., (2000): Remote sensing of land use and vegetation for mesoscale hydrological studies. International Journal of Remote Sensing 21, 213–233.
- SULEBAK, J.R., ETZELMQLLER, B., AND SOLLID, J.L. (1997): Landscape regionalization by automatic classification of landform elements. Nor. Geogr., Tidsskr. 51 (1), 35– 45
- TSVIELI, Y., ZANGVIL, A. (2007): Synoptic climatologial analysis of Red Sea Trough and non- Red Sea Trough rain situation over Israel, Adv. Geoci., 12, 137-143.
- US ARMY CROPS OF ENGINEERS (1987): Engineering and design hydraulic design navigation dams, Engineer manual, No. 1110-2-1605.
- US ARMY CROPS OF ENGINEERS (2003): Division 5100 erosion and sediment control, Kansas City Metropolitan Chapter, American Public Works Association.
- VERSTAPPEN, H. (1983): the applied geomorphology, International Institute for Aerial Survey and Earth Science (I.T.C), Enschede, Netherlands, Amsterdam, Oxford, New York.
- VISERAS, C., CALVACHE, M.L., SORIAC, J.M. AND FERNÁNDEZA, J. (2003): Differential features of alluvial fans controlled by tectonic or eustatic accommodation space, Examples from the Betic Cordillera, Spain. Geomorphology, 50: 181-202.
- WALTER, H. (1963): Water supply of desert plants. In: Rutter, A.J., Whitehead, E.H. (Eds.), the Water Relations of Plants. Blackwell, London, pp 394.
- WALTERS, M, O. (1990): "Transmission Losses in Arid Regions, J. Hydraulic Engng, 116:129-138.
- WATT, W., CHOW, K. (1985): A general expression of basin lags time. Can. J. Civil Engng 12(2), 294-300.
- WESTON, K. J., ROY, M. G. (1994): 'The Directional Dependence of the Enhancement of Rainfall over Complex Orography', Meteorol. Applications 1, 267 275
- WHITTAKER, R.H. (1967): Gradient analysis of vegetation. Biological Reviews 42, 207–264.
- WILLIAMS, G. (1988): Fluvial Processes in Dryland Rivers. Berlin and New York: Springer-Verlag, 346 p.; reprinted 2002 by Blackburn Press, Caldwell New Jersey.
- YAIR, A. (1983): Hillslope hydrology water harvesting and areal distribution of some ancient agricultural systems in the northern Negev Desert. Journal of Arid Environments 6, 283–301.
- YAIR, A. (1996): Spatial variability in runoff in semiarid and arid areas. In: Rubio, J.L., Calvo, A. (Eds.), Soil Degradation and Desertification in Mediterranean Environments. Geoforma, Logron, pp. 71–90.
- YAIR, A. (2003): Hydrological processes In small arid catchments: scale effects of rainfall and slope length, Elsevier, geomorphology 61, 155-169.
- YAIR, A., DANIN, A. (1980): Spatial variation as related to the soil moisture regime over an arid limestone hillside, northern Negev, Israel. Oecologia 47, 83–88.

- YAIR, A., ENZEL, Y. (1987): The relationship between annual rainfall and sediment yield in arid and semiarid areas. The case of the northern Negev, Catena, Supplement 10, 121–135
- YAIR, A., KLEIN, M. (1973): The influence of surface properties on flow and erosion processes on debris covered slopes in an arid area. Catena 1, 1 –14
- YAIR, A., LAVEE, H. (1985): Runoff generation in arid and semi- arid zones, in hydrological forecasting, edited by Anderson, chapter 8, pp. 182-220.
- YEKUTIELIT, I., MANDELBROT, B. (1994): Horton-Strahler ordering of random binary trees, I. Phys. A: Math. Gen., Printed in the UK, 27 pp. 285-293.
- YU, B., ET AL (2000): The relationship between runoff rate and lag time and the effects of surface treatments at the plot scale, Hydrological Sciences-Journal-des Sciences Hydrologiques, 45(5) 709-726.
- ZAKARIA, T. (1993): Climate of Sinai Peninsula and the east Coast of Egypt, a study in climate geography, MSc, Thesis, Geography, Dept., Fac. Arts, Zagazig University (in Arabic).
- ZERNIT, E. R. (1932): Drainage patterns and their significance, Columbia University, Jour. Geol. 40, pp. 498-521
- ZIV, B., DAYAN, U., AND SHARON, D. (2004): A mid-winter, tropical extreme flood-producing storm in southern Israel: Synoptic scale analysis: Meteorology and Atmospheric Physics, v. 88, p. 53–63.
- ZOHARY, M. (1962): Plant Life of Palestine, Israel and Jordan. Ronald Press, New York, p. 262.

*Aut**horities:***

- EGYPTIAN MINERAL RESOURCES AUTHORITY.
- METEOROLOGICAL AUTHORITY.
- SOUTHERN SINAI GOVERNATE.
- REMOTE SENSING AUTHORITY.
- CENTRAL AGENCY FOR PUBLIC MOBILISATION AND STATISTICS.
- DESERT RESEARCH CENTER.

Some network places:

-http://www.uwsp.edu/geo/faculty/ritter/geog101/textbook/fluvial_systems/drainage_patterns.html
- http:// www.nesdis.noaa.gov/satellite.html
- http://en.wikipedia.org/wiki/Relative_humidity
- http://iflorinsky.narod.ru/rr.htm
- http://museum.gov.ns.ca/mnh/nature/nhns/t3/t3-2.pdf
- http://www.arabicnews.com/ansub/Daily/Day/980317/1998031712.html
- http://www.fao.org/ag/agl/swlwpnr/reports/y_nf/egypt/e_soils.htm
- http://www.isprs.org/publications/related/ISRSE/html/papers/988.pdf

- http://www.sli.unimelb.edu.au/gisweb/DEMModule/DEM_T_Sl.Htm
- http://www .state.nj.us/dep/waters hedmgt
- http://crustal.usgs.gov/laboratories/luminescence_dating/section4.html